

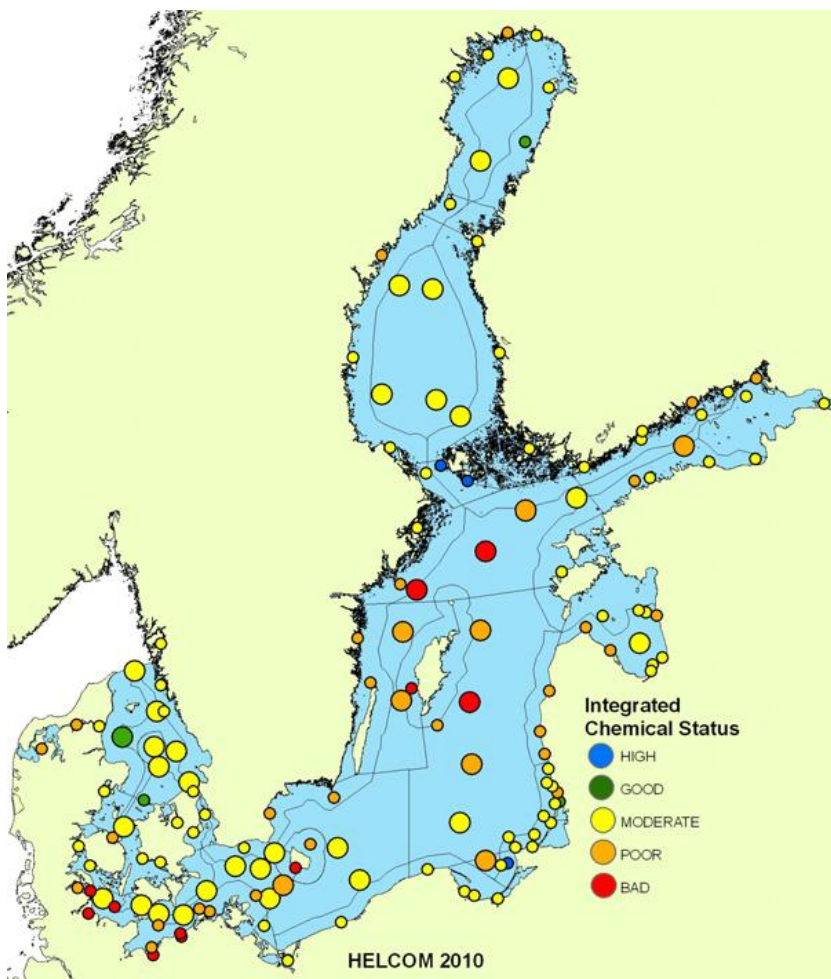
## **Final Report**

# **FEHMARNBELT FIXED LINK HYDROGRAPHIC SERVICES (FEHY)**

## **Marine Water - Baseline**

# **Hydrography, Water Quality and Plankton of the Baltic Sea**

**E1TR0057 - Volume I**



**Prepared for: Femern A/S  
By: DHI/IOW Consortium**

in association with LICEngineering, Bolding & Burchard and Risø DTU

**Responsible editor:**

FEHY consortium / co DHI  
Agern Allé 5  
DK-2970 Hørsholm  
Denmark

FEHY Project Director: Ian Sehested Hansen, DHI  
www.dhigroup.com

Please cite as:

FEHY (2013). Fehmarnbelt Fixed Link.

Marine Water- Baseline.

Hydrography, Water Quality and Plankton of the Baltic Sea.

Report No. E1TR0057 - Volume I

Report : 194 pages

**May 2013**

**ISBN 978-87-92416-27-8**

**Maps:**

Unless otherwise stated:

DDO Orthofoto: DDO®, copyright COWI

Geodatastyrelsen (formerly Kort- og Matrikelstyrelsen), Kort10 and 25 Matrikelkort

GEUS (De Nationale Geologiske Undersøgelser for Danmark og Grønland)

HELCOM (Helsinki Commission – Baltic Marine Environment Protection Commission)

Landesamt für Vermessung und Geoinformation Schleswig-Holstein (formerly Landesvermessungsamt Schleswig-Holstein) GeoBasis-DE/LVermGeo SH

Model software geographic plots: Also data from Farvandsvæsenet and Bundesamt für Seeschifffahrt und Hydrographie

**Photos:**

Photos taken by consortium members unless otherwise stated

© Femern A/S 2013

All rights reserved.

The sole responsibility of this publication lies with the author. The European Union is not responsible for any use that may be made of the information contained therein.



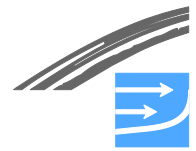


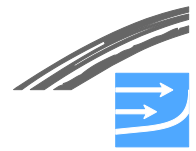
## TABLE OF CONTENTS

1	EXTENDED SUMMARY .....	1
1.1	Hydrography of the Baltic Sea .....	1
1.1.1	Driving forces.....	2
1.1.2	Estuarine Circulation and Water Masses.....	6
1.1.3	Regular inflow and major inflows .....	8
1.1.4	Mixing processes .....	10
1.1.5	Resulting salinities, temperatures and water levels .....	12
1.1.6	Marine optics, transparency .....	18
1.2	Nutrients and oxygen in the Baltic Sea .....	20
1.2.1	Seasonal nutrient cycles .....	21
1.2.2	Long-term trends.....	22
1.2.3	Inorganic nutrients in the depth .....	22
1.2.4	Oxygen .....	24
1.3	Cyanobacteria and phytoplankton in the Baltic Sea .....	25
1.3.1	Spatial and seasonal distribution.....	25
1.3.2	Long-term trends in phytoplankton composition .....	28
1.3.3	Long-term trends in total phytoplankton biomass and primary production.....	28
1.4	Present pressures .....	28
1.4.1	Major constructions.....	28
1.4.2	Ship traffic.....	28
1.4.3	Eutrophication and hazardous substances .....	29
1.5	Consequences of climate change .....	31
2	THE AREA – NATURAL CONDITIONS AND EXTERNAL FORCING .....	33
2.1	Geographical setting .....	33
2.1.1	Bathymetric data and hypsography .....	34
2.1.2	Geographical structure of the Baltic Sea .....	41
2.1.3	Hydrographic implications.....	47
2.2	River runoff to the Baltic Sea.....	49
2.2.1	Discharge data and the HBV model .....	49
2.2.2	Regional inputs, seasonal and inter-annual variability.....	53
2.3	Nutrient inputs .....	57
2.3.1	Riverine input.....	61
2.3.2	Atmospheric deposition of nutrients .....	64
2.4	Meteorological conditions in the Baltic Sea area .....	66
2.4.1	Observational and model data .....	67
2.4.2	Typical transient weather patterns .....	69
2.4.3	Seasonal meteorological conditions over the Baltic Sea .....	71
2.4.4	Inter-annual variations.....	76
3	HYDROGRAPHICAL STATE OF THE BALTIC SEA.....	78
3.1	Sea Level.....	78
3.1.1	Introduction .....	78
3.1.2	Tides.....	78
3.1.3	River inflow.....	78
3.1.4	Density difference.....	78
3.1.5	Wind set-up .....	79
3.1.6	Seiching .....	81
3.1.7	Climate change .....	82
3.1.8	Extreme water levels.....	82
3.2	Waves and tides in the Baltic Sea .....	84
3.2.1	Wind-induced waves .....	84
3.2.2	Tides.....	88



3.3	Baltic water masses — stratification and horizontal gradients .....	94
3.3.1	Regional distribution of salinity .....	97
3.3.2	Temperature .....	105
3.3.3	Stratification .....	107
3.3.4	Optical water types .....	108
3.4	Estuarine Circulation .....	110
3.4.1	Long-term exchange .....	110
3.4.2	Major Baltic Inflows.....	112
3.5	Wind-Driven Currents.....	115
3.5.1	Ekman current and transport.....	115
3.5.2	Upwelling, coastal jets and Kelvin waves.....	116
3.5.3	Interaction of the coastal zone and the open sea .....	118
3.6	Turbulence and mixing .....	119
3.6.1	Bulk estimates for basin-scale mixing .....	120
3.6.2	Mixing processes.....	121
3.6.3	Entrainment in buoyancy-driven inflows.....	121
3.6.4	Internal wave mixing.....	123
3.6.5	Upwelling and mixing .....	124
3.6.6	Other mixing processes .....	125
3.7	Sea ice .....	127
3.7.1	Baltic Sea .....	127
4	NUTRIENTS AND OXYGEN IN THE BALTIC SEA.....	131
4.1	Nutrients .....	131
4.1.1	Seasonal nutrient cycles .....	131
4.1.2	Long-term trends.....	132
4.1.3	Inorganic nutrients in the depth.....	135
4.2	Oxygen conditions.....	136
4.2.1	Introduction .....	136
4.2.2	Surface layer.....	137
4.2.3	Deep water conditions .....	139
5	CYANOBACTERIA AND PHYTOPLANKTON IN THE BALTIC SEA .....	144
5.1	Data basis.....	144
5.2	Factors determining phytoplankton .....	146
5.3	Spatial distribution .....	147
5.4	Seasonal succession.....	150
5.5	Primary production.....	153
5.6	Long-term trends.....	154
5.6.1	Species composition.....	155
5.6.2	Non-indigenous species .....	157
5.6.3	Chlorophyll and total biomass.....	157
5.6.4	Primary production.....	158
6	PRESENT PRESSURES.....	161
6.1	Major constructions.....	161
6.2	Ship traffic and its effects .....	161
6.2.1	High-speed traffic .....	161
6.2.2	Oil spill .....	162
6.3	Eutrophication and hazardous substances .....	164
6.3.1	Eutrophication .....	164
6.3.2	Hazardous substances .....	165
6.4	Fishery .....	169
6.4.1	Commercial fishing.....	169
7	EXPECTED CLIMATE CHANGE .....	171





7.1	Overview .....	171
7.2	Future development .....	173
8	REFERENCES.....	178
8.1	Literature .....	178
8.2	Computer code.....	194
9	GLOSSARY .....	195

Lists of figures and tables are included as the final pages

Note to the reader:

In this report the time for start of construction is artificially set to 1 October 2014 for the tunnel and 1 January 2015 for the bridge alternative. In the Danish EIA (VVM) and the German EIA (UVS/LBP) absolute year references are not used. Instead the time references are relative to start of construction works. In the VVM the same time reference is used for tunnel and bridge, i.e. year 0 corresponds to 2014/start of tunnel construction; year 1 corresponds to 2015/start of bridge construction etc. In the UVS/LBP individual time references are used for tunnel and bridge, i.e. for tunnel construction year 1 is equivalent to 2014 (construction starts 1 October in year 1) and for bridge construction year 1 is equivalent to 2015 (construction starts 1st January).

# 1 EXTENDED SUMMARY

The present report provides a baseline description of the Baltic Sea conditions, undertaken as part of the Fehmarnbelt Hydrography (FEHY) services to Femern A/S.

The report is part of the planned baseline description for the Fehmarnbelt Fixed Link EIA. Separate baseline descriptions are being prepared for the local conditions in Fehmarnbelt and adjacent waters.

The Baltic Sea baseline will serve as reference for potential effect of the Fixed Link extending beyond the local baseline descriptions into the Baltic Sea area. The baseline description is based on literature and dedicated Baltic Sea modelling undertaken as part of the Fehmarnbelt Fixed Link EIA.

## 1.1 Hydrography of the Baltic Sea

The Baltic Sea belongs to the big estuaries of the world. The border between it and the North Sea is the border between Kattegat and Skagerrak, i.e. Kattegat is defined as part of the Baltic Sea and Skagerrak is part of the North Sea. In the following the hydrography, flow and stratification (salinity and temperature) of the Baltic Sea are described, see Fig. 1.1 and

Table 1.1.

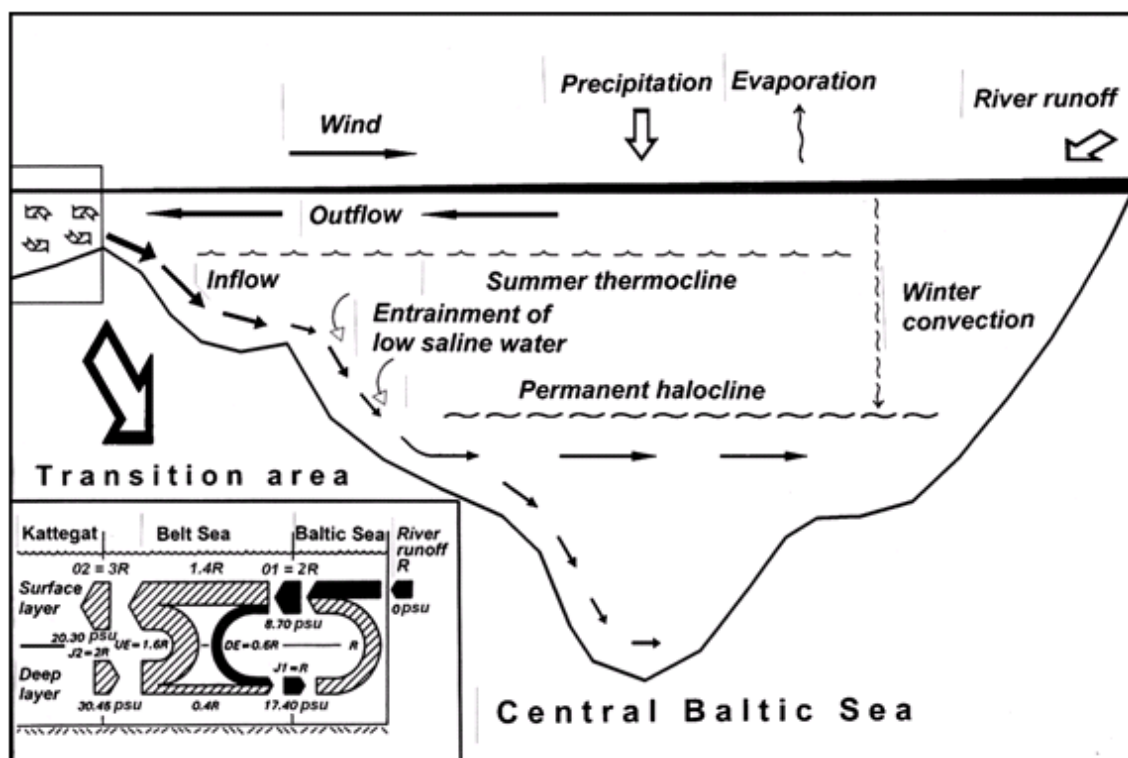


Fig. 1.1 Sketch of water exchange in the Baltic Sea (redrawn after (Lass and Matthäus 2008)).



Table 1.1 Water and salt balance of the Baltic Sea after (Lass and Matthäus 2008). The table provides annual water mass ( $\text{km}^3$ ) and salt transports (Gt) for the relations shown in Fig. 1.1. Extending the above scheme we present the total fresh water input  $F=R+(P-E)$ , with river runoff  $R$ , and precipitation and evaporation ( $P-E$ ) derived from (Lindau 2002) for the period 1980-1995.  $R=446 \text{ km}^3$ ,  $P-E=25 \text{ km}^3$ .

	Kattegat	Belt Sea (+Sound)		Central Baltic Sea
<b>Surface layer</b>	← 3F=1,413 $\text{km}^3$ 28.7 Gt	← 1.4F=659 $\text{km}^3$ 5.73 Gt	← 2F=942 $\text{km}^3$ 8.20 Gt	
<b>Exchange</b>		↑ 1.6F=754 $\text{km}^3$ 23.0 Gt	↓ 0.6F=283 $\text{km}^3$ 2.46 Gt	↑ 1F=471 $\text{km}^3$ 8.20 Gt
<b>Bottom layer</b>	→ 2F=942 $\text{km}^3$ 28.7 Gt		→ 0.4F=188 $\text{km}^3$ 5.74 Gt	

### 1.1.1 Driving forces

The driving forces that determine the flow and stratification in the Baltic Sea can be divided into:

1. Oceanographic conditions in the North Sea (high salinity, wind set-up and tide);
2. Hydrology of the adjacent watershed (river discharge and low salinity); and
3. Meteorological conditions (wind, air pressure and heat exchange).

### Bathymetry of the Baltic Sea

The total surface area of the Baltic Sea is  $411,700 \text{ km}^2$  and the volume  $21,100 \text{ km}^3$ . The bathymetry of the Baltic Sea characterised by contractions and sills that influences the currents and mixing between the water masses is shown in Fig. 1.2.

The first bathymetrical feature to notice is the Baltic transition area, which is the relatively shallow, contracted connection between the North Sea and the Central Baltic Sea. It contains the sea areas Kattegat, northern part of Sound, Great Belt, Little Belt and Fehmarnbelt. The border between the Baltic transition area and the Central Baltic Sea are the Darss and Drogden sills. The maximum depth at the two sills is only about 18 m and 7 m, respectively. The transition area limits the inflow of highly saline water from the North Sea into the Central Baltic Sea and in this manner it has a significant impact on the hydrographical conditions inside the Central Baltic Sea. If and when highly saline water masses originating from the North Sea pass the two sills, they are trapped inside the Central Baltic Sea by the sills and propagate further into the Central Baltic along the bottom. The highly saline water masses can only leave the Central Baltic Sea again by being entrained into the upper less saline water mass at the surface and together with it they flow out of the Baltic Sea again.

The second bathymetrical feature to notice is the three basins in the southwestern Central Baltic Sea, named the Arkona, Bornholm and Gotland Basins. The deepest connection between the Arkona and Bornholm Basin is the Bornholm Channel located north of Bornholm, and the deepest connection between the Bornholm and Gotland Basins is the Stolpe Channel (or Slupsk Furrow). When highly saline water

flows across the sills into the Central Baltic Sea it propagates along the deepest connections, i.e. from the Arkona Basin through the Bornholm Channel into the Bornholm Basin and there from through the Stolpe Channel into the Gotland Basin.

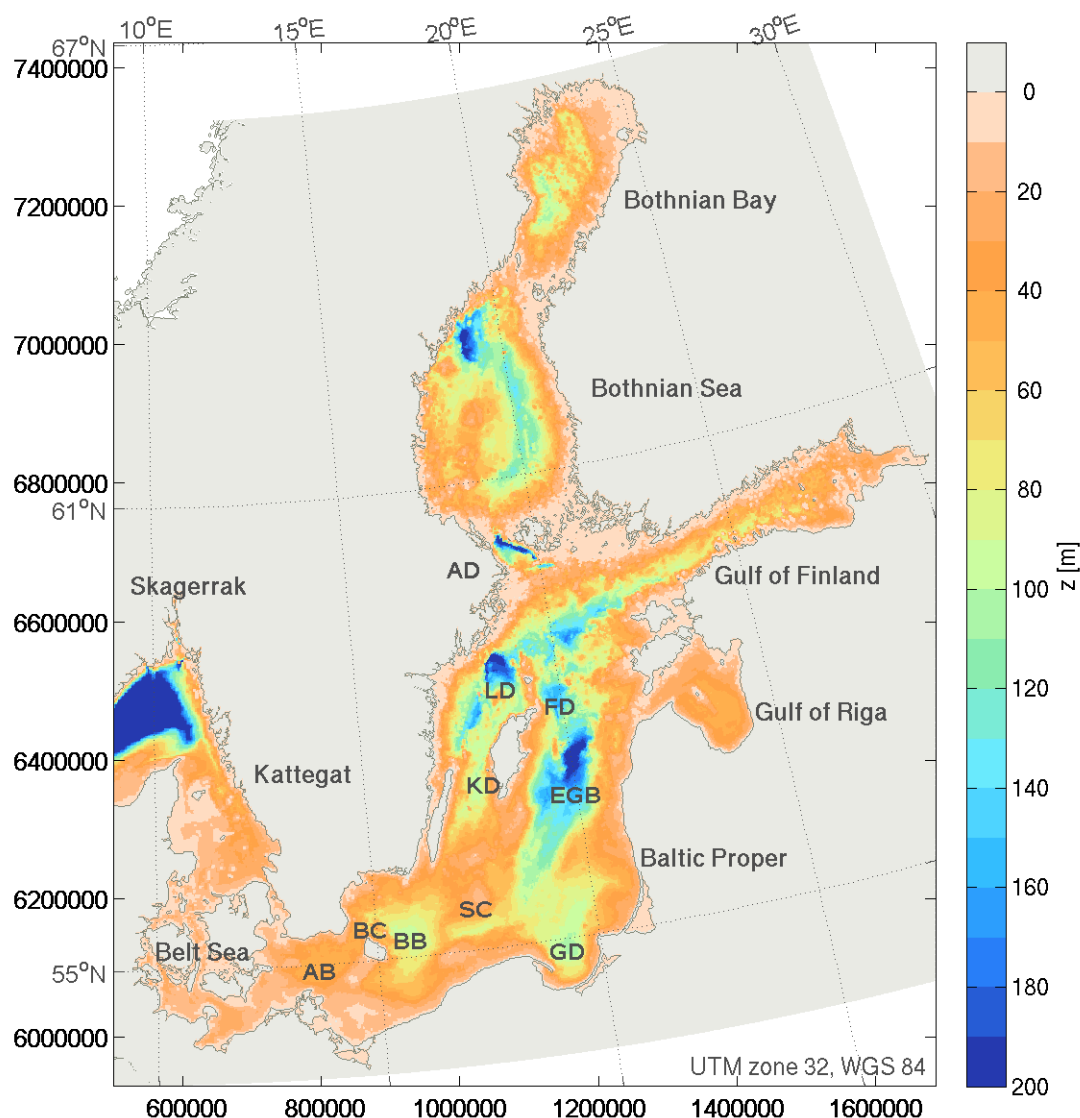


Fig. 1.2 Bathymetry and geographical structures of the Baltic Sea. Water depths refer to (Seifert et al. 2001). Water depth is cut off at 200m. Acronyms indicate some basins and connecting channels: Arkona Basin (AB), Bornholm Channel (BC), Bornholm Basin (BB), Stolpe Channel (SC, also called Slupsk Furrow), Gdansk Depression (GD), Eastern Gotland Basin (EGB), Landsort Deep (LD), Fårö Deep (FD), Karlsö Deep (KD) and Aland Deep (AD).

### Oceanographic conditions in the North Sea

The average salinity in the North Sea is 35 psu and close to the salinity in the oceans, because of the North Sea's wide opening towards the Atlantic Ocean. Therefore water masses in the North Sea are denser than water masses in the Baltic Sea being brackish. In the northern Kattegat or southeastern Skagerrak the North Sea water masses subside (at the Northern Kattegat front, see e.g. (Jakobsen 1997)) and flow under the lighter water masses in the Baltic transition area, towards the bathymetrical restriction at the two sills at Drogden and Darss. In connection with wind-driven exchange flow between the North Sea and the Central Baltic Sea, the dense water mass is then lifted across the two sills and continues into the Central Baltic Sea. In recent years, inflow events have also been observed un-



der calm forcing conditions during summer. These relatively warm, saline plumes could be tracked into the Central Baltic Sea (Feistel et al. 2003c).

Tidal waves propagate from the Atlantic Ocean into the North Sea and continue along an anti-clockwise path through the North Sea. They separate at the Skagerrak and only partly propagate into the Baltic Sea. On their way, the tidal amplitudes decrease dramatically and they are only of limited importance for the flow and stratification in the Central Baltic Sea. But they do contribute to the instantaneous flow through the transition area and the vertical mixing of the water masses.

### **Hydrology of the adjacent watershed**

Fig. 1.3 shows the main rivers of the Baltic Sea. The mean runoff is  $14,136 \text{ m}^3/\text{s}$  (standard deviation of annual values  $\pm 1,545 \text{ m}^3/\text{s}$ ) according to (HELCOM 2009b). The difference of direct precipitation and evaporation  $P - E$  to and from the surface of the Baltic Sea is estimated to range from around  $700 \text{ m}^3/\text{s}$  (Lindau 2002) to  $1,300 \text{ m}^3/\text{s}$  (HELCOM 1986), which corresponds to roughly 5%-10% of the river runoff.

The runoff specifications for the ten largest rivers are summarized in Table 1.2.

The fresh water surplus to the Baltic Sea creates a low saline water mass close to the sea surface that flows towards the North Sea, wherefore the water masses in the Baltic Sea are stratified.

If there was no river inflow to the Baltic Sea the water masses in the Baltic would be oceanic (see also (Bo Pedersen and Møller 1981)) and its ecosystem would be completely different. Hence the river inflow is of crucial importance for the conditions in the Baltic Sea.

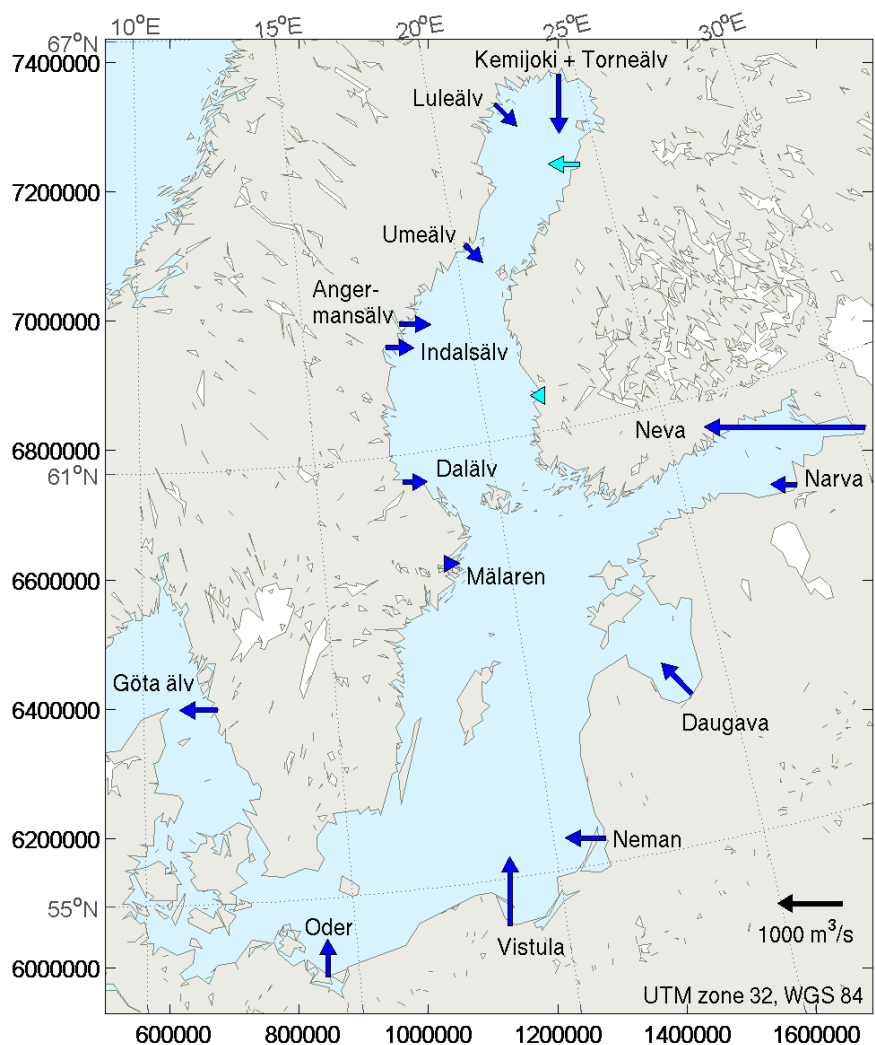
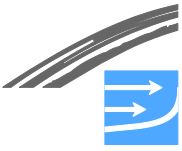


Fig. 1.3 Major rivers contributing to the Baltic Sea water budget. Dark blue arrows indicate specific river runoff, light blue arrows show accumulated diffuse sources. The Göta älv is shown for although it empties into the Kattegat. Torneälv and Kemijoki have been summed up as their mouths are located only 15 km apart. Values from (Mikulski 1970) and (Bergström & Carlsson 1994).

Table 1.2 The ten largest rivers of the Baltic Sea system, including the Belt Sea, Sound and Kattegat, their approximate drainage area and mean annual runoff 1950-1999 (Bergström and Carlsson 1994)

River	Drainage area (km <sup>2</sup> )	Mean annual runoff (m <sup>3</sup> /s)
Neva	281,000	2,460
Vistula	194,400	1,065
Daugava	87,900	659
Neman	98,200	632
Göta älv	50,100	574
Oder	188,900	573
Kemijoki	51,400	562
Ångermanälven	31,900	489
Luleälven	25,200	486
Indalsälven	26,700	443



### **Meteorological conditions**

High and low air pressures fields pass Scandinavia on a weekly time-scale and raise or depress the water levels in the North Sea and Baltic Sea, respectively. The water level difference it causes between the North Sea and the Central Baltic Sea drives an exchange flow between the two seas that either transports low saline waters from the Central Baltic Sea out to the North Sea or higher saline water masses from the North Sea into the Central Baltic Sea. Hence the wind driven exchange flow enhances the estuarine circulation. Actually the wind driven exchange in the Danish Straits is an order of magnitude bigger than the net outflow generated by the freshwater runoff and therefore it is difficult to identify and quantify the density driven circulation in flow measurements collected in the straits. Furthermore the wind shear stress on the sea surface produces turbulence that mixes the water masses.

As just described, the wind can set-up and set-down water levels in the North Sea and Baltic Sea, respectively. When the wind changes or ceases, two-dimensional seiches are generated, i.e. the wind set-up oscillates (and partly turns in a counter clockwise direction) in the North Sea and inside the semi-enclosed Central Baltic Sea. The seiching can cause an extra exchange flow in the transition area.

Inside the Central Baltic Sea, and also, but with less importance, in the transition area, the wind also creates:

- Ekman current in the more open sea areas;
- Coastal jets closer to the coast line;
- Kelvin waves on sea surface, thermocline or halocline; and
- Upwelling of water masses from below either the thermocline or the halocline.

All these resulting currents, i.e. have an impact on the redistribution and mixing of the waters in the area and the water chemistry.

Furthermore, during summer the water masses are heated and during winter they are cooled by the heat exchange with atmosphere. The heating creates a warm low-density layer at the surface with a thermocline located in the upper 20-30 m of the water column, both in the North Sea and in the central Baltic Sea.

#### **1.1.2 Estuarine Circulation and Water Masses**

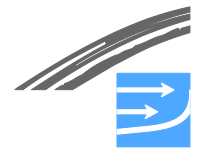
The estuarine circulation is a relatively slow continuous exchange flow driven by the freshwater surplus in the Baltic Sea, partly diminished by the bathymetry constraints, mainly the Darss and Drogden Sills, and enhanced by the wind driven exchange flow.

In the estuarine circulation only two original water masses are involved (see Fig. 1.1):

1. Water from the Baltic rivers with a salinity of 0 psu; and
2. Water from the Atlantic Ocean with a salinity of 35 psu that has flown into the North Sea

All water masses found in the Baltic Sea are a mixture of these two original water masses (only a limited amount of water from the German Bight can be found in the Kattegat, see e.g. (Jakobsen 2000). On the basis of a water mass salinity in the





Baltic Sea one can determine the ratio of the two original water masses. E.g. a water mass with the salinity 17.5 psu consists of half river water and half Atlantic water. In the summer, the original water masses are both warm and in winter they are both cold. This triviality is mentioned, because it is important for the temperature of the lower layers inside the Baltic Sea, see later.

The river water flows in the upper layer at the surface towards the North Sea (Fig. 1.1). Along the path lower laying higher saline water are entrained and mixed with the river water, whereby both its salinity and its volume increases. In the Arkona Basin the salinity has increased to be 8 psu (23% Atlantic water). Through the transition area the salinity increases further to be about 25 psu (71% Atlantic water). Finally it leaves the Kattegat and continues as the Norwegian Coastal Current towards the Atlantic Ocean.

Atlantic water in the North Sea subsides in the southeastern Skagerrak or in the northern Kattegat and flows below the upper layer along the sea bed and through the transition area, and regularly, but not continuously, into the Central Baltic Sea. Note that its last contact with atmosphere is at the entrance to the Baltic transition area. Along the path in the transition area, upper laying lower saline waters are entrained and mixed with the Atlantic water, whereby its salinity decreases. In the Fehmarnbelt the salinity has decreased to be about 21 psu. When the bottom water is lifted across the sills, it plunges into the Arkona Basin and continues into the Central Baltic Sea initially as a dense bottom current (cf. Fig. 1.4). This dense bottom current follows the deepest connections, while being diluted, until it meets a water mass with identical density. At this point it leaves the sea bed and intrudes the water column and continues as an intermediate layer. Hence inside the Central Baltic Sea the structure of the water column below the upper layer is complicated with many intrusions and both the salinity and temperature can vary. Only strong inflows through the transition area are of barotropic nature so that the entire water column is advected across the sills and sinks below the local surface layer in the adjacent Baltic basins. Small inflows can also happen under stratified conditions with only the dense bottom water from the transition area leaking across the sills, which then contributes to the salinity budget of the Baltic Sea. The details of strong and weak inflows are discussed in more detail in Chapter 1.1.3.

Beside the Fehmarnbelt (Darss Sill) pathway the Sound (Darss Sill) exchanges water with the Baltic Proper. The Sound exchange was studied in details as part of the Øresund fixed link study (ØL 1997). The Sound can for most purposes be considered a stratified channel, where the water discharge through the channel is driven by the water level difference between Kattegat and Arkona Basin. The water discharge is only to a minor extent driven by the local wind over the Sound and the density difference between the boundaries due to the shallow Darss Sill. During southwards flow high saline water from Kattegat can be lifted locally across the Drogden sill. And in general larger parts of the Drogden sill area are stratified during a south flowing current than during a north flowing current. During northwards flow the narrow contraction at Helsingør-Helsingborg can act as an internal hydraulic control on the flow and hence impact the extent of the salt water wedge in the Sound. Even the density differences in the Sound are not important in driving the flow through the Sound, the stratification lubricates the flow, i.e. decreases the retarding friction on the flow. Hence the stratification in the Drogden Sill area decreases the contribution to the specific resistance of the Sound from the sill area.

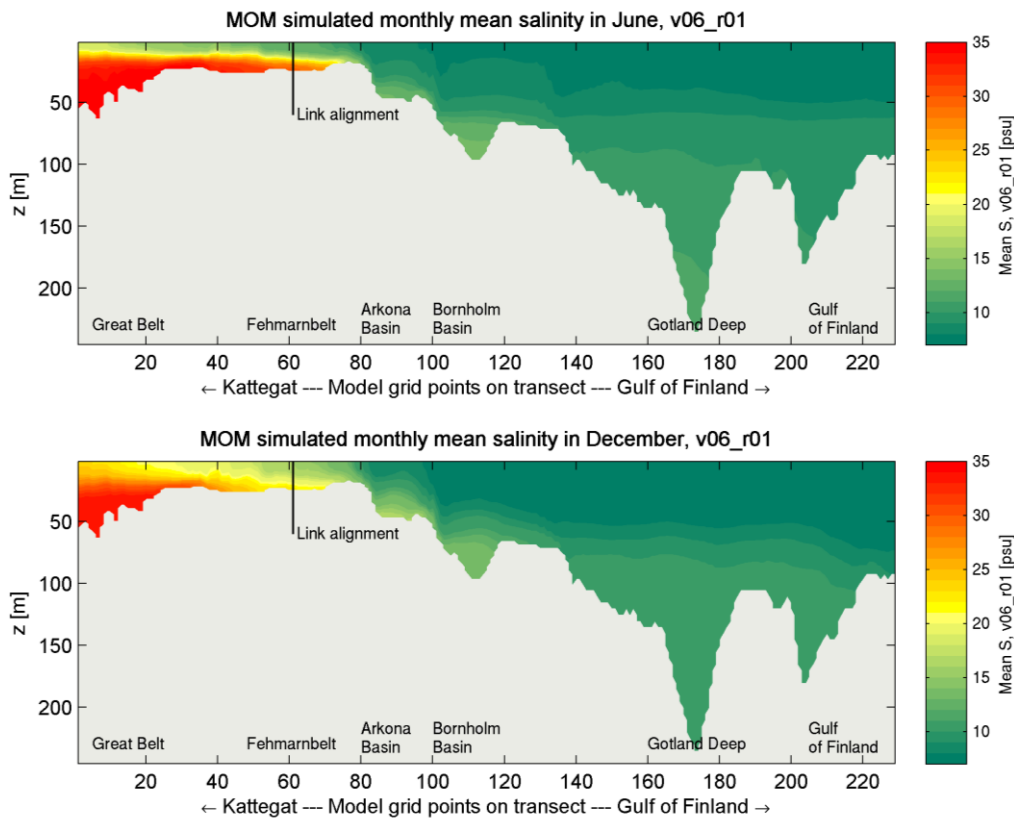
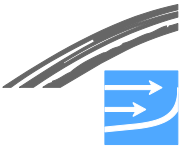


Fig. 1.4 Cross-section showing simulated longitudinal salinity distribution as monthly means from Great Belt through Fehmarnbelt and into the Baltic Proper, where the vertical line shows the position of the planned link (FEHY MOM model, version v06\_r01).

The heat (and oxygen) exchange with the atmosphere takes only place in the water mass at the sea surface. Hence if the Atlantic water in the North Sea water is cold when it subsides and flows into the Baltic Sea, then it stays cold and the temperature is only increased through mixing with warm water masses and vice versa. In this manner the temperature of the intrusions into the Central Baltic Sea signals when they subsided on their way into the Baltic Sea. The travel time can range from months to years (it is noted that the 'older' the water mass, the lower the oxygen content; which is important for marine biology).

The residence time for the upper layer in the Central Baltic Sea is about 30 years. The waters below the upper layer consist of numerous layers and intrusions with different salinity, temperature and age (taken from when it flew into the Central Baltic Sea). Hence it is more difficult, or at least makes less sense, to define one residence time for the lower laying water masses in the Central Baltic Sea. Even so values between 1 to 10 years can be found in literature. It has been noted that in general the higher the salinity of a water mass flowing into the Central Baltic Sea is, the longer its residence time in the Central Baltic Sea will be.

### 1.1.3 Regular inflow and major inflows

The instantaneous water flows through the Danish Straits are primarily driven by air pressure and wind fields and secondarily by tide and density differences. The flow direction is typically three days outwards and two days inwards, but the durations vary considerably. The ratio between the discharges (not salt transports) through the Belt Sea (Darss Sill) and the Sound (Drogden Sill) is 8:3 (Jakobsen & Trébuchet 2000). The smaller transports through the Sound in combination with the shallower sill depth had earlier lead to the assumption that the transport of highly sa-



line water masses through the Sound into Central Baltic Sea is only of minor importance. But recent detailed measurements have revealed that the transport through the Sound is actually considerable and that there is a net salt transport into the Central Baltic Sea through the Sound (Lintrup & Jakobsen 1999) that has to be compensated by a net salt transport out through the Belt Sea, see (Jakobsen & Ottavi 1997).

On average, the net transport flows through Little Belt, Great Belt and Sound according to the relation 1:7:3 (Jakobsen 1980; Jakobsen and Trebuchet 2000). This has been derived from the long-term water budget of the Baltic Sea (HELCOM 1986) and was confirmed by current meter observations at Drogden Sill, Darss Sill and Little Belt. However, estimates of transport derived from single stations can only represent the magnitude of order of the flow through the entire cross-section. Because of changes in stratification estimated salt transport are even more uncertain. Reliable transports through cross-section can be calculated from numerical models which provide continuous data in space and time. Moreover the volume conservation of the models assures a realistic water budget of the Baltic Sea. One of the regional models established as part of the Fehmarnbelt link study gives the annual mass and salinity transports shown in Table 1.3. The model results also show that the fluctuation in transport is regularly several times larger than the net transport. The salt transports are nearly balanced over the 18 years period with a net flow less than 1 Gt/year. The small values given in the table correspond to a minor transient decrease in the Baltic Sea salinity over the period.

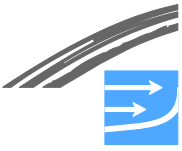
*Table 1.3 Annual volume and salt transports across Drogden Sill, Darss Sill and Fehmarnbelt as simulated by the MIKE Regional Model (ID6.42) for the period 1990-2007.*

	<b>Volume inflow [km<sup>3</sup>]</b>	<b>Volume outflow [km<sup>3</sup>]</b>	<b>Net volume transport [km<sup>3</sup>]</b>	<b>Salt inflow [Gt]</b>	<b>Salt outflow [Gt]</b>	<b>Net salt transp. [Gt]</b>
Drogden Sill	564	-767	-203	7.8	-7.6	0.12
Darss Sill	1,283	-1616	-333	16.1	-16.4	-0.33
Total Central Baltic	1,847	-2,383	-536	23.8	-24.0	-0.21

The duration of the inflows and outflows are determined by the meteorological conditions and a scenario that can cause longer inflows are for example:

- First, a relatively stable high air pressure field over Scandinavia. It will force water out of the Central Baltic Sea and thereby lower the mean sea level inside the Central Baltic Sea; and it shall be followed by
- Second, a relatively stable low air pressure field over Scandinavia. It will, together with the low mean sea level inside the Central Baltic Sea, force a large water volume into the Central Baltic Sea.

The longer the inflow is, the bigger the volume and the higher the salinity are of the water mass crossing the sills and flowing into the Central Baltic Sea. And the bigger the volume and the higher the salinity, the longer the water mass will propagate along the sea bed inside the Central Baltic Sea and replace the existing water at the bottom. Only in connection with especially large inflows the water mass follows the bottom all the way through the Central Baltic Sea without intruding the water column. Such large inflows are referred to as Major Baltic Inflows. Recent Major Baltic Inflows are shown in Fig. 1.5. During the last 25 years only few Major Baltic Inflows took place. Because of the often strong winds during the Major Baltic Inflows, a large mixing of the inflowing water mass takes place already in the Arkona Basin.



During the Major Baltic Inflow of 1993 the transport through the Great Belt and the Sound was measured, see (Jakobsen 1995). The data analysis revealed that the volume of the highly saline water mass ( $S > 17$  psu) transported through the Belt Sea (Darss Sill) was  $88 \text{ km}^3$ , while through the Sound it was  $66 \text{ km}^3$ . Hence also during major inflows, the transport through the Sound contributes significantly to the total inflow (43%) and thereby the replacement of the densest bottom waters in the Central Baltic Sea.

The inflowing dense water masses during a Major Baltic Inflow replace the water masses already located at the bottom. As the density of this new bottom water is high, it can stay there for years until a new major inflow takes place. But because of internal seiching, the dense water mass is slowly mixed with higher laying water masses of less density and hence the density in the bottom water slowly decreases in the years following the major inflow event. Therefore the chance of replacement increases as time passes (the required density of the inflowing water decreases in time).

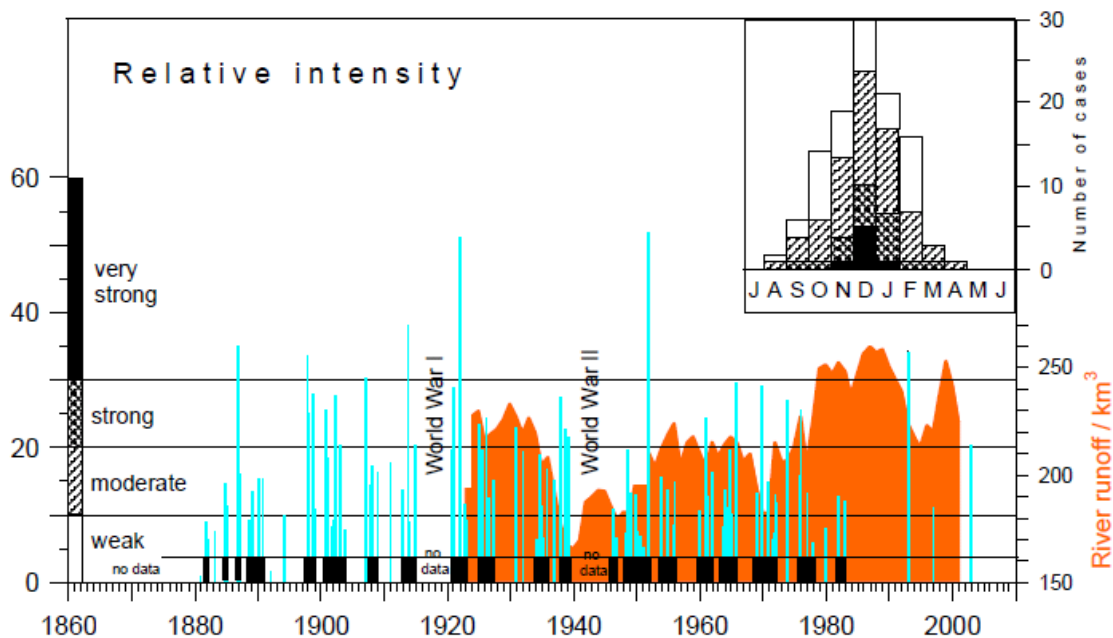


Fig. 1.5 Major Baltic inflows between 1880 and 2007 and their seasonal distribution (upper right) shown in terms of their relative intensity and five year running means of river runoff to the Baltic Sea (inside the entrance sills) averaged from September to March (shaded). Black boxes on the time axis: major inflows arranged in clusters (Matthäus et al. 2008). Intensities: 0 equals an inflow of 5 days duration with  $S=17\text{‰}$  (17 psu), 100 equals an inflow of 30 days duration with  $S=24\text{‰}$ .

#### 1.1.4 Mixing processes

The entrainment and mixing of the water masses along their path through the Baltic Sea are determined by:

- Wind stirring induced by surface shear stress and breaking surfaces waves;
- Cooling of the sea surface (or more correctly free penetrative convection);
- Current shear across thermocline or halocline;
- Current shear towards the sea bed;



- Double diffusion. It is generated by either an instable temperature or instable salinity stratification and can for example have impact the intrusions;
- Internal waves that break at the pycnocline or at topographical obstacles.

The exact contribution of each of the processes is difficult to determine and still under investigation.

The winds and the currents are the most important sources to the mixing in the Baltic Sea and one can in general divide their relative importance roughly dependant on the local bathymetrical features:

- In contraction and sill areas and in channels, the entrainment and mixing caused by currents are the most important ones. Areas are for example Belt Sea, Sound, Bornholm Channel and Stolpe Channel; and
- In more open sea areas, the entrainment and mixing caused by winds are most important. Areas are for example Kattegat, Arkona Basin, Bornholm Basin and Gotland Basin.

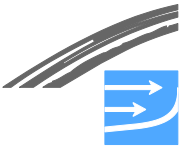
The division is only a rough separation and details can be discussed.

Wind speed varies during the year and is generally lower during the summer season than during the winter season. Hence the mixing caused by the wind varies over the year. As water currents to a large extent are forced by the winds, also the mixing caused by currents varies during the year and is in phase with the wind variation. This seasonal variation in winds and currents causes the stratification in the Baltic Sea to be stronger during the summer season and weaker during the winter season.

Furthermore, during the summer season a thermocline is located in the upper 20-30 m of the water column that protects the halocline from the wind stirring. During fall mainly the wind stirring, but also the free penetrative convection, destroys the thermocline layer. When the thermocline layer is completely destroyed during fall, the entrainment from the halocline starts and it continues until the next spring when the thermocline is build up again.

The mixing can be enhanced or diminished locally at:

- Upwelling and downwelling areas of either thermocline or halocline. In areas with upwelling, the layer thickness is reduced and that increases the mixing locally (and vice versa for areas with downwelling);
- Fronts. The stability of the water column is low close to fronts and hence a significant mixing can take place at fronts (eddies and beddies);
- Along boundaries of dense bottom currents. The stability of the water column is low in areas where the halocline meets the sea bed and the production of turbulent kinetic energy is large and hence an enhanced mixing can be found locally along these boundaries (secondary flows also impact the mixing in these areas); and
- Man-made structures as for example bridges and ferries. This topic will not be treated in this report.



### **1.1.5 Resulting salinities, temperatures and water levels**

#### **Salinity**

The Baltic Sea can loosely be characterized by two main types of water. In the surface layer, which extends from the sea surface to the thermocline, low density water with an average salinity of around 7 psu is found. 1 psu is close to 1 g salt per kg sea water or 1‰ but the units represent different methods. The Practical Salinity Unit psu is derived from the conductivity of seawater, while g/kg is a mass ratio, which is equal to parts per thousand (‰).

The surface layer salinity shows a small seasonal cycle in response to the seasonal runoff characteristics. The other dominant water mass is the more saline, and thus denser, bottom water. This water fills the deep basins east of Bornholm island and around Gotland island. Between the surface and bottom layers, the so-called winter water exists, which is formed during winter and separated by a thermocline from the surface layer at summer.

Salinity in the Baltic Sea decreases eastward from the Belt Sea to the Baltic Proper and reaches its lowest values in the Bay of Bothnia (Fig. 1.6). In the main basins the mean circulation is counter-clockwise and therefore salinity is usually slightly higher in the eastern parts of basins than in the western areas.

#### **Kattegat**

In the eastern Kattegat a clear two-layer stratification is given with a permanent halocline at depths of about 15 m. Surface salinity varies from 18‰ to 26‰ while bottom salinity may reach up to 34‰ (Leppäranta and Myrberg 2009). In contrast to this, the western part features average depths of only 10 m which is shallower than the upper layer's thickness in the east. Therefore a well-mixed water column is normally found in the western Kattegat (Bo Pedersen and Møller 1981).

#### **Belt Sea and Sound**

In the Belt Sea a two-layer structure is generally found like in the Kattegat. As of today, the upper layer consists of outflowing Baltic Sea water with average salinities between 8 psu and 12 psu showing a high intraannual variability (cf. Fig. 3.10 and Fig. 3.12), whereas the bottom water originates from the Kattegat or the North Sea respectively. Bottom salinity in the northern Belt Sea can reach 34 psu while it is already diluted to below 28 psu in the Fehmarnbelt due to internal mixing and entrainment of fresher surface water. Although currents in the Fehmarnbelt show a high variability, salinity is more inert. Early in the year one will observe isohaline waters that slowly develop into a proper stratification. A bottom salinity maximum is found in summer due to the absence of strong wind-induced mixing. With the onset of autumnal winds barotropic in- and outflow increases and thus bottom salinity decreases again due to vertical mixing (König 2004).

In the Sound, three water masses can be found: surface water from the Arkona Sea (7-8 psu), Kattegat surface water (18-26 psu) and bottom water from the Kattegat with salinities between 32 psu and 34 psu.



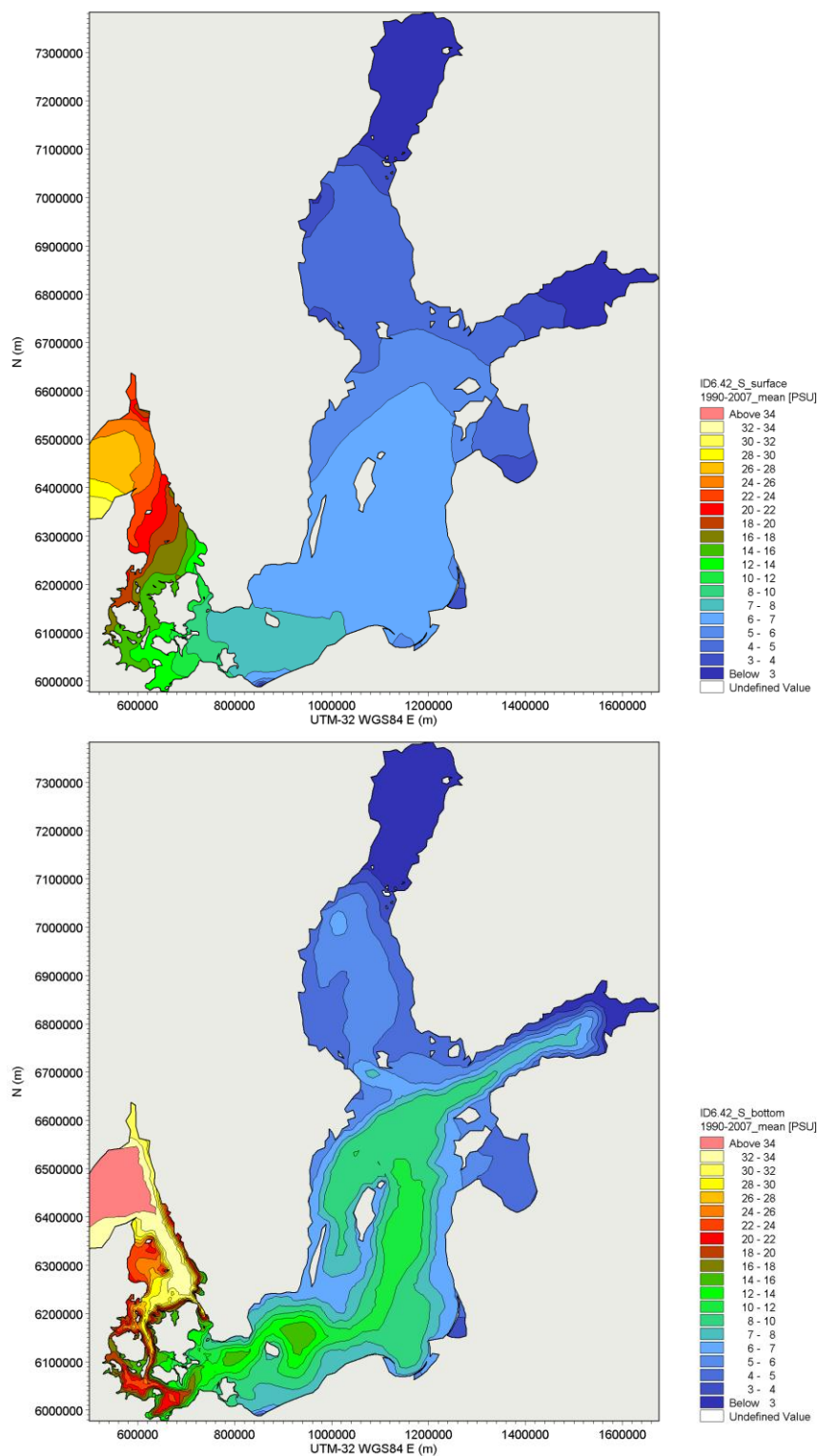


Fig. 1.6 Mean surface (upper panel) and bottom (lower panel) salinity (1990-2007) of the Baltic Sea simulated with the MIKE numerical model (FEHY, 2010/b). A clear gradient between the northern Baltic Sea and the Kattegat is visible.





### **Arkona Basin**

In the Arkona Basin, the surface salinity is around 8 psu, the halocline is situated between 20 m and 30 m, indicating a maximum thickness of the mixed layer of 2/3 of the entire water column. Bottom salinity can reach 22 psu.

### **Bornholm Basin**

Here, the surface salinity varies between 7 psu and 8 psu (up to 9 psu according to observations from ICES, 2010) with an upper layer thickness of up to 60 m. The salinity of the lower layer can reach 13 – 17 psu depending on strong saline inflows. During stagnant periods of weak inflows, salinity and thus density decreases in the deep zones of the Bornholm Basin.

### **Gotland Sea**

The Gotland Sea with its eastern and western sub-basins comprises most of the Baltic Proper and contains about half of the water volume of the entire Baltic Sea. In the Eastern Gotland Basin the halocline is found at 60 m to 80 m depth with an upper layer salinity of 6.5 psu - 8 psu. Below the halocline there is an almost linear increase in salinity to 9 psu - 12 psu at 100 m and 11 psu - 13 psu at 200 m depth in the deep basins (Fig. 1.7) Interdecadal cycles with periods of 20-30 years exist in surface salinity but instantaneous standard deviation is very small ( $\sigma = 0.28$  psu). Bottom salinity of the last 50 years shows a slightly greater standard deviation ( $\sigma = 0.43$  psu) due to the stagnation period from the mid-1980s to mid-1990s. Coastal areas though show a somewhat lower salinity due to river runoff. In the northern part of the Gotland Sea, surface salinity is lower than in the east because of the cyclonic Gotland gyre: Gotland Basin surface water mixes with water from the Gulf of Finland and the Bothnian Sea which results in surface salinities of 6 psu - 7 psu and a bottom salinity of about 11 psu.

### **Northeastern Gulfs**

The surface layer is dominated by freshwater from the most voluminous river of the entire Baltic Sea catchment, the river Neva which results in a continuous east-west gradient in the Gulf of Finland with salinities of 0 psu at the Neva mouth to 7 psu in the western Gulf. Also a halocline is only found in these parts of the Gulf of Finland, at depths of 60 m to 80 m. The bottom layer originates of surface water from the eastern Gotland Basin, and has salinity of 7 psu to 9 psu in the western parts, 5 psu to 8 psu in the central Gulf. The eastern Gulf of Finland is covered with ice in winter, which can last into April.

The Gulf of Bothnia differs greatly in stratification. Water masses here are formed by exchange with the Northern Gotland Basin and by river runoff. The overall stratification is weak and thermohaline mixing reaches into the deep layers. In deep zones though, stratification is strong enough to prevent autumnal deep convection and such bottom water can only be renewed by advection from the south. A weak halocline exists in the Bothnian Sea at depths of 60m to 80 m and in the Bay of Bothnia at 50 m to 60 m.

Salinity at the surface is 5 psu - 6 psu in the Åland Sea while bottom salinity typically varies between 7 psu and 7.5 psu. As in the Bothnian Sea, the lower layer in the Åland Sea is mostly formed by surface waters from the Gotland Basin that are stratified below the less dense local surface water, although a small portion of saline Gotland Basin deep water flows in over some sills and contribute to the deeper layer in the Åland Sea and eventually the Bothnian Sea. In exchange, an equivalent volume of surface water is transported into the Northern Gotland Basin. This mechanism strengthens stratification in the Bothnian Sea (Leppäranta & Myrberg 2009).

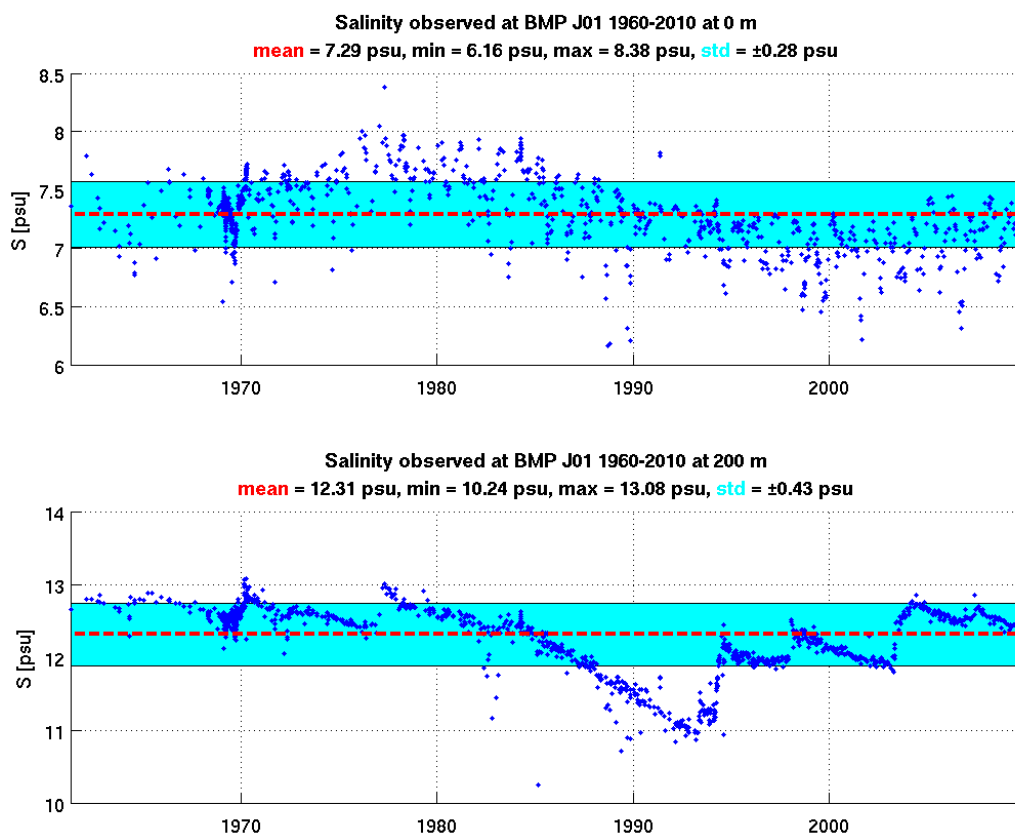


Fig. 1.7 Observed salinity at 0 m (upper panel) and 200 m (lower panel) at station BMP J01 in the Eastern Gotland Basin (ICES, 2010).

Table 1.4 shows the basic statistics of salinity at the sea surface and in the bottom layer in the main basins of the Baltic Sea (cf. Fig. 1.2). The minimum and maximum values describe the full range of salinity which was ever observed. Typical conditions are depicted by the mean values. The differences between surface and bottom salinity are a measure for the average strength of stratification. The variability is expressed by the standard deviation (STD) and more comprehensibly by the variation coefficient, which is the quotient of standard deviation and mean salinity as a percentage of change within the range of  $\pm 1$  standard deviation. This indicates the low salinities in the central and northern Baltic Sea, with variation coefficients around  $\pm 3$ -7%. Only the salinity in Gulf of Finland and Gulf of Riga, which is subject to strong fresh water discharges, shows salinity variation coefficients of  $\pm 10$ %. Higher bottom salinity in the Eastern Gotland Basin in comparison to the Western Gotland Sea reveals the long-term cyclonic circulation of inflowing saline water. The entrance pathway of inflows is also found in the increasing bottom salinities in Bornholm Basin and Arkona Basin, where the variability of the bottom salinity is highest, indicating the strong fluctuation of inflow pulses. Mean salinity is constantly increasing in Belt Sea, Sound and southern Kattegat from 12.7 psu to 19.5 psu at the surface to 20.8 psu to 33.9 psu at the bottom. The variability is high between 10-23% within the whole water column in the shallow Mecklenburg Bight and Kiel Bight. Outflowing brackish water causes also high variation in the surface layer of Great Belt, Sound and Kattegat, but the deeper layers are always filled with saline water.

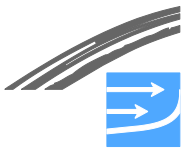


Table 1.4 Long-term statistics of surface and bottom salinity in Baltic Sea basins at the sea surface and in the bottom layer (after Feister et al. 2008). Potential outliers indicated by brackets.

Basin	Lon., lat.	Depth (m)	Min.	Max.	Mean	STD	Var. coeff. (%)	N
<b>Bothnian Bay</b>	22-23°E 64-65°N	0-10	2.6	4.5	<b>3.4</b>	0.22	<b>6</b>	2,029
		10-140	3.3	5.0	<b>4.2</b>	0.28	<b>7</b>	1,039
<b>Bothnian Sea</b>	19-20°E 61-62°N	0-10	3.4	6.2	<b>5.8</b>	0.25	<b>4</b>	1,825
		100-140	4.8	7.7	<b>6.6</b>	0.33	<b>5</b>	1,182
<b>Gulf of Finland</b>	25-26°E 59-60°N	0-10	3.0	8.4	<b>5.3</b>	0.60	<b>11</b>	3,174
		80-110	6.0	11.0	<b>9.1</b>	0.80	<b>9</b>	915
<b>Gulf of Riga</b>	23-24°E 57-58°N	0-10	1.4	7.4	<b>5.2</b>	0.54	<b>10</b>	1,382
		40-60	5.0	6.8	<b>5.8</b>	0.28	<b>5</b>	916
<b>Eastern Gotland Basin</b>	20-21°E 57-58°N	0-10	5.8	8.6	<b>7.0</b>	0.31	<b>4</b>	20,675
		230-240	9.5	13.7	<b>12.4</b>	0.46	<b>3</b>	3,538
	17-18°E 57-58°N	0-10	5.7	8.9	<b>6.9</b>	0.32	<b>5</b>	5,053
<b>Bornholm Basin</b>	16-17°E 55-56°N	0-10	(3.1)	9.4	<b>7.4</b>	0.27	<b>4</b>	21,552
		80-90	8.9	20.5	<b>16.0</b>	1.41	<b>9</b>	1,426
<b>Arkona Basin</b>	13-14°E 55-56°N	0-10	6.0	21.5	<b>8.0</b>	0.51	<b>6</b>	17,417
		40-50	7.3	25.9	<b>15.1</b>	3.49	<b>23</b>	8,416
<b>Mecklenburg Bight</b>	11-12°E 54-55°N	0-10	(5.1)	26.8	<b>12.7</b>	2.96	<b>23</b>	39,742
		20-30	7.5	31.4	<b>20.8</b>	3.88	<b>19</b>	16,221
<b>Kiel Bight</b>	10-11°E 54-55°N	0-10	(5.0)	29.5	<b>15.8</b>	3.27	<b>21</b>	30,602
		30-60	9.0	34.1	<b>23.5</b>	2.30	<b>10</b>	7,115
<b>Great Belt</b>	10-11°E 55-56°N	0-10	7.4	33.3	<b>19.0</b>	4.03	<b>21</b>	74,991
		40-60	22.6	33.9	<b>30.5</b>	2.10	<b>7</b>	648
<b>Sound</b>	12-13°E 55-56°N	0-10	(4.8)	(35.7)	<b>12.7</b>	5.04	<b>40</b>	58,315
		40-60	21.7	35.2	<b>32.3</b>	1.85	<b>6</b>	13,282
<b>Southern Kattegat</b>	11-12°E 56-57°N	0-10	8.9	33.9	<b>19.5</b>	3.65	<b>19</b>	14,449
		50-110	32.3	35.0	<b>33.9</b>	0.57	<b>2</b>	1,004

### Water temperature

Water temperature in the Baltic Sea is as well determined by the two-layer stratification that arises from the above named salinity features. The upper layer is subject to a strong annual cycle through air-sea interaction and solar radiation. This leads to the formation of a warm seasonal surface layer with a thermocline in summer: after the ice-melt in spring, a thin layer at the very surface is quickly heated by solar radiation and reaches a temperature of maximum density,  $T_m$ , of 1.5°C to 3°C. Typical depths of the thermocline are stated within 5 m – 100 m, depending on geographical location, although the depth of the summer thermocline is stated within 15 m - 30 m throughout the entire Baltic Sea (Leppäranta & Myrberg 2009).

At the lower edge of this layer a dicothermal layer is formed when the water is heated from above but cooled by the colder bottom water, so-called "winter water", at the same time. This dicothermal water mass is referred to as "old winter water", it is a specific phenomenon of the Baltic Sea and other ice-covered seas.



The lower layer is isolated from atmospheric effects and therefore temperature changes here are mainly due to temperature of the inflowing water from the North Sea water. These changes are very weak. Typical bottom water temperatures range from 4°C to 6°C.

### **Water level**

The water levels in the North Sea – Baltic Sea system is determined by:

- Tides propagating from the Atlantic Ocean into the North Sea and further into the Baltic Sea;
- River inflow to the Baltic Sea;
- Density differences due to differences in salinity and temperature;
- Wind set-up and barometric pressure conditions in the Baltic Sea and the North Sea, respectively;
- Seiching in the two seas due to changing wind fields (see, e.g., (Wübbler and Krauss 1979); and
- Climate change

Tides propagate from the Atlantic Ocean into the North Sea and further into the Baltic Sea. Along their path the tidal amplitude increases, because of reduced water depth (shoaling), and decreases, because of bed friction (energy dissipation). In Kattegat at Hornbæk the tidal amplitude, or intensity coefficient, is 15 cm (sum of four tidal constituents: M<sub>2</sub> + S<sub>2</sub> + K<sub>1</sub> + O<sub>1</sub>). The amplitude decreases through the Danish Straits and is 7.5 cm at Gedser. Inside the Central Baltic Sea the amplitude is less than 5 cm.

The river inflow to the Central Baltic Sea lifts the water level to be higher inside the Central Baltic Sea than in the Kattegat and the North Sea. The water level lift is nearly constant inside the Central Baltic Sea, but varies over the Danish Straits. Because of the river inflow the water level is lifted to be located about 4 cm higher in the southwestern Baltic Sea than in the Kattegat (calculated by the energy equation and the resistance of the Danish Straits; see also Fig. 1.8 for a numerical simulation).

As salinity at the sea surface increases from 0-3 psu in the innermost of the Baltic Sea to a mean value of 24.8 psu in Kattegat at Læsø Nord, the density of the water increases from its minimum value at the innermost Central Baltic Sea towards the North Sea. This density variation causes a water level lift. The highest lift is found in the innermost of the Baltic Sea wherefrom it decreases gradually towards the North Sea. The water level is located about 4 cm higher in the southwestern Baltic Sea than in the Kattegat because of these density differences.

Hence the total lift from river inflow and density difference is from 4 cm to 8 cm (the contributions should not simply be added). From measurement it is found to be 6 cm (Jakobsen et al. 1997; Jakobsen & Trébuchet 2000; and Jakobsen et al. 2010), but the value is uncertain.

In addition, high and low air pressures fields pass Scandinavia on a weekly time-scale and set-up or set-down the water levels in the North Sea and Baltic Sea. The actual value of high and low water levels depends on the air pressure and wind fields (the wind shear stress on the sea surface increases with the wind speed to power 2). It is remarked that high water levels in Kattegat and low water level in



the Arkona Basin forces an inflow to the Baltic Sea. Low water levels in Kattegat and high water level in the Arkona Basin force an outflow from the Baltic Sea.

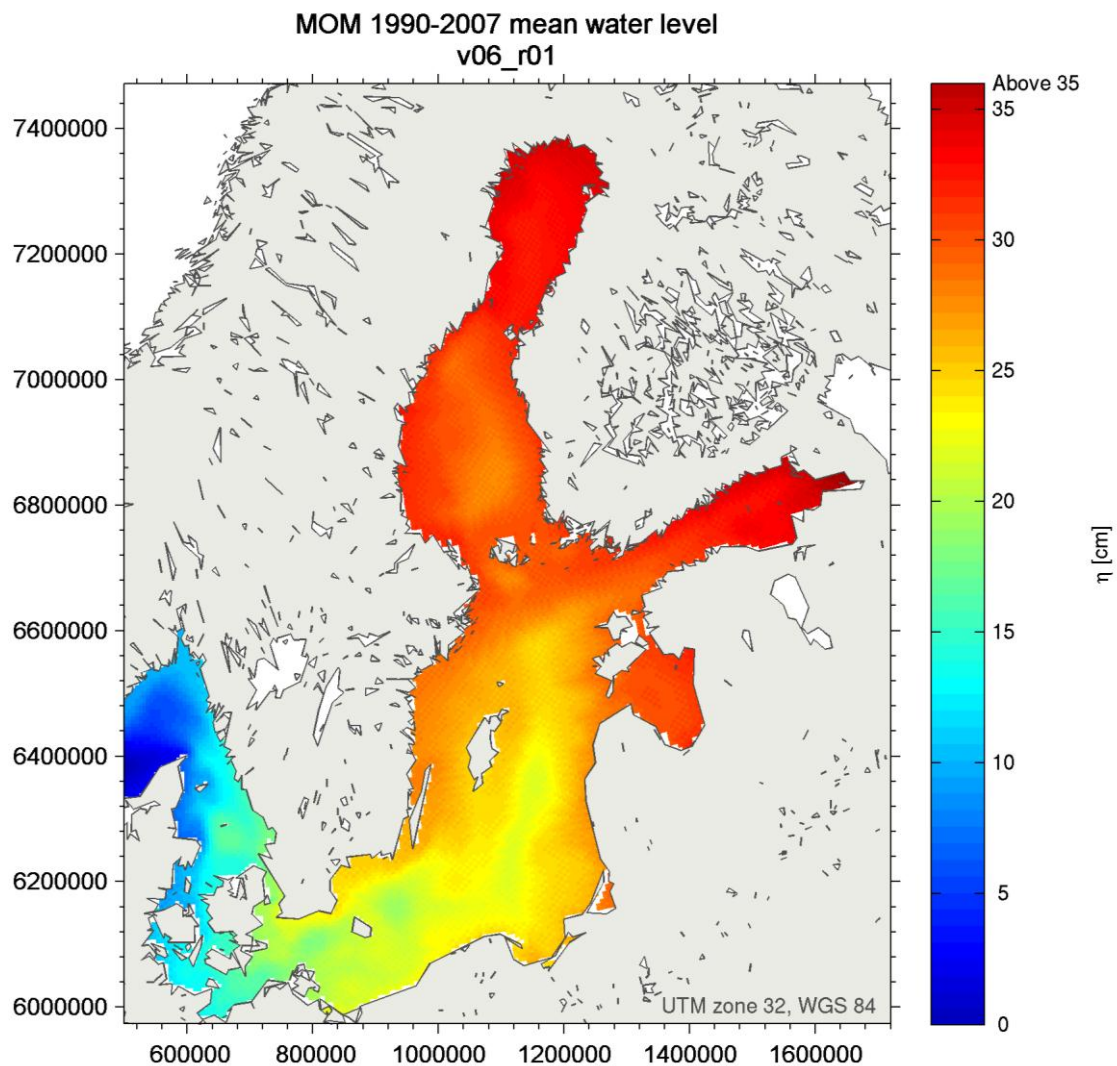
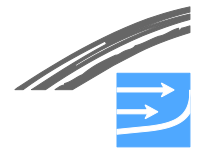


Fig. 1.8 Mean water level (1990-2007) of the Baltic Sea simulated with the MOM numerical model (FEHY, 2013c). A clear gradient between the northern Baltic Sea and the Kattegat is visible. Local depressions due to large gyres exist in sub-basins like the Bornholm Basin or the Bothnian Sea.

### 1.1.6 Marine optics, transparency

The knowledge about optical features of Baltic Sea water is largely based on irradiance data. A long time series (> 100 years) of Secchi depths exists (see Fig. 1.9) and few records are available from water samples and in-situ soundings. Most optical research has been carried out in the southwestern Baltic Sea but more recently a number of programmes have been established in the Gulf of Finland. Depending on time and location, the present level of Secchi depths in the Baltic Sea varies from 5 m to 10 m. Coastal areas are generally more turbid than open basins, and turbidity there increases even during runoff peaks when large amounts of suspended matter is washed into the sea. As the Secchi depth is related to the scale of light attenuation, it can be used to infer physical properties of sea water. Mean Secchi depth in the Baltic has significantly decreased during the last 100 years due to anthropogenic influence. A major cause is eutrophication which has led to an increase of colored dissolved organic matter (CDOM) and chlorophyll in the Baltic Sea and in the lakes of its drainage (Leppäranta & Myrberg 2009).





A high content of CDOM and suspended matter which strongly influences light transfer is typical for Baltic Sea water masses. The inversion for optical measurements of water properties in such optically highly complex waters needs not be unique. The large amount of CDOM turns the Baltic Sea water brownish. In a 2004 study, Sipelglas et al. concluded that for variability of the attenuation coefficient, CDOM was the main optical component in their data set. Generally, chlorophyll is also a major factor in optical properties, not least due to its seasonal variability.

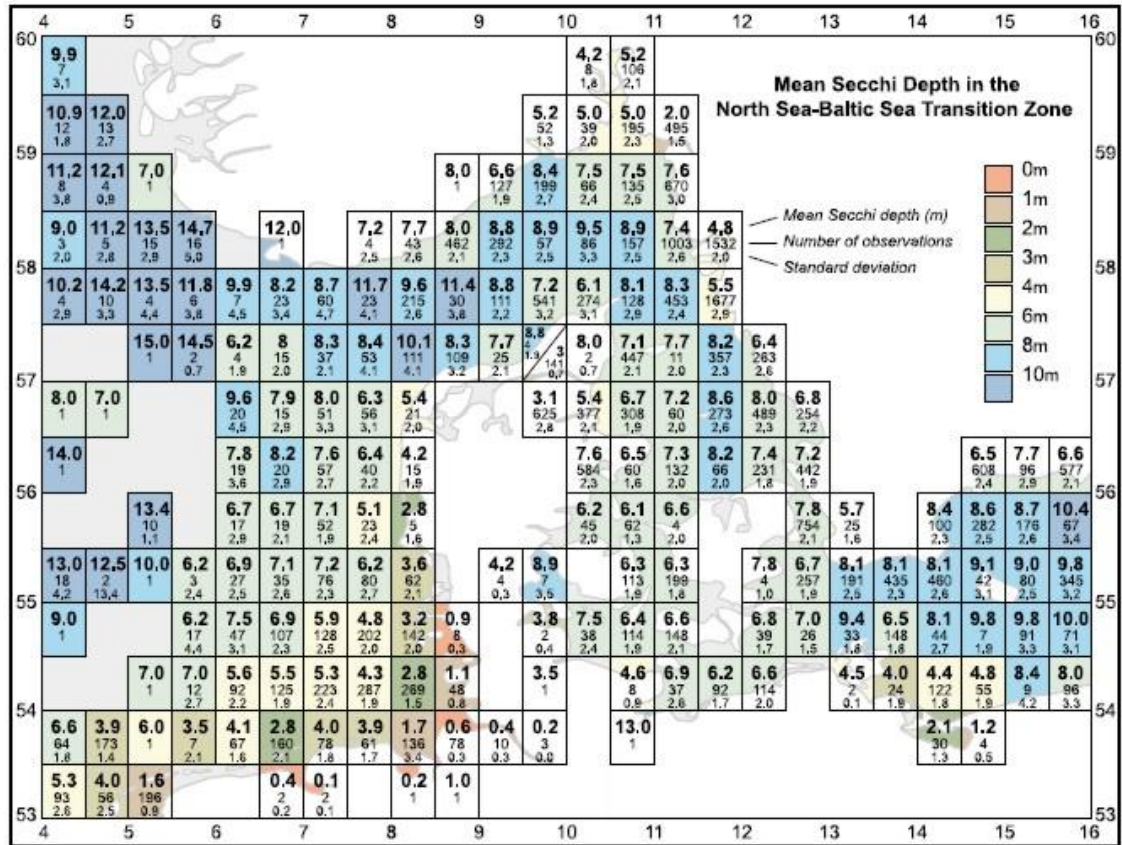
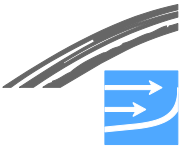


Fig. 1.9 Mean Secchi depth (top number), number of observations (middle number) and standard deviation (bottom number) for  $0.5^{\circ} \times 0.5^{\circ}$  squares for the transitional zone of the North Sea - Baltic Sea in the period 1902-1999; from (Aarup 2002). Most straits in the Belt Sea show a mean Secchi depth of 6 m while it increases to 8 m in the deeper parts of the Kattegat and also in the Arkona and Bornholm Sea. Reprinted from *Oceanologia*, Vol. 44, No. 4, Figure 2, p. 332, with the publisher's permission.

Sea ice and snow cover have as well a great impact on light transfer, depending on their wetness and layer thickness. Reflectance measurements show that in the early melting seasons the reflectance of snow becomes lower and has a weak minimum at 550 nm with an overall reflectance  $>0.4$ . In sea ice, the main optical impurities are made up by gas bubbles, included brine pockets and chlorophyll. Other studies showed that snow on sea ice causes a strong attenuation but a significant amount of light can pass into the water column once the ice is not covered by snow any more. Furthermore, the apparent optical properties of water below sea ice differ from those of ice-free water because incoming light is much more diffuse under an ice cover. One of the most important applications in marine optics in the Baltic Sea, especially remote sensing, is currently the mapping of harmful algae blooms. However it is not clear how to separate the signal of climatic change from local anthropogenic effects.



## 1.2 Nutrients and oxygen in the Baltic Sea

The Baltic Sea is endangered by anthropogenic nutrient inputs modifying the structure and function of the ecosystem (Nixon 1995, Aertjeberg et al. 2003). Eutrophication (see Chapter 6.3) is analogous to the natural aging in the broadest sense of the word, the increased supply of plant nutrients to waters due to human activities in the catchment areas that result in an increased production of algae and higher water plants (EUTROSYM 1976). Thereby the excessive input of nitrogen and phosphorus is the main concern. Fig. 1.10 gives a conceptual model of these sources.

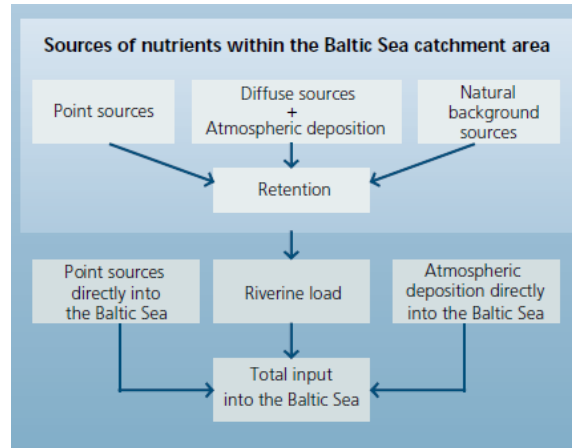


Fig. 1.10 Conceptual model of nutrient input sources to the Baltic Sea (HELCOM 2010a – holistic assessment).

(HELCOM 2010b) reported that for the period of 2001 – 2006, the averaged annual total waterborne input of nitrogen (riverine load, coastal areas, direct point and diffuse sources) amounted to 641,000 t. An additional quarter of the total nitrogen inputs is caused by atmospheric deposition. This pathway amounts to 198,000t N in 2006. In total, yearly around 840,000 t of nitrogen are introduced into the Baltic Sea. Fig. 2.17 gives an overview of the contribution of different sources. About 80% of the diffuse sources originate from agriculture, about 10% are discharged from point sources such as municipal wastewater treatment plants or industry. Transboundary inputs from inland countries without a Baltic Sea coastline are mainly coming from Belarus and Ukraine. It has to be mentioned also that 17% are due to natural background losses.

For phosphorus, the averaged annual input for the period 2001-2006 amounts to 30,200 t (HELCOM 2010/a/b). It is believed that the airborne phosphorus deposition accounts for a maximum of 5%. Exact measured or modelled data are not reported. Around 20% of the inputs are coming from point sources whereby wastewater treatment plants contribute to 90% of this source. Again, 80% of the diffuse sources can be related to agriculture. Natural background losses amount to 16% of the total input. The five largest sources of phosphorus and nitrogen are the rivers Vistula, Neva, Oder, Daugava and Nemunas. Thus, the highest nutrient enrichment pressure is on the Baltic Proper, the Gulf of Finland and the Gulf of Riga (HELCOM 2010a).

A study by (Larsson et al. 1985) suggests an increase in total phosphorus loading by about eight times, and in total nitrogen load by about four times from the catchment area due to human activities from the early 20<sup>th</sup> century to the 1980s, see Table 1.5.





Table 1.5 Estimated total nitrogen and phosphorus inputs (tons/year) into the Baltic Sea during the 1980s and before the beginning of the 20th century (Larsson et al. 1985).

	<b>Nutrient</b>	<b>Rivers</b>	<b>Atmosphere</b>
Mid of the 1980s	Phosphorus	51,600	5,500
Beginning of the 20 <sup>th</sup> century		6,800	2,800
Mid of the 1980s	Nitrogen	640,500	322,000
Beginning of the 20 <sup>th</sup> century		150,000	83,000

A model study by Schernewski and Neumann (2005) to describe the trophic state of the Baltic Sea a century ago compared the early 20<sup>th</sup> century with the nutrient load during the 1980s. They calculated a riverine load reduction of 68% for nitrogen and 76% for phosphorus hundred years ago. Taking all loads, including atmospheric deposition, the load at that time was only one quarter of today's inputs.

One can conclude that despite differences in the various estimates and calculations a man-made increase in nitrogen and phosphorus inputs to the Baltic Sea by a factor of four at least can be given.

### 1.2.1 Seasonal nutrient cycles

The distribution of inorganic nutrients in the surface layer of the Baltic Sea is characterized by a pronounced seasonality with reaching high concentrations in winter, the seasons with lowest biological activity, and a decrease to around the detection limit during the period of high biological productivity which is beginning in early spring and ending in late summer (Nausch and Nehring 1996; Nausch & Lysiak-Pastuszek 2002). Due to the long-lasting winter in the central Baltic Sea a typical homogenous nutrient level between early February and end of March/beginning of April is formed. In the Arkona Basin and especially in the western Baltic Sea the spring bloom starts much earlier, often already at the beginning of March or in the second half of February. It has been shown that intensive nitrogen-fixing blooms are mainly based on regenerated phosphate, changes in the internal phosphorus pool (Nausch et al. 2004) and on additional phosphorus supply by upwelling processes (Nausch et al. 2009; Lass et al. 2010). During autumn, first phosphate and later also nitrate concentrations start to increase due to the intensification of decomposition processes. In February of the following year, again typical winter concentrations are reached. See Fig. 1.11 for annual cycles of phosphate and nitrate.

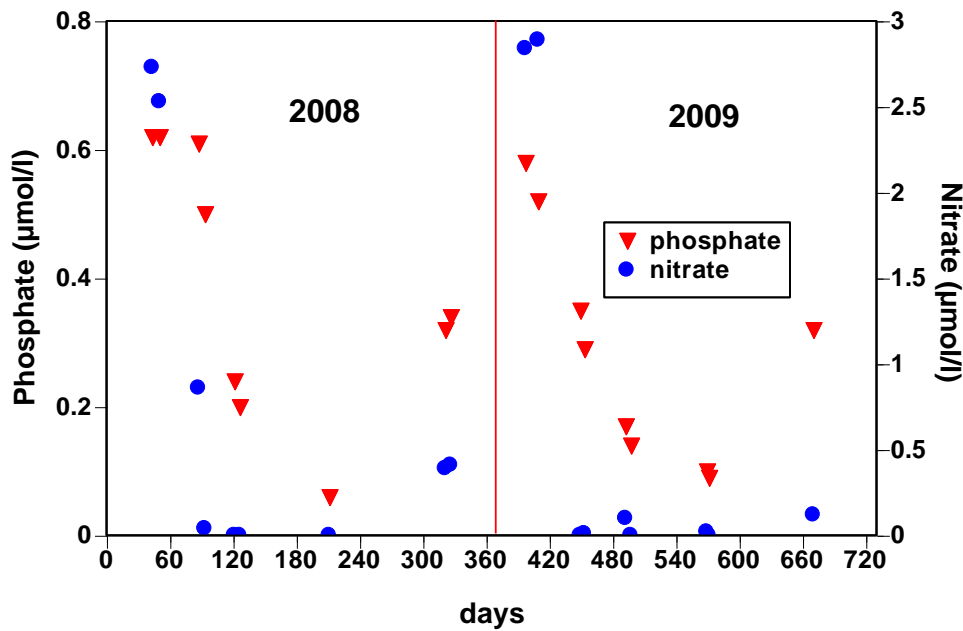
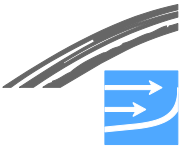


Fig. 1.11 Annual cycle of phosphate and nitrate 2008 and 2009 in the surface layer (0 – 5 m) in the Arkona Sea (measurements at station 113/BMP K05),( ICES 2010).

The reason for the different seasonal cycles of phosphate and nitrate is a disturbed Redfield ratio. Phytoplankton incorporates carbon, nitrogen and phosphorus in a molar ratio of around 106:16:1 (Redfield et al. 1963). When primary production is limited by light, a similar ratio is found in seawater caused by the mineralization of organic matter. In the Baltic Sea, denitrification in suboxic water layers and at the sediment surface is thought to be responsible for this anomaly. First measurements at the end of the 1950/beginning of 1960s give also a molar N/P ratio of 7-10.

### 1.2.2 Long-term trends

Fig. 1.12 demonstrates long-term trends for the eastern Gotland Basin. At the beginning of the time series, before regular monitoring cruises started, only few data, especially for nitrate + nitrite are available. In Nausch et al. (2008) data are summarized for 5 (10) year periods. In the Bornholm Basin and the eastern Gotland Basin phosphate concentrations are similar for the period 1958/68 and 1969/1973. They range between 0.21 and 0.34 µmol/l. In contrast to coastal areas where eutrophication is an already long-lasting phenomenon the open seas seems not to be affected strongly at that time. For nitrate, rare data of the periods 1958/68 and 1969/73 differ, but it is generally accepted that background concentrations are in the range of 2.0 – 2.5 µmol/l (Nausch et al. 2008). Phosphate and nitrate concentrations started to increase in the late 1970s and remained on a high level since the 1980s. The phosphate winter concentrations and the concentrations of inorganic nitrogen recently observed are nearly twice as high as the background concentrations. These results are clear signs of eutrophication.

### 1.2.3 Inorganic nutrients in the depth

Nutrient concentrations in the deep basins of the Central Baltic Sea are closely correlated with the hydrographic regime governed by the alternation between Major Baltic Inflows (MBIs) and stagnation periods. In the presence of oxygen, phosphate is partly bound in the sediments and onto settling particles in the form of an iron-III-hydroxophosphate complex. If the system turns from oxic to anoxic conditions, this complex is reduced by hydrogen sulphide (Hille et al. 2005). Phosphate and iron(II) ions are liberated leading to an increase in phosphate in the water column.

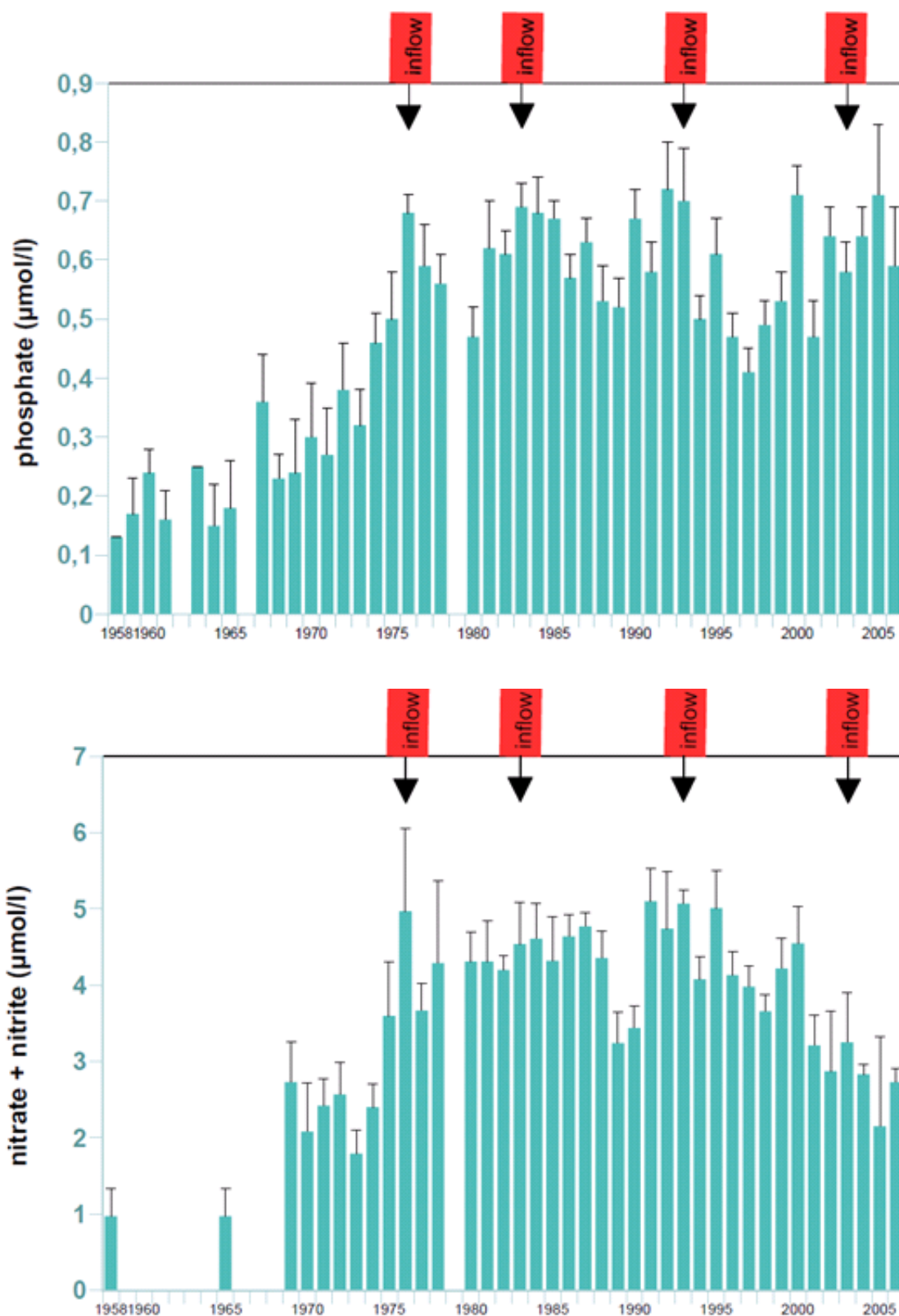
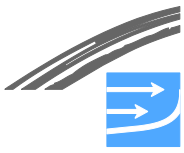


Fig. 1.12 Mean phosphate and nitrate+nitrite concentrations in the mixed winter surface layer (0 – 10 m) pooling five stations in the eastern Gotland Basin from 1958 to date (1962, 1966, and 1979 no data). Major Baltic Inflows are marked with red tags. Figures taken from (Nausch et al. 2008).

A detailed description of the nutrient situation in the Baltic Sea can be found in the annually published assessments of the Baltic Sea (e.g. the latest report by (Nausch et al. 2009).



### 1.2.4 Oxygen

The oxygen budget of the sea is characterized by the input from the atmosphere and through primary production of algae and submerged vegetation and the consumption through respiration, decomposition of organic matter and loss to the atmosphere. Temperature and salinity cause stratification but vertical circulation, advection and convection can influence the oxygen content. The oxygen situation in the surface layer is normally good. Changes in the oxygen content here are mainly caused by the annual cycles of temperature and the seasonally differing production and consumption processes (Matthäus 1978, Nausch et al. 2009). Below permanent or temporarily occurring pycnoclines, however, a significant loss of oxygen can take place because in these water layers the absence of light prevents production processes and only oxygen consumption is relevant. The oxygen consumption can be so intensive that anaerobic conditions occur and the formation of hydrogen sulphide starts as in the deep basins of the central Baltic Sea. These different features can be seen in a transect from the Darss Sill to the northern Gotland Basin (Fig. 1.13).

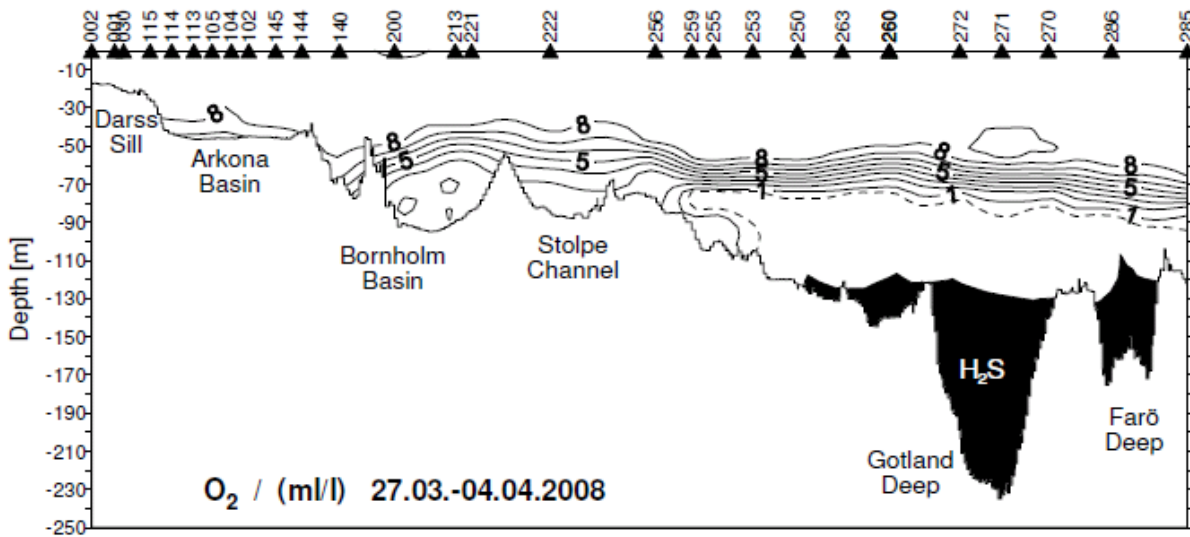


Fig. 1.13 Vertical distribution of oxygen resp. hydrogen sulphide between Darss Sill and northern Gotland Basin in March/April 2008 (from Nausch et al., 2009).

In the mixed surface layer, low temperature in winter causes high solubility of oxygen, but productivity is minor. In spring, temperature still remains on a low level, but the spring bloom of phytoplankton generates an additional oxygen supply. The rapid temperature increase, starting mid-May, diminishes oxygen solubility. During summer the observed saturation is only 6 – 7 ml/l. Autumnal cooling leads to an increase of the oxygen content in the surface layer.

In the shallow western Baltic Sea and in the Arkona Basin (max. depth 47 m), also in the bottom near layer an annual cycle can be observed. During winter time, vertical mixing takes place down to the bottom. Additionally, frequent inflow processes cause water renewing. Thus, the bottom water is relatively well supplied during winter and spring. The development of the thermocline in late spring/winter prevents deep reaching vertical convection. Together with the increased mineralization of organic substances, the oxygen saturation decreases in summer and autumn. Intensified cooling of the surface waters and storm events in autumn dissolve the thermocline, leading again to mixing down to the bottom in winter. Due to the importance of these processes in the Fehmarnbelt region they are described more in detail in the special Fehmarnbelt Baseline Report (FEHY 2010a).



In the more eastern basins of the Central Baltic Sea, a permanent halocline exists, preventing vertical mixing down to the bottom. Therefore, the oxygen situation is coined through the occurrence or absence of barotropic or baroclinic inflow events. Not only Major Baltic Inflows of higher saline water, but also regular inflows of lower volumes of water frequently penetrate across the Darss and Drogden Sills, pass the Arkona Basin, and are trapped in the deep water of the Bornholm Basin causing a high variability in temperature, salinity and oxygen concentration. In contrast to the Bornholm Deep, no regular seasonal variations can be observed in the Gotland Deep, Fårö Deep, Landsort and Karlsö Deep. The so far latest MBI was detected in January 2003 followed by a stagnation period which continues until today. The oxygen system reacted as described before. From 1993 onwards, stagnation effects were observed also in the western Gotland Basin. The 2003 inflow had only small effects on the oxygen conditions there (Nausch et al. 2005, 2006) owing to the relatively high salinity in the deep water which caused a higher stability of stratification and hampering vertical exchange.

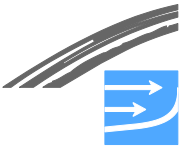
### **1.3 Cyanobacteria and phytoplankton in the Baltic Sea**

Marine phytoplankton is the principal primary producer and is influenced by hydrological and biological parameters. However, the marine phytoplankton itself influences a cascade of biological and hydrological parameters, especially during the eutrophication process: increasing nutrient input goes along with increasing phytoplankton biomass and leads to decreasing light penetration, which hampers the growth of macrophytes and higher plants. The loss of macrophyte cover changes the structure of the benthic habitat with negative consequences for benthic diversity and fish breeding. In addition, excessive blooms of plankton lead to increasing oxygen consumption and finally oxygen depletion. Increasing nutrient supply results in an increase of duration and frequency of algal blooms. For this baseline report several national projects, eight phytoplankton and six chlorophyll a (chl-a) HELCOM long-term stations were analysed on seasonal basis.

#### **1.3.1 Spatial and seasonal distribution**

In general the vertical gradients of biomass and primary production are stronger than the horizontal gradients. They depend mainly on light penetration and stratification. The horizontal distribution is associated with the estuarine gradients (trophic conditions and salinity), the upwelling gradients (nutrient availability, temperature and salinity), and the large scale marine gradients of decreasing salinity from Kattegat to the Bothnian Sea. Within the west-northeast gradient the regional species composition changed on basis of main taxa groups as well as on basis of individual taxa. According to (Wasmund & Siegel 2008) the diversity seems to be lowest in the Bornholm and Gotland Basin due to unfavourable salinity conditions for both marine and limnetic species. Diatoms decreased along the west-east gradient towards lower salinities, whereas cryptophytes and dinophytes increased. Bloom forming cyanobacteria normally represent the main phytoplankton group during summer in the eastern and northern parts (Fig. 1.14). Especially the diazotrophic (N-fixing) potential harmful species, like *Nodularia spumigena* and *Aphanizomenon* spp. are adapted to the conditions in the Baltic Proper, but have rarely been observed in the Kattegat and the northern Gulf of Bothnia (Kahru et al. 1994; Wasmund 1997).

The horizontal distribution of chl-a concentration is similar to that of phytoplankton biomass and is determined by the main horizontal gradients in the Baltic Sea. The primary production (Table 1.6) is also changing along the estuarine gradients, but maximum is not always found in the periods of high nutrient concentrations, because of lower light penetration caused by suspended or dissolved colored substances in high productive regions. In addition the shorter vegetation periods (light



and temperature) lead to lower annual production in the northern parts of the Baltic Sea.

Table 1.6 *Phytoplankton primary production in the different sea areas (values from the 1990s). Data are compiled from various literatures by Wasmund & Siegel (2008).*

Baltic Sea region	Annual total primary production
Kattegat/Belt Sea/Arkona Sea	190 [g C m <sup>-2</sup> y <sup>-1</sup> ]
Bornholm Basin	193 [g C m <sup>-2</sup> y <sup>-1</sup> ]
East Gotland Basin	208 [g C m <sup>-2</sup> y <sup>-1</sup> ]
Bothnian Sea	48 [g C m <sup>-2</sup> y <sup>-1</sup> ]

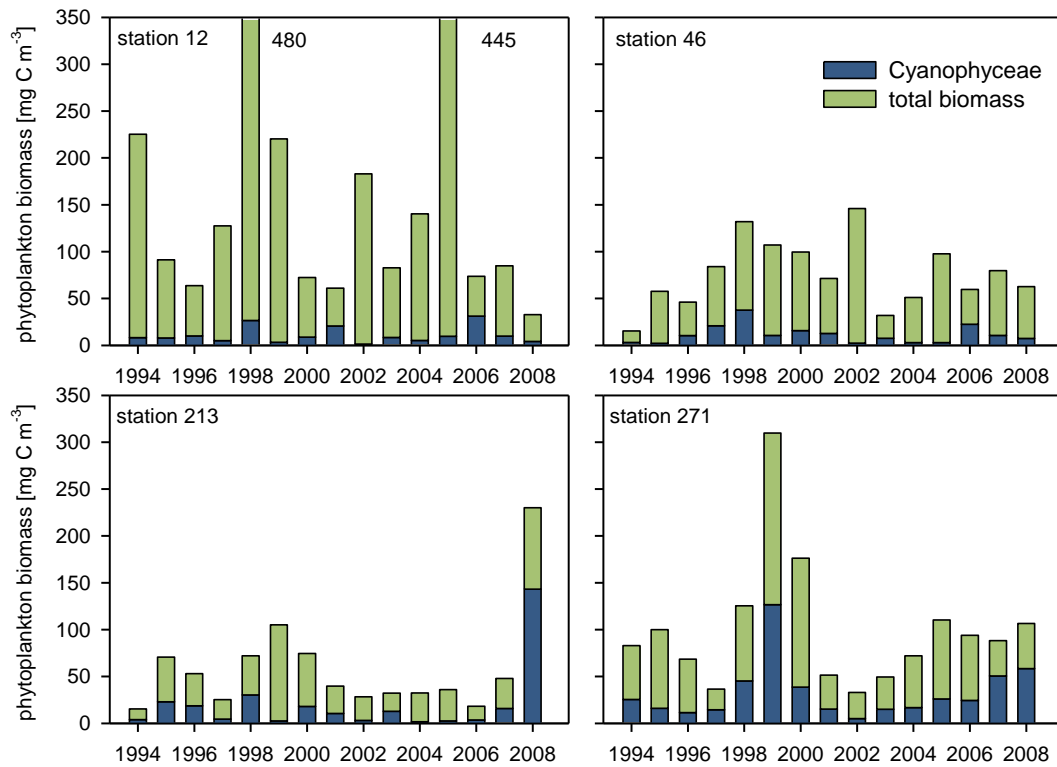


Fig. 1.14 *Proportion of Cyanophyceae on total biomass (integrated sample of 0-10 m depth) for summer long-term data in various Baltic Sea areas (see Fig. 5.1 for station positions). To assure comparable data, summer was defined as mean values for July and August in all investigated areas.*

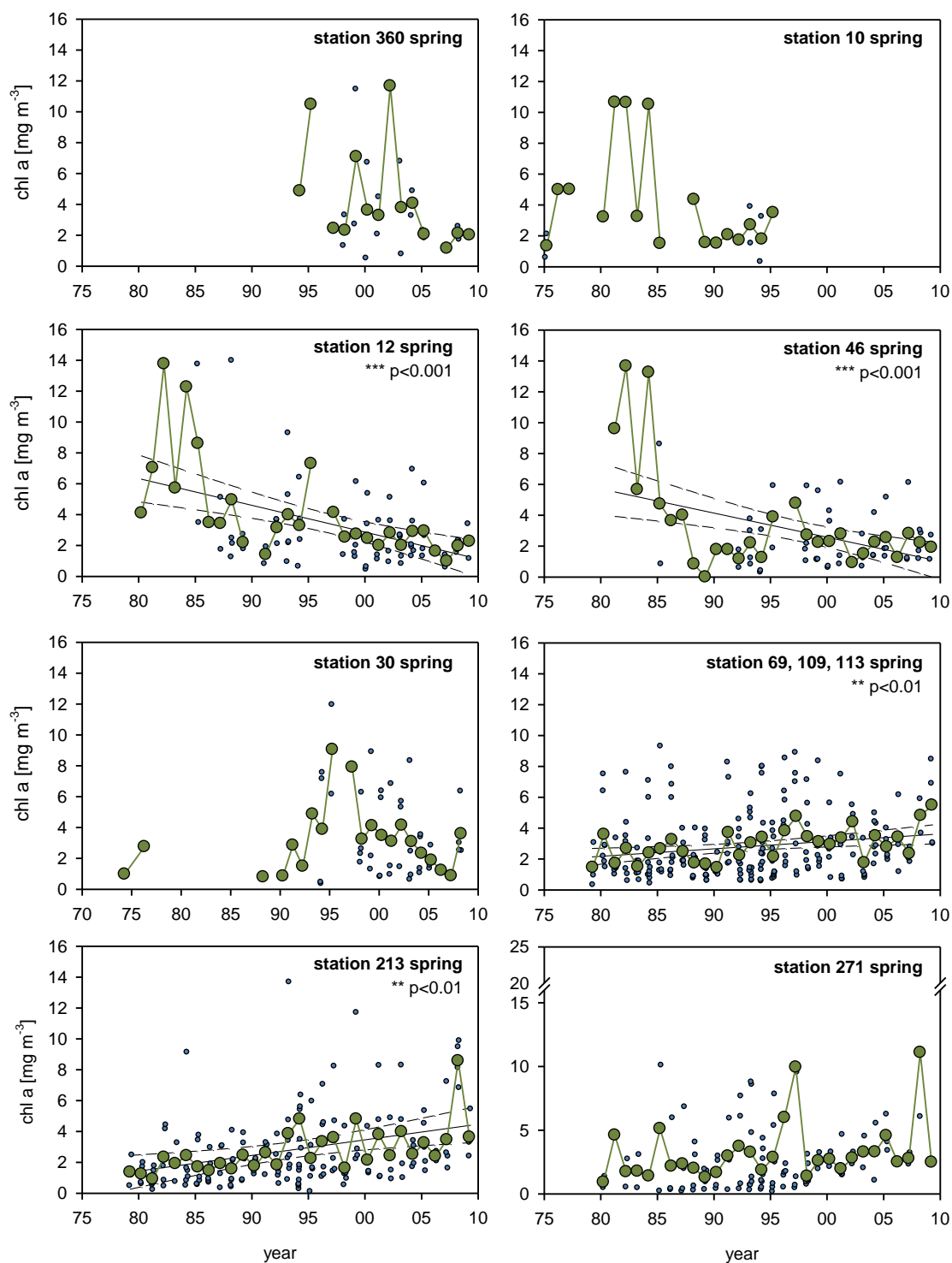


Fig. 1.15 Long-term investigation of chl-a concentration (mean of 0-10 m depth), both for seasonal means (green circles) and original data (blue circles) for the spring season. Updated data series of (Wasmund and Uhlig 2003) and (Wasmund et al. 2009). Lines represent linear regression and 95% confidence intervals for original data sets (blue). See Fig. 5.1 for position of stations.





### **1.3.2 Long-term trends in phytoplankton composition**

Changes in phytoplankton composition and biomass are indicators for changes in the marine environment. The anthropogenically induced eutrophication and changes in climate conditions may be considered as major forces for system alteration.

A significant reduction in diatoms in spring was observed for many areas in the northern Baltic Proper, Gotland Sea, Belt Sea and Kattegat. For the southern Baltic Sea this trend is not significant. A shift in spring from diatoms to dinoflagellates is proposed for the northern parts of the Baltic (HELCOM 1996). Upward trends for diatom autumn blooms were found in the western Gotland Sea, Belt Sea and Kattegat (Wasmund et al. 2007), whereas the autumn bloom has not changed in western parts of the Baltic Sea (Wasmund et al. 2007). In the Baltic Proper and the Belt Sea upward trends were found in all seasons for dinoflagellate (Dinophyceae) abundance, whereas downward trends were found in the Kattegat and Sound.

Cyanobacteria blooms have been reported from the open Baltic Sea already in the 19th century, but their intensity and frequency seem to increase (Finni et al. 2001). During the last decade intensive blooms have been detected by satellite imaging in 1999, 2003, 2005 and 2006. (Wasmund & Uhlig 2003) reported downwards trends in the Baltic Proper, with high biomasses in 1979–1981, 1985–1986, 1991–1993 and 1998. The decreasing trend is confirmed for the most Baltic Sea areas under consideration of more recent data by (Jaanus et al. 2007). Increasing trends are reported for the northern Baltic regions (Suikkanen et al. 2007).

### **1.3.3 Long-term trends in total phytoplankton biomass and primary production**

According to (Wasmund et al. 2007) in Kiel Bight the total phytoplankton biomass increased in the last century from approximately 55 mg C m<sup>-3</sup> up to 83-216 mg C m<sup>-3</sup> (2001-2003). (Rydberg et al. 2006) reported a doubling of primary production in the Western Baltic within the last 50 years. While significant downward trends in chl-a occurred for the Mecklenburg Bight (Wasmund & Siegel 2008), (Fig. 1.15) and Kattegat (HELCOM 2009a), a slight but significant increase of chl-a was observed for the Arkona Basin and the Bornholm Sea (Wasmund & Siegel 2008, Fig. 1.15). Increasing biomass and chl-a values in open waters of the Baltic Sea, were also reported from (Jaanus et al. 2007) and (HELCOM 2009). A minor downward trend could be found for the Baltic Proper from 1974 up to 2008 (Håkansson and Lindgren 2008).

## **1.4 Present pressures**

### **1.4.1 Major constructions**

The Baltic Sea is affected by a number of anthropogenic impacts like large offshore and onshore constructions, shipping, pollution and eutrophication. The bridges across the Danish Straits are all designed as zero solutions and are thus not supposed to affect the hydrography of the Baltic Sea directly. While it has been shown in the QuantAS study (HELCOM 2009d) that the effect on the hydrography and ecology of the Baltic Sea of offshore wind farms is negligible in shallow waters, the impact of future offshore windfarms that may comprise up to 1,000 turbines is yet unclear.

### **1.4.2 Ship traffic**

Ship traffic has two main effects on the Baltic Sea. On the one hand, high-speed ferries may affect nearby coasts due to the wakes they produce while sailing with full speed. Wave systems at such speeds may contain so-called solitonic waves that are very different from waves induced by conventional ships (Soomere 2006). Wake waves may reach heights around 1 m (Soomere and Rannat 2003). Studies by (Erm and Soomere 2004, 2006) in Tallinn Bay have also shown local resuspen-

sion of light sediments in the wakes of fast ferries sailing in water depths that range from about 2 m to 15 m.

The other effect is the general increase of shipping at conventional speeds. A risk occurs in certain areas like the Great Belt or in the Gulf of Finland where traffic of oil tankers is ever more increasing (cf. Fig. 1.16). Collisions or grounding of oil tankers pose a threat of severe oil spills that will affect the Baltic Sea ecosystem for decades due to the slow exchange of water masses in the Baltic.

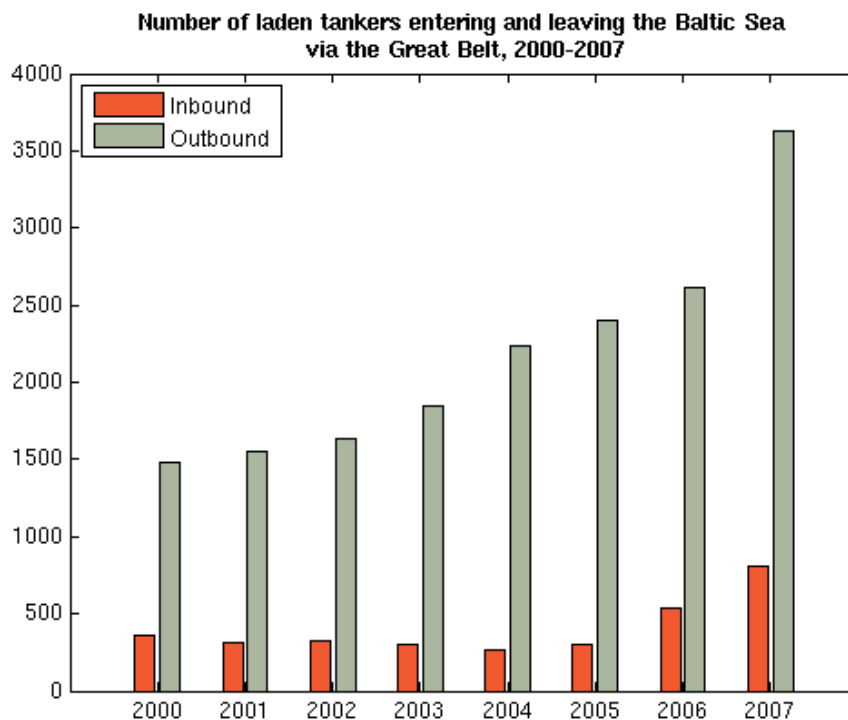


Fig. 1.16 Number of laden tankers entering and leaving the Baltic Sea via the Great Belt. Figure redrawn with data from (HELCOM 2009e).

### 1.4.3 Eutrophication and hazardous substances

In 2009, the Helsinki Commission published for the first time a consistent classification of eutrophication. All in all 189 sea areas were classified, among them 172 coastal areas and 17 open sea areas (Fig. 1.17). Only the open waters of the Bothnian Bay and the Swedish parts of the northeastern Kattegat are classified as "areas not affected by eutrophication". It is commonly accepted that the open parts of the Bothnian Bay are close to pristine and that the northeastern Kattegat is influenced by Atlantic waters. In the coastal zone, 161 areas show signs of eutrophication, only 11 have a good ecological status. Consequently, HELCOM comes to the conclusion that eutrophication is still a major concern despite measure undertaken so far. There the so-called "Baltic Sea Action Plan" which was adopted 2007 by all Contracting Parties of the Helsinki Commission, is aimed to reduce nutrient input further.

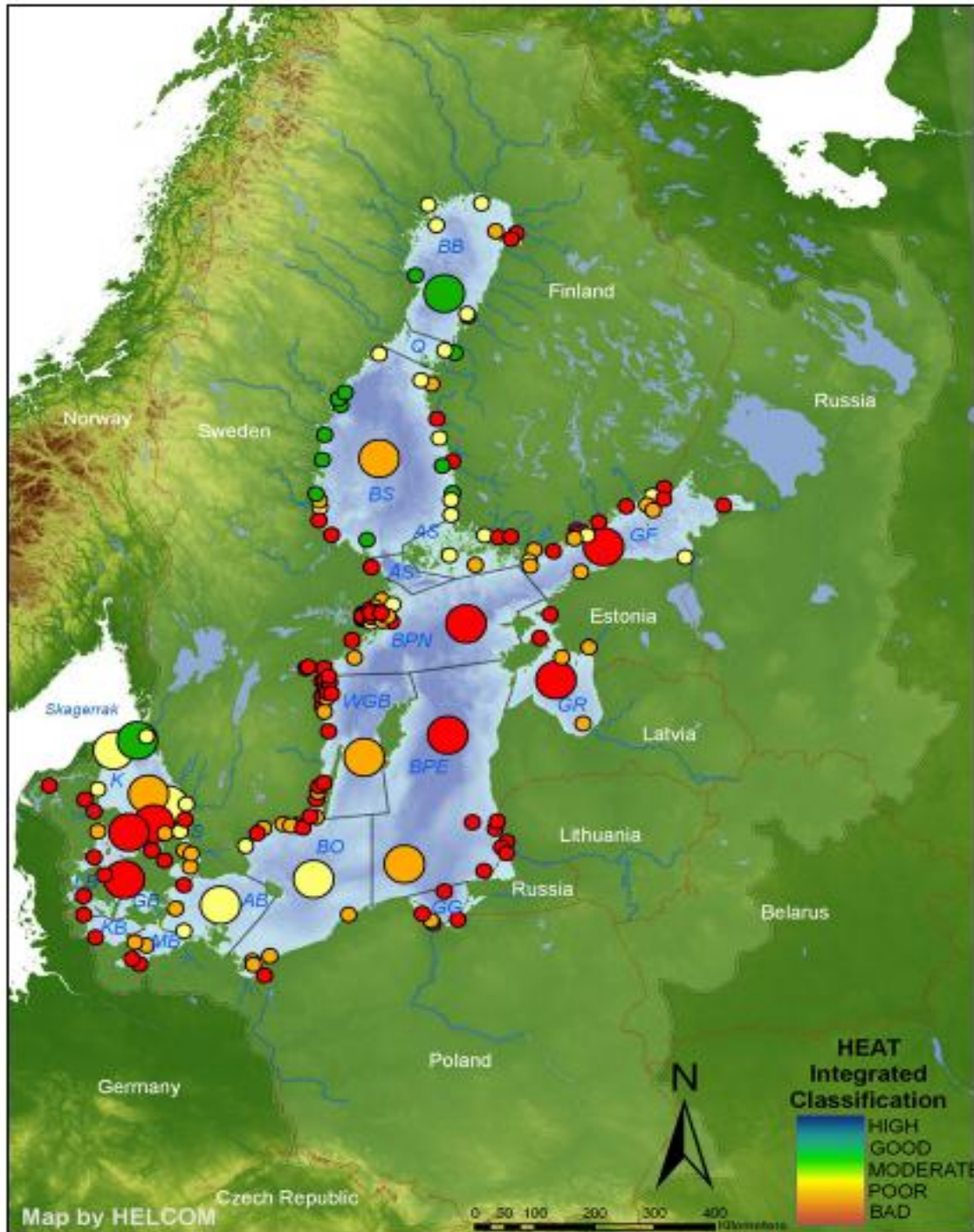


Fig. 1.17 Integrated classification of the eutrophication status of the Baltic Sea. Large circles represent open sea areas, small circles show coastal areas. Very good status (blue, not existent, good status (green) describes "areas not affected by eutrophication" while moderate (yellow), poor (orange) and bad (red) are equivalents to "areas affected by eutrophication" (HELCOM 2009a)

The Baltic Sea has been exposed to an extensive use of chemicals since the beginning of industrialization in the area and its marine environment has a long history of contamination; therefore the Baltic Sea has often been referred to as the most polluted sea in the world (HELCOM 2010c). Hazardous substances, also known as pollutants, can accumulate in the marine food web up to levels which are toxic to



marine organisms, particularly predators. They may also represent a health risk for people, e.g. by consumption of contaminated sea food. Once they are released into the Baltic Sea, hazardous substances can remain in the water for very long periods. (HELCOM 2010c) defines substances as hazardous if they are toxic, persistent and bioaccumulative, or very persistent and very bioaccumulating. Substances that affect hormone and immune systems are also considered hazardous.

According to (HELCOM 2010c), the assessment of hazardous substances in the Baltic Sea using data from 1999–2007 on concentrations of hazardous substances in biota, sediments or seawater shows that the goal of the Baltic Sea Action Plan to attain a “Baltic Sea with life undisturbed by hazardous substances” has not been reached. 137 out of 144 areas assessed were classified as “moderate”, “poor” or “bad” and were therefore classified as being “disturbed by hazardous substances”. This indicates that the entire Baltic Sea was an area with a high contamination level from 1999–2007. With the exception of the northwestern Kattegat, all open-sea areas of the Baltic Sea were classified as being “disturbed by hazardous substances” (HELCOM 2010c). 98 of the 104 coastal assessment units were classified as being “disturbed by hazardous substances”. So, for the entire Baltic Sea, only seven units were assessed as “undisturbed by hazardous substances”. There are however encouraging signs of decreasing trends of certain substances and an improvement in the health status of some top predators.

## **1.5 Consequences of climate change**

The Baltic Sea climate is embedded in the general atmospheric circulation system of the Northern hemisphere with mean westerly air flow of annually varying intensity. The strong westerly air flow provides maritime, humid air transport into the southwestern and southern parts of the Baltic Sea basin, while in the eastern and northern parts the maritime westerly air flow is weakened, providing continental climate conditions. There is a permanent exchange of air masses of different features resulting in a great variability of weather. The air pressure system formed by low pressure near Iceland and high pressure around the Azores Islands is known to affect the weather and circulation in the Baltic Sea basin. Furthermore, high/low pressure systems over Russia may influence the climate and circulation in the Baltic Sea basin, in particular in the north-eastern parts. These systems show a distinct annual cycle. In the autumn and winter season southwesterly air flow intensifies due to the amplifying Icelandic low pressure. During spring and summer Azores High extends into mid-Europe and the southwesterly air flow weakens.

The warming trend for the Baltic Sea basin in the last century is in the order of 0.08°C/decade and therefore larger than the global trend of 0.05°C/decade. A pronounced warming started around 1990 which is related to the accelerating global warming trend.

Climate change in the Baltic Sea basin is related to global climate change. Possible future development, climate projections, in the Baltic Sea basin are based on global models, scenarios, and data. Changes in the global climate can be driven by natural variability and as a response to anthropogenic forcing. Natural variability is due to solar variability, volcano eruptions, and associated with internal dynamics of the earth’s system. The most important anthropogenic force is the emission of greenhouse gases, and hence an increasing concentration of greenhouse gases in the atmosphere. Relevant anthropogenic greenhouse gases are carbon dioxide, methane, and nitrous oxide. Greenhouse gases reduce the transparency of the atmosphere for infrared (thermal) radiation, and as a result the heat budget of the earth’s system changes with increasing temperature of the lower atmosphere. Estimates of different factors influencing the global climate suggest that the largest contribution



to the observed warming in the last century is attributed to an increase in greenhouse gas concentration.

For the assessment of a future climate development global climate models together with emission scenarios are used. Different emission scenarios (SRES: IPCC special report on emission scenarios) have been developed by the IPCC (Intergovernmental Panel on Climate Change). The SRES scenarios follow four storylines, each based on different assumptions concerning the factors that might drive the development of human society during the next 100 years. Multi-model simulations of different SRES scenarios show an expected global warming of 2-4°C at the end of the century. Scenarios of A1 and A2 storylines show a stronger warming than scenarios of B1 and B2 storylines. However, a changing climate will be felt at a regional scale and strategies for adaption and protection have to be based on regional climate.

For the Baltic Sea basin RCM simulations show a positive temperature trend. In winter and spring the temperature increase is stronger compared to summertime in the northeastern part of the Baltic Sea basin and in the southwestern part the increase is stronger in summer. Furthermore, daily maximum temperature in summer will increase from 3°C up to 10°C. For precipitation the simulations show an increase in winter, while in summer projections show an increase in the northern part and a decrease in the southern part. Extreme precipitation events generally show an increase in winter. The sea ice season will decrease by 1-2 months in the northern part and 2-3 months in the central part of the Baltic Sea. The sea surface temperature will increase by 2-4°C and would be strongest in May and June and in the southern and central basins.

Global sea level rise will propagate into the Baltic Sea as well. The most recent projections are up to +1 m at the end of the 21<sup>st</sup> century according to a dedicated Fehmarnbelt climate change effect workshop (FEHY 2009).

The combined effect of the increased precipitation, increased evaporation due to temperature increase and a sea level rise of up to 1 m on the salinity of the Baltic Sea are not yet known.





## **2 THE AREA – NATURAL CONDITIONS AND EXTERNAL FORCING**

### **2.1 Geographical setting**

The Baltic Sea is a marginal basin of the world ocean located in the northern temperate climate zone of Europe. According to the Helsinki Commission, it is one of the world's largest bodies of brackish water (HELCOM 2010d) that comprises the waters bordered by the Swedish, Finnish, Estonian, Latvian, Lithuanian, Russian, Polish, German and Danish coasts to the lines Falsterbo-Stevns Klint and Gedser-Darsser Ort (HELCOM 2006). This definition of the Baltic Sea excludes the transition area of Belt Sea, Sound and Kattegat. In general though "Baltic Sea" comprises also the whole sea area south off the tip of the Jutland peninsula at 57°45' northern latitude, i. e. the Kattegat is included. To the north the Skagerrak follows, which is considered as the transition into the North Sea. Because of the Norwegian trench, the Skagerrak is a wide and deep channel with maximum water depth below 700 m. Including the transition area, the Baltic Sea extends from 9°30' to 30° of eastern longitude, and 54° to 66° of northern latitude, see Fig. 2.1. The Baltic is a semi-enclosed, intra-continental sea which is nearly completely surrounded by land masses. The only connection to the North Sea is the narrow and shallow Danish Straits which restrict the water exchange with the ocean. The inner Baltic Sea is a series of sub-basins which are divided by sills, shoals and islands. The sub-basins are connected by rather narrow channels which limits the exchange and renewal of particularly the bottom water masses.

Geological surveys have shown that the Baltic Sea did not exist before the Pleistocene. Instead there was a wide plane around a big river system emptying into the southern North-Sea that was called the Eridanos by (Overeem et al. 2002) while it was previously known as the Baltic River System (Gibbard 1988; Bijlsma 1981). This fluvio-deltaic system, that drained most of north-western Europe, developed during the Late Cenozoic as a result of simultaneous uplift of the Fennoscandian shield and accelerated subsidence in the North Sea Basin. Several glaciation episodes during the Pleistocene scooped out the river bed into the current sea basin with a distinctive structure of sub-basins. By the time of the last, or Eemian Stage, the so-called Eemian Sea was in place. From that time the area underwent a number of geologic transformations determined by submergence or emergence of the region due to the weight of ice shields and subsequent isostatic readjustment, and by the connecting channels it found to the North Sea/Atlantic system: either through the Danish Straits or at what are now the large lakes of Sweden. Many of these periods clearly reflect a complex changing of water temperatures and salinity which in turn lead to faunal changes (Björck 1995).

The current geographical sub-division of the Baltic Sea is discussed in Chapter 2.1.2 on the basis of a gridded bathymetry.

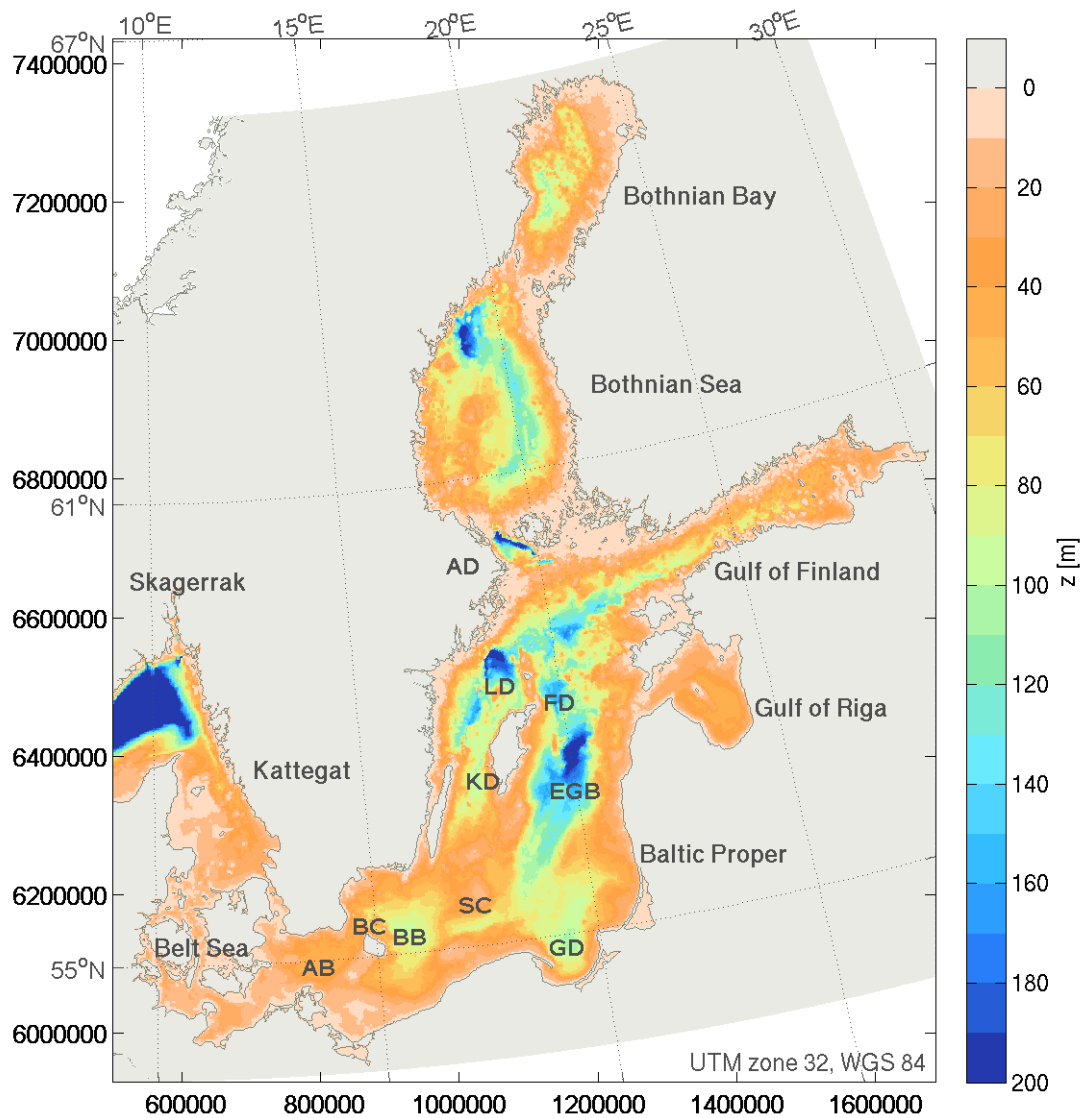
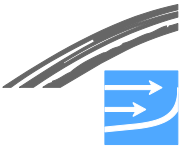
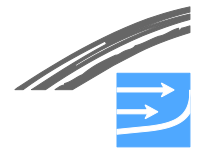


Fig. 2.1 Bathymetry and geographical structures of the Baltic Sea. Water depths refer to Seifert et al. (2001). Water depth is cut off at 200 m. Acronyms indicate some basins and connecting channels: Arkona Basin (AB), Bornholm Channel (BC), Bornholm Basin (BB), Stolpe Channel (SC, also called Slupsk Furrow), Gdansk Depression (GD), Eastern Gotland Basin (EGB), Landsort Deep (LD), Fårö Deep (FD), Karlsö Deep (KD) and Aland Deep (AD).

### 2.1.1 Bathymetric data and hypsography

The main dimensional characteristics of the Baltic Sea and its sub-basins, like surface area, volume, maximum and mean water depth, are described in summarizing reports as (Fonselius 1995), (HELCOM 2002), and in textbooks as (Läpperanta, Myrberg (2009). However, for detailed studies, local budgets, and the set-up and evaluation of numerical models, an accessible bathymetric data set is necessary. The global data sets provided by GEBCO and Smith and Sandwell (1997) show rather strong deviations for the Baltic Sea. Hence, the digitized data set of the bathymetry of the Baltic Sea, compiled by Seifert et al. (2001), has become a commonly used basis for Baltic Sea applications. The latest version of the data is provided via the web site [www.io-warnemuende.de/iowtopo](http://www.io-warnemuende.de/iowtopo) of the Institut für Ostseeforschung Warnemünde (IOW). The data are also available as digital supplement in (Feistel et al. 2008).





The IOW bathymetry comprises the area 9°-31°E and 53°30'-66°N, i. e. the whole Baltic Sea including Kattegat and partly Skagerrak, see Fig. 2.1. The grid spacing is regular with respect to geographical coordinates with a resolution of 2' in longitude and 1' in latitude, which corresponds to approximately 2 km. Eq. (2.1) specifies the location of the midpoints of the grid cells

$$\begin{aligned}x(i) &= 9^\circ\text{E} + (i - 1/2)\Delta x & \Delta x &= 2' & i &= 1 \dots 660 \\y(j) &= 53^\circ 30'\text{N} + (j - 1/2)\Delta y & \Delta y &= 1' & j &= 1 \dots 750\end{aligned}\quad (2.1)$$

The resulting mean water depth is shown in Fig. 2.1 in UTM32 projection, but the Baltic bathymetry data set refers to a regular grid in geographical longitude and latitude as specified by Eq. (2.1). The color bar is confined to 300 m in order to emphasize the depth structure of the Baltic Sea. For later reference main substructures of the Baltic Sea are indicated in Fig. 2.1.

The different regional data density is illustrated in Fig. 2.2 showing the occupation number  $n_{wet}$  of depth samples allocated to each grid cell. Negative occupation numbers, which occur along the coasts, indicate where lacking data have been replaced by spatial interpolation of neighboring cells. Skagerrak, Kattegat, and the northern Baltic Sea including the Gulf of Finland are only covered by the IOW1995 and the related DK0 data sets (see Seifert et al. 2001) yielding 4-6 samples. The 5 m isobath of the GEOBALT sea chart provide a better coverage for parts of the Baltic Proper, especially in regions with steep bottom gradients, whereas plane areas are also occupied by only 4-6 data samples. A high data density was available for the Belt Sea which is not in the scope of this report.

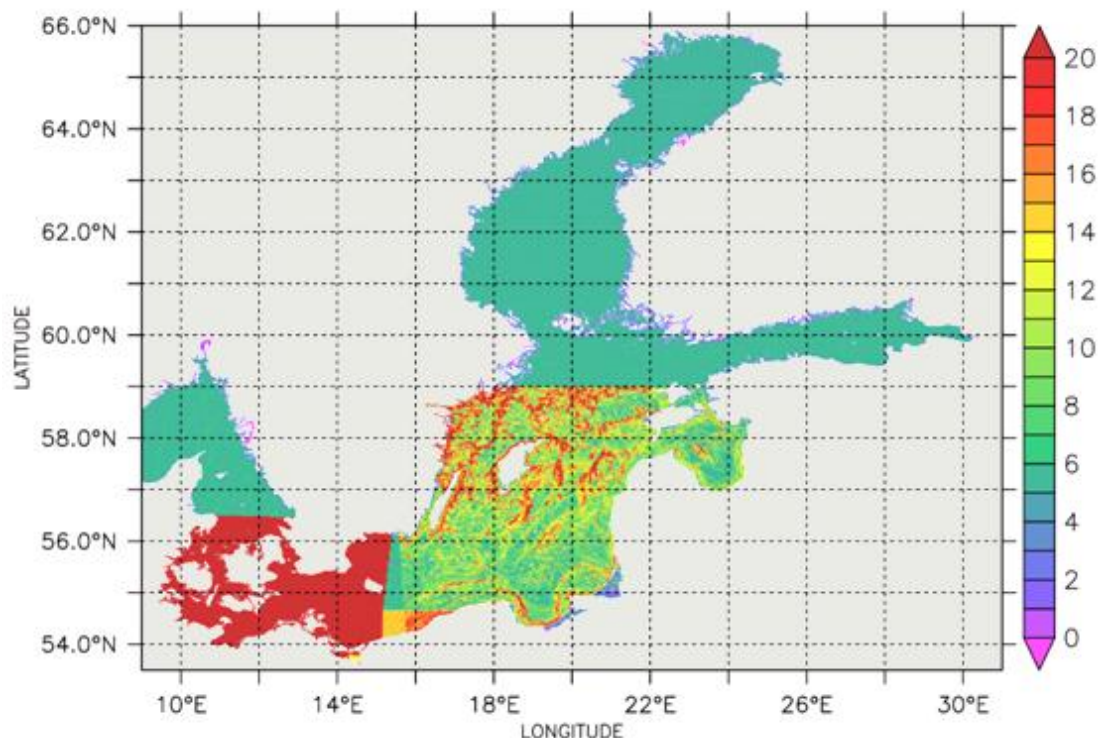


Fig. 2.2 Number of water depth samples per grid cell (see Eq. 2.1) used for IOW Baltic Sea bathymetry.

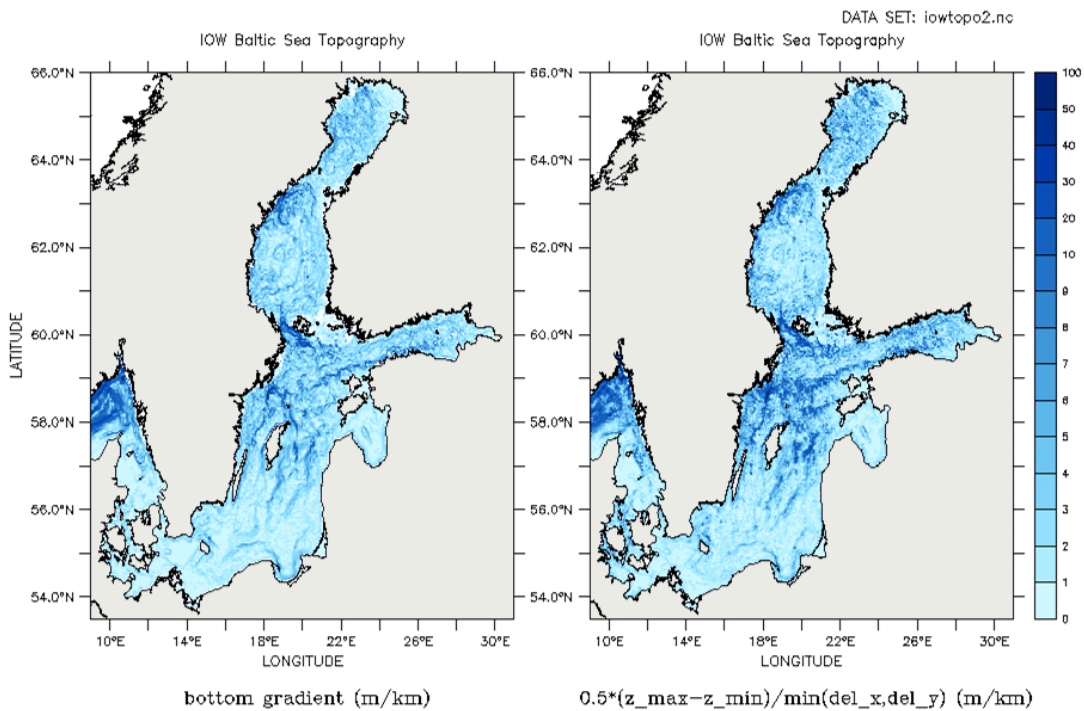
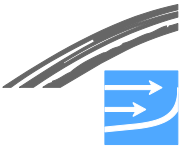


Fig. 2.3 Relation between the gradient of the sea bottom and the range of variation of water depth samples.

The range of variation provides information about the local minimum and maximum water depth as far as these are right met by the available samples. Moreover,  $(z_{\max}-z_{\min})$  divided by the grid spacing ( $\Delta_{lon}, \Delta_{lat} \approx 2$  km) yields an estimate for the local bottom gradient. Fig. 2.3 demonstrates that this relation holds for the Baltic bathymetry. The bottom gradient in the left panel was calculated from the mean water depth by central differences. Note that this estimate is derived on grid scale, whereas the actual depth variation might be larger on smaller length scales. The factor of 0.5 applied for the range of variation in the right panel is an average value chosen to fit to the same scale. Both pictures clearly show the steep slope of the Norwegian trench in Skagerrak, the Ronne Bank southwest of island Bornholm, the Stolpe Channel, the rims of Gdansk Deep and Eastern Gotland Basin, and the high variability of the sea bottom in the northern Baltic Proper. Despite the rather coarse sampling even the Aland trench and the main slopes of the Gulf of Finland and the Bothnian Sea are resolved.

The frequency of occurrence plot in Fig. 2.4 shows that only 24% of the sea bottom is flat with gradients below 1 m/km corresponding to depth variations of at least  $\pm 1$  m within a grid cell. Since a similar close correspondence, as shown in Fig. 2.3, exists between the bottom gradient and the standard deviation of the depth samples,  $z_{stdv}$  is overestimated within 76% of the Baltic Sea area. Flat areas are mainly located in the southern Baltic Sea, but even in Belt Sea around 30% of the area exhibit bottom gradients above 2 m/km (not shown here). The maximum bottom gradient of 82 m/km corresponds to differences of about  $\pm 100$  m found for corresponding grid cells in data set comparisons.

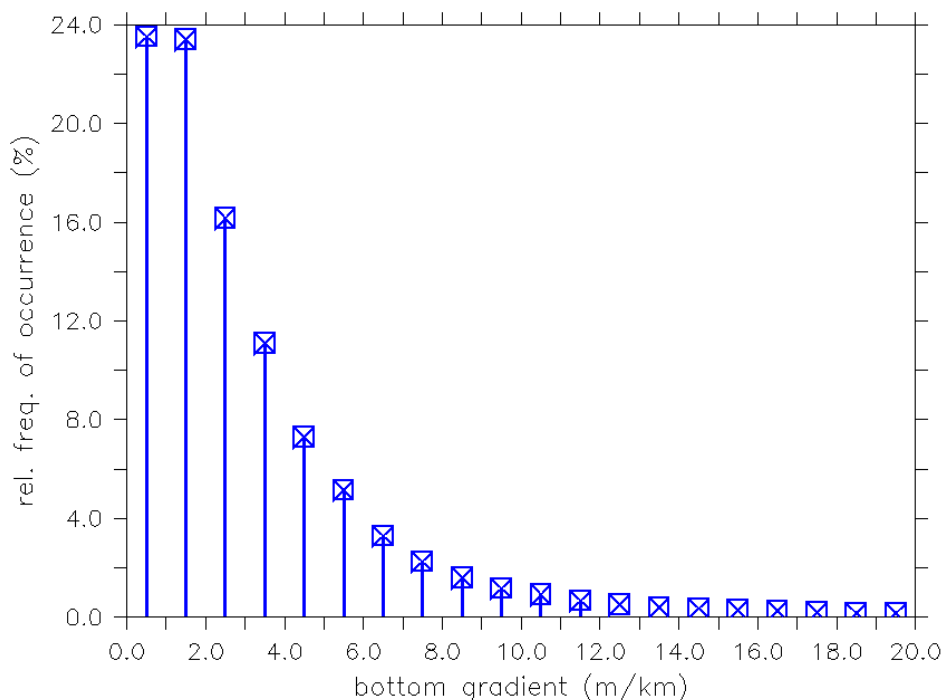
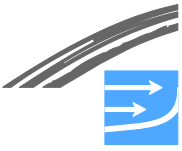


Fig. 2.4 Relative frequency of occurrence of sea bottom gradients in bins of 1m/km derived from the 2 km Baltic Sea grid Eq. (2.1).

The gridded bathymetry allows to evaluate the open sea surface and the enclosed volume of water for any sub-basin of the Baltic Sea and for any reference water depths. This leads to the hypsographic curves, shown in the left panel of Fig. 2.5. In order to cover several orders of magnitude the abscissa is on logarithmic scale. The hypsography demonstrates that area and volume of the Baltic Sea decay exponentially with water depth from roughly 411,700 km<sup>2</sup> and 21,100 km<sup>3</sup> at the surface to 51,000 km<sup>2</sup> and 1,700 km<sup>3</sup> in 100 m depth, and only 2,300 km<sup>2</sup> and 70 km<sup>3</sup> in 200 m depth. Between 220 and 240 m the decrease is weaker indicated by a reduced slope of the hypsographic curves. Below 250 m the remaining volume of 14 km<sup>3</sup>, which is mainly enclosed in Landsort Deep, quickly converges to zero. More details are discussed in the following subsection.

The right panel of Fig. 2.5 indicates the relative errors of surface area and volume which were derived from the standard deviation of the depth samples.

The blue curve in right panel of Fig. 2.5 shows that the relative uncertainty of the volume of the Baltic Sea is below ±5% down to 10 grid cells comprising only 1 km<sup>3</sup> of water, whereas the 95% confidence range grows up to ±25% below 250 m depth. The range of variation of the surface area is indicated by green symbols, because this quantity shows some scatter, especially around 240 m where the number of open grid cells decreases rapidly.



Hypsography of Baltic Sea (iowtopo2)

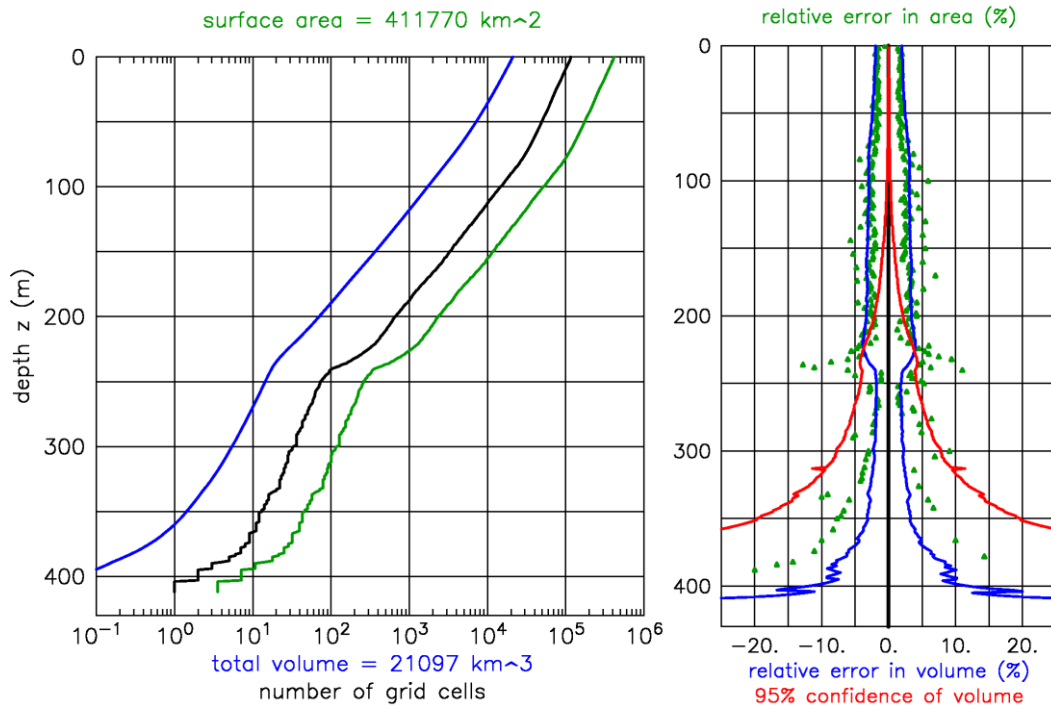


Fig. 2.5 Open sea surface ( $\text{km}^2$ , green curves) and enclosed water volume ( $\text{km}^3$ , blue curves) in dependence on water depth (left panel) and relative errors (right panel) for an assumed variation of sea level of  $\pm 1 \text{ m}$ . The black curve corresponds to number of open grid cells and the red curve shows the 95% confidence range of volume. Note that Baltic Sea includes Belt Sea and Kattegat.

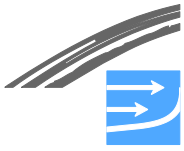
Finally, the surface area and the volume of the main Baltic sub-regions derived from the gridded IOW Baltic Sea bathymetry are provided in Table 2.1 and compared to the data of (HELCOM 2002). According to the HELCOM division maps, provided in the digital supplement of (Feistel et al. 2008), the reference area "Gulf of Bothnia" corresponds to Bothnian Bay, Bothnian Sea, and Åland Sea, the Baltic Proper is sub-divided into a northern, western, eastern and southern part, and comprises also the Bornholm Basin as well as the Arkona Basin, whereas Belt Sea-Kattegat summarizes the westernmost 7 region masks indicated by colors in Fig. 2.6.



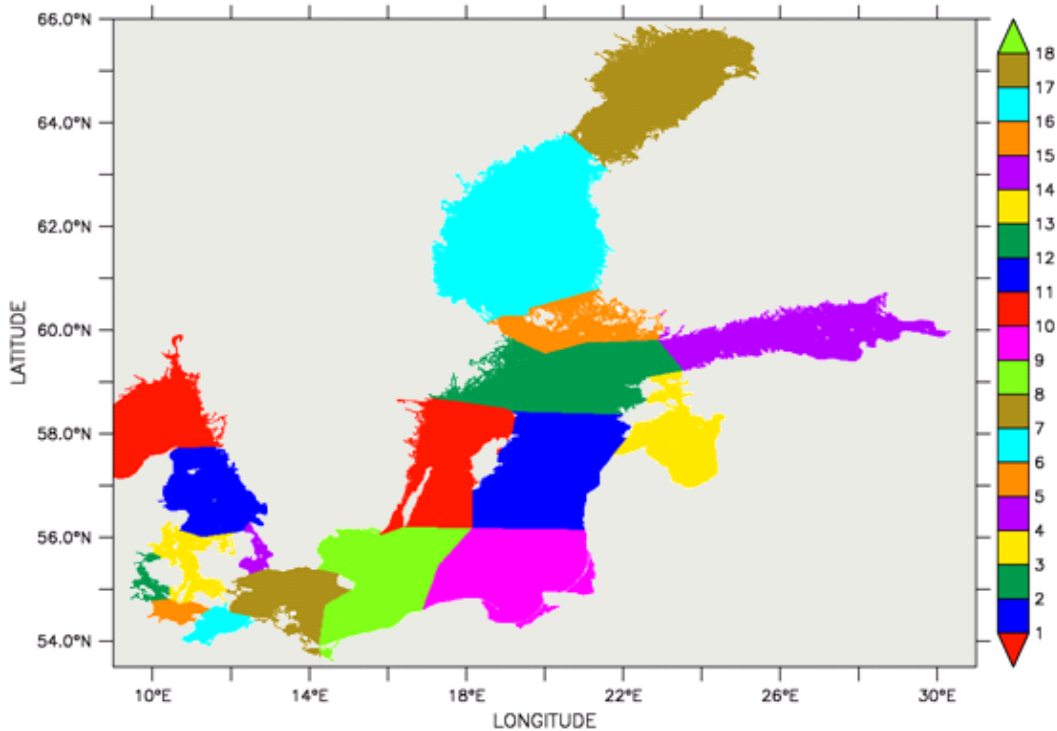
Table 2.1 Area, volume, and mean water depth derived from IOW gridded bathymetry compared to (HELCOM 2002). The sub-division of the Gulf of Bothnia refers to (Leppäranta & Myrberg 2009), statistics for sub-divisions of the Baltic Proper are not specified in (HELCOM 2002). Sub-basin figures in italics.

Region	Area (km <sup>2</sup> )		Volume (km <sup>3</sup> )		Mean depth (m)	
	IOW	HELCOM	IOW	HELCOM	IOW	HELCOM
Gulf of Bothnia	115,280	115,516	5,892	6,389	51.1	55.3
<i>Bothnian Bay</i>	<i>35,640</i>	<i>36,260</i>	<i>1,317</i>	<i>1,481</i>	<i>37.0</i>	<i>40.8</i>
<i>Bothnian Sea</i>	<i>64,560</i>	<i>64,886</i>	<i>4,118</i>	<i>4,308</i>	<i>63.8</i>	<i>66.4</i>
<i>Åland Sea</i>	<i>15,080</i>	<i>14,370</i>	<i>457</i>	<i>580</i>	<i>30.3</i>	<i>40.4</i>
Gulf of Finland	29,750	29,600	1,040	1,100	35.0	37.2
Gulf of Riga	18,580	16,330	420	424	22.6	26.0
Baltic Proper	206,050	211,069	12,972	13,045	63.0	61.8
<i>Northern Baltic Proper</i>	<i>37,450</i>	-	<i>2,706</i>	-	<i>72.3</i>	-
<i>Eastern Gotland Basin</i>	<i>42,630</i>	-	<i>3,699</i>	-	<i>86.8</i>	-
<i>Western Gotland Basin</i>	<i>30,090</i>	-	<i>2,005</i>	-	<i>66.6</i>	-
<i>Southern Gotland Basin</i>	<i>39,330</i>	-	<i>2,380</i>	-	<i>60.5</i>	-
<i>Bornholm Basin</i>	<i>38,000</i>	-	<i>1,734</i>	-	<i>45.6</i>	-
<i>Arkona Basin</i>	<i>18,550</i>	-	<i>448</i>	-	<i>24.2</i>	-
Belt Sea – Sound - Kattegat	42,110	42,408	773	802	18.4	18.9
<b>Baltic Marine Area</b>	<b>411,770</b>	<b>415,266</b>	<b>21,097</b>	<b>21,721</b>	<b>51.2</b>	<b>52.3</b>

It should be noted that the "Baltic Marine Area" defined by HELCOM as shown in Table 2.1 has a slightly larger area and volume than the explicitly stated sub-basins. Also there is a difference of 20 km<sup>3</sup> in the partial volumes of the Gulf of Bothnia between (HELCOM 2009a) and (Läpperanta and Myrberg 2009). Taking into account that the reference areas used in HELCOM 2002) are not completely identical with the HELCOM division maps, the agreement between IOW and HELCOM data is rather good. However, the IOW estimates, except the area of the Gulf of Riga, tend to give lower values than HELCOM. The regional sea surfaces agree well within ±1%, corresponding to a difference of -3496 km<sup>2</sup> for the entire Baltic Sea. The larger deviations for Gulf of Riga and Baltic Proper yield -1.2% if both areas are taken together. The reason for this negative bias is differences in the landmask. Of course the choice of the landmask is somewhat arbitrary and dependent on grid resolution, but it is based on the detailed high resolution coastal shore lines of (Wessel and Smith 1996). An underestimation of fjords, river inlets and coastal bays by the chosen landmask should be compensated by neglecting most of the small islands of the Swedish-Finnish archipelago since each grid cell corresponds to 3 - 4 km<sup>2</sup>. Differences introduced by evaluating cell areas on a spherical earth of 6370.5 km radius instead of the WGS84 ellipsoid, see (Feistel et al. 2008) are +0.1%, i. e. negligible. Hence, some 1000 land grid cells remain questionable along the coasts.



DATA SET: masks\_helcom\_regions\_17.lst



HELCOM Baltic Sea regional basins

Fig. 2.6 Regional masks of main sub-basins of the Baltic Sea. Colors and numbers indicate the regional masks. 1: Skagerrak (not part of Baltic Sea), 2: Kattegat, 3: Little Belt, 4: Great Belt, 5: Sound, 6: Kiel Bight, 7: Mecklenburg Bight, 8: Arkona Basin, 9: Bornholm Basin, 10: Southern Gotland Basin, 11: Western Gotland Basin, 12: Eastern Gotland Basin, 13: Northern Baltic Proper, 14: Gulf of Riga, 15: Gulf of Finland, 16: Åland Sea, 17: Bothnian Sea, 18: Bothnian Bay.

The volumes predicted by the IOW data set show a stronger negative bias. The water masses enclosed in the Kattegat-Belt Sea region and in the entire Baltic Sea deviate by -3 to -4%. This is comparable with the variation derived above for the IOW data if the water level is shifted by a constant offset of  $\pm 1$  m, see Fig. 2.5. However, since deviations in volume  $V$  and sea surface area  $A$  partly compensate by division, the mean depth  $H=V/A$  are shifted only by -2 to -3% (-0.6 to -1.1 m). But the differences in mean water depth of -2.2 m to -4.2 m in the Gulf of Finland, in the Gulf of Riga, and in the Gulf of Bothnia indicate a distinct offset of the IOW data within these regions. The neglect of the enhanced sea level in the northern Baltic because of the diminishing salinity might only explain an offset below 0.5 m in mean water depth. This implies the suggestion that a systematic offset was introduced into the IOW bathymetry by sampling these regions only from rather large scale sea charts which tend to under-estimate water depth, especially in regions with archipelagos and shoals like the Åland Sea, which is off by -21% of volume.

In contrast to that the good agreement found for the Baltic Proper, -2.4% less sea surface with a lack of -0.6% of water volume, leading to a 1.2 m deeper mean water depth, seems to indicate the state-of-the-art limit of uncertainty. Note that the detailed GEOBALT sea chart, providing isobaths in steps of 5 m, and the MESODYN data were available for this region. The sub-division of the Baltic Proper in Table 2.1





according to the HELCOM masks in Fig. 2.6 clearly shows that the Eastern Gotland Basin is the largest and deepest basin within the Baltic Sea.

In respect of an uncertainty around  $\pm 1\%$  the data for sea surface and water volume may be rounded to 3 significant digits.

### **2.1.2 Geographical structure of the Baltic Sea**

#### **Regional scale structure**

The area from Kattegat to the Drogden Sill in Sound and the Darss Sill is the Baltic transition zone which plays the key role for the water exchange, because its main hydrographical function is the limitation of the inflowing and outflowing water masses and the transformation of the saline signature, see Chapters 3.3 and 3.4. On regional scale the Baltic Sea is divided into Bothnian Bay, Bothnian Sea, Åland archipelago, Gulf of Finland, Gulf of Riga, Baltic Proper, Belt Sea, and Kattegat as indicated in Fig. 2.1 and Fig. 2.6. For the following short description we provide the frequency distribution of water depth in Fig. 2.7 and the depth and enclosed volume of bottom water in Table 2.2 for the main basins and connecting channels. The closing depth describes the depth below which there is no exit to and from a basin. The frequency distribution shows the partial area of sea bottom within a range of water depth. Thus areas shallower than 20 m cover around 15-20% in Baltic Proper, Bornholm Basin, and Bothnian Sea, whereas more than 40% are shallow in the Bothnian Bay and about 75% in the Åland Sea. This supports the suggestion that the shallow bias of sea charts plays a role for the reliability of the IOW bathymetry in these regions. The following description is focused on the propagation of saline inflow across the sill depth between basins and the enclosed pool of bottom water, because the salinity, temperature and the content of dissolved oxygen in the deep basins are key indicators for the long-term development of the Baltic Sea and its ecosystem.



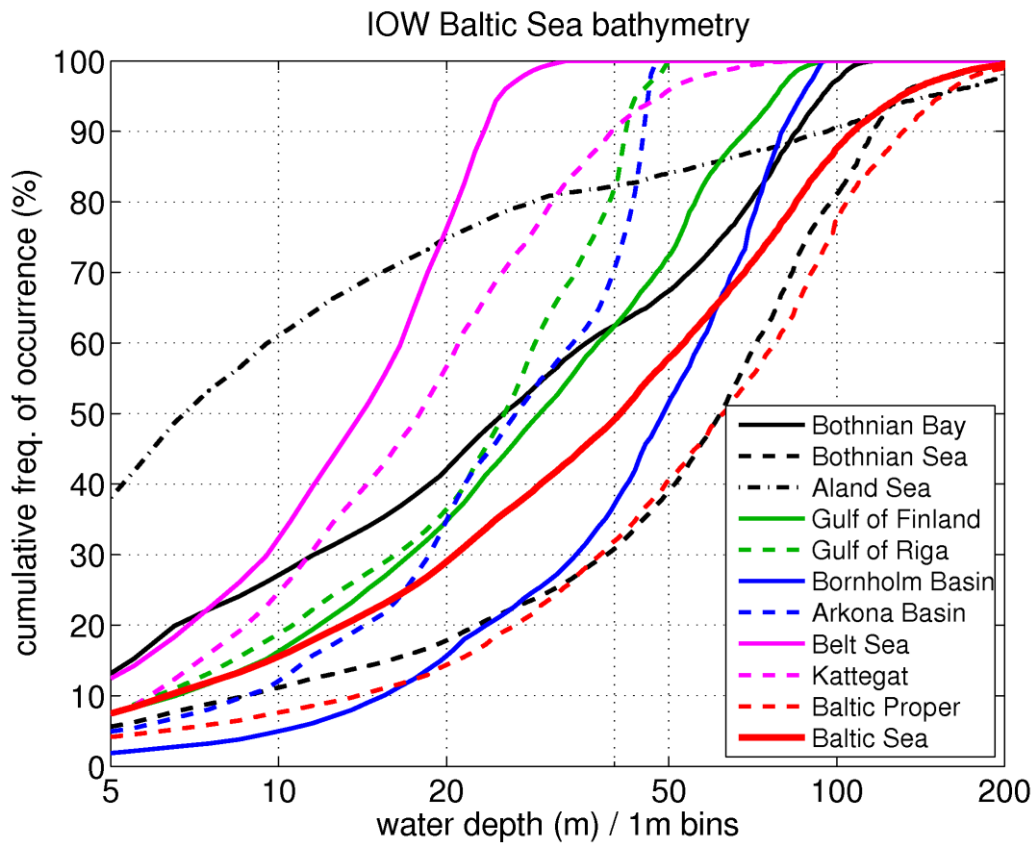


Fig. 2.7 Cumulative frequency of occurrence of water depth derived from the IOW Baltic Sea bathymetry providing partial areas within depth intervals, see Fig. 2.6 for regional subdivisions.

Table 2.2 Closing depth and enclosed volume of bottom water in main basins and connecting channels of the Baltic Sea (excluding transition area) derived from the IOW bathymetric data set.

<b>Basin/channel</b>	<b>Closing depth (m)</b>	<b>Maximum depth (m)</b>	<b>Enclosed area (km<sup>2</sup>)</b>	<b>Enclosed volume (km<sup>3</sup>)</b>
Arkona Basin	47	55	390 ± 390	0.3 ± 0.3
Bornholm Sea	66	101	8010 ± 240	100 ± 10
Stolpe Channel	76	94	730 ± 100	4 ± 1
Gdansk Deep	90	115	3630 ± 190	31 ± 4
Eastern Gotland Sea	140	249	6530 ± 135	207 ± 7
Central Gotland Basin	168	249	2460 ± 60	80 ± 2
Norrkoping Deep	140	203	805 ± 30	13 ± 1
Landsort Deep	160	463	1450 ± 15	72 ± 2
Gulf of Riga	22	66	9570 ± 400	120 ± 10
Aland Deep	75	280	1780 ± 10	122 ± 2
Bothnian Sea	75	290	24000 ± 400	750 ± 25
Bothnian Bay	20	130	21000 ± 570	770 ± 20

### Transition zone

The Kattegat is part of the transition zone to the North Sea with medium depths around 10-60 m. The western part of the Kattegat off Jutland is shallower than 15 m, whereas a deeper entrance channel lies in the eastern part off the coast of



Sweden. This channel is connected with the Danish Straits only through very narrow furrows in the sea bottom with depths around 30 m. Little Belt, Great Belt, and Oreound, contain the limiting cross sections for the water exchange. The inlet of Little Belt is very narrow. The northern mouth of the Sound and the Drogden Sill at its southern end have comparable minimum cross sections below 100,000 m<sup>2</sup>, however, the mouth is narrow (4 km) but deep (20-30 m), whereas the Drogden Sill is very shallow (5-9 m) with a wide opening (15 km), see also (Jacobsen 1980). The transition zone extends to the shallow Darss Sill 18-20 m, with the Kiel Bight and the Mecklenburg Bight as buffer volumes. This area is described in more detail in the baseline report devoted to the Fehmarnbelt region.

### **Arkona Basin**

The Arkona Sea is the first basin of the actual Baltic Sea. This basin is directly entered by the saline inflows coming across the shallow Darss Sill and Drogden Sill. The Arkona Sea is a rather small and shallow area, the central basin below 30 m depth covers approximately 6,000 km<sup>2</sup> with 70 km<sup>3</sup> of water and the maximum water depth is around 50-55 m. Therefore the Arkona Basin may be nearly completely filled up by stronger inflow events above 50 km<sup>3</sup>. Smaller inflows are accumulated and mixed until the saline bottom water spills over the small sill at the entrance of Bornholm Channel which is the connection channel to the following Bornholm Basin. The salinity of the bottom water in Arkona Basin is decisive for the further propagation into the deep Baltic basins. Due to its shallowness the basin might be completely ventilated by gale winds. Consequently, an essential amount of saline water is mixed up and leaves again with outflowing water. Because of this transformation of salinity the Arkona Basin plays a key role in the water exchange of the Baltic Sea. The inflow plumes coming over Drogden Sill have a higher salinity and branch around the shallow Kriegers Flak, whereas bottom water entering over Darss Sill flows in predominantly along the southern rim of the basin. To the east the Arkona Basin is confined by the island of Bornholm and the adjoining shoals of the Rønne Bank and the Oder Bank which allow only the exchange of surface water. However, the basin is not really closed. Using the deepest data  $z_{\min}$  allocated to the IOW bathymetry grid cells, the closing depth listed in Table 2.2 reaches down to 47 m in Bornholm Channel. Hence, less than 1 km<sup>3</sup> of bottom water is enclosed and a rather permanent flow of saline water onwards into the central Baltic Sea takes place. Stabilized by geostrophic adjustment some 10 km<sup>3</sup> of bottom water may circulate within the basin. The average retention time of bottom water in the Arkona Basin has been estimated by (Lass et al. 2005) as 10-30 days. Since the influence of surface waves is weak below 15 m, the central Arkona Basin is an accumulation area of fine grained sediments (Leipe et al. 2008).

### **Bornholm Basin**

The Bornholm Sea east off island Bornholm is the first deep basin of the Baltic Proper reaching water depth around 100 m. The surface area indicated in Fig. 2.6 covers about 27,000 km<sup>2</sup> and 1330±30 km<sup>3</sup> of water. The central basin is closed at the Stolpe Channel below 66 m depth comprising 100 km<sup>3</sup> of bottom water. Hence only very strong inflow events may refill this buffer volume totally. Normally, pulses of saline water enter through Bornholm Channel, and it depends on the salinity and temperature of the incoming water whether the bottom pool is replaced or if the inflow interleaves between the halocline and seabed. Saline plumes propagate further into the Baltic Proper if elevated bottom water washes over the small sill in front of the Stolpe Channel, which is the connection to the central Baltic Proper in the east, see below. Because of the permanent halocline, which establishes in Bornholm Sea between 50-60 m, the basin is permanently stratified and therefore subject to stagnation periods with regular occurrence of anoxia in deeper layers. Moreover, substantial sedimentation takes place in the central Bornholm Basin. Since the opening to the channel off island Öland is around 50 m depth this connection contributes only to the exchange of surface water.

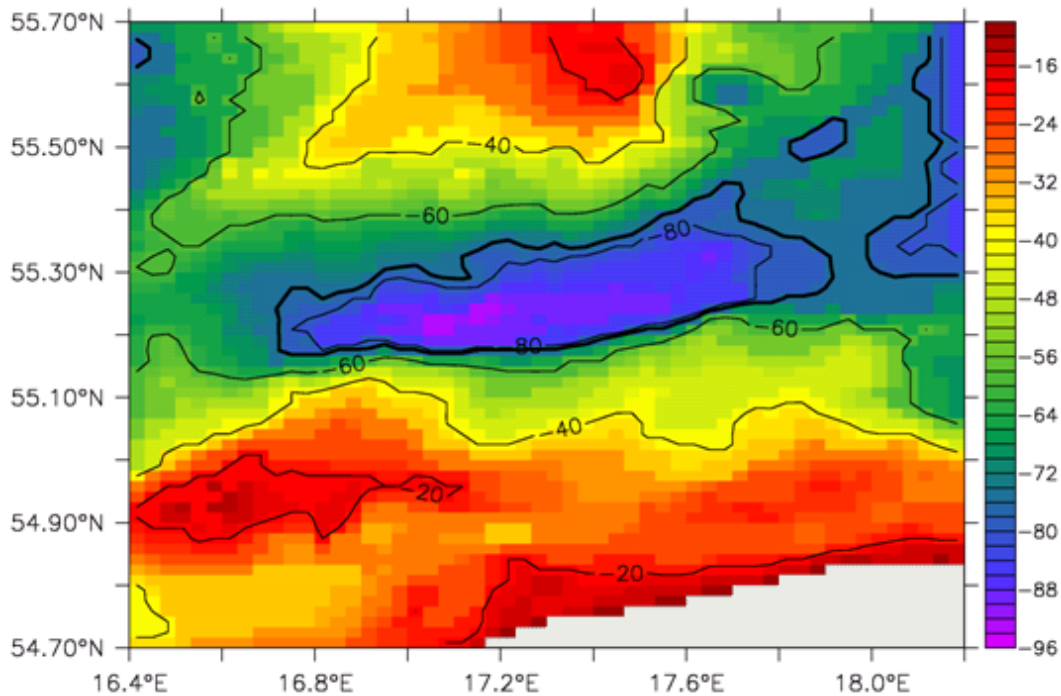


Fig. 2.8 Bathymetry of Stolpe Channel connecting Bornholm Basin to the west with Baltic Proper to the east. Bold isoline indicates closing water depth of 70 m (data from Seifert et al., 2001).

### Stolpe Channel

The Stolpe Channel is a straight channel between the Bornholm Basin and the southern Baltic Proper which extends over approximately 100 km from 16.5°-18°E and 55°-55.5°N, see Fig. 2.8. The lateral boundaries are the Slupsk Bank off the Polish coast in the south and the open sea elevation of the Southern Middel Bank in the north. These elevations “block” the deep water exchange with the Western Gotland Sea (see below). Hence, Stolpe Channel is the only pathway of saline bottom water into the Baltic Proper. The average cross section below the halocline depth of 60 m is around 350,000 m<sup>2</sup>, but only 3000 m<sup>2</sup> at the western sill to Bornholm Basin. A shallow area above 75 m at the eastern end is not an essential obstacle for bottom flow because the channel broadens up. However, an enclosed volume of 4 km<sup>3</sup> below 76 m reaching down to a maximum depth of 94 m may buffer some saline water. The propagation of saline plumes through Stolpe Channel has recently been described by Piechura, Beszczynska-Möller (2004) and Paka et al. (2006).

### Baltic Proper

Here the Baltic Proper is identified with the central Baltic Sea as indicated in Fig. 2.6. Often also the Bornholm Basin, the Arkona Basin, and the Pomeranian Bight are included, as for instance by (HELCOM 2002). The Baltic Proper is a rather deep basin: only 14% of the surface area of 163,000 km<sup>2</sup> are shallower than 20 m, but 25% are deeper than 100 m leading to a mean depth of 62 m. A zonal division into a southern, central, and northern part along 56°N and 58°N roughly corresponds to the main sub-basins. The southern part covers an area of 44,000 km<sup>2</sup> enclosing 2500 km<sup>3</sup> of water. The central and the northern Baltic Proper are of rather equal dimensions of 60,000 km<sup>2</sup> and 4600 km<sup>3</sup>, and 59,000 km<sup>2</sup> and 4,200 km<sup>3</sup>, respectively. However, the mean depth of 77 m and 71 m indicate the central part contains a larger amount of bottom water.

### Southern Baltic Proper and Gdansk Depression

The southern Baltic Proper is dominated by the Gdansk Depression which forms a half-open bay along the coast of Poland. The central basin encloses 30 km<sup>3</sup> of bot-



tom water below 90 m. The maximum water depth is around 115 m. To the north the basin is confined by the Klaipeda Bank the offshoots of which reach down to 55.2°N. Thus saline inflow plumes branching from Stolpe Channel to the south and interleaving below 85 m are trapped in the Gdansk Depression. Because of this relative constriction of the bottom water, oxygen conditions and sedimentation depend essentially on the input of nutrients and suspended matter by river Vistula. (HELCOM 2009) states seasonal and long-term hypoxia for the whole basin.

### Central Baltic Proper and Eastern Gotland Sea

The central Baltic Proper is sub-divided by island Gotland and the adjoining submarine elevations into the Western and Eastern Gotland Sea. The eastern part is dominated by the Gotland depression (see Fig. 2.9), which forms a channel-like structure at the sea bottom, sloping continuously down from 100 m in the south to 250 m in the central basin east off Gotland. The next depression to the north (Farö Deep) is sub-divided by a sill area around 140 m. The Eastern Gotland Basin is considered as the main indicator area for the hydrographic conditions in the Baltic Proper because it contains the largest bottom water pool of the Baltic Sea. Around 210 km<sup>3</sup> covering an area of 6500 km<sup>2</sup> are enclosed below 140 m depth (see Fig. 2.9), and 80 km<sup>3</sup> below 168 m within the central basin. Because of the strong permanent halocline in 70-90 m, which separates surface waters of 6-8 psu salinity from bottom waters with 11-13 psu, this basin is subject to long lasting periods of stagnation leading to hypoxic and anoxic conditions, which are only interrupted by stronger inflow events. Saline bottom water spreads from the Stolpe Channel along the steep eastern rim of the Gotland depression directly into the Eastern Gotland Basin. However, ventilation of deeper layers only takes place if the saline plumes carry enough salinity and oxygen to renew the bottom water. Intensive observations provided long-term time series revealing the interchange of long-term stagnation with ventilation events.

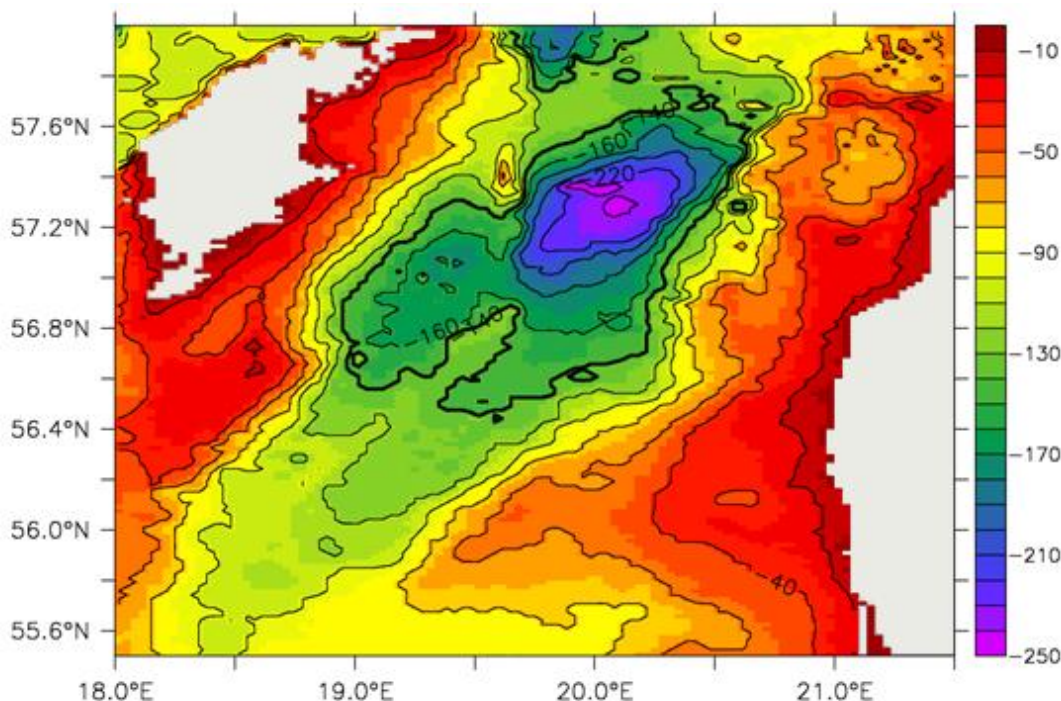


Fig. 2.9 Bathymetry of the central Baltic Proper showing the Gotland Depression (below -100 m water depth) and the Eastern Gotland Basin, which is enclosed below -140 m (bold black line). Data from (Seifert et al. 2001).





### **Northern Baltic Proper and Landsort Deep**

The bathymetry of the Northern Baltic Proper is highly variable, showing many depressions below 100 m depth which are interspersed with small scale elevations. The region is directly connected with the Gulf of Finland to the east. Low saline surface water is exchanged with the Gulf of Bothnia across the shallow Åland Sea (see below). The bottom water in this region is subject to permanent hypoxia because deep saline inflow pulses arrive not directly, but are absorbed and transformed in Eastern Gotland Basin. The basin-wide circulation of deep water around island Gotland is hindered by the elevation of the Middle Banks in the south. The largest sub-basin is located at Landsort Deep, a narrow cleft with steep walls reaching down to a maximum depth around 460 m. The basin is closed below 160 m comprising 70 km<sup>3</sup> of stagnant bottom water. Landsort Deep is a second indicator area for the hydrographic conditions in the Baltic Proper which is regularly controlled by observations.

### **Gulf of Finland**

The Gulf of Finland is not a basin enclosing a pool of bottom water, but an elongated trench with a westward sloping bottom down to below 100 m depth, extending along 330 km, if one excludes the Bay of St. Petersburg, which is separated by a dam. This area of the sea covers 29,000-29,600 km<sup>2</sup> and comprises a volume of 1005-1100 km<sup>3</sup>, see Table 2.1. The cross channel depth profile is asymmetric. A shallow archipelago spreads off the northern coast, whereas the southern part shows a steep coastal decline. The coast line is cliffy, and the sea bottom has a complex structure of alternating elevations and depressions. The part off 26°E forms a shallow bay of 28 m mean depth, whereas the western part is a channel with a cross section around 3 km<sup>2</sup>. This large interface allows intensive water exchange with the northern Baltic Proper. However, due to heavy riverine nutrient loads long-term hypoxia occurs below 80 m (HELCOM 2009a). The strong input of fresh water of approximately 130 km<sup>3</sup>/year, mainly by rivers Neva and Narva discharging in the eastern part, establishes a permanent gradient in surface salinity between 3-7 psu and maintains a permanent vertical stratification of the water body. The brackish surface water leaves the Gulf of Finland predominantly along the northern coast, leading to inflow in the south connected with eddies in the shear zone, see for instance the high resolution model study of Andrejev et al. (2004).

### **Gulf of Riga**

The Gulf of Riga is a relatively isolated basin with a surface area of 16,000 km<sup>2</sup> containing 400 km<sup>3</sup> of water. The main connection to the Baltic Sea is the flat and narrow Irben Strait with a sill depth of 22 m and a minimum cross section around 400,000 m<sup>3</sup>. The volume enclosed below the sill depth is 120 km<sup>3</sup>. The small straits between the islands in the north play a minor role. Suur Strait, for example, has a cross section of 36,000 m<sup>2</sup> with a sill depth of only 10 m. Hence, the Gulf of Riga exchanges only surface water with the Baltic Proper. Together with an average fresh water river discharge of 1,100 m<sup>3</sup>/s, mainly by river Daugava, the water is diluted to salinities of 5-6.5 psu and salinity differences between surface and bottom water are around 1 psu. Therefore, the water body is only weakly stratified, even during the summer thermocline. Thus the rather shallow water body with a maximum depth of 66 m is ventilated by wind action and seasonal convection. Temperature observations show a seasonal signal over the whole water column. Consequently hypoxic conditions are rare in spite of heavy riverine nutrient loads, see (HELCOM 2009). An observation based description of the hydrography of the Riga Gulf has been given by (Kõuts 1993).

### **Åland Sea**

The Åland Sea consists of the deep Åland Trench off the Swedish coast and the very shallow Archipelago Sea off Finland, yielding a special hypsography since 60% of



the area are of less than 10 m depth. This is approximately the sill depth of the archipelago according to the IOW bathymetry. The small north-south channels through the archipelago with 30-40 m depth, mentioned by (Leppäranta and Myrberg 2009), are not resolved by the IOW bathymetry grid Eq. (2.1). This confirms the suggestion that water depth is systematically under-estimated, especially in the flat areas of the northern Baltic Sea, by sampling from sea charts. The Åland Trench is a deep depression limited by sill regions of 75 m. Hence it encloses a considerable pool of 120 km<sup>3</sup> of bottom water which is comparable with Bornholm Basin and Eastern Gotland Basin. However, despite a maximum depth around 300 m (Leppäranta and Myrberg 2009), (IOW grid only 280 m) the bottom water is sufficiently ventilated due to weak stratification. Bottom salinities of 6.5-8 psu correspond to surface salinity of the Baltic Proper.

### **Gulf of Bothnia**

Because of the Åland Sea the Gulf of Bothnia is a rather isolated part of the Baltic Sea, which consists of two sub-basins, the southern Bothnian Sea and the northern Bothnian Bay. According to the dimensions listed in Table 2.1 the surface area of Bothnian Sea is 2:1 to Bothnian Bay and the volume ratio is 3:1. The distribution of water depth in Bothnian Sea is similar to Baltic Proper, but Bothnian Bay is obviously more shallow, see Fig. 2.7. The central deep of Bothnian Sea is an elongated depression reaching down to 290 m in the northwest, whereas bottom depths below 100 m occur at several places in Bothnian Bay. The main depression in the Bothnian Bay with a maximum depth of 130 m is located in the southern part of the bay, just north of the shallow region of Kvarken, which divides both sub-basins. The sill depth of Kvarken is around 18-20 m. Therefore the enclosed volume of 770 km<sup>3</sup> in Bothnian Bay is nearly the same as in the larger Bothnian Sea. But the latter refers to the sill depth of 75 m in Åland Sea (see Table 2.2). Because of its isolation and the strong fresh water input by rivers the Bothnian Gulf is characterized by low salinity brackish water. The mean yearly river runoff is around 190 km<sup>3</sup> (40% of the total Baltic), which discharge to equal parts into both sub-basins. Salinity profiles show 3-5 psu in the Bothnian Bay and 5-7 psu in the Bothnian Sea. Thus the weak stratification is also determined by the cold bottom water of 0-4 °C, see (Leppäranta and Myrberg 2009). Due to seasonal convection the whole water column is well ventilated, avoiding occurrence of low oxygen conditions.

#### **2.1.3 Hydrographic implications**

Main hydrographical characteristics of the Baltic Sea are essentially dependent on its geographical location and structure. Due to the shallow transition zone with the narrow Danish Straits and the fresh water input the Baltic Sea is one of the largest brackish water reservoirs in the world with a strongly stratified water body. The sub-division into basins, which are partly isolated by submarine sills, contributes to the large horizontal and vertical gradients in salinity and temperature. Rather isolated basins, like the Gulf of Bothnia and the Gulf of Riga, show less stratification allowing seasonal ventilation of the deep water by convection. On the contrary, the deep basins of the central Baltic Sea suffer regularly from long-term stagnant periods leading to hypoxic and anoxic conditions. The ventilation of these basins depends on the oxygen import by saline inflow. However, inflow is considerably constrained by bathymetry. Saline plumes are weakened or completely absorbed by mixing while passing shallow Arkona Sea. The following Bornholm Basin may buffer even strong inflows in the order of 100 km<sup>3</sup>. Moreover, this large pool acts like a retention basin where bottom water gets aged before being lifted over the Slupsk Sill. After passing Stolpe Channel the inflow branches partly into the Gdansk Deep. Further mixing with ambient waters occurs during the propagation into the Eastern Gotland Basin. Therefore, a considerable amount of inflow water interleaves somewhere below the permanent halocline and only strong events can renew the stagnant bottom water in the deep Baltic Basins.





Finally, bathymetry determines the deep circulation in the Baltic. In general, the basin-wide deep gyres are cyclonic, since inflow comes from the south and propagates along the eastern rims of the basins. The course of bottom near currents is determined by topographic steering. Internal eddies may be generated and destroyed by interaction of currents with elevations of the sea bottom, see Reissmann (2005). Last, but not least, the exchange between deep and surface waters is essentially influenced by the interaction of the sloping ground with internal waves at interfaces like the halocline.

## 2.2 River runoff to the Baltic Sea

### 2.2.1 Discharge data and the HBV model

The strong horizontal and vertical gradients of salinity in the Baltic Sea are maintained by the fresh water input discharging from rivers. Precipitation over sea plays a negligible role because it is nearly balanced with evaporation, see Chapter 2.4. However, the drainage area shown in Fig. 2.10, i. e. the surrounding land region, which discharges into the Baltic, covers 1,730,000 km<sup>2</sup>, an area more than four times larger as the sea surface. This area catches a considerable amount of precipitation which is partly discharged by the rivers to the Baltic Sea. Because of the seasonal variation in precipitation and evaporation, especially the storage of water during winter by ice and snow, the river runoff shows a distinct seasonal distribution with peak values in spring.

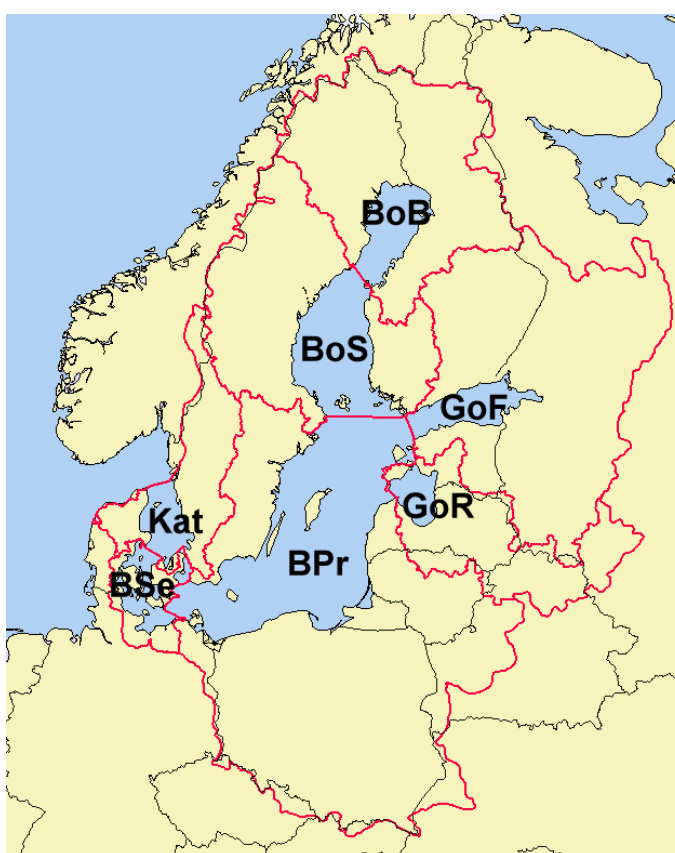


Fig. 2.10 Sketch of the drainage area of the Baltic Sea sub-divided into Bothnian Bay (BoB), Bothnian Sea (BoS), Gulf of Finland (GoF), Gulf of Riga (GoR), Baltic Proper (BPr), Belt Sea (BSe), and Kattegat (Kat), taken from the *Baltic Environmental Atlas* (<http://maps.grida.no/baltic>).

Estimations of the river runoff as a constitutive part of the water balance of the Baltic Sea have been undertaken since the beginning of the 20<sup>th</sup> century, for example by Spethmann (1912) and Witting (1919). However, systematic observations comprising the whole Baltic drainage area were initiated only in the 1950ies. Based on improved measurements and computations of river discharges contributed from all Baltic states (Mikulski 1970) discussed the "Inflow of river water to the Baltic Sea in the period 1951-1960". This overview specifies 65 discharge locations around the Baltic with corresponding catchment area (km<sup>2</sup>), river runoff (m<sup>3</sup>/s) and specific runoff (l/s/km<sup>2</sup>), describing the drainage yield. The seasonal cycle is shown by monthly mean runoff from the main Baltic sub-basins: Bothnian Bay, Bothnian Sea, Gulf of Finland, Gulf of Riga, and Central Baltic including the Belt Sea. The maxi-



mum regional discharge shows a time shift to the northeast due to delay in melting of ice and snow. Peak runoff occurs in March-April in the western and Central Baltic, in April-May in the Riga Gulf, and in May-June in the Gulf of Finland and Gulf of Bothnia, where enhanced discharge may last until July-August.

(Mikulski 1982) extended the analysis of river runoff to the Baltic Sea by providing printed tables of monthly, yearly, and decadal mean discharge within the period 1921-1975 to the above mentioned main drainage basins, counting Baltic Proper and Belt Sea as extra regions and adding Kattegat. The total monthly runoff to the Baltic Sea and Kattegat, derived from these data, are available from the digital supplements to (Feistel et al. 2008).

A more comprehensive runoff database for the period 1950-1990 was compiled by (Bergström and Carlsson 1994); (see Table 2.3 for the 10 largest rivers and Fig. 2.11 for the location of major river runoffs into the Baltic Sea) who evaluated data from some 200 river flow stations around the Baltic, whereas (Mikulski 1982) was based on only 17 rivers. However, it is shown that both data sets agree well within the overlap period 1950-1975 with respect to total runoff. Larger differences were found for Bothnian Sea and Baltic Proper. By merging both data sets for 1921-1990 it is shown that the average river runoff of 15,210 km<sup>3</sup> varies about ±9% even on decadal time scale. The driest period was 1941-1950 with a mean runoff of 13,940 m<sup>3</sup>/s, whereas 1971-1980 was the wettest decade with 16,690 m<sup>3</sup>/s. The data for 1950-1990 are provided by (Bergström and Carlsson 1993) in graphs displaying monthly and annual mean discharge to 6 main Baltic sub-basins. The main characteristics of these basins are shown in Table 2.4. Note that the Danish Belt Sea, the Sounds and Kattegat are considered as one region. The specific runoff, which relates the mean river discharge to the drainage area, indicates that Gulf of Bothnia, Danish Belt Sea, the Sounds and Kattegat are relatively wet areas. The effect of riverine fresh water input to the Baltic sub-basins may be illustrated by relating the discharge to the sea surface and the water volume. The sea level rise, which would occur if the basins were closed, indicates that the surface water is especially diluted in the Gulf of Finland, the Bothnian Bay, and the Gulf of Riga. The same strong effect of river input is found for these regions with respect to the total water volume.

Table 2.3 The ten largest rivers of the Baltic Sea system, including the Belt Sea, Sound and Kattegat, their approximate drainage area and mean annual runoff 1950-1999 (Bergström & Carlsson, 1994)

River	Drainage area (km <sup>2</sup> )	Mean annual runoff (m <sup>3</sup> /s)
Neva	281,000	2,460
Vistula	194,400	1,065
Daugava	87,900	659
Neman	98,200	632
Göta älv	50,100	574
Oder	188,900	573
Kemijoki	51,400	562
Ångermanälven	31,900	489
Luleälven	25,200	486
Indalsälven	26,700	443

The flushing time, needed to fill up the empty basins by river discharge, is only 10-15 years, which is one order of magnitude less than the time scale of the Baltic Proper. On average, river runoff corresponds to a sea level rise around 1 m per

year and a flushing time of about 45 years for the Bothnian Sea and the total Baltic Sea.

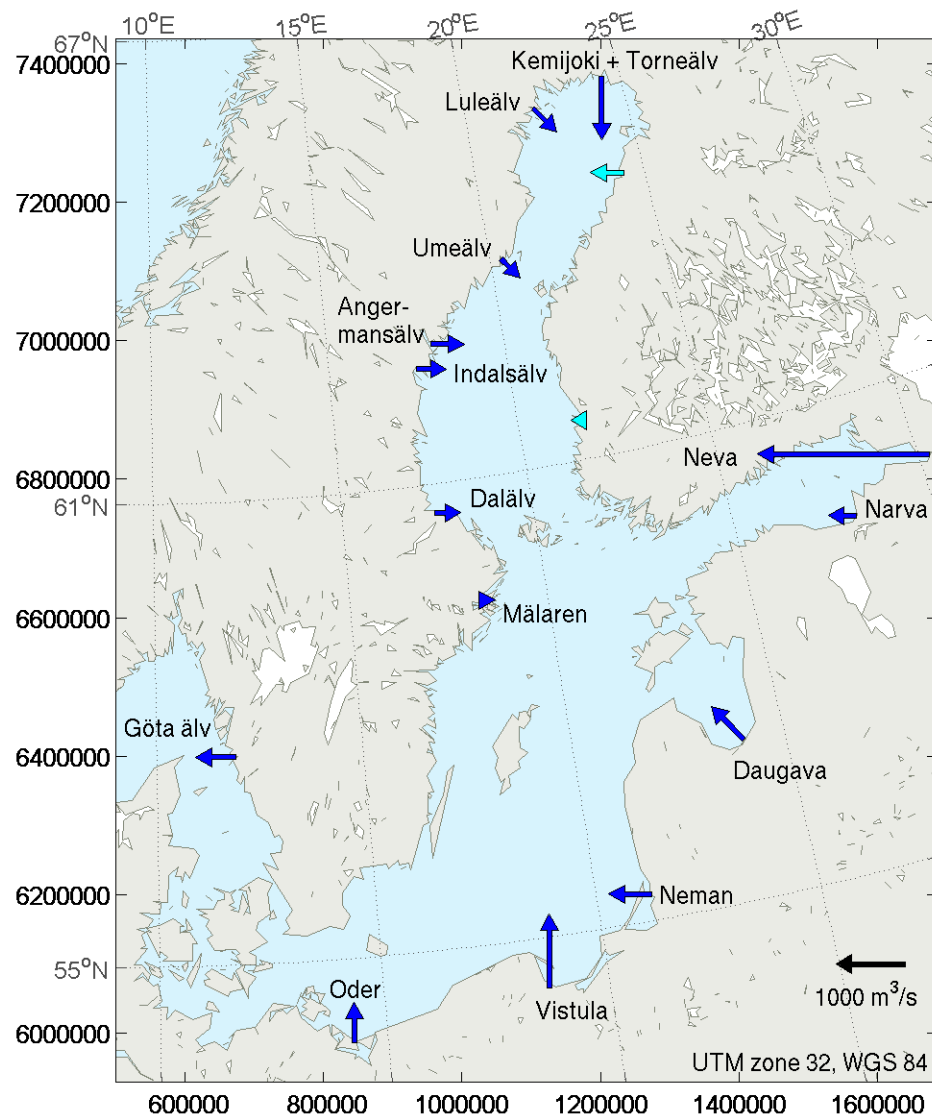


Fig. 2.11 Major rivers contributing to the Baltic Sea water budget. Dark blue arrows indicate specific river runoffs, light blue arrows show accumulated diffuse sources. The Göta älv is shown for although it empties into the Kattegat. Torneälv and Kemijoki have been summed up as their mouths are located only 15 km apart. Values from Mikulski (1970) and Bergström and Carlsson (1994).

The typical yearly cycle of river discharge to the sea is discussed by (Bergström and Carlsson 1993) on the basis of climatological monthly means, i. e. the runoff within each month averaged over the whole period. Seasonal variation, showing a slight trend to higher discharge in the northern Baltic basins during winter in the decade 1980-1990, is demonstrated on the basis of annual means.

The database provided by (Bergström and Carlsson 1993) is continued by the Swedish Meteorological and Hydrological Institute (SMHI) by updating every year the mean annual river discharge to Bothnian Bay, Bothnian Sea, Gulf of Finland, Gulf of Riga, Baltic Proper and the total Baltic Sea (restricted to these 5 sub-basins), published in HELCOM indicator fact sheets, see (HELCOM 2009b). Since 2003 the discharge data rely on the hydrological HBV model run by SMHI. This is a conceptual



model relating precipitation and air temperature to evapotranspiration and soil moisture. The model is based on 700-800 synoptic weather stations and derives the runoff from the sub-regions of the drainage area via routing through the land topography, taking into account the seasonal water storage by snow cover and the regulating effect of lakes and artificial reservoirs. The HBV model introduced by (Bergström 1976) is continuously improved at SMHI and regularly calibrated with discharge data. The potential of HBV to reproduce the observed river runoff into the Baltic Sea and to simulate climate change effects was demonstrated by (Graham 2000). Besides daily discharge of fresh water the HBV model also provides input loads of nutrients (tons/day). Ammonium (NH<sub>4</sub>), Nitrite (NO<sub>2</sub>), and Nitrate (NO<sub>3</sub>) are components of the dissolved inorganic nitrogen (DIN), which sums up with dissolved organic nitrogen (DON) to the total nitrogen load (N<sub>tot</sub>=DIN+DON). Dissolved organic phosphorus (DOP) is implicitly given by specifying total phosphorus (P<sub>tot</sub>) and phosphate (PO<sub>4</sub>), which is identical with dissolved inorganic phosphorus (DIP).

Table 2.4 Characteristics of the main Baltic sub-basins in relation to river discharge. Mean river runoff and drainage area after (Bergström and Carlsson 1993), sea surface and water volume taken from (HELCOM 2002).

Sub-basin	Mean annual river runoff 1950-1990		Drainage area km <sup>2</sup>	Specific runoff l/s/km <sup>2</sup>	Sea surface km <sup>2</sup>	Sea level rise m	Water volume km <sup>3</sup>	Freshwater flushing time years
	m <sup>3</sup> /s	km <sup>3</sup> /y						
Bothnian Bay	3,104	98	261,000	11.9	36,260	2.70	1,480	15
Bothnian Sea	2,860	91	230,000	12.4	79,250	1.15	4,890	54
Gulf of Finland	3,556	112	421,000	8.4	29,600	3.78	1,100	10
Gulf of Riga	1,020	32	132,000	7.7	16,330	1.96	420	13
Baltic Proper	3,610	114	584,000	6.2	211,070	0.54	13,050	114
Belt Sea, Sound, Kattegat	1,159	37	101,000	11.5	42,410	0.87	800	22
Total area	15,310	483	1,729,000	8.9	414,920	1.16	21,740	45

The FEHY data set for the river discharge into the Baltic Sea is a compilation made by DHI from the daily HBV model estimates for 1999-2009 provided by SMHI and monthly data compiled in the framework of the IKZMODER project (see below) for 1970-1998. The data set has a daily resolution, but with constant discharges during months until 1998. The FEHY data set is focused on the greater Fehmarnbelt area by specifying runoff and nutrient loads for 34 locations in the Belt Sea and Sounds, and 13 in Kattegat, but only 13 discharge sites in the Baltic Sea and Glomma river in Skagerrak. The nutrient data have been completed with the riverine input of silicate besides inorganic nitrogen (NH<sub>4</sub>, NO<sub>2</sub>+NO<sub>3</sub>) and phosphate (PO<sub>4</sub>). Detritus and dissolved organic nutrients are differentiated into carbon, nitrogen and phosphorus content, and into the refractory and labile parts, respectively.

IKZMODER is a sub-project for integrated coastal zone Management (IKZM – Integriertes Küsten-Zonen Management) associated to the German branch of the European Union for Coastal Conservation (EUCC). The IKZMODER data provide monthly mean values for runoff and nutrient concentrations of 20 rivers discharging



into the Baltic Sea, Belt Sea, and Kattegat. These rivers represent the runoff from the total adjacent drainage area. The IKZMODER data are mainly based on the Baltic Environmental Database (BED, <http://nest.su.se/nest>) hosted by the Baltic Nest Institute at Stockholm University and were updated for rivers Oder, Peene, Warnow, Schwentine, and Trave with local observations. The data compilation is documented in an Excel file. Runoff reflects the inter-annual variations between 1960-2002, whereas realistic annual cycles for riverine nutrient loads were derived from Stålnacke et al. (1999) for the period 1970-1993. The nitrogen components (ammonium, nitrate and detritus) are considered to be 75% of the total load which is available for biological production. Dissolved inorganic phosphate is assumed to be 50% of the total phosphorus content. For long-term model experiments the data set was extrapolated back to 1948 and continued after 2003 by using the monthly means averaged over the 10-year periods 1960-1969 and 1993-2002, respectively. Estimated background concentrations were inserted for missing nutrient data. Moreover, the data were corrected by yearly scaling factors to follow the total regional runoff provided by SMHI via (HELCOM 2007b).

### **2.2.2 Regional inputs, seasonal and inter-annual variability**

In the following the riverine inputs to the Baltic Sea, excluding the transition area (Belt Sea, Sound and Kattegat), will be discussed on the regional scale. The total discharge into the Baltic Sea derived from the FEHY data set is shown in Fig. 2.12. It is obvious that full time resolution only applies to HBV data from 1999, whereas before daily time steps are filled with monthly mean runoff taken from the IKZMODER data set. The bold line marks the average discharge, which is 14,347 m<sup>3</sup>/s (452 km<sup>3</sup>/year) and 14,777 m<sup>3</sup>/s (466 km<sup>3</sup>/year) within the two periods (excluding the transition area). The range of variance is indicated by thin lines corresponding to one standard deviation of ±4,884 m<sup>3</sup>/s and ±4,302 m<sup>3</sup>/s, respectively. Remarkably, the variation of river runoff is of the same order of magnitude on daily and monthly time scale. It is only reduced by 10% to ±3,922 m<sup>3</sup>/s if calculated from monthly mean HBV data.

The coefficient of variation, which is the relation between standard deviation and mean value, is around 30%, indicating a high variability of the river discharge. Runoff above 20,000 m<sup>3</sup>/s occurs nearly every year, peak events exceed 30,000 m<sup>3</sup>/s, whereas dry periods fall below 10,000 m<sup>3</sup>/s. Using mean values and standard deviation as reference it should be noted that the probability distribution of river discharge is skewed to higher values: Low discharge periods lie mainly within the lower bound of the range of variation whereas peak events regularly go essentially beyond, see Fig. 2.12.

The inter-annual variation is shown in Fig. 2.13 by the time integral of river discharge expressed in km<sup>3</sup>. The FEHY data (red line) are compared with the yearly runoff (black line and symbols) provided by SMHI via (HELCOM 2009b), and the scaled IKZMODER data (blue line). The HELCOM data yield an average yearly river discharge to the Baltic Sea of 446 ± 49 km<sup>3</sup>, corresponding to 14,136 ± 1545 m<sup>3</sup>/s (standard deviation). This is near to the long-term mean of 14,151 m<sup>3</sup>/s derived by (Bergström and Carlsson 1993) for the period 1950-1990 (note that the total runoff in Table 2.4 includes also the Belt Sea, the Sound and Kattegat.) The standard deviation of ± 49 km<sup>3</sup> also characterizes the variability of river discharge on decadal time scale. The FEHY data set yields 418, 484, 452, and 471 km<sup>3</sup>/year for the decadal periods 1970-1979 to 2000-2009. With respect to this the change in mean runoff and standard deviation between the IKZMODER and HBV data, as shown in Fig. 2.12, is small and well within the range of natural variability. The coefficient of variation is reduced to 11% for yearly runoff, indicating that the three times higher variability on monthly time scale is introduced by the annual cycle (discussed below). Nevertheless, the inter-annual differences are considerable, exceeding ±100 km<sup>3</sup>, for instance during the dry year 1976 or the wet years 1981 and 1998.





Moreover, Fig. 2.13 shows that 1977-1995 was a rather “quiet” period with annual changes around 10-30 km<sup>3</sup> during 1977-1980, 1982-1986, and 1989-1995.

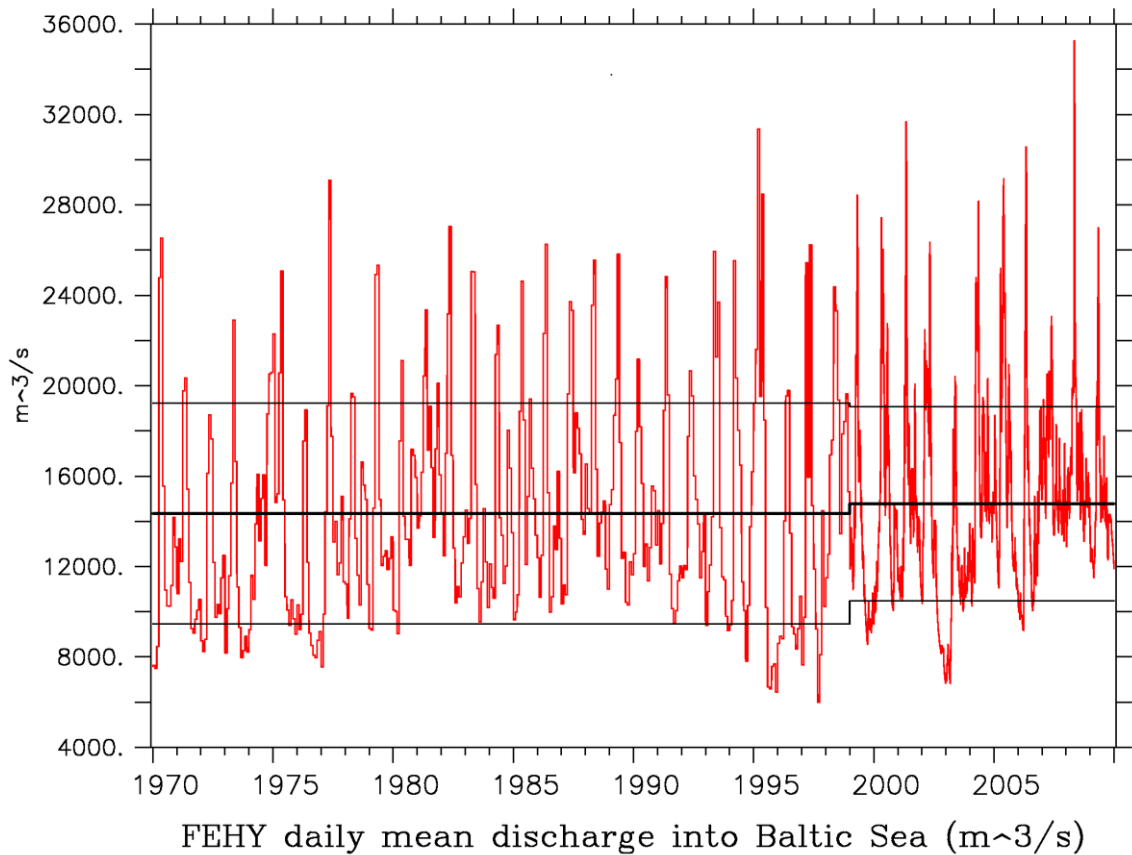


Fig. 2.12 Total river discharge (m<sup>3</sup>/s) into the Baltic Sea (excluding transition area) derived from FEHY data set. The bold black lines indicate the long-term mean runoff, and thin lines the range of variation by one standard deviation.

It is not clear why the HBV data applied for FEHY from 1999 show a similar time behavior, but do not reproduce the HELCOM yearly runoff, which is also based on HBV. A request to SMHI for an explanation of this discrepancy is pending.

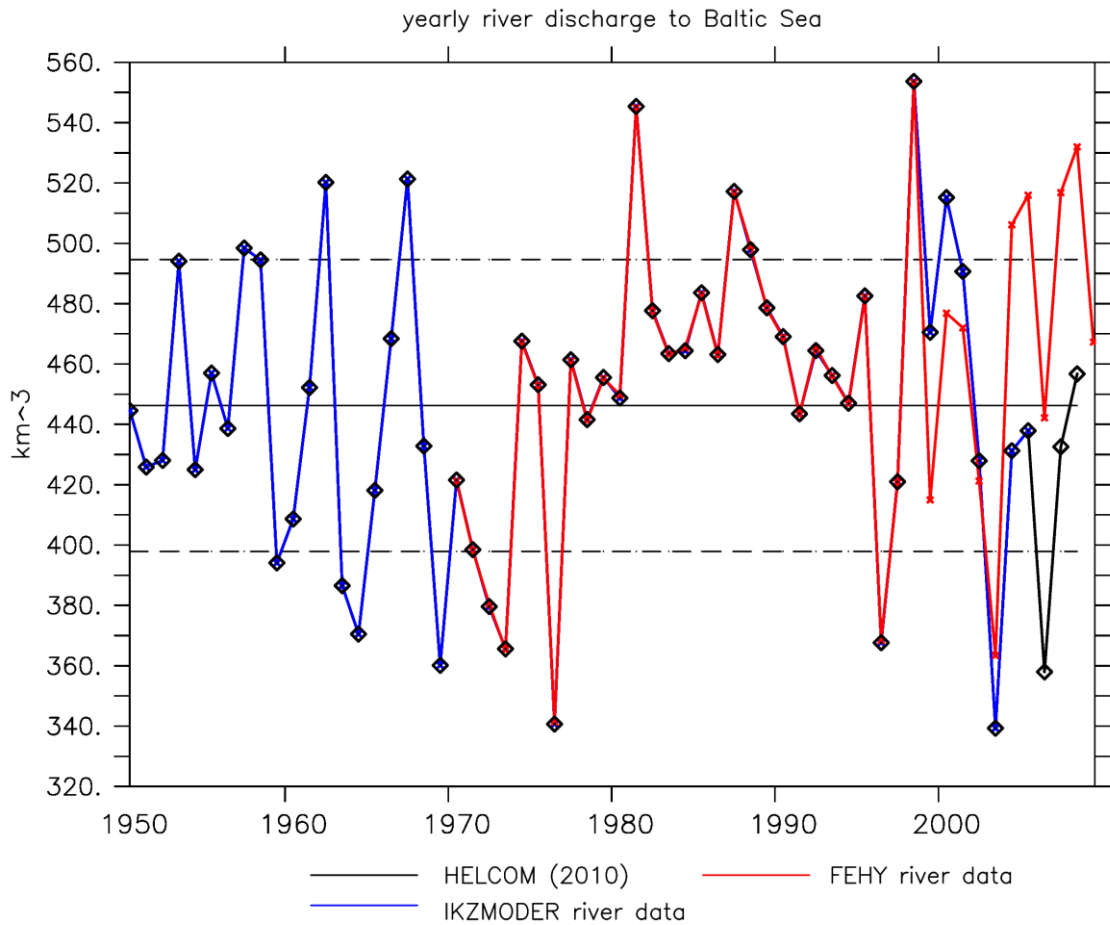


Fig. 2.13 Inter-annual variation of yearly river discharge ( $\text{km}^3$ ) to the Baltic Sea. (HELCOM 2010) refers to (Kronsell and Andersson 2010).

The distribution of the yearly river runoff to the Baltic sub-basins is shown in Fig. 2.14. With respect to the absolute discharge all basins, except Gulf of Riga, obtain comparable fresh water input from rivers. On average 22%, 20%, 25% and 26% of the total runoff is discharged into Bothnian Bay, Bothnian Sea, Gulf of Finland and Baltic Proper, corresponding to 90-120  $\text{km}^3$  per year. The mean runoff into Gulf of Riga is only 7% or 30  $\text{km}^3$ . However, the local effects, expressed by sea level rise and flushing time are dependent on the dimensions of the basin (see Table 2.4). Moreover, the regional distribution of the runoff shows strong inter-annual variation which shifts the regional focus intermittently. For example 1980-1981 when Baltic Proper got a peak runoff of 160  $\text{km}^3$ , or during 1989-1992 when a nearly constant discharge of 130  $\text{km}^3$  entered the Gulf of Finland while the runoff to Baltic Proper dropped down to 85  $\text{km}^3$ .

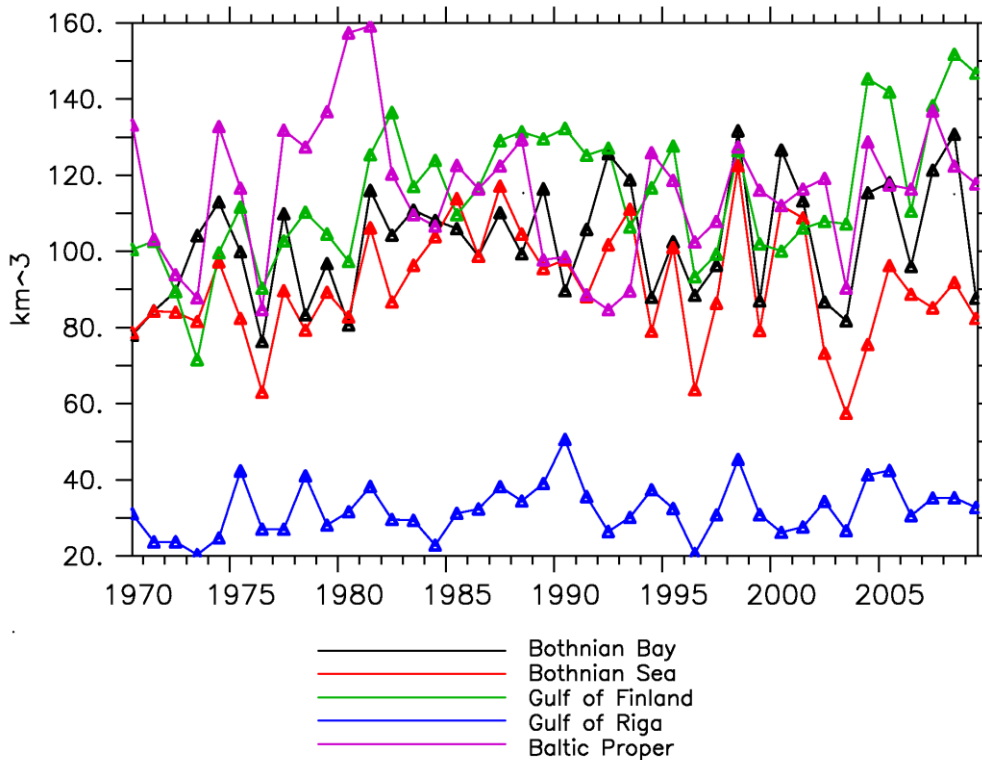


Fig. 2.14 Contribution of Baltic sub-basins to the yearly river runoff according to (Kronsell and Andersson 2010).

The annual cycle of river discharge into the Baltic Sea is displayed in Fig. 2.15 by means of climatological monthly averages. i. e. the average monthly river runoff in the periods 1970-1999 indicated by dashed lines and 1999-2000 by bold curves, respectively. The separation into periods reveals some distinct differences between the HBV model data and the IKZMODER data compilation. Both data sets show the yearly maximum river runoff in April and especially in May as a consequence of the snow melt during spring, however, the HBV model predicts a summer discharge from July to September which is 1,700-2,300 m<sup>3</sup>/s ( $\approx 5 \text{ km}^3/\text{month}$ ) stronger on average. Moreover, the maximum and minimum monthly HBV discharges show less amplitude and variation, which partly might be attributed to the fact that HBV covers only 11 years whereas stronger extremes occurred during the preceding 30-years period. The monthly annual cycle looks rather different within the Baltic sub-regions due to the snow melt time as mentioned earlier. Likewise, winter is the minimum runoff season in the northern regions whereas summer is the dry period in Gulf of Riga and Baltic Proper. The strongest yearly signal occurs in Bothnian Bay, where mean monthly discharge varies between 2,000-8,000 m<sup>3</sup>/s. The flat yearly cycle in Bothnian Sea (2,000-4,000 m<sup>3</sup>/s in HBV data) is influenced by the river regulation in Sweden and Finland, see (Carlsson and Sanner 1994).

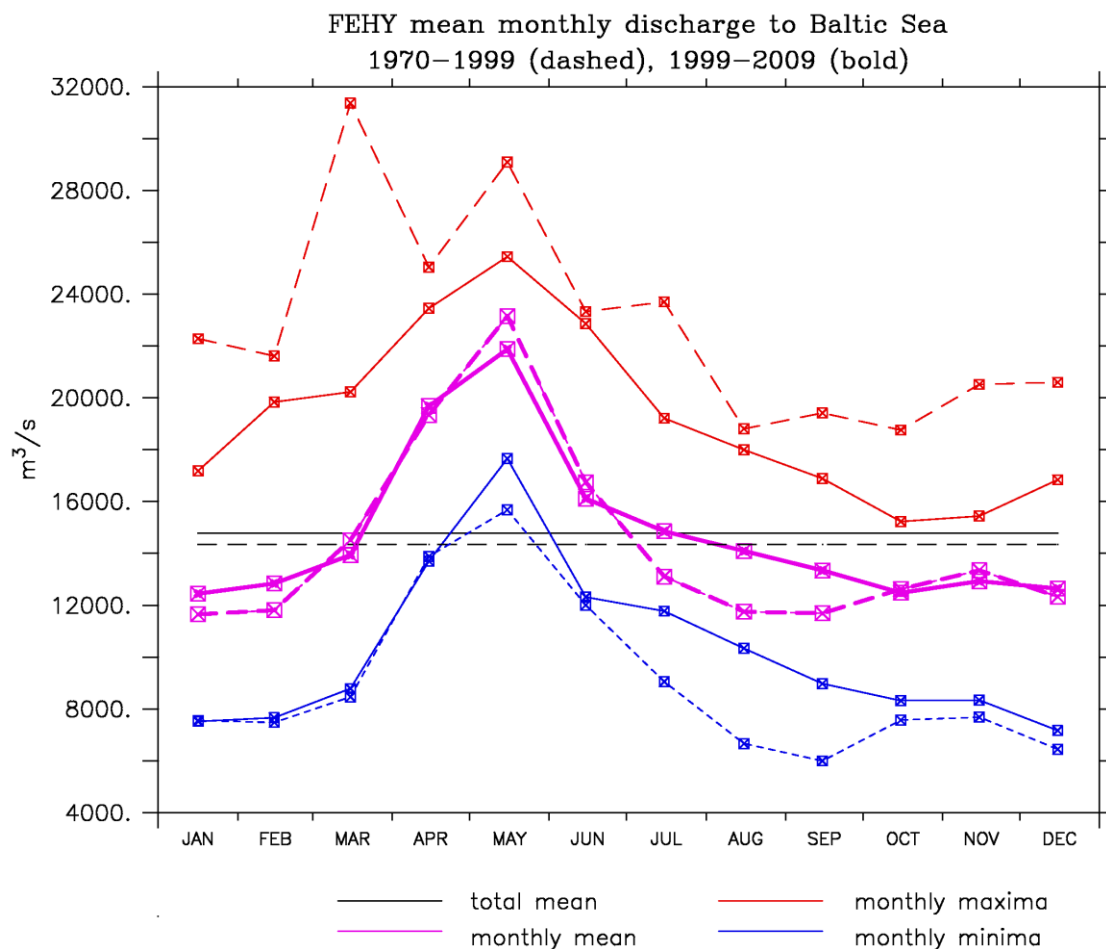


Fig. 2.15 The annual cycle of river runoff ( $m^3/s$ ) shown by climatological monthly means.

### 2.3 Nutrient inputs

Eutrophication of marine systems is still of major concern worldwide. Especially coastal areas and semi-enclosed basins like the Baltic Sea are endangered by anthropogenic nutrient inputs modifying the structure and function of the ecosystem (Nixon, 1995, Aertjeberg et al., 2003). Eutrophication (see Chapter 6.3) is analogous to the natural aging in the broadest sense of the word, the increased supply of plant nutrients to waters due to human activities in the catchment areas that result in an increased production of algae and higher water plants (EUTROSYM 1976). Mainly the excessive input of nitrogen and phosphorus has to be considered. Different land-based sources as well as atmospheric deposition have to be taken into account.

Fig. 2.16 gives a conceptual model of these sources.

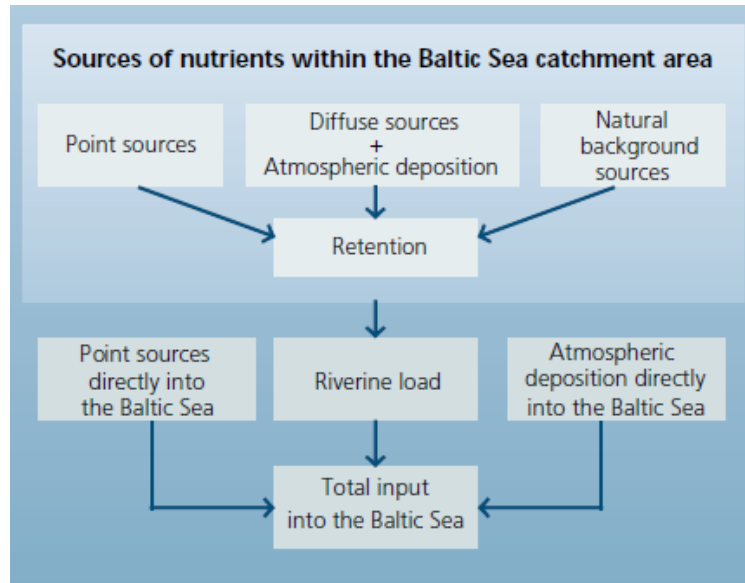
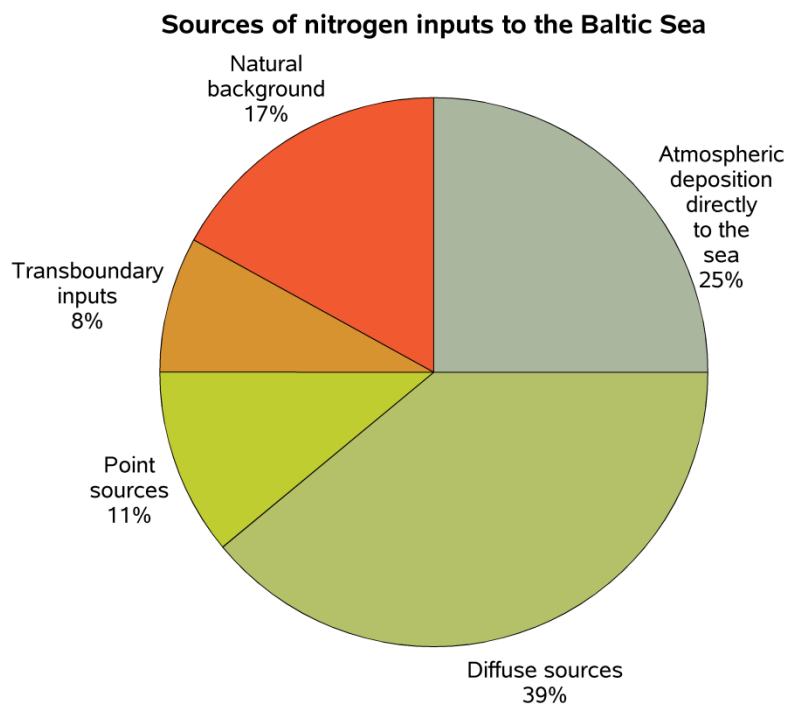


Fig. 2.16 Conceptual model of nutrient input sources to the Baltic Sea (HELCOM 2010a – holistic assessment).

The most recent evaluation of the nutrient load to the Baltic Sea is “The Fifth Baltic Sea Pollution Load Compilation (PLC 5)” (HELCOM 2010b) which is based on measurements in the years 2001–2006. For this period, the averaged annual total waterborne input of nitrogen (riverine load, coastal areas, direct point and diffuse sources) amounted to 641,000 t. An additional quarter of the total nitrogen inputs is caused by atmospheric deposition (see Chapter 2.3.2). This pathway amounts to 198,000 t N in 2006. In total, yearly around 840,000 t nitrogen are introduced into the Baltic Sea. Fig. 2.17 gives an overview of the contribution of different sources. About 80% of the diffuse sources originate from agriculture, about ten percent are discharged from point sources such as municipal wastewater treatment plants or industry. Transboundary inputs from inland countries with no Baltic Sea coastline are mainly coming from Belarus and the Ukraine. It has to be mentioned also that 17% are due to natural background losses.



*Fig. 2.17 Proportion of different nitrogen sources to the Baltic Sea. Point sources include both coastal and inland point sources. Transboundary inputs have not been divided into point or diffuse sources (redrawn from HELCOM 2010a/b).*

For phosphorus, the averaged annual input for the period 2001-2006 amounts to 30,200 t (HELCOM 2010a/b). It is believed that the airborne phosphorus deposition accounts for a maximum of 5%. Exact measured or modelled data are not reported. Around 20% of the inputs are coming from point sources whereby wastewater treatment plants contribute to 90% of this source. Again, 80% of the diffuse sources can be related to agriculture. Natural background losses amount to 16% of the total input (Fig. 2.18).

The five largest sources of phosphorus and nitrogen are the rivers Vistula, Neva, Oder, Daugava and Nemunas. Thus, the highest nutrient enrichment pressure is on the Baltic Proper, the Gulf of Finland and the Gulf of Riga (HELCOM 2010a).

Comparing the recent observation period 2001-2006 with the previous one (1995-2006), the total load of nitrogen decreased by 13.7% and the load of phosphorus by 15.3%. However, also a decrease of the annual runoff of 9.8% was measured between the same periods. Therefore, it is obvious that around two-thirds of the observed decrease in nutrient inputs can be explained by differences in the hydrological conditions (HELCOM 2009c). Nutrient inputs can vary considerably from year to year. Years with high runoff are characterized by high nutrient discharge leached from the soil, dry years show lower nutrient inputs. The atmospheric deposition of nitrogen has declined by about one third since 1980 and by 8% since 1995, but it increased during the assessment period 2003-2007 (Bartnicki 2009).





### Sources of phosphorus inputs to the Baltic Sea

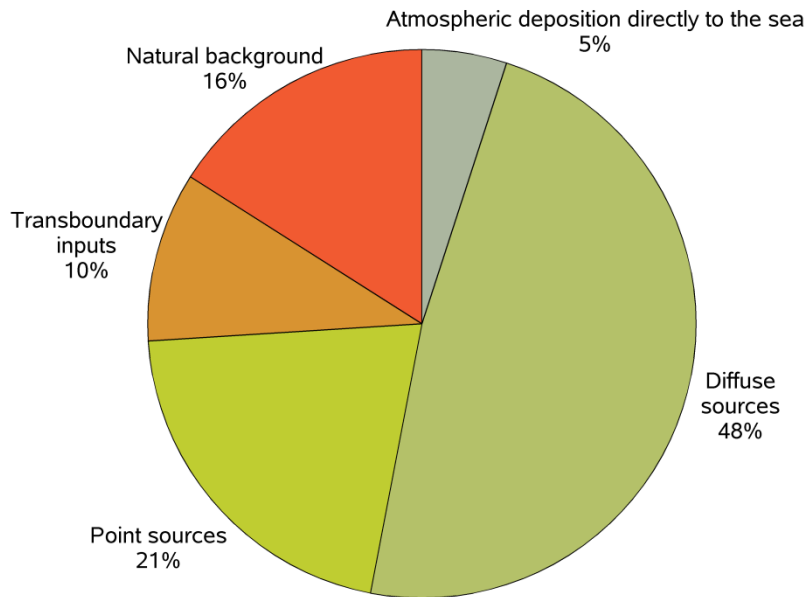
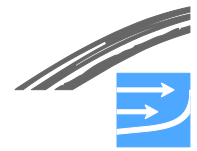


Fig. 2.18 Proportion of different phosphorus sources to the Baltic Sea. Point sources include both coastal and inland point sources. Transboundary inputs have not been divided into point or diffuse sources (redrawn from HELCOM 2010 a/b).

Different attempts were made to estimate the nutrient inputs a century ago when man had little influence. (Larsson et al. 1985) have done one of the first estimates (Table 2.5). Their calculation suggests an increase in total phosphorus loading by about eight times, and in total nitrogen load by about four times from the catchment area due to human activities. It is remarkable that they used present nutrient concentrations in northern Swedish rivers as natural background conditions. From that it can be concluded that the northern Baltic Sea is less affected by the increase in nutrient inputs compared to the rest of the Baltic Sea which is more under anthropogenic influence. (Rosenberg et al. 1990) and (Jansson and Dahlberg 1999) calculated a threefold increase of the nitrogen load to the Baltic Sea and an increase of the phosphorus input by a factor of five using the 1940s data as reference.

Table 2.5 Estimated total nitrogen and phosphorus inputs (tons/year) into the Baltic Sea during the 1980s and before the beginning of the 20th century (Larsson et al. 1985)

	Nutrient	Rivers	Atmosphere
Mid of the 1980s	Phosphorus	51,600	5,500
Beginning of the 20 <sup>th</sup> century		6,800	2,800
Mid of the 1980s	Nitrogen	640,500	322,000
Beginning of the 20 <sup>th</sup> century		150,000	83,000



More recently, Schernewski and Neumann (2005) used a model simulation to describe the trophic state of the Baltic Sea a century ago and compared this time with the nutrient load during the 1980s. They calculated a riverine load reduction of 68% for nitrogen and 76% for phosphorus hundred years ago. Taking all loads, including atmospheric deposition, the load at that time was only one quarter of today's inputs. They argue that the riverine phosphorus loads were lower compared to the nitrogen loads. In conclusion, despite differences in the various estimates and calculations a man made increase in the nitrogen and phosphorus inputs to the Baltic Sea by a factor of four at least can be given.

### 2.3.1 Riverine input

The eutrophication of the Baltic Sea is mainly caused by the heavy input of nutrients with river discharge. Riverine nutrient loads consist of discharges and losses from different sources within a river's catchment area, including discharges from industry, municipal wastewater treatment plants, losses from agriculture and managed forests, as well as natural background losses and atmospheric deposition over land which is washed into the rivers. According to the (HELCOM 2004) pollution report, diffuse sources (mainly agriculture) contribute almost 60% of the nitrogen and 50% of the phosphorus river loads. Usually, input data for rivers also include the runoff of direct and diffuse sources along the adjacent coastal area within the corresponding catchment region.

According to the recent environmental assessment compiled by (HELCOM 2009a/b) about 75% of the nitrogen and at least 95% of phosphorus enter the sea via rivers. Therefore, the nutrient loads connected with river discharge are critical input data for water quality modeling. The river discharge data set used for FEHY assessments and modeling is an up-to-date compilation (HELCOM 2010e); see also (FEHY 2013c), which specifies the different components of nutrient inputs, i.e. the dissolved and particulate fractions, for the period 1970-2009.

Table 2.6 Yearly mean riverine inputs of nutrients to the Baltic Sea (total amounts of nitrogen (N) and phosphorus (P) in ktons).

Period	N / kt	P / kt	Reference
2001-2006	641	30.2	(HELCOM 2009a)
2001-2006	640 ± 82	29.5 ± 4.0	FEHY compilation
1970-1979	803 ± 224	33.1 ± 9.4	
1980-1989	935 ± 149	41.4 ± 8.0	
1990-1999	823 ± 180	39.7 ± 6.6	
2000-2009	655 ± 73	30.4 ± 3.8	
<b>1970-2009</b>	<b>805 ± 196</b>	<b>36.3 ± 8.7</b>	

The (HELCOM 2009a) assessment of the yearly mean riverine input of the total amount of nitrogen and phosphorus to the Baltic Sea, including Belt Sea and Kattegat, is compared in Table 2.6 with the average annual loads of the river discharge data set used for FEHY modelling. Good agreement is found for the period 2001-2006. However, the decadal averages and the total mean for 1970-2009 show considerable variation (expressed by one standard deviation) on inter-annual and decadal time scale. This is also evident from Fig. 2.19. Moreover, the (HELCOM 2009b) graphic for 1994-2006 in Fig. 2.20 demonstrates that the nutrient load variations are mainly determined by the annual discharge of river water. The trend to decreasing nutrient inputs in recent years is also followed by the FEHY data set. The long-term average input of nitrogen to the Baltic Sea is around 800 kt/year, but only 655 kt/year in recent years.

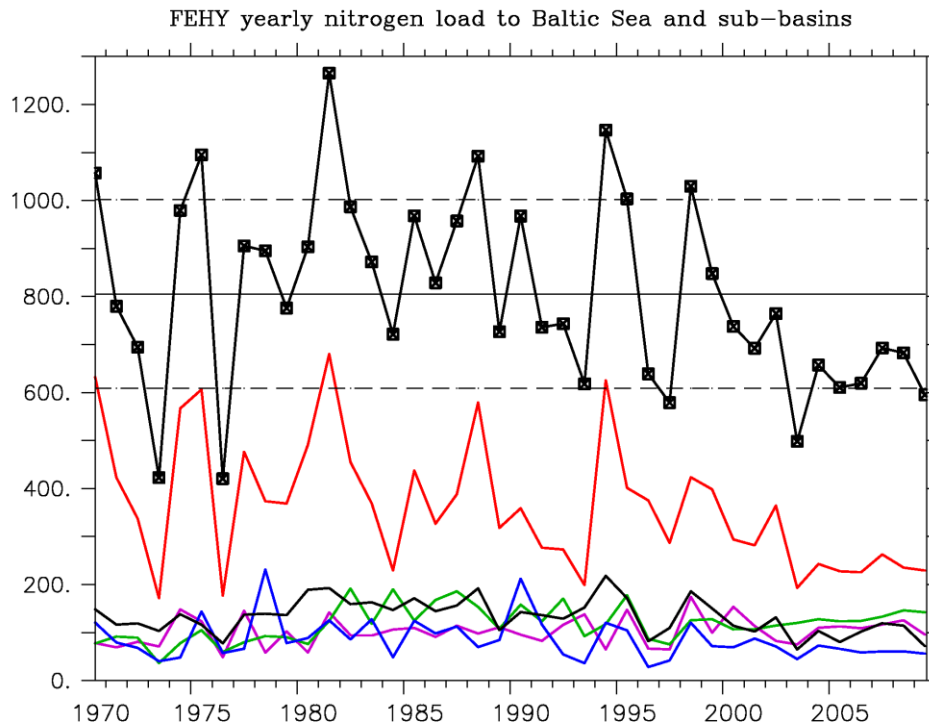


Fig. 2.19 Annual mean riverine input of nitrogen (kt) to the Baltic Sea and its sub-basins. Coloured lines represent: Gulf of Bothnia (magenta), Gulf of Finland (green), Gulf of Riga (blue), Baltic Proper (red), and Belt Sea (black). The bold black line with symbols denotes the total yearly input to the Baltic, straight lines indicate the long-term average and the variation by one standard deviation (dashed). Source: FEHY compilation data.

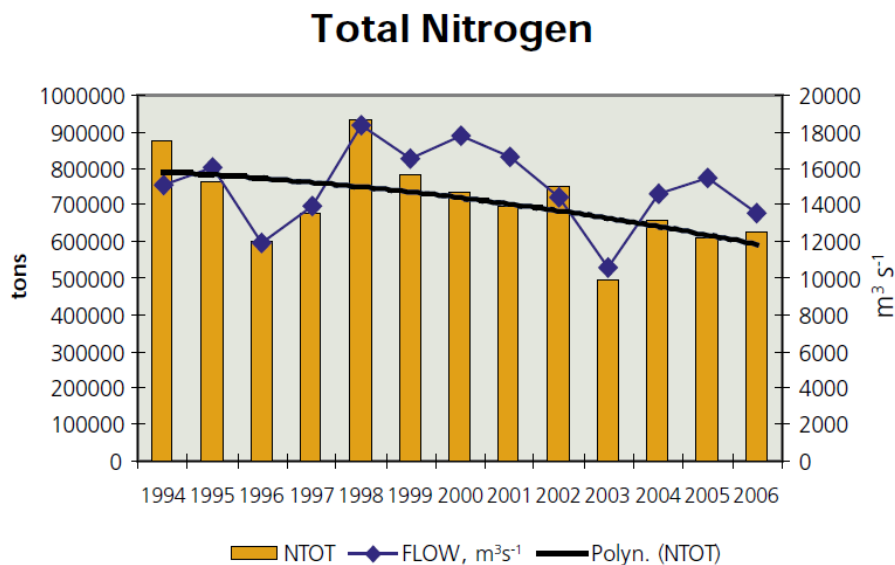


Fig. 2.20 Riverine and direct source inputs of total nitrogen into the Baltic sea for 1994-2006 taken from (HELCOM 2009b).

According to the molar Redfield Ratio of N:P=16:1, the phosphorus loads are an order of magnitude smaller, about 30 - 35 kt/year, however the inter-annual variation is again rather high ( $\pm 15 - 30\%$ ), see Table 2.6 and Fig. 2.21. Like for nitrogen, phosphorus inputs show a maximum during the 1980s and a decreasing trend afterwards.

The regional distribution of riverine nutrient loads is indicated in Table 2.7. Note that (HELCOM 2009a) data refer to 2006, whereas FEHY compilation data are averaged over the period 1970-2009 to include the effect of large inter-annual variations. The absolute inputs show that the highest amounts of nitrogen and phosphorus enter the Baltic Proper, see also the colored curves for the Baltic sub-basins in Fig. 2.19 and Fig. 2.21. However, the regional impact of nutrients is better characterized by the specific areal loads. If the amount of nutrients is related to the sea surface, then Gulf of Finland and Gulf of Riga appear as the most affected sub-basins, whereas Belt Sea and Baltic Proper show less impact. The relative inputs are smallest in Gulf of Bothnia, where rivers discharge from partly pristine catchment regions. The regional distribution of riverine nutrient loads is reflected by the ecological status of the sea. Gulf of Bothnia is mainly qualified as good and moderate by (HELCOM 2009b) eutrophication assessment, whereas the other parts of the Baltic Sea, including Åland Sea, are predominantly considered as poor or bad. Nutrient loads are related to the sea surface because the river inputs are primarily consumed by algae blooms in the surface layer. However, the regional relationships shown in Table 2.7 remain the same, if loads are related to the water volume within the sub-basins (not shown).

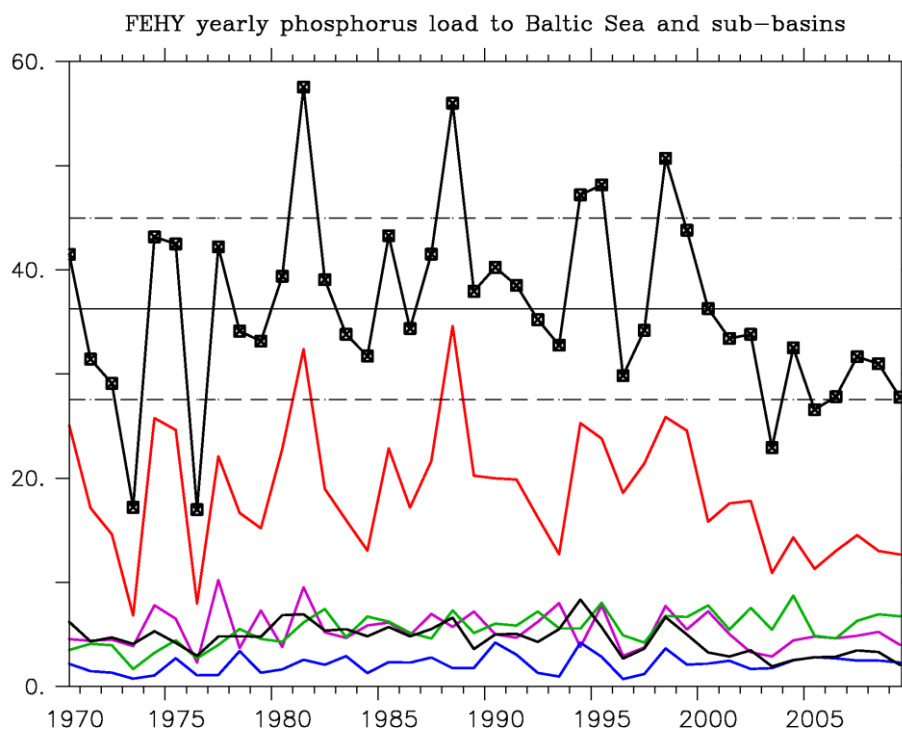


Fig. 2.21 Annual mean river input of phosphorus (kt) to the Baltic Sea and its sub-basins. Coloured lines represent: Gulf of Bothnia (magenta), Gulf of Finland (green), Gulf of Riga (blue), Baltic Proper (red), and Belt Sea (black). The bold black line with symbols denotes the total yearly input to the Baltic, straight lines indicate the long-term average and the variation by one standard deviation (dashed). Source: FEHY compilation data.



Table 2.7 Regional distribution of riverine nutrient inputs (absolute amounts in kt and area specific loads in t/km<sup>2</sup>). (HELCOM 2009a) data refer to 2006 and FEHY compilation data are averaged over the period 1970-2009.

Sub-basin	Sea surface	HELCOM		FEHY		HELCOM		FEHY	
		Nitrogen loads				Phosphorus loads			
	km <sup>2</sup>	kt	t/km <sup>2</sup>	kt	t/km <sup>2</sup>	kt	t/km <sup>2</sup>	kt	t/km <sup>2</sup>
<b>Bothnian Gulf</b>	115,510	109	0.94	102	0.88	4.6	0.04	5.4	0.05
<b>Gulf of Finland</b>	29,600	130	4.39	119	4.00	5.0	0.17	5.5	0.19
<b>Gulf of Riga</b>	16,330	58	3.55	86	5.27	2.7	0.16	2.1	0.13
<b>Baltic Proper</b>	211,070	228	1.08	365	1.73	12.9	0.06	18.6	0.09
<b>Belt Sea, Sound, Kattegat</b>	42,410	102	2.41	1	1.25	2.8	0.07	4.6	0.11

### 2.3.2 Atmospheric deposition of nutrients

The water quality of the Baltic Sea is also influenced by the deposition of nutrients from the atmosphere, particularly 25% of all Nitrogen inputs into the Baltic Sea result from atmospheric loads (cf. Fig. 2.17). Atmospheric deposition shows seasonal and inter-annual variation dependent on meteorological conditions. Wind determines the distribution of emissions. Wet deposition is clearly linked to precipitation, whereas dry deposition is relatively constant.

The atmospheric deposition of nitrogen in oxidized (NO<sub>x</sub>) and reduced (NH<sub>y</sub>) form plays a substantial role for the Baltic Sea, since inputs are 10-40% of the river loads. The most important sources of NO<sub>x</sub> are the emissions caused by fossil fuel combustion for energy production, road and ship traffic, whereas NH<sub>y</sub> is predominantly produced by agriculture (fertilization and livestock breeding). The emission zone is much larger than the Baltic river catchment because atmospheric transports extend over some 10<sup>3</sup>-10<sup>4</sup> km. (Bartnicki et al. 2007) estimate that 32% of the atmospheric nitrogen is imported from countries outside the Baltic drainage area, for instance from Great Britain, Ukraine and France.

The emission, distribution and deposition of nitrogen and others pollutants by the atmosphere is monitored for the Baltic Sea in the framework of the European Monitoring and Evaluation Programme (EMEP). Comprehensive estimates of nitrogen deposition are calculated, based on observational emission data, by the unified EMEP model run at Meteorological Synthesizing Centre – West of EMEP in Oslo. A complete description of the model and its applications is available online (<http://www.emep.int>). The performance of the recent model version is described by (Bartnicki and Valiyaveetil 2008) for atmospheric nitrogen deposition to the Baltic Sea in the periods 1997-2003 and 2000-2006. The accuracy of the model predictions is estimated as ±30%. A regularly updated overview of nitrogen deposition to the Baltic is provided by (HELCOM 2009f) indicator fact sheets.

Fig. 2.22 shows the regional distribution of annual nitrogen deposition to the main Baltic sub-basins taken from (HELCOM 2009f). The different scales on the inserted time series indicate distinct regional differences in absolute inputs. Baltic Proper gains per annum atmospheric loads around 110 kt, whereas the other basins receive only 10-30 kt, respectively. The regional impact of these loads becomes evident, if the annual depositions are related to the sea surface, see Table 2.8, where the mean annual loads for the period 1995-2007 are listed based on the data provided by (HELCOM 2009f). The inter-annual variation is indicated by one standard deviation. The area specific inputs are rather low in Gulf of Bothnia and Gulf of Finland and moderate, compared to the Baltic mean, in Gulf of Riga and Baltic Proper. Despite relatively small receiving sea surface, the high impact regions are Belt Sea and Kattegat, where annual atmospheric deposition corresponds to nitrogen inputs

of approximately 1 t/km<sup>2</sup> or 1 g/m<sup>2</sup>. In contrast to that, the annual fluxes entering the central Baltic basins and Bothnian Gulf are only 0.5-0.3 t/km<sup>2</sup>. Atmospheric nitrogen inputs to Belt Sea and Kattegat are also considerably high (40%) in comparison to nutrient river discharges. In the northern basins the relationship between atmospheric and river loads is distinctly below the average of 33% because of lower fluxes into Gulf of Bothnia and small receiving surfaces of Gulf of Finland and Gulf of Riga.

Oxidized and reduced nitrogen fractions are in the same order of magnitude, see Fig. 2.22. However, a detailed analysis reveals slight north-south gradients. The deposition of NO<sub>x</sub> prevails in the northern regions, whereas NO<sub>y</sub> is predominant in the southern basins. For a detailed analysis of regional emission and deposition of nitrogen to the Baltic Sea see (Bartnicki and Valiyaveetil 2008).

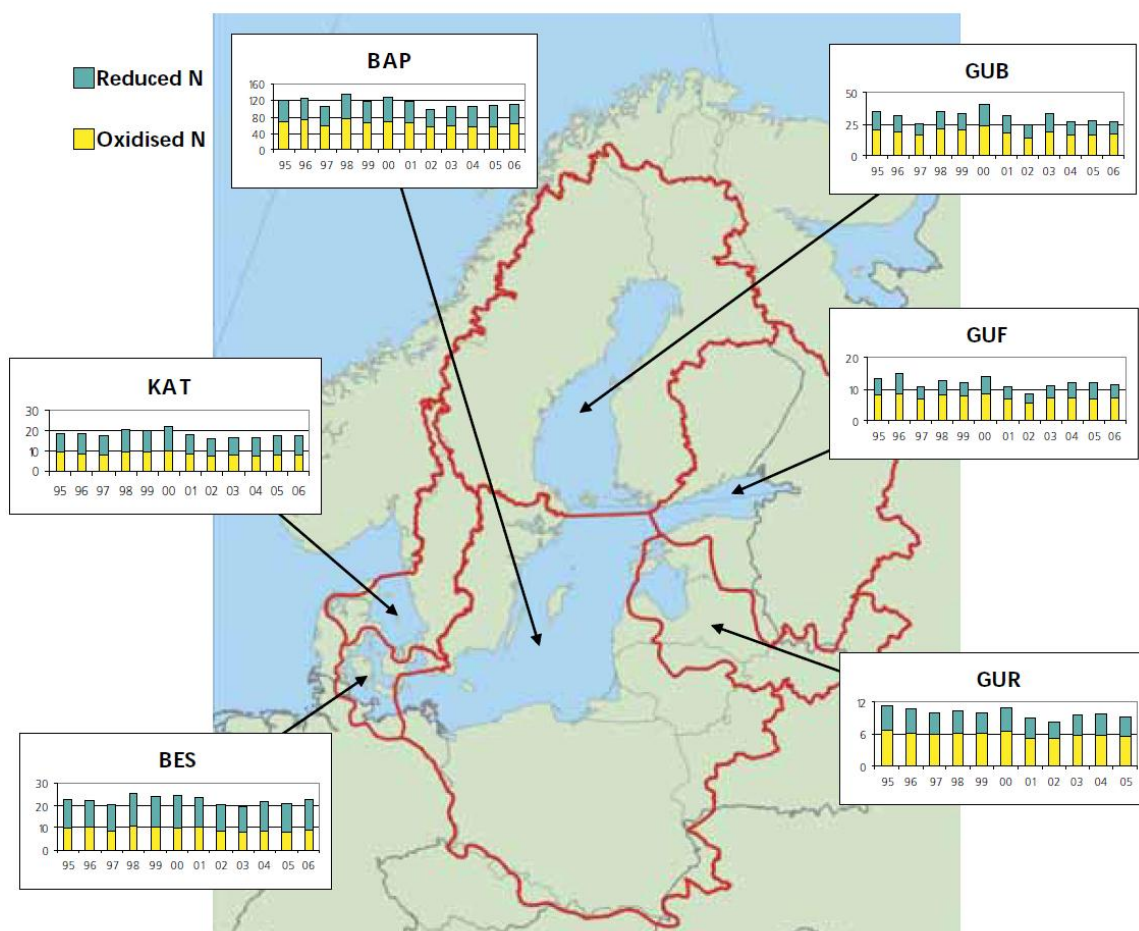


Fig. 2.22 Regional distribution of atmospheric nitrogen deposition divided into oxidized (NO<sub>x</sub>) and reduced (NH<sub>y</sub>) fractions taken from (HELCOM 2009f), see Table 2.8 below for explanation of regional acronyms.



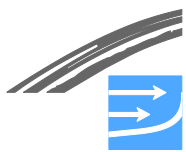


Table 2.8 Average atmospheric deposition of total nitrogen in 1995-2009 after (HELCOM 2009f) in relation to nitrogen riverine loads in 2006 after (HELCOM 2009a) and to sea surface according to (HELCOM 2002). Regional acronyms refer to Fig. 2.22.

Sub-basin	Sea surface	River loads	Atmospheric deposition		
			absolute	relative	ratio
	km <sup>2</sup>	kt	kt	t/km <sup>2</sup>	%
Gulf of Bothnia (GUB)	115,510	109	30 ± 5	0.26	23
Gulf of Finland (GUF)	29,600	130	12 ± 2	0.40	8
Gulf of Riga (GUR)	16,330	58	9 ± 1	0.55	13
Baltic Proper (BAP)	211,070	228	115 ± 10	0.54	33
Belt Sea (BSE)	42,410	102	22 ± 2	0.97	40
Kattegat (KAT)			18 ± 2		
<b>Baltic Sea</b>	<b>414,920</b>	<b>627</b>	<b>206 ± 19</b>	<b>0.50</b>	<b>33</b>

The atmospheric deposition of phosphorus to the Baltic Sea is often neglected based on the assumption that the contribution is only 1-5% of riverine loads (HELCOM 2006). Even the EMEP monitoring does not provide current data on atmospheric phosphorus inputs. A recent study by Rolff et al. (2008) analyzed nitrogen and phosphorus deposition measurements during 2001-2002 at four observational sites in the Baltic, one at the Swedish coast and three on island in the open sea. The observed deposition rates for total phosphorus show a large range of variation between 0.0028-0.0158 t/km<sup>2</sup>/year, with higher deposition near the coasts. The N/P ratio of atmospheric inputs is found between 50-200, indicating that phosphorus loads are relatively small compared to nutrient river discharge with N/P around 20-30 (see Table 2.7). However, extrapolated onto the whole Baltic Sea surface the observed deposition rates lead to atmospheric phosphorous loads of 1-6 kt/year (rivers around 30 kt/year). This input should not be neglected because it can contribute to local effects, for instance in sustaining cyanobacteria blooms during summer by providing phosphorus to the nutrient depleted surface layer.

## 2.4 Meteorological conditions in the Baltic Sea area

As for any sea, the state of the Baltic Sea depends essentially on the forcing driven by the meteorological conditions in the overlying atmosphere. The main control parameters are air pressure, air temperature, cloudiness, humidity, precipitation, and wind.

Pressure gradients in the atmosphere determine direction and strength of the wind, which generates waves at the sea surface and pushes currents in the sea. Moreover, air pressure has an influence on the elevation of the sea surface, an excess pressure of 1 hPa corresponds to a sea surface depression of 1 cm, approximately. However, large sea level fluctuations are caused by wind driven transports and wind setup at the coasts. The decay of wind input by breaking waves and internal friction provides turbulent energy to the sea which contributes to internal mixing. Cloud cover controls the amount of direct solar irradiation which inputs thermal energy to the water body and maintains photosynthesis by algae. The thermal stratification and the heat fluxes across the sea surface are influenced by the air temperature and the humidity of the atmosphere. Heating during summer stabilizes the water column, whereas cooling during autumn and winter leads to deep mixing by convection. But in a brackish sea, like the Baltic Sea, heating in spring also yields convection because of the anomaly of the sea water density. Air temperature also determines the amount of sea ice. Precipitation implies an input of fresh water (and possibly of dissolved nutrients and pollutants, see sections 2.2 and 2.3), to the sur-



face layer, which is counteracted by evaporation from the sea. As indicated by these examples, all interactions between atmosphere and sea involve several control parameters. Moreover, the coupling is interactive – the state of the atmosphere depends on the underlying sea. The quantification of the energy and material fluxes across the sea surface yields different, non-linear relationships with a rather high uncertainty, albeit based on observations. There is for instance a variety of relations for estimating the wind stress transferred to the sea from the wind in 10 m height. Therefore, the discussion is focused on meteorological quantities which are directly derived from measurements.

Meteorological forcing is especially effective in a marginal sea like the Baltic Sea. Coastal regions and shallow basins are subject to total mixing by stormy winds. Because of the strong stratification of the brackish sea water, the spatial scale of dynamic response patterns, like eddies and coastal currents, is only some 1-5 km, see (Fennel et al. 1991). Hence, even small basins, like the Mecklenburg and Lübeck Bights, develop local currents which vary quickly with changing weather on the time scale of days. The long-term fluctuations of the meteorological conditions, as for instance the seasonal cycle, affect the whole Baltic Sea. Consequently, time scales between hours and inter-annual variations have to be considered to characterize the forcing and the response of the Baltic Sea.

#### **2.4.1 Observational and model data**

The description of the meteorological conditions over the open Baltic Sea is hampered by the limited availability of observations. Continuous long-term time series were only taken by meteorological services at coastal stations and islands. The main source of information from open sea is the weather reports taken by voluntary observing ships. Compiled ship data sets are provided by the ICOADS (International Comprehensive Ocean-Atmosphere Data Set) web site (ICOADS 2010). Since the 1990s satellites and self-sustaining buoys are delivering open sea data. Because measurements are often scattered or interrupted by device failure or environmental impact, weather models, which are checked by observations, provide complementary data sets, comprehensive in space and time.

The atmospheric forcing conditions over the Baltic Sea will be described on the basis of ship data compiled by (Miętus 1998), some available meteorological stations, and the SN-REMO downscaling (Feser et al. 2001), which was used to drive the regional Baltic Sea models for the period 1970-2007. The reliability of SN-REMO model data was estimated by comparing with observations on different time scales.

(Miętus 1998) compiled a meteorological data set for the climate period 1961-1990 from voluntary ship observations. This data set is provided by web site (ICOADS 2010). The data are concentrated around the main shipping routes. Thus central and southern Baltic Proper are well covered, whereas data density is sparse in the northern Baltic Sea (see Fig. 2.23). Because temporal resolution is arbitrary, these data can be used to calculate climatological monthly and seasonal means. For locations with high data density monthly mean values may be derived. This has been applied to calculate a monthly time series for a pseudo-station in the Eastern Gotland Basin, which describes the typical weather conditions in the Central Baltic Proper.



Table 2.9 List of meteorological stations for which data of air pressure (P), air temperature (T), wind (W), cloudiness (C), relative humidity (R) and precipitation (N) were available. Frequency denotes basic time resolution. DWD refers to German Weather Service. The data record for Eastern Gotland Basin is derived from Miętus (1998). Tables of climatological monthly means at Swinoujscie, Utö, and Kemi, were taken from (Leppäranta and Myrberg 2009).

Station	Longitude	Latitude	Period	Frequency	Data coverage
Darss Sill mast (IOW)	12°42'E	54°42'N	2000-2010	hourly	87-91% (T,W,R)
Arkona Sea buoy (IOW)	13°52'E	54°53'N	10/2002-2010	hourly	87-89% (P,T,W,R)
Heligoland (DWD)	07°53'E	54°10'N	1952-2010	daily	65% (P,T,W,C,R,N)
Warnemünde (DWD)	12°04'E	54°01'N	1947-2010	daily	56% (W) 94-100% (T,W,C,R,N)
Greifswald (DWD)	13°24'E	54°02'N	1947-2010	daily	51-57% (P,T,W,C,R,N)
Eastern Gotland Basin	20°00'E	57°30'N	1961-1990	monthly	66% (P,T,W,C,R)
Swinoujscie	14°10'E	53°52'N	1961-1990	clim. monthly means	(T,W,C,R,N)
Utö	21°23'E	59°47'N	1961-1990		
Kemi	24°35'E	65°47'N	1961-1990		

The available data sets from meteorological stations, listed in, were selected for the following reasons:

- station located at open sea or near the coast at sea level,
- and availability of multi-year time series.

The first criterion is relevant, since meteorological measurements at land are biased by effects from the relief of the landscape. This bias plays a role in the narrow channels and the small basins of the Belt Sea because of the near coasts, but it is assumed to be small at Darss Sill and negligible in the centre of Arkona Sea, see Fig. 2.19. The stations Darss Sill and Arkona Sea belong to the German monitoring network MARNET operated by IOW on behalf of Federal Maritime and Hydrographic Agency (BSH). These are two open sea records with a data coverage around 90% running from February 2000 and October 2002 until now. The time resolution of one hour corresponds to the SN-REMO model data. Measurements from the buoy in Fehmarnbelt, provided by BSH, were not used because only 10-22% of the period is covered by data. The daily time series provided by German Weather Service (Deutscher Wetterdienst, DWD) are long-term records at coastal stations covering the period from 1947 until now. Heligoland, located in German Bight in North Sea, was included in order to take into account one more open sea station. These data as well as Darss Sill and Arkona allow for the consideration of long-term averages like climatological monthly and seasonal means and the discussion of inter-annual variations.

SN-REMO is a recent regional downscaling project run at GKSS Research Center Geesthacht, Germany. The model provides atmospheric fields with hourly time resolution for the period 1948-2007 covering Europe, see (Feser et al. 2001) and Weisse et al. (2005). It relies on the regional weather model REMO with a ground resolution of 0.5 degrees, corresponding approximately to a grid spacing of 56 km

in latitude, and around 30 km in longitude. This is rather coarse with respect to the geographical structure of the Belt Sea.

With respect to the northern Baltic Sea we refer to the description of “Weather and climate in the Baltic Sea region” in the book by (Leppäranta and Myrberg 2009) who also applied the Miętus (1998) data. The climatological monthly means for Swinoujście, Utö and Kemi are cited from this source.

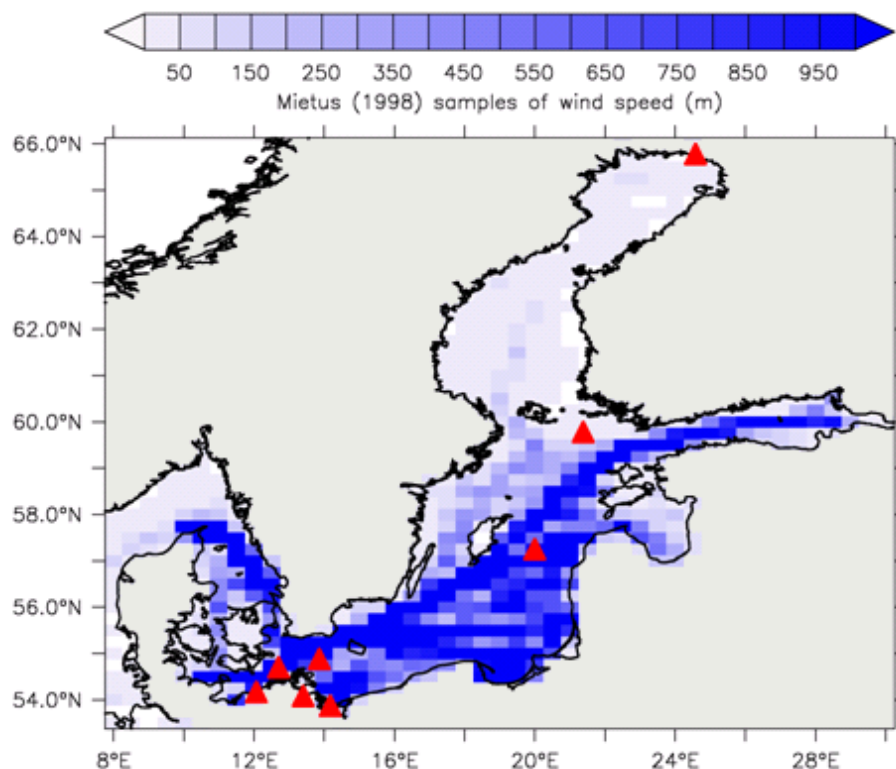


Fig. 2.23 Number of wind speed samples from voluntary ships compiled for ICOADS by Miętus (1998). Red symbols indicate location of meteorological station from west to east: Warnemünde, Darss Sill, Greifswald, Arkona Basin, Swinoujście, Eastern Gotland Basin, Utö, and Kem, see Table 2.9. (Heligoland in North Sea not shown.)

#### 2.4.2 Typical transient weather patterns

On daily time scale weather conditions are usually classified as “Grosswetterlagen” based on the large-scale distribution of air pressure, characterized by “lows” and “highs” which are accompanied by cyclonic and anticyclonic wind systems. Intersections fronts between cold and warm air often lead to heavy precipitation. The example shown in Fig. 2.24 is taken from the classification used by Deutscher Wetterdienst (DWD) as described by (Gerstengarbe and Werner 2005). It represents a typical weather pattern where a low over Scandinavia and a high over Spain lead to strong westerly winds over the Baltic Sea. Fig. 2.25 demonstrates that this pattern is well reproduced by the SN-REMO model data.

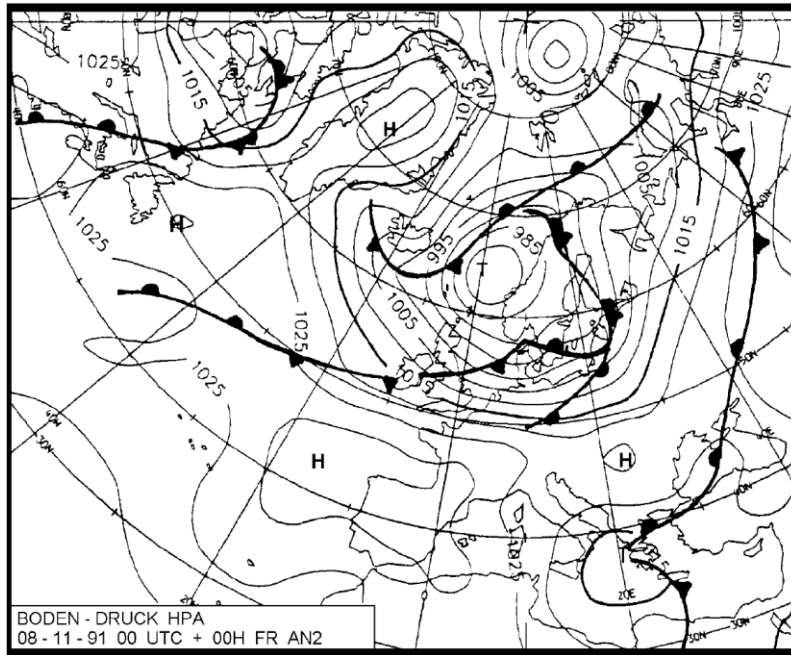


Fig. 2.24 A typical cyclonic weather pattern over Europe taken from the classification of Deutscher Wetterdienst (DWD) by (Gerstengarbe and Werner 2005).

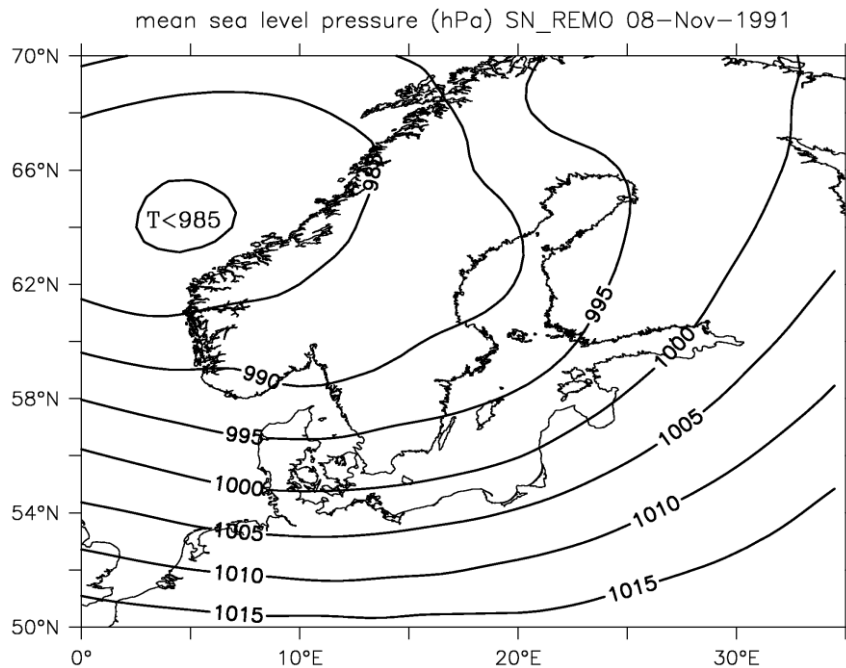


Fig. 2.25 The cyclonic weather pattern of 8 Nov. 1991 simulated by SN-REMO, compare to Fig. 2.24. Note different area and map projection.

After Tiesel (2008) other typical pattern in the Baltic region are high pressure fields of Omega shape providing long-lasting calm weather, whereas cyclonic tracks of the Vb type (after the classification scheme introduced by (van Bebber 1819) often are connected with dangerous stormy winds and heavy precipitation events. Examples are the exceptional storm surge in the southwestern Baltic in 1872 and the flood in 2002, which lead to a strong outflow of polluted water from Oder river. Even the calm Omega conditions may have hydrographical implications. E.g. the re-



cently observed baroclinic warm inflows of saline water into the Baltic in 2002 and 2003 occurred under such forcing.

### 2.4.3 Seasonal meteorological conditions over the Baltic Sea

The typical long-term meteorological forcing conditions over the Baltic Sea are discussed with seasonal resolution in order to characterize the annual variation. The meteorological seasons refer to December, January, and February (DJF) for winter, March, April, May (MAM) for spring and so on. The following figures were derived from SN-REMO model fields, which provide continuous time series comprising the whole Baltic area. Climatologic averages refer to the full SN-REMO period 1948-2007. The discussion will show that the model reflects regional and seasonal differences in a realistic way. Moreover, the forcing applied for long-term runs of Baltic Sea models is characterized.

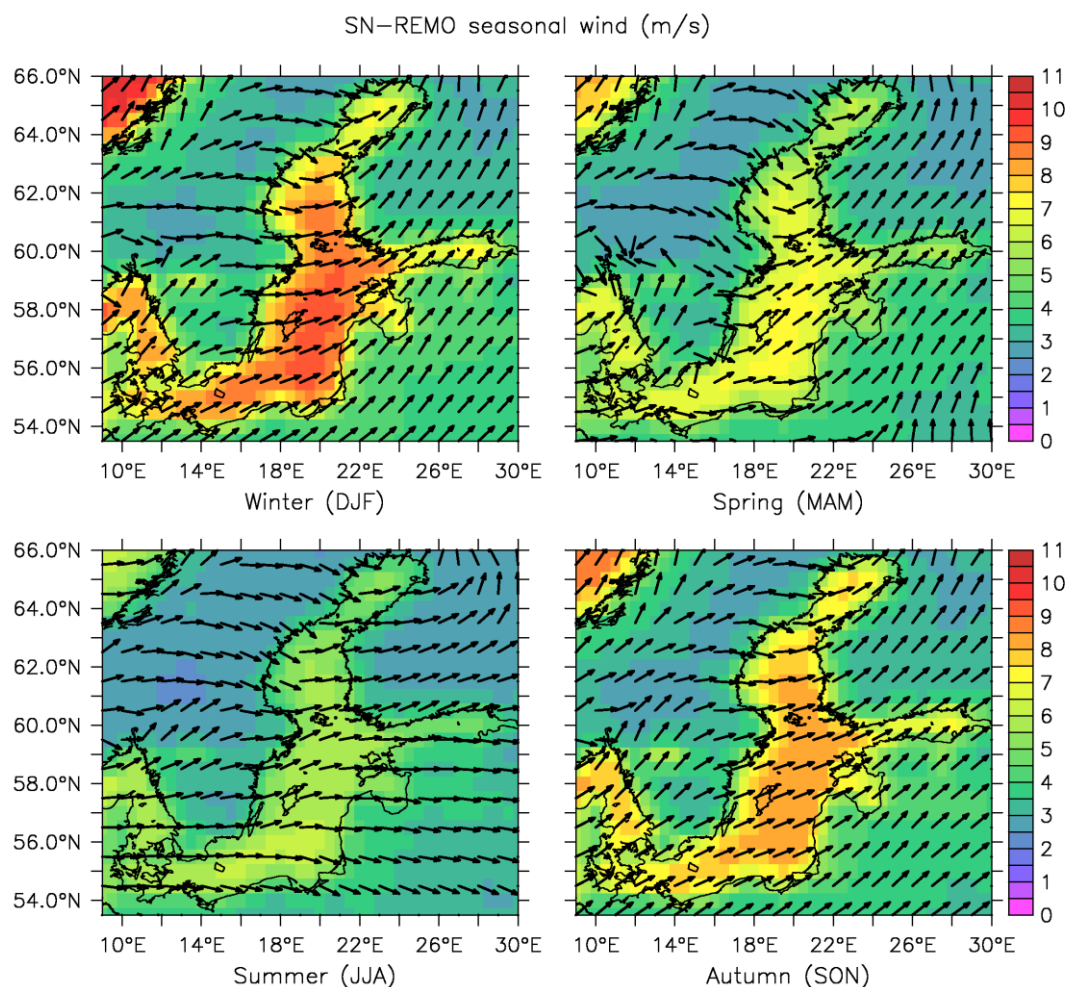


Fig. 2.26 Seasonal wind over the Baltic Sea. Colours depict the seasonal mean of absolute wind speed (m/s) and unit arrows indicate the direction of the mean wind vector (note vector length independent of wind speed).

The seasonal wind fields over the Baltic are displayed in Fig. 2.26, where unit arrows indicate the mean vectorial wind direction and colors corresponds to the seasonal mean of absolute wind speed. Wind speed shows a clear seasonal cycle and a distinct land-sea contrast even in the rather coarse SN-REMO model grid. Enhanced wind speed is resolved for all Baltic basins. Maximum wind occurs in the central Baltic Proper where the fetch length, i. e. the distance from land is largest. The seasonal variation is characterized by mean wind speed around 9, 7, 6, and 8 m/s





during winter, spring, summer, and autumn in the Eastern Gotland Basin at 20°E and 57°N. This agrees well with the seasonal Baltic winds redrawn from Miętus (1998) in the book of (Leppäranta and Myrberg 2009). Realistic wind is crucial for modeling since the energy input on waves and currents go with the second power of wind speed. A small bias, as found for the control stations, may be compensated by tuning the parameterization applied for calculating wind stress. In contrast to wind speed, the variation of wind direction shows only a weak seasonal signal. In accordance to the sketches after (Miętus 1998), southwesterly winds are predominant over the Baltic Sea in winter, summer, and autumn. During spring SN-REMO predicts also the tendency to circular winds in southern Baltic and Bay of Bothnia. However, the model wind is too directional emphasizing western and eastern wind components. Easterly winds, which may yield a substantial lowering of the Baltic Sea level as a typical pre-condition for saline inflows (see Matthäus & Schinke, 2004), if lasting for days to weeks, are not seen in seasonal averages, because westerly winds prevail during the whole year.

**Frequency classes of mean wind speed and direction from 2002 to 2010 at Arkona Basin**

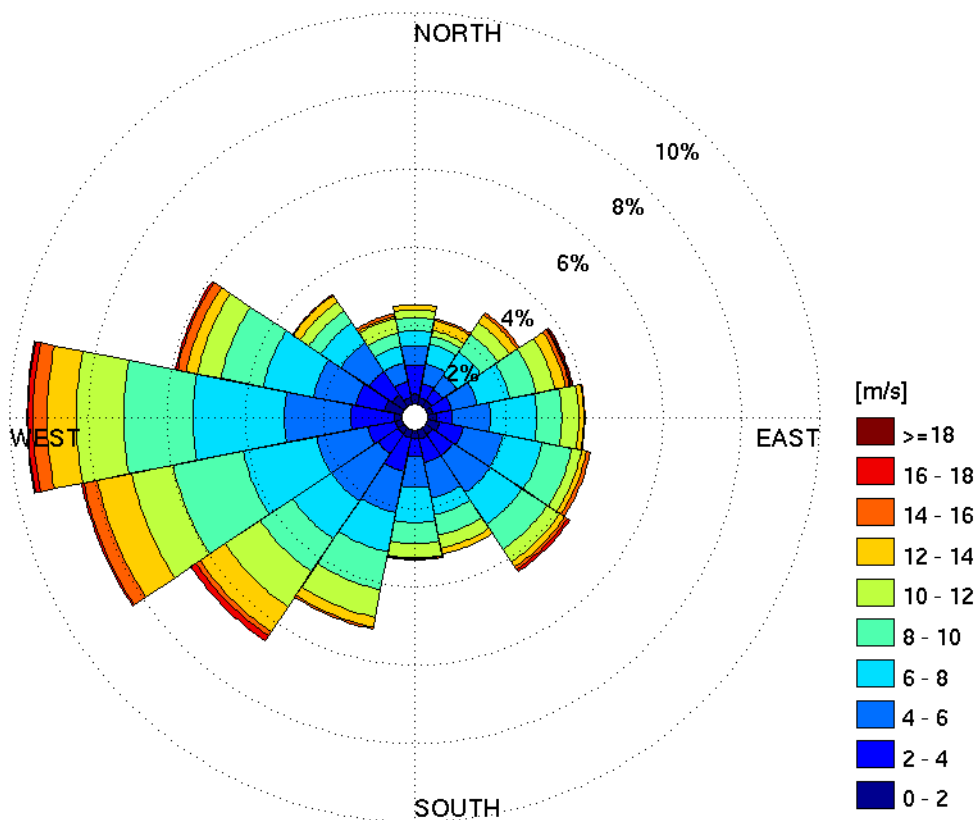


*Fig. 2.27 Rosette plot of daily mean wind vectors observed at Arkona station. Classification into 16 directional bins reveals frequent occurrence of westerly to southwesterly winds.*

The observed distribution of wind direction is displayed in Fig. 2.27 for the open sea station in Arkona Basin. The size of sectors corresponds to the frequency of occurrence and color indicates the wind speed. Thus, the predominance of westerly to southwesterly winds is obvious, but the occurrence of even strong winds from east-

erly to southeasterly and northwesterly directions is also clearly seen. The annual mean speed is 7.2 m/s at this station.

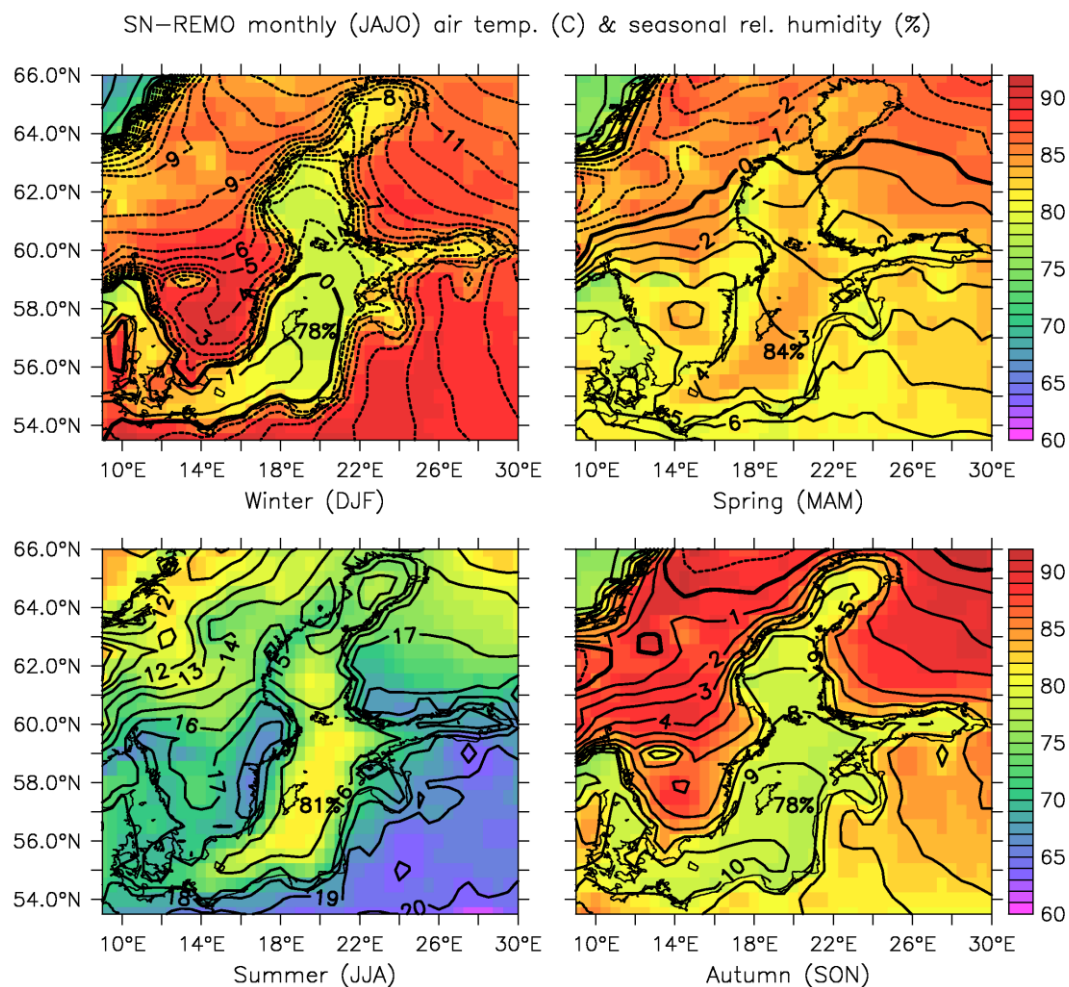


*Fig. 2.28 Climatological monthly means of air temperature (isolines in °C) over seasonal mean relative humidity (%). (JAJO) refers to the central months of the seasons: January, April, July, and October.*

Since air temperature follows a strong annual variation, it is represented in Fig. 2.28 by the climatological average of the central month of the season, i.e. for January, April, July and October. Nevertheless, the correlation to relative humidity is obvious, which is shown on seasonal scale by colors. Both parameters show a distinct land-sea contrast and a seasonal cycle. Air temperature differences between land and sea are strongest during summer and winter, when the sea stores or releases thermal energy. Heat release keeps the mean air temperature over central to southern Baltic and over Kattegat above zero and even in Gulf of Bothnia the isolines of decreasing air temperature are deflected to north. The zero isoline of air temperature in January and April roughly indicates the area of regular seasonal ice cover. The Baltic Proper below 59°N is affected only during severe winters, when negative air temperatures last over weeks. In July monthly mean air temperature is around 16°C in the central Baltic and between 14-15°C in the Gulf of Bothnia, however, this average signal is superposed by a daily temperature cycle of up to -5 to +10°C. The weak annual variation of relative humidity is indicated in Fig. 2.28 by 78%, 84%, 81% and 78% at 20°E and 57°N in the Baltic Proper which is biased by -5 to -10% in comparison to station measurements. Anyway, the land-sea contrast



of higher humidity over sea in spring and summer, and lower humidity during autumn and winter, is well reflected by SN-REMO.

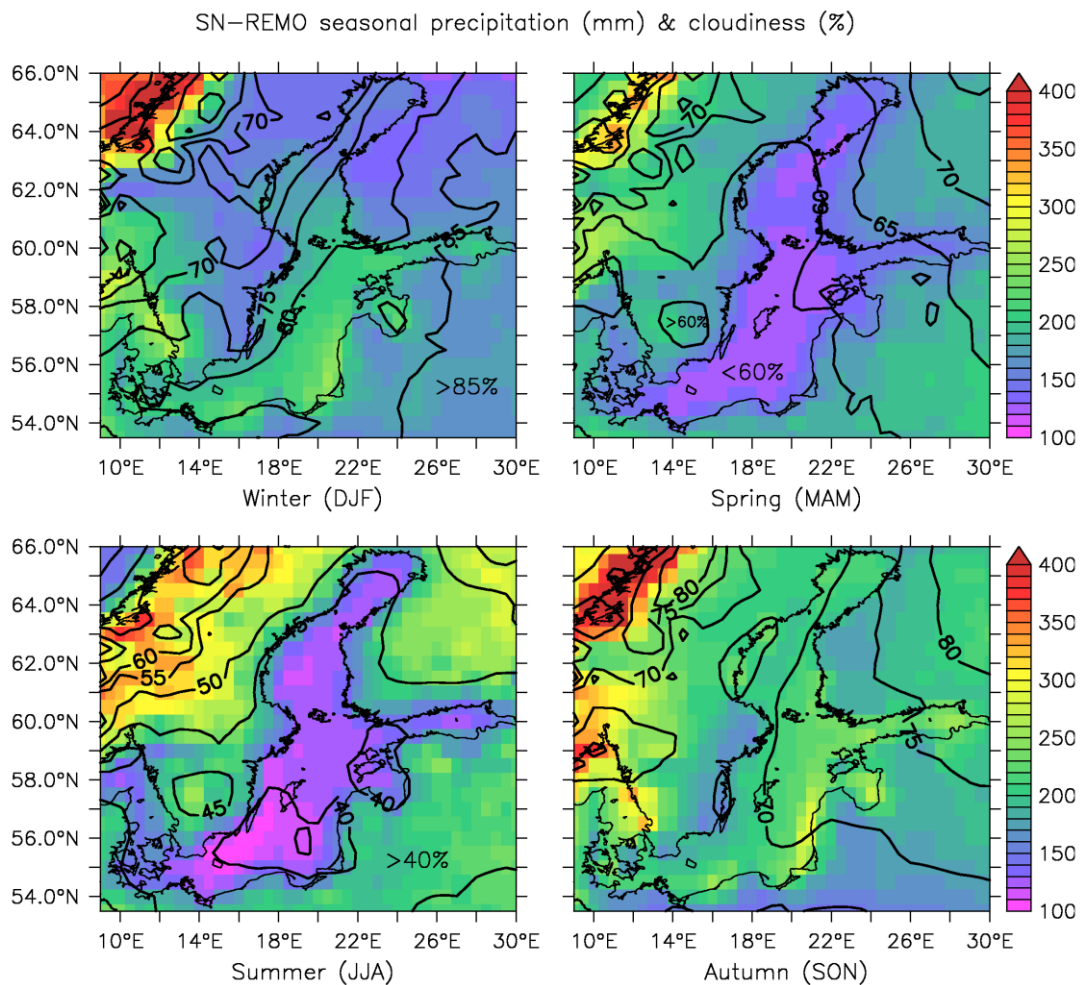


Fig. 2.29 Mean seasonal sum of precipitation (colours in mm) and average cloudiness indicated in 5% steps by isolines as predicted by SN-REMO for 1947-2007.

SN-REMO provides distributions of cloudiness and precipitation which reveal distinct regional and seasonal patterns as seen in Fig. 2.29. During spring and summer precipitation is substantially less over sea (<150 mm) than over adjacent land areas (>200 mm). Maximum precipitation occurs over Kattegat and Baltic Proper in autumn and winter, especially at eastern coasts which are exposed to cyclones accompanied by westerly winds. This effect is evident, albeit the Baltic Sea is sheltered against heavy weather coming in from the Atlantic by the Scandinavian mountains and the Danish islands. The regional minimum along the western coasts of Sweden between 56-60°N suggest that the Baltic Sea may enhance precipitation from passing cyclones. This is well known for heavy snowfall at the German coasts occurring if tracks go from northeast to southwest across the whole Baltic Proper, see Tiesel (2008). As a consequence of seasonal ice cover, precipitation is rather uniformly distributed in the area of the Bothnian Bay and Bothnian Sea during autumn and winter.

In general, the seasonal patterns and the substantial differences between land and sea imply that precipitation over sea might not easily be interpolated from stations at coasts and land. This has already been emphasized by the estimation of the water balance of the Baltic Sea by (HELCOM 1986). A rough map for the period 1931-



1960 shows annual precipitation over sea in the range of <600 mm till >700 mm (not shown) with a similar regional distribution as the SN-REMO weather model. Data based precipitation over the Baltic Sea has been calculated by (Lindau 2002) from ICOADS weather observations onboard ships for the period 1980-1995. The monthly averages range from 10 mm/month to 150 mm/month around a total mean of 50 mm/month, which corresponds to 150 mm/season or 600 mm/year. The data reveal a weak annual variation from 30 mm/month in spring to 60 mm/month in summer and autumn, and precipitation is around 50 mm/month during winter. Evaporation over the Baltic Sea shows an opposite seasonal signal, leading to an annual excess of precipitation of 65 mm/year.

Table 2.10 Regional contribution of precipitation minus evaporation (P-E), 1980-1995, after Lindau 2002) in relation to annual mean river runoff (HELCOM 2009c) in 1950-2008.

Basin	Area (km <sup>2</sup> )	Lindau P-E		HELCOM river runoff (km <sup>3</sup> /year)	(P-E)/river (%)
		mm/month	(km <sup>3</sup> /year)		
Bothnian Bay	35,640	12.0	5.1	100	5.1
Bothnian Sea	79,640	7.0	6.7	90	7.4
Gulf of Finland	29,750	5.0	1.8	112	1.6
Gulf of Riga	18,580	0.0	0.0	32	0.0
Baltic Proper	206,050	3.5	8.7	112	7.8
Belt Sea, Sound	21,690	14.0	3.6	7	51.4
<b>Baltic Sea (excluding Kattegat)</b>	<b>391,350</b>	<b>5.5</b>	<b>25.8</b>	<b>453</b>	<b>5.6</b>

The difference P-E between precipitation and evaporation is regionally distributed over the Baltic Sea from high values of 12-14 mm/month in the North and over Belt Sea to a balance around zero in the central Baltic Sea. The (P-E) data specified in Table 2.10 are estimated areal means from a map provided by (Lindau 2002). The absolute contribution of P-E to the water balance is only some km<sup>3</sup> per year. This corresponds to 5-8% of the fresh water input by rivers to the Gulf of Bothnia and the Baltic Proper, which is representative for the total mean of the Baltic Sea. Because of its small area and strong river runoff the ratio is only 1.6% in the Gulf of Finland and negligible in the Riga Gulf. However, in Belt Sea the net atmospheric fresh water flux is comparable with the river input.

The large-scale distribution of cloudiness derived from SN-REMO, shown in Fig. 2.29, resembles the seasonal plots after Miętus (1998). The local minima and maxima suggested by Miętus (1998) for Baltic basins are smoothed out in the model fields, however, the minimum cloudiness (<65%) in autumn along the Swedish coast off island Öland and in Bothnian Sea between 60-64°N is reproduced. The bias around -10% is obvious for summer when the model predicts only 40-45% cloud cover over the Baltic Sea. During winter, spring, and autumn, the mean cloudiness is more realistic around 80%, 60% and 70%, respectively.

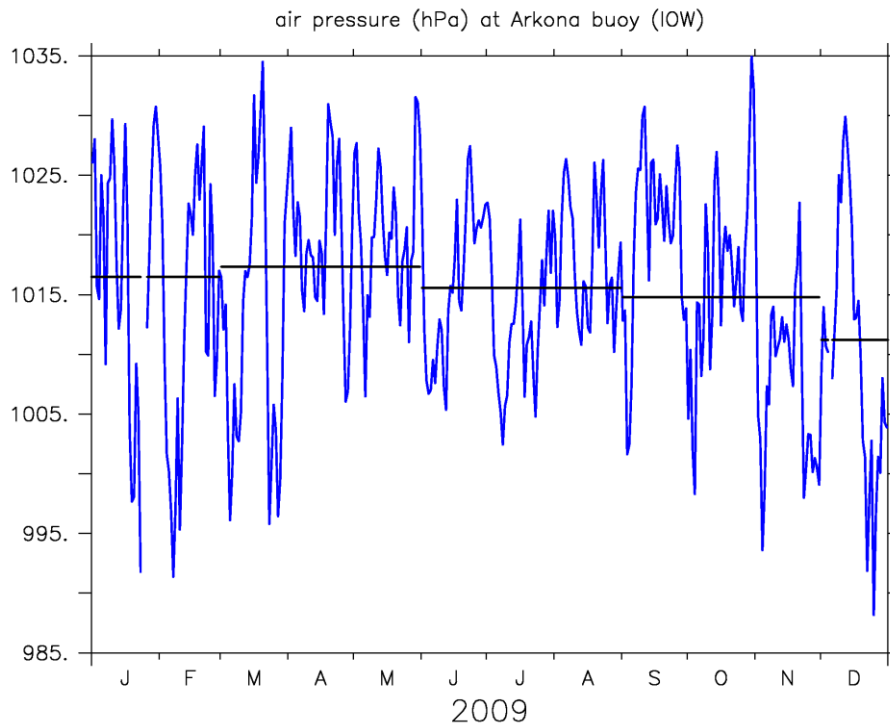


Fig. 2.30 Daily mean air pressure (hPa) observed in 2009 at buoy station in Arkona Basin. Horizontal black lines indicate seasonal averages.

Seasonal distribution of air pressure is not shown, because lows and highs varying on daily time scale, are completely smoothed out. The remaining background signal is an average north to south pressure gradient between 1009-1013 hPa in winter, 1010-1014 hPa in autumn, and only 1010-1012 hPa in summer. During spring the mean air pressure over the Baltic Sea is around 1013 hPa. An example for the daily variation of air pressure is shown in Fig. 2.30 based on the observations at the open sea buoy station in Arkona Basin. Seasonal means, indicated by horizontal lines, vary within 5 hPa. The smallest seasonal variation occurs in summer. The higher variation of air pressure during autumn and winter is caused by strong cyclones (low air pressure) which are accompanied by tempestuous winds.

#### 2.4.4 Inter-annual variations

Finally, the long-term meteorological forcing of the Baltic Sea is characterized by the behavior of yearly mean air temperature and wind speed over the Baltic Proper. The curves displayed in Fig. 2.31 represent areal means of the SN-REMO predictions comprising the region 14-24°E and 54-60°N.

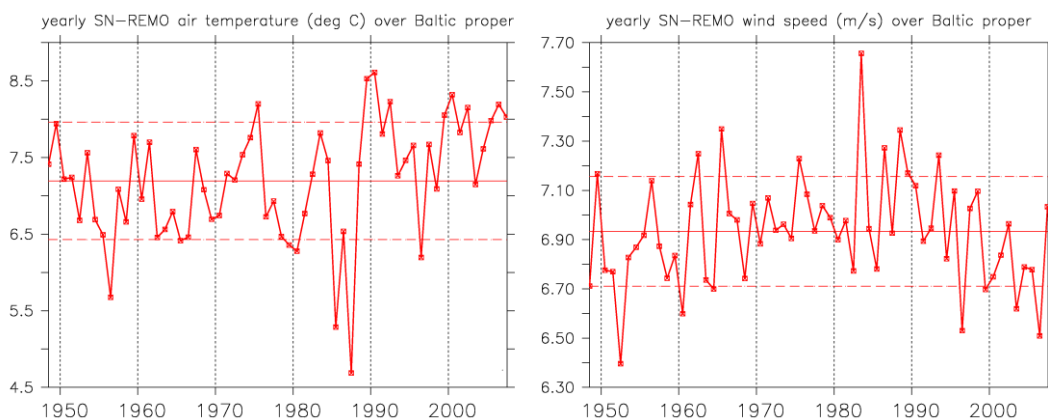


Fig. 2.31 SN-REMO model prediction of yearly mean air temperature (left panel) and wind speed (right panel) over the Baltic Proper.

The range of variance of yearly averages is again indicated by  $\pm 1$  standard deviation, depicted as dashed lines in Fig. 2.31. With respect to that, 1956, 1985-1987, and 1995 may be considered as exceptionally cold years. On the other hand, the frequent excess of the upper data range after 1990 clearly illustrates the increasing temperature trend in recent years. In contrast to air temperature wind speed shows an intermittent maximum between 1970-1990 and a decreasing trend afterwards. The enhanced mixing by stronger wind forcing explains the increase of surface salinity within the Baltic Proper observed in the same period, see (Feistel et al. 2008a). Regional model runs of the Baltic Sea forced with SN-REMO reproduce this effect in surface salinity.





### **3 HYDROGRAPHICAL STATE OF THE BALTIC SEA**

#### **3.1 Sea Level**

##### **3.1.1 Introduction**

The water levels in the North Sea – Baltic Sea system is determined by, see (Jacobsen 1980) where a review of literature up to year 1980 can be found, and (Lass et al. 1987):

- Tides propagating from the Atlantic Ocean into the North Sea and further into the Baltic Sea;
- River inflow to the Baltic Sea;
- Density differences due to differences in salinity and temperature;
- Wind set-up and barometric pressure conditions in the Baltic Sea and the North Sea, respectively;
- Seiching in the two seas due to changing wind fields (see, e.g., (Wübber and Krauss 1979); and
- Climate change.

Some of these topics are treated in detail elsewhere in the report and will only be mentioned briefly in the following.

##### **3.1.2 Tides**

Tides propagate from the Atlantic Ocean into the North Sea and further into the Baltic Sea. Along their path the tidal amplitudes increases, because of reduced water depth (shoaling), and decreases, because of bed friction (energy dissipation). In Kattegat at Hornbæk the tidal amplitude, or intensity coefficient, is 15 cm (sum of four tidal constituents: M2 + S2 + K1 + O1). The amplitude decreases through the Danish Straits and is 7.5 cm at Gedser. Inside the Central Baltic Sea the amplitude is less than 5 cm.

Hence the tides contribute to the water level variation. Inside the Central Baltic Sea the contribution is maximum  $\pm 7.5$  cm.

##### **3.1.3 River inflow**

The river inflow to the Central Baltic Sea lifts the water level to be higher inside the Central Baltic Sea than in the Kattegat and the North Sea. The water level lift is nearly constant inside the Central Baltic Sea, but varies over the Danish Straits. Because of the river inflow the water level is lifted to be located about 4 cm higher in the southwestern Baltic Sea than in the Kattegat (calculated by the energy equation and the resistance of the Danish Straits; see also Fig. 3.2 for a numerical simulation of water levels in the Baltic Sea).

##### **3.1.4 Density difference**

The salinity at the sea surface increases from 0-3 psu in the innermost of the Baltic Sea to a mean value of 24.8 psu in Kattegat at Læsø Nord. The higher the salinity the higher the density (ignoring the variation in temperature) and hence the density of the water increases from its minimum value at the innermost Central Baltic Sea towards the North Sea. The biggest salinity and density gradients are found at



the Danish Straits, where the salinity increases from 8 psu in the southwestern Baltic Sea to 25 psu in the Kattegat.

The density variation causes a water level lift. The highest lift is found in the innermost of the Baltic Sea wherefrom it decreases gradually towards the North Sea. The water level is located about 4 cm higher in the southwestern Baltic Sea than in the Kattegat, because of the density differences (calculated by the momentum equation).

Hence the total lift from river inflow and density difference is from 4 cm to 8 cm (the contributions should not simply be added). From measurement it is found to be 6 cm (Jakobsen et al., 1997; Jakobsen & Trébuchet, 2000; and Jakobsen et al., 2010), but the value is uncertain.

### **3.1.5 Wind set-up**

High and low air pressures fields pass Scandinavia on a weekly time-scale and set-up or set-down the water levels in the North Sea and Baltic Sea.

An example of a typical low pressure field is shown in Fig. 3.1 below. The related wind field causes set-ups and -downs in the North Sea and Baltic Sea, respectively, with:

- High water levels along the west coast of Jutland and in the Skagerrak and Kattegat;
- Low water levels in the Arkona Basin; and
- High water levels in the northeastern Baltic Sea.

The actual value of high and low water levels depends on the air pressure and wind fields (the wind shear stress on the sea surface increases with the wind speed to power 2). It is remarked that high water levels in Kattegat and low water level in the Arkona Basin forces an inflow to the Baltic Sea.

If it instead is a high air pressure field the situation is reversed with:

- Low water levels along the west coast of Jutland and in the Skagerrak and Kattegat;
- High water levels in the Arkona Basin; and
- Low water levels in the northeastern Baltic Sea.

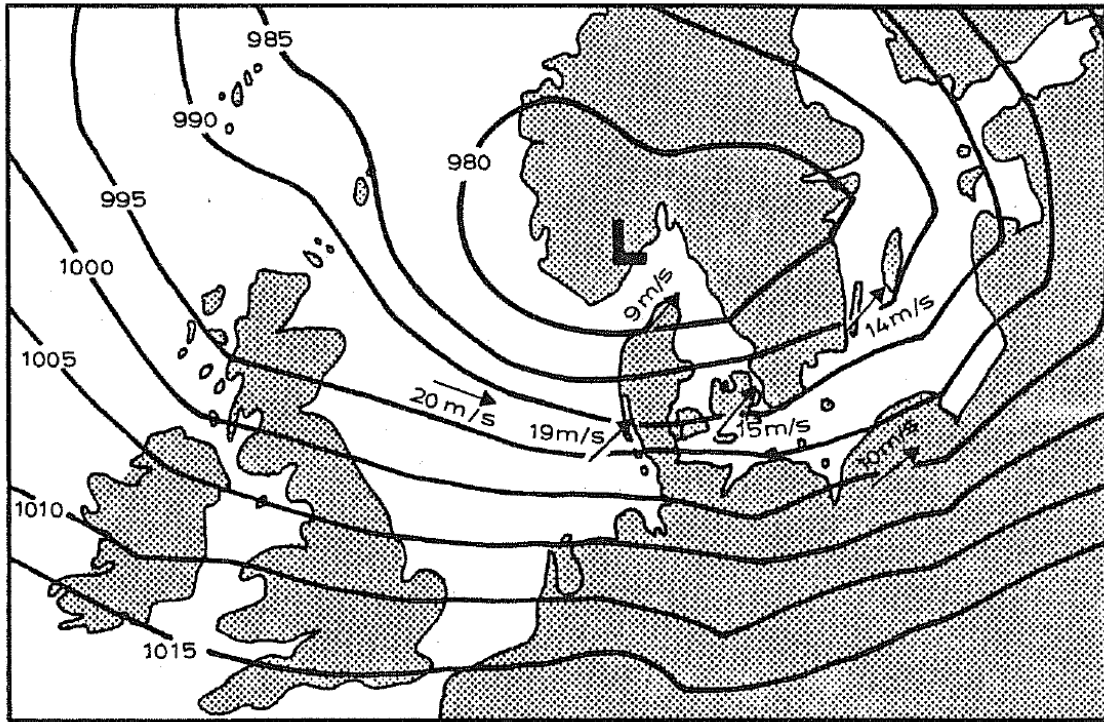
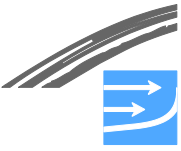
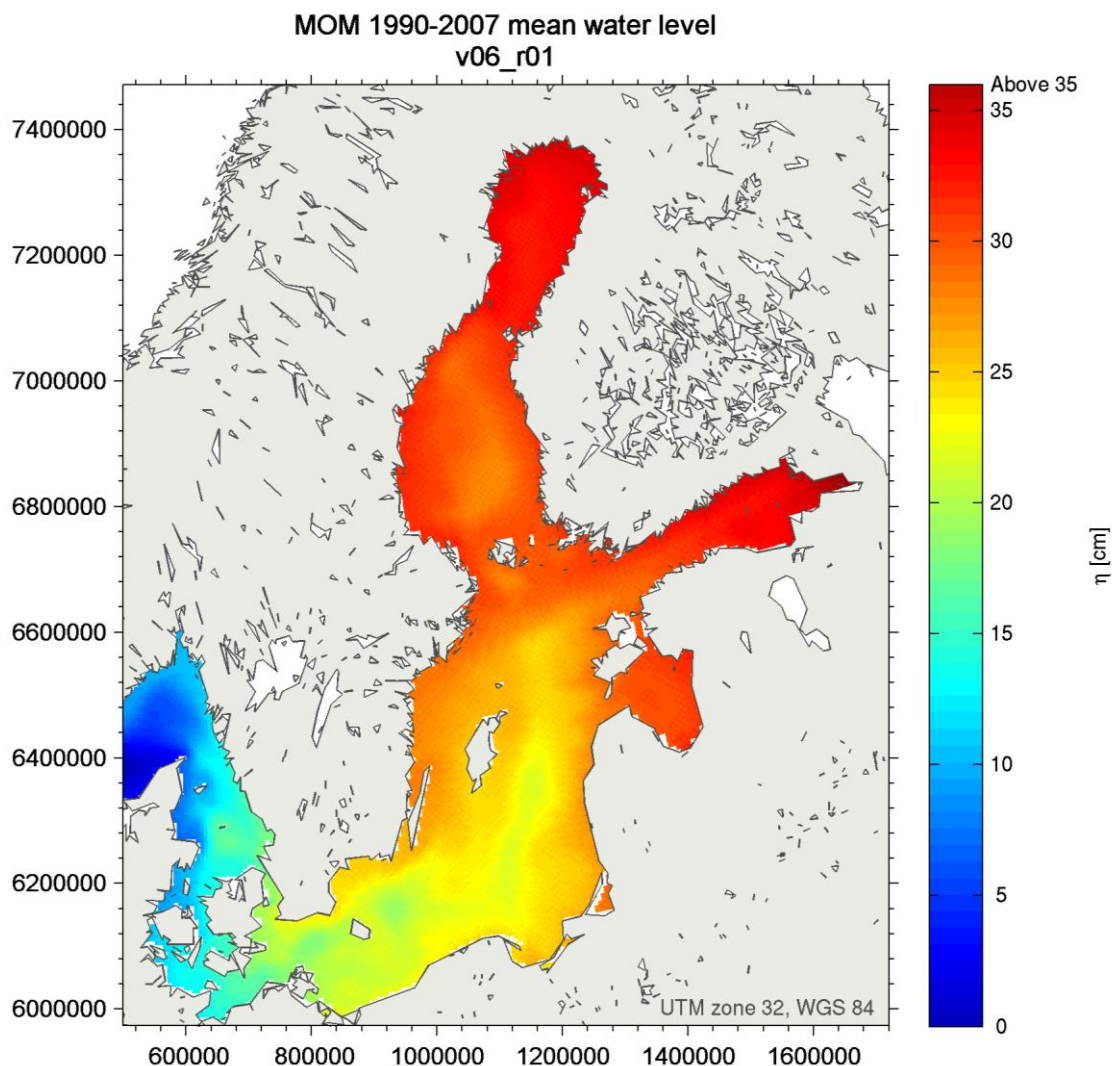


Fig. 3.1 Low air pressure field over the North Sea - Baltic Sea system (from 24 December 1977 at 12:00).



*Fig. 3.2 Mean water level (1990-2007) of the Baltic Sea simulated with the MOM numerical model (FEHY, 2013c). A clear gradient between the northern Baltic Sea and the Kattegat is visible. Local depressions due to large gyres exist in sub-basins like the Bornholm Basin or the Bothnian Sea.*

It is remarked that the low water level in Kattegat and high water level in the Arkona Basin forces an outflow from the Baltic Sea.

### **3.1.6 Seiching**

As explained in the previous chapter, the wind can set-up and set-down water levels in the North Sea and Baltic Sea, respectively. When the wind changes or ceases two-dimensional seiches are generated, i.e. the wind set-up oscillates (and partly turns in a counter clockwise direction) in the North Sea and inside the semi-enclosed Central Baltic Sea.

The periods of the two-dimensional seiches in the Central Baltic Sea are (Wüßer and Krauss 1979):

- Mode 1: 31.0 hours;
- Mode 2: 26.4 hours; and
- Mode 3: 22.4 hours.



In general, the lower the mode is, the more important it becomes. Here in the sense that the lowest mode causes the largest water level variations.

It is noted that because of the seiching in the Baltic Sea high and low water levels can be observed some days after a storm.

### **3.1.7 Climate change**

It is anticipated that climate change will raise water levels and increase extreme storm wind speeds in the future (see Chapter 7). For example up to +1 m and + 3 m/s by year 2100. Both effects will lead to higher water levels in the Baltic Sea:

- if the water levels in the world oceans are raised by 1 m then it will cause the water levels in the Baltic Sea to be permanently raised by 1 m; and
- if extreme storm wind speeds are increased, then storm surge levels will go up. If storm wind speed for example is increased from 27 m/s to 30 m/s, then the storm surge set-up is increased by very roughly 23%.

### **3.1.8 Extreme water levels**

Storms cause extreme water level in the North Sea – Baltic Sea system. One such case occurred in the period 12-14 November 1872 (Colding 1881), see Fig. 3.3. The maximum water levels in the Fehmarnbelt during this storm are about 9 feet (2.7 m).



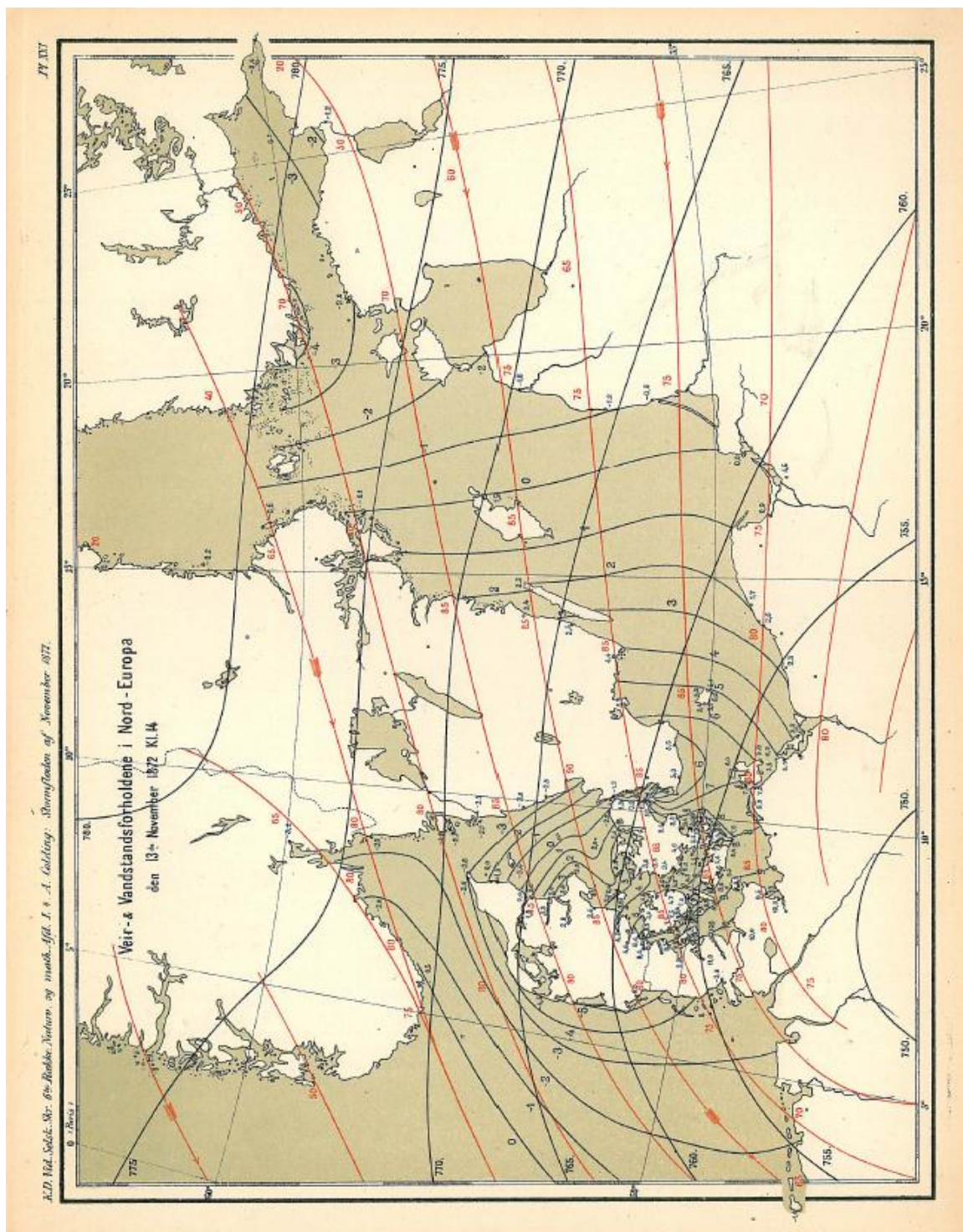


Fig. 3.3 Storm surge in the Baltic Sea on the 13 November 1872 at 14:00. From (Colding 1881).





## 3.2 **Waves and tides in the Baltic Sea**

Sverdrup and Munk (1947) presented a fundamental work for the study and prediction of surface waves. They analyzed observations about wave heights from ships' logs, and from these they derived prediction methods for wind sea, swell, and surf. During this work, it was discovered that observers on board a ship usually select and enter into the log only those wave features that significantly strike their eyes. In connection with studies of the statistical structure of the wind sea state, Longuet-Higgins (1952) found out that this wave height is equivalent to an average value that is composed of the upper third of the heights of all waves. Today this is generally called the significant or characteristic wave height, an important measure for the characterization of the sea state.

For decades, the interest in the sea state of the Baltic Sea has only been limited. In his "Handbuch der Wellen der Meere und Ozeane" (Manual of Sea and Ocean-Waves), (Bruns 1955) devotes only two pages to the waves in the Baltic Sea. He thus states (Bruns 1955, p. 103) that "only a small number of systematic wave measurements..." were performed....and a survey of the variability of the wave elements with the sea state or the wind conditions over many years is lacking." A wave of 9 m height was reported south of Öland island by (Bruns 1963) but a widespread opinion remained that sea state in the Baltic Sea is negligible and so it was studied only sporadically until the late 1960s (Schmager et al., 2009). Experimental, theoretical, and empirical sea state studies were initiated in the 1970s and forecast methods for wind seas in shelf areas were used to calculate tabular wave heights in the Baltic Sea. As of today, a broad spectrum of sea state information is available. Almost all Baltic Sea littoral states provide forecasts for a wide variety of different sea state parameters. Local ship-induced waves are treated in Chapter 6.2.1 of this report.

### 3.2.1 **Wind-induced waves**

Schmager et al. (2009) write: "Sea state is called wind sea, if it is stimulated by the wind and if it increases under the influence of the wind. If the wind speed decreases or the waves move out of the wind field, the appearance of the sea state on the sea surface becomes more even. This sea state is called swell." A schematic diagram of wind sea and swell is given in Fig. 3.4. Growth and height of the wind sea state are decisively influenced by changes in the average wind speed related to a height of 10m above sea level. A 10% increase in wind speed will result in a 10–15% increase in wave height, or in other words, an error of 10% in the determination of the wind speed results in a wave height error of the same order of magnitude (Schmager et al., 2009).

#### **Wave-generating factors**

The length of a wind field, in which the direction and speed of the wind are approximately constant, is called the *fetch*. In sea areas similar to the Baltic Sea, the wind direction determines this fetch and thereby the wave growth. If the development of wind-induced waves starts during offshore winds leeward of a coast, the wave heights will increase in the direction of the open sea, and the fetch is calculated from the distance to the coast. It is notable in this context that the dimensions of the wind field have to be such that the width of the field is at least equal to its length. In the Baltic Sea, such conditions are found only for easterly winds off the coast of the Baltic states and for southerly winds off the Polish coast (Schmager et al., 2009). Schmager et al. (2009) state also that "the values for the fetch in the Baltic Sea that are found in the relevant literature sometimes appear strikingly odd." Early calculations considering only the geometry of the water covered areas found fetch lengths of 700 km and values from other publications presenting fetches of more than 750 km are considered excessive. They state that maximum values of 350 km are realistic instead, as presented by Quandt (1980). Such extreme

fetches can occur in the Gdansk Depression and off the eastern area of the Polish coast for northerly and north-easterly winds.

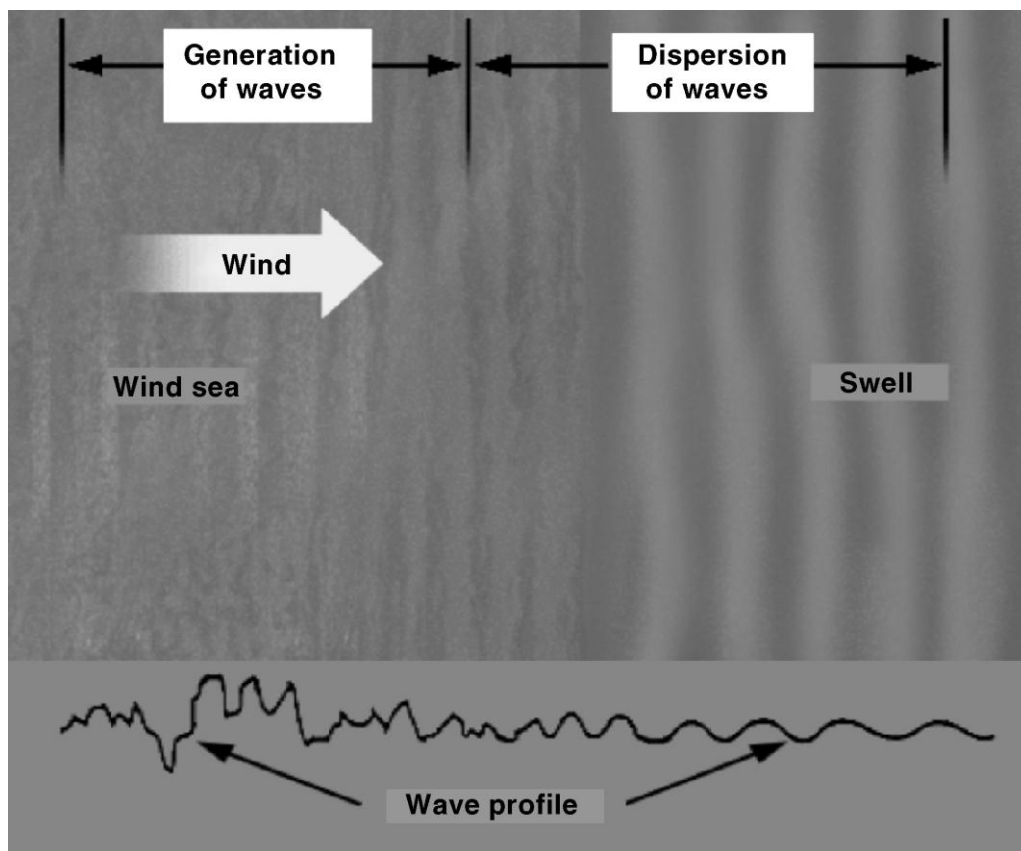


Fig. 3.4 Schematic diagram of wind sea and swell (from Schmager et al., 2009). While the initial wind-induced sea state shows superpositions of high frequencies, dispersion of surface waves leads to swell with longer periods.

The time or duration a wind of constant direction and speed is able to transfer its energy to the sea surface is called the *wind duration*. Depending on fetch and wind speed, the wind must blow for a specific period of time (minimum wind duration) to generate specific wave heights and periods. According to Schmager et al. (2009), a sea state growth that is independent of the fetch, occurs in the Baltic Sea only at wind speeds of up to 16 knots ( $\approx 8$  m/s) with a minimum wind duration of 24 h.

*Water depth* is another factor that influences the generation of surface waves. Because the distinction between shallow water and deep water waves depends not on water depth per se but on the ratio of wave constituents to water depth, the highest significant waves that form in the Baltic Sea at water depths of 30 m and a wind strength of 5 Bft ( $\approx 10$  m/s) still have to be treated as deep sea state, since their wave length just exceeds 40 m, making them long waves compared to water depth.

An overview of wave parameters in the Baltic Sea is given in Fig. 3.5 with exemplary values listed in Table 3.1.

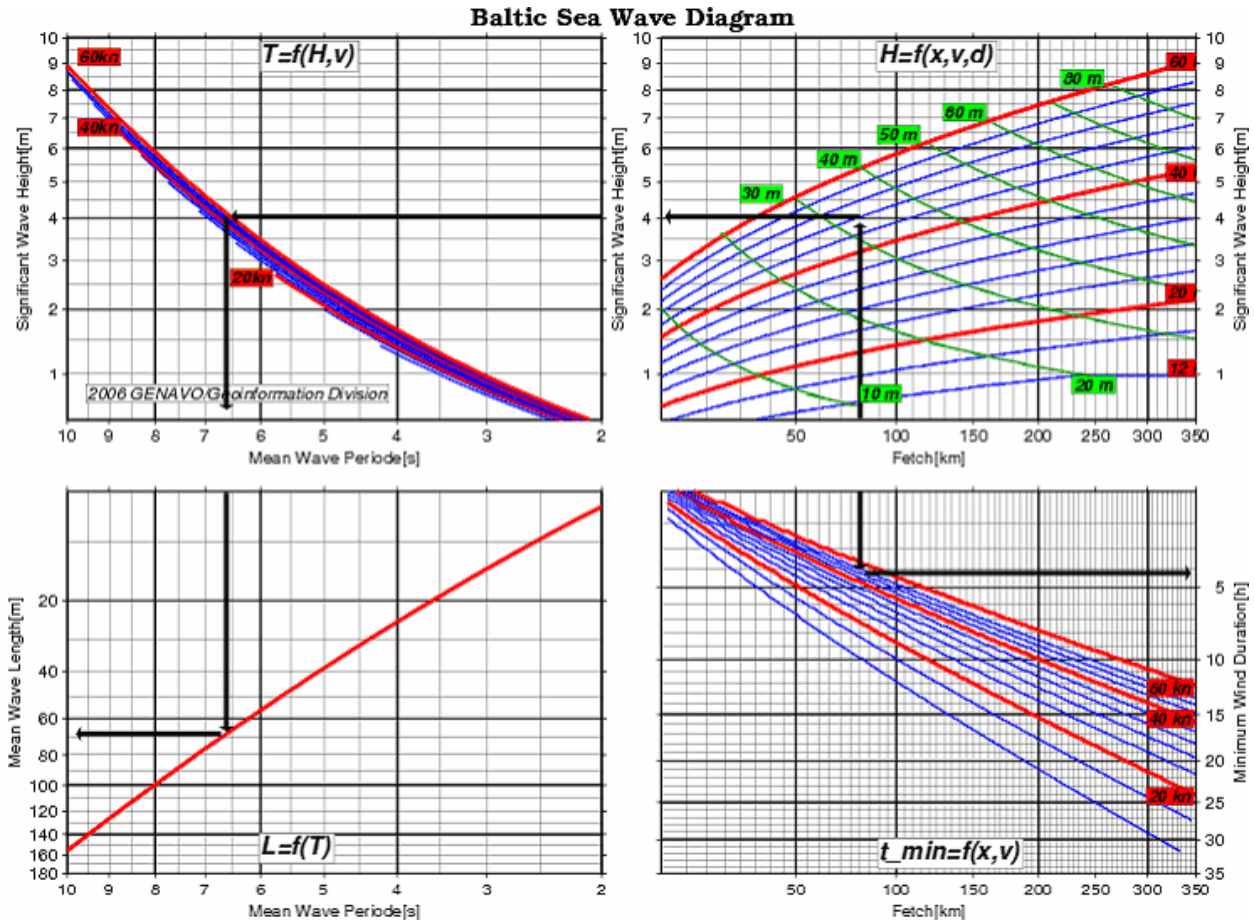


Fig. 3.5 Baltic Sea wave diagram (from Schmager et al., 2009). To use the diagram, fetch and wind speed (knots) must be known, so one can follow the the path indicated by the black arrows from a known point in the lower right panel. The arrows given represent values listed in Table 3.1 below

Table 3.1 Sea state parameters determined from the wave diagram in Fig. 3.5.

<b>Fetch</b>	80 km
<b>Wind speed</b>	46 kn (23.6 m/s)
<b>Significant wave height</b>	4 m
<b>Average wave period</b>	6.6 s
<b>Average wave length</b>	68 m
<b>Minimum water depth</b>	32 m
<b>Minimum wind duration</b>	4 h

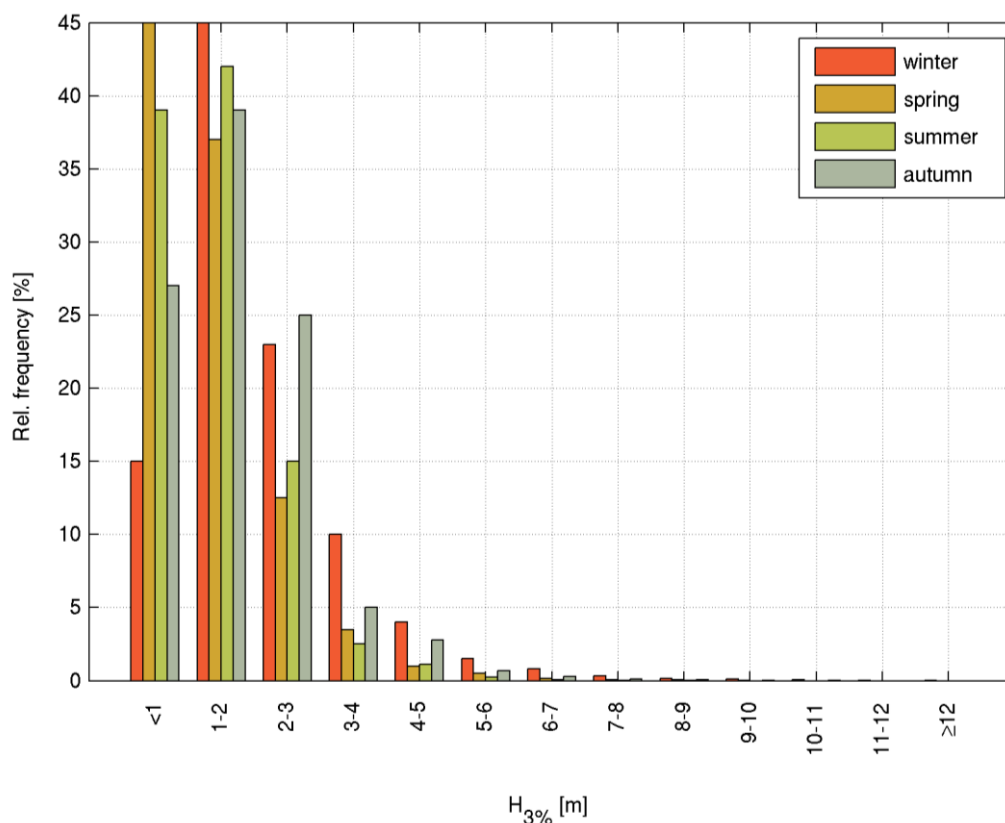


Fig. 3.6 Frequency Distribution of the wave height  $H_{3\%}$  in the Baltic Sea east of  $15^\circ\text{E}$  and south of  $60^\circ\text{N}$  (redrawn with data from Registrar of the USSR, 1974).

A climatology of wave heights was published by the Registrar of the USSR in 1974. In accordance with Soviet regulations, the wave height  $H_{3\%}$  at the lower limit of the top 3% of the wave was used as a measure for the height of the waves. This measure is identical with the highest waves in the sea state. These statistics show that the occurrence of extreme waves with a height of more than 12 m (corresponding to a significant wave height  $H_s = 9$  m) in the Baltic Sea must be expected, even if their frequency is very low (Schmager et al., 2009). An example for the Baltic Sea east of  $15^\circ\text{E}$  and south of  $60^\circ\text{N}$  (an area that includes Baltic Proper, Gulf of Riga and Gulf of Finland, cf. Fig. 1.2) as calculated in the Registrar's climatology is shown in Fig. 3.6. It reveals that throughout the seasons of the year, the likelihood of waves with heights greater than 4 m is less than 5%.

A more recent climatology of wave heights for 20 subareas of the Baltic Sea was compiled by Deutscher Wetterdienst (DWD) based on their marine weather archive. This climatology and a corresponding numerical model hindcast by the German GKSS research center (Weisse, 2007) showed the following results according to Schmager et al. (2009):

- the highest significant wave (9 m) was observed in January at the western part of the Gulf of Finland;
- extreme wind seas with significant heights of 8-8.5 m are prevalent in the northern, central, and southern Baltic Proper but concentrate in the Eastern Gotland Basin off the coast of Latvia and Lithuania and in the entrance to the Gulf of Finland;



- the GKSS simulation showed a maximal wave height of 10.2 m for the Gdansk Depression which was attributed to hurricane "Anatol" in December 1999;
- two hot spots with significant wave heights greater than 10 m can be found in the Gdansk Depression and west of the Latvian coast.

### 3.2.2 Tides

Tides are a large-scale oceanic phenomenon which is driven by the gravitational forces of the moon and the sun. Due to the motion of the celestial bodies and the rotation of the Earth the deflection of the sea surface propagates as basin-wide tidal waves through the oceans under the influence of the restoring gravity of the Earth and the Coriolis force. Tides consist of a superposition of periodic constituents, the so-called partial tides, which are related to the orbital periods of the Moon  $T_m \approx 27.3$  days and the Sun  $T_s \approx 365.24219$  days (tropical year), and combinations of both with the period of earth's rotation  $T_e = 24$  h, see below.

Full tides develop in the large oceanic basins because the weak gravity of moon and sun requires a large effective length to deflect the sea surface. In the rather shallow North Sea the tides are mainly co-oscillations with the Atlantic Ocean. In the Baltic Sea, however, both tidal forcings are weak. Internal tides are limited because of the rather small extension of the sub-basins, and the co-oscillations are nearly damped out by the narrow and shallow Danish Straits. The tidal signal reaches only some centimeters which is considerably less than the effects of wind and seiches. Therefore, the Baltic Sea is often considered as a "practically non-tidal sea", see (Alenius et al. 1998), and consequently there have been only a limited number of investigations devoted to tides in the Baltic Sea.

An early investigation of the tides comprising the whole Baltic Sea was carried out by Witting (1911) who came to the conclusion that the Baltic Sea has its own internal tides. Detailed analyses of the tides in the Gulf of Bothnia and the Gulf of Finland were carried out by (Lisitzin 1943 and 1944). Based on the spectra of 31 gauge records observed in 1958 (Magaard and Krauss 1966) derived tidal amplitudes and phases. The state of knowledge about tides in the Baltic was summarized in Defant (1961): "The sum of the principal constituents  $M_2 + S_2 + K_1 + O_1$  is about 100 cm in the North Sea and decreases in the Skagerrak and Kattegat to below 20 cm, in the Belts to about 10 cm, in the Baltic to between 5 and 2 cm and in the Gulf of Bothnia mostly below 2 cm. In the Gulf of Finland there seems to be a gradual increase to nearly 10 cm." A recent review has been given by (Schmager et al. 2008).

Usually the tidal conditions in an area of the sea are characterized by the following constituents which yield the major contributions to the diurnal and semi-diurnal tidal sea level elevation:

**$M_2$** , the principal lunar semidiurnal cycle which represents the rotation of the earth with respect to the moon.

**$S_2$** , the principal solar semidiurnal tide generated by the rotation of the earth with respect to the sun.

**$K_1$** , a lunisolar diurnal constituent which expresses the effect of the moon's declination.

**$O_1$** , the lunar diurnal constituent which together with  $K_1$  mainly accounts for diurnal tides.



The relation  $F = (O_1 + K_1) / (M_2 + S_2)$  between the amplitudes of the two diurnal and semi-diurnal partial tides yields the form number  $F$ , indicating whether the tides are predominantly diurnal or semi-diurnal or of a mixed type:

- $0 < F < 0.25$  semidiurnal,
- $0.25 < F < 1.5$  mixed, mainly semidiurnal,
- $1.5 < F < 3.0$  mixed, mainly diurnal,
- $3.0 < F$  diurnal.

The sum of the four *amplitudes*  $I = M_2 + S_2 + K_1 + O_1$  is the intensity index, i. e. the maximum contribution of the tides to sea level elevation if all constituents are superposed in phase.

Each tidal constituent is characterized by its period  $T$ , the amplitude  $A$ , and a phase shift  $\varphi$  related to a reference time and geographical longitude. Co-tidal maps, like Fig. 3.7 show the propagation of the flood tide by progress in time or in phase angle. The amplitudes and phases of local tides depend mainly on the local gravitational potential, the water depth, bottom friction, and the structure of the coast line. A sloping bottom in a narrowing coastal bay may considerably enhance the tidal amplitudes. Local tides are determined by harmonic analysis of sea gauge records which yields a least-squares fit onto Fourier components like  $A_{M_2} \cos(2\pi t / T_{M_2} - \varphi_{M_2})$  for the  $M_2$  constituent.

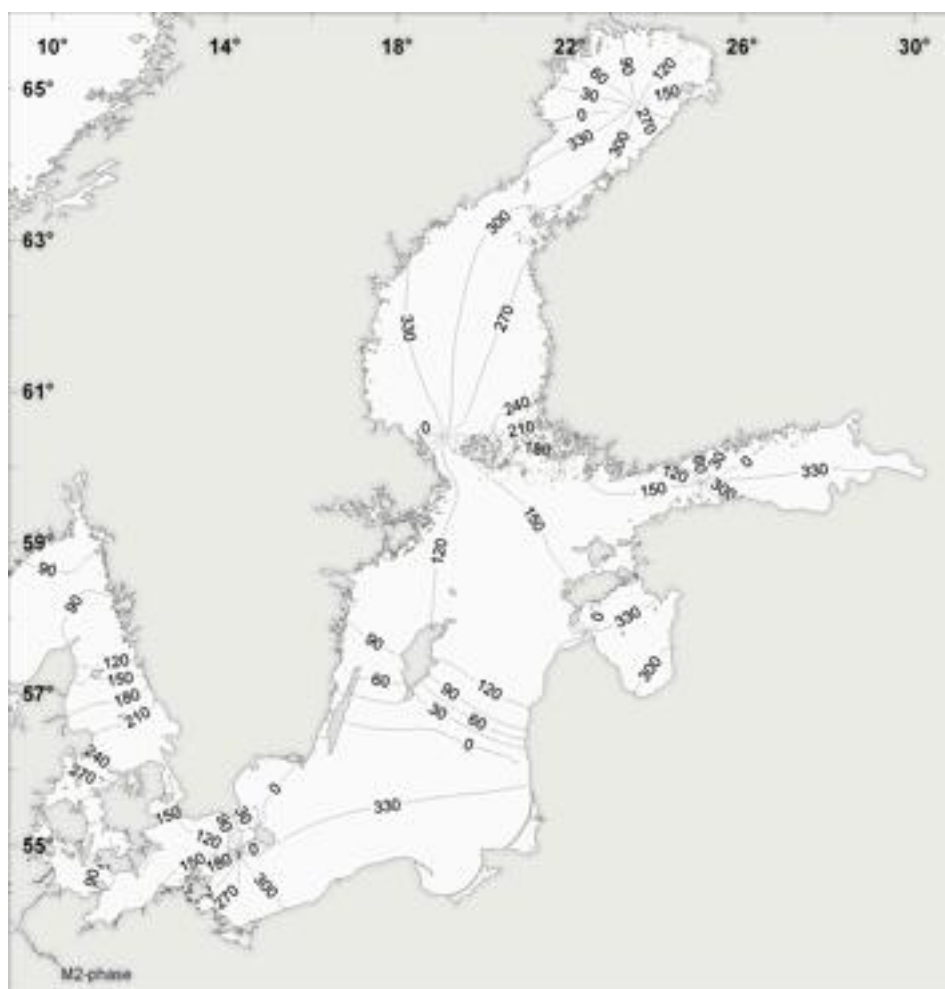


Fig. 3.7 Computed phases of the  $M_2$  partial tide in the Baltic referred to the passage of the moon through the Greenwich meridian; figure by Müller-Navarra in (Schmager et al. 2008).





The spectral analysis of gauge records is another frequently used tool to analyze local tides. This has been applied by (Magaard and Krauss 1966) who showed that the semi-diurnal partial tides cause distinct spectral peaks, especially in the Kattegat and Belt Sea level which are influenced by co-oscillation with the tides coming in through Skagerrak. Analysis of the form number  $F$  revealed that semi-diurnal tidal signals play also a role in the Åland Sea, whereas the diurnal constituents are predominant in the Gulf of Bothnia and the Gulf of Finland. This investigation was restricted to the coastal regions where tide gauge data were available.

Müller-Navarra (in Schmager et al., 2008) emphasizes the importance of internal tides in the Baltic Sea. For that reason the tidal potential of the moon and the sun is included into the operational forecast model at BSH. The distribution of the form number within the Baltic Sea shown in Fig. 3.8 was derived from a tidal analysis of a model run for the year 2005. The dominance of diurnal tides is confirmed by  $F > 3$  for the Bothnian Bay and the Gulf of Finland, but also found in the Gulf of Riga, off Lithuania, southwest off Bornholm, and north-west off the Åland archipelago. The Bothnian Sea and the southern Baltic show mixed tides. The semi-diurnal tides in the central northern Baltic Sea are a model prediction which might not be proven by gauge data.

The intensity index  $I$  derived from the model results is given in millimeters by Fig. 3.9. According to that, the maximal amplitudes of the semi-diurnal and diurnal constituents may reach 10-20 cm in the Kattegat with higher elevation at the Danish coast, 5 cm-20 cm in the Belt Sea, and 1 cm-3 cm within the open Baltic. Only in the rear end of the Finnish Gulf tides may contribute 5 cm-8 cm to the sea level elevation.

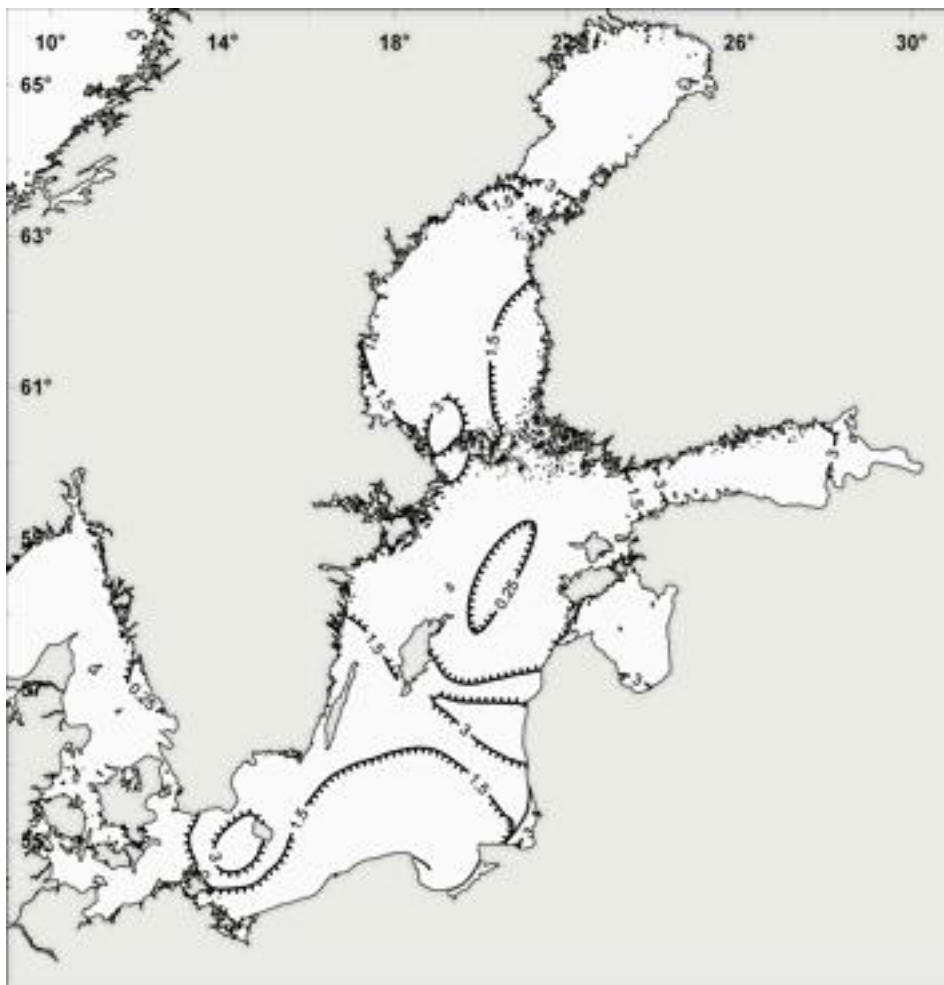


Fig. 3.8 Form number  $(O1+K1)/(M2+S2)$  indicating dominance of diurnal, semi-diurnal, and mixed tides; figure by Müller-Navarra in (Schmager et al. 2008).

As an example the co-tidal map of the semi-diurnal partial tide M2 is shown in Fig. 3.7. The progression of the tidal wave is expressed in 0 degrees - 360 degrees. By that it is obvious that the M2 tide rotates clockwise through Bothnian Sea and northern Baltic Proper, within the Gulf of Finland, and around Bornholm. Within the Bothnian Bay an exceptional anti-clockwise amphidrome is found. The amphidromic points, where the tidal elevation of M2 is nearly zero, coincide with the regions, where the diurnal tides are predominant, see Fig. 3.8.

Using the tidal fitting toolbox for MATLAB provided by (Grindsted 2008) the set of gauge records specified in Table 3.2 has been analyzed. The calculations are based on three selections of tidal constituents: daily refers to the semi-diurnal and diurnal tides  $M2 + S2 + K1 + O1$ , yearly denotes the yearly cycle  $T_s$  and its sub-harmonics to  $T_s/8$  and all means the major 35 partial tides plus yearly cycle and sub-harmonics to  $T_s/8$ .

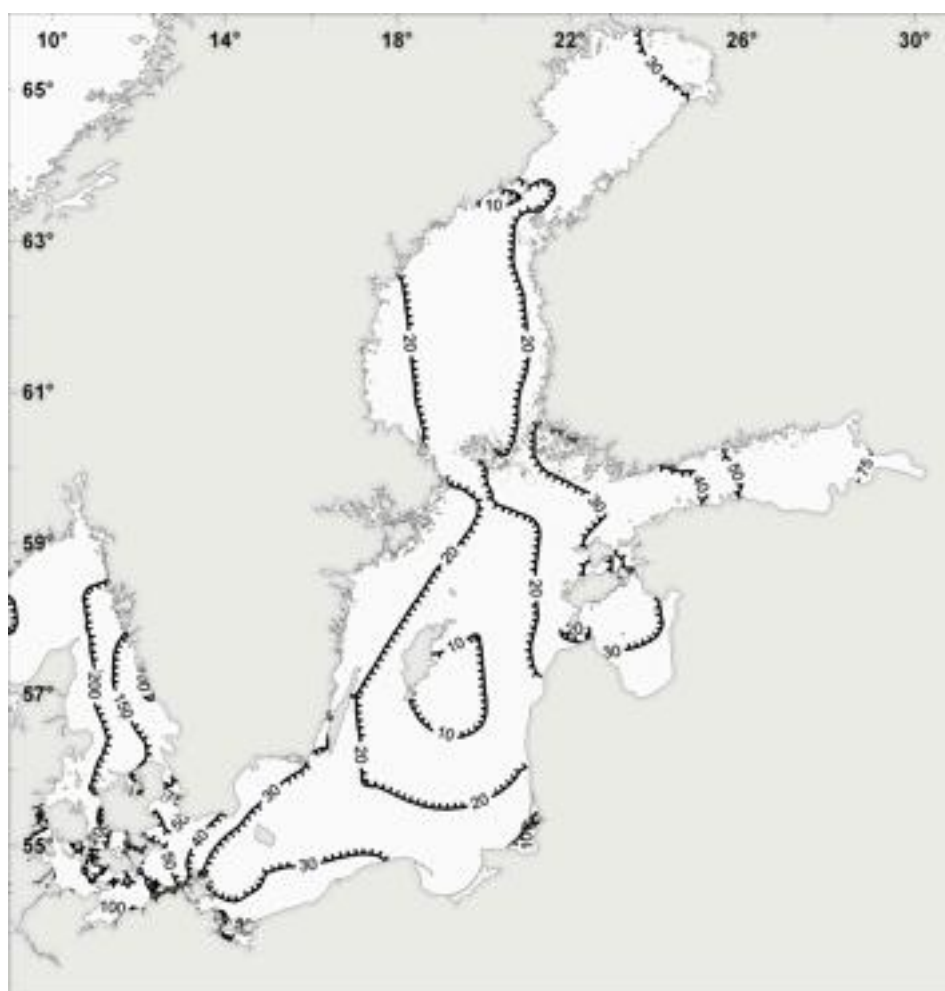


Fig. 3.9 Intensity coefficient (mm) of the four leading tides in the Baltic Sea ( $M2+S2+K1+O1$ ), figure by Müller-Navarra in Schmager et al. (2008).

The tidal explained variance  $100\sigma_t/\sigma_\eta$  represents the percentage of the variance



$$\sigma_{\eta} = \sqrt{\sum_{n=1}^N (\eta_n - \bar{\eta})^2 / N} \quad (3.1)$$

of the observed sea level  $\eta$ , which is reflected by the sum of tidal constituents taken into account. The tidal root mean square (rms) sea level corresponds to the square root  $\sqrt{\sigma}$  which is a measure of the standard deviation of the sea level from the long-term mean which is subtracted for analysis.

The results in Table 3.2 demonstrate that the rms deviation of the observed sea level at the coasts is between 20-30 cm within the Baltic Sea and Kattegat. The tidal contributions, however, show regional differences. Taking into account all tidal constituents typically 10-30% of the observed variance is reproduced in Kattegat, and 10-20% in the Baltic Sea. This is also the case in the Great Belt and the Sound, but coastal gauges located in the adjoining basins of the Belt Sea, like Gedser, Kiel, Travemünde, Warnemünde, and Wismar, are well below 10%. Correspondingly, the tidal rms of sea level elevation is around 10 cm in Kattegat, Danish Straits, and Baltic Sea, but only 5 cm in the basins of Belt Sea. Korsør and Slipshavn show around 10 cm.

The different tidal characteristics become more clear if only the semi-diurnal and diurnal constituents or the yearly cycle with its sub-harmonics are considered. Semi-diurnal and diurnal partial tides play no role within the Baltic Sea, the explained variance is around 1% and the contribution to amplitude is between 1-3 cm only. Nearly the full tidal signal in the Baltic Sea is allocated to the yearly cycle and its sub-harmonics. In contrast to that, the semi-diurnal and diurnal constituents yield the major tidal signal in Kattegat and Danish Straits, however, the long-term contributions are in the same order of magnitude, i.e. 5 cm-10 cm in rms elevation. The regional differences in tidal amplitudes reflect the low-pass filter characteristic of the Danish Straits: the high frequent tides in Kattegat are effectively damped out, whereas the low frequent constituents pass through. The fact that the "yearly rms elevations" in the Baltic Sea are even higher, especially in the Gulf of Bothnia and the Gulf of Finland, indicates an enhancement of the low frequent co-oscillation of the Baltic Sea by internal tides. However, since the tidal fitting is a formal decomposition of the observed sea level with respect to the prescribed periods, the long-term part may contain contributions which are caused by other reasons as for instance the seasonal cycle of wind forcing.

Finally, Müller-Navarra (in Schmager et al. 2008) points out that even small tidal signals may play a role within oceanic basins like the Baltic Sea. Because pressure disturbances by sea level elevations affect the whole water column, tides generate barotropic currents and contribute to the displacement of internal interfaces. These signals are periodically changing and are permanently in effect. Hence, tides may contribute to bottom currents and internal mixing, especially under calm meteorological forcing. However, no investigations of these effects are known for the Baltic Sea.



Table 3.2 Tidal fitting of the sea level elevation recorded at gauge stations. Daily refers to partial tides  $M2+S2+K1+O1$ , yearly to the annual cycle and its sub-harmonics, and all comprises the major 37 tidal constituents plus the yearly contributions, see text. The tidal contribution to the observed rms of sea level is given in relative (%) and absolute (cm) units.

Gauge	Tidal explained variance (%)			Tidal rms sea level (cm)			Observed rms (cm)	Period
	daily	yearly	all	daily	yearly	all		
<b>Kattegat</b>								
Göteborg	6.5	8.8	17.1	5.1	6.0	8.3	20.2	2002-2005
Smögen	12.2	9.4	21.8	7.9	7.3	10.5	22.5	1978-2007
Kungsvik	12.3	9.6	23.9	8.4	5.9	11.7	23.9	2002-2005
Ringhals	3.5	8.2	14.2	3.5	6.6	7.2	19	1994-2002
Skagen	18.8	6.1	30.2	10.0	5.6	12.7	23.1	2005-2007
<b>Belt Sea</b>								
Gedser	2.7	3.0	7.5	3.7	3.9	6.2	22.7	2006-2007
Hornbæk	6.8	3.9	13.9	5.8	4.4	8.2	22.1	2006-2007
Kiel-Holtenau	2.4	2.7	7.9	3.8	3.6	6.9	24.5	2005-2007
Korsør	16.2	2.4	22.0	8.8	3.3	10.2	21.8	2006-2007
Slipshavn	23.4	4.1	30.1	10.4	5.0	11.8	21.5	2006-2007
Travemünde	3.8	4.4	9.7	4.7	5.0	7.5	24.1	2005-2007
Viken	8.0	8.9	18.5	5.6	5.9	8.5	19.8	2002-2005
Warnemünde	2.6	3.0	5.8	3.5	3.8	5.3	21.9	1969-1993
Wismar	2.8	2.4	5.6	4.0	3.8	5.7	24.1	1977-2001
<b>Baltic Sea</b>								
Foglö	0.1	18.8	19	0.8	9.4	9.5	21.8	1977-2002
Hamina	0.8	14.6	15.5	2.5	10.6	11	27.8	1977-2002
Helsinki	0.8	20.4	21.5	2.2	10.9	11.2	24.1	2005-2007
Kalix	0.2	17.1	17.6	1.2	12.1	12.3	29.3	2005-2007
Kaskinen	0.1	21.4	21.8	0.9	11.2	11.3	24.1	2005-2007
Kemi	0.2	15.4	16.0	1.5	12.2	12.4	31.0	2005-2007
Klagshamn	2.8	11.0	14.5	3.1	6.2	7.2	18.8	2002-2005
Koserow	0.4	5.0	5.6	1.4	4.7	5.0	21.1	1997-2007
Kungsholmsfort	0.5	16.0	16.9	1.4	7.8	8.0	19.5	2002-2005
Landsort	0	20.5	21.0	0.4	9.2	9.3	20.4	2001-2002
Sassnitz	0.4	6.0	6.5	1.3	5.0	5.2	20.3	1969-1997
Simrishamn	0.6	8.4	10.1	1.6	5.6	6.1	19.3	2006-2007
Skånör	1.6	9.5	11.7	2.7	6.6	7.3	21.3	2002-2005
Spikarna	0.1	17.4	17.5	0.7	9.3	9.3	22.3	1973-2004



### 3.3 **Baltic water masses – stratification and horizontal gradients**

The term *water mass* refers to a body of water with a given set in salinity-temperature values. The signatures of water masses can be displayed in a so-called T/S-diagram where temperature is plotted over salinity in a two-dimensional scatter plot. Such diagrams are helpful to identify different water masses, their origins and their development.

The Baltic Sea can loosely be characterized by two main types of water. In the surface layer, which extends from the sea surface to the thermocline, low density water with an average salinity of around 7 psu is found (note that 1‰ or 1 psu is close to 1g salt per kg sea water). This layer shows a seasonal cycle in response to the atmospheric temperature changes. The thermocline is located at depths between 20 m and 30 m. The other dominant water mass is the more saline, and thus denser, bottom water. This water fills the deep basins east of Bornholm island and around Gotland island. These two major water bodies establish a permanent two-layer stratification in the Baltic. Between the surface and bottom layers, the so-called winter water exists, which is formed during winter and separated by the surface layer. This specific system of water masses gives rise to a number of biological species that have adapted to the present state of the Baltic Sea ecosystem. E.g. a detailed analysis of the plankton species in the greater Fehmarnbelt area and their dependence on salinity and temperature is given in the Preliminary Baseline Analysis by (FEMA 2010).

The high amount of freshwater supply to the Baltic Sea by river discharge and precipitation causes a strong outflow into the North Sea that accounts for 60% of the North Sea's freshwater supply. This equates to an average annual discharge of 480 km<sup>3</sup> of low-density freshwater at the surface into the North Sea (Leppäranta & Myrberg 2009). The outflow is balanced by a saline and dense inflow from the North Sea into the bottom layer. The main front between the water occurs in the Kattegat and the Skagerrak, where mixing leads to an increase in surface salinity up to oceanic levels. Compared to the dynamics in this entrance area, temporal changes in salinity of the Baltic Proper are rather small. Since the pathway of outflowing water through the Belt Sea is significantly longer than through the Sound, the outflowing water in the Sound is much less saline than the outflow through the Belt Sea. These two water masses follow different paths through the Kattegat along the Swedish and Danish coastlines respectively while their salinity increases due to entrainment. For a schematic view of the Baltic Sea water balance including riverine contribution see Fig. 3.11 and Table 3.3.

The inflow along the trenches of the Belt Sea and across the main sills is not always confined to the bottom layer, but is frequently in a barotropic mode. The volume of such instantaneous in- and outflows is up to 25 km<sup>3</sup> with a salinity of 8‰ to 28‰ (Leppäranta & Myrberg 2009) but much larger volumes may occur during so-called Major Baltic Inflows. An important factor is the strong entrainment of surface water with low salinity originating from the Baltic Proper into the saline bottom layer outside the sill areas. This and internal mixing of the dense bottom flow lead to considerably lower bottom salinity in the Baltic Proper compared to that in the Kattegat region. Strength and duration of such inflows are key factors for the salinity of deep saline inflows into the Baltic Sea. The greatest part of such inflows are more or less continuously occurring short events with only moderate salinity and are responsible for an overall stratification of two layers in the Baltic; yet they are usually not dense enough to replace bottom water in the deep basins of the Baltic Proper. The infrequent major inflows of saline water (see Chapter 3.4.2) are therefore very important for the ventilation and renewal of the deep basins. (Krauss and Brügge 1991) write: "The greatest renewal during the last 40 years occurred in 1951 (Wyrтки 1954), followed by a stagnation period until 1963". Meier et al. (2004)

states that “during the past two decades the frequency of major inflows has decreased”. Significant inflows have occurred only 3 times: in 1983, 1993, and 2003”. One of the major obstacles for saline inflows on their way into the deep basins of the Baltic Sea is the Darss Sill at approximately 12° 40' E, a shallow sill with depths of 20 m and less. Measurements in the area show an extremely high variability of salinity with occasional changes of 1.5 psu and more within an hour (cf. Fig. 3.10).

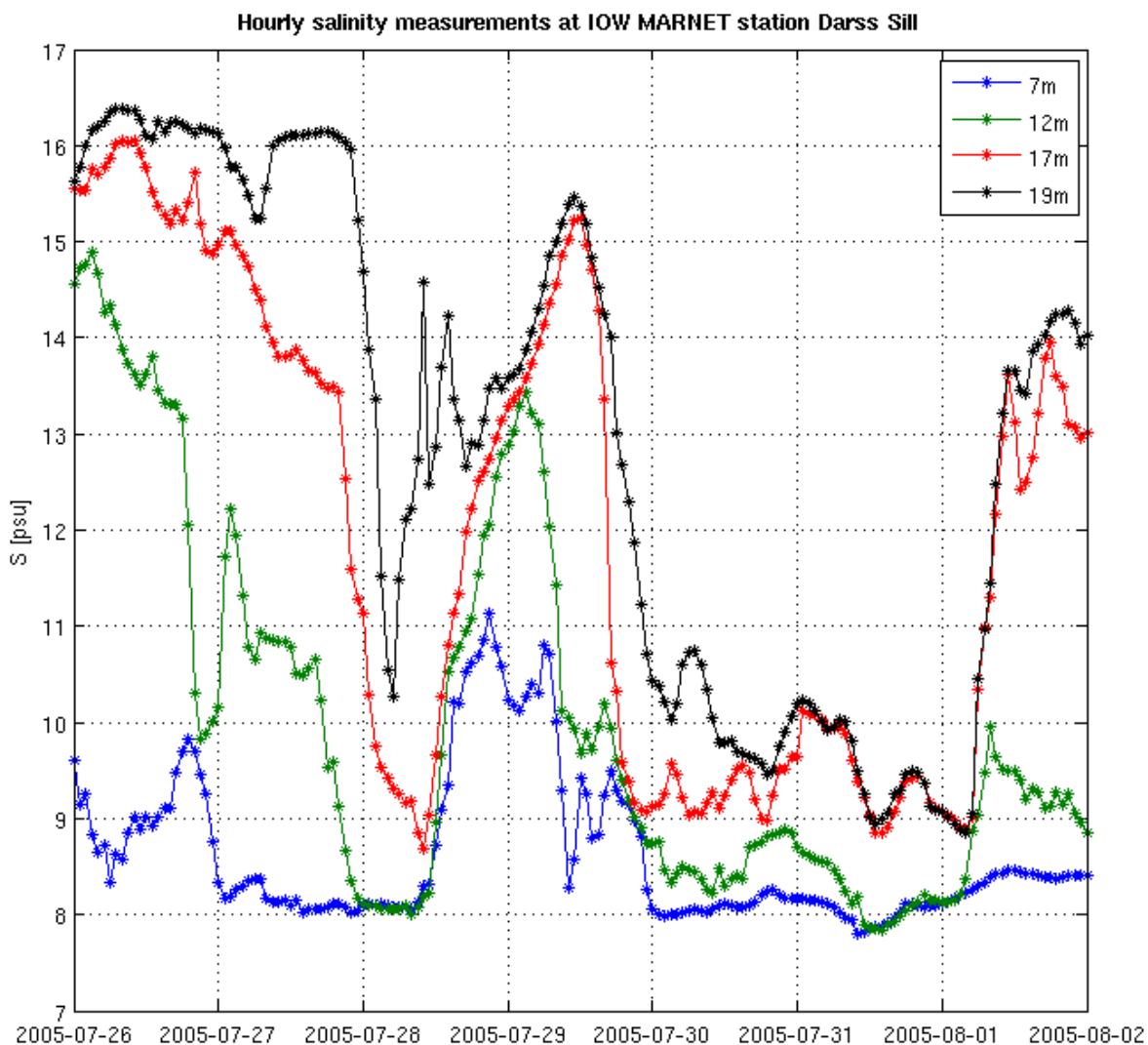


Fig. 3.10 Hourly salinity time series in the summer of 2005 at different depth levels from a fixed monitoring station at the Darss Sill, position: 54° 42' N, 12° 42' E (IOW data, own work). Note the generally high variability in salinity below 7 m depth, especially at 19 m on July 28.



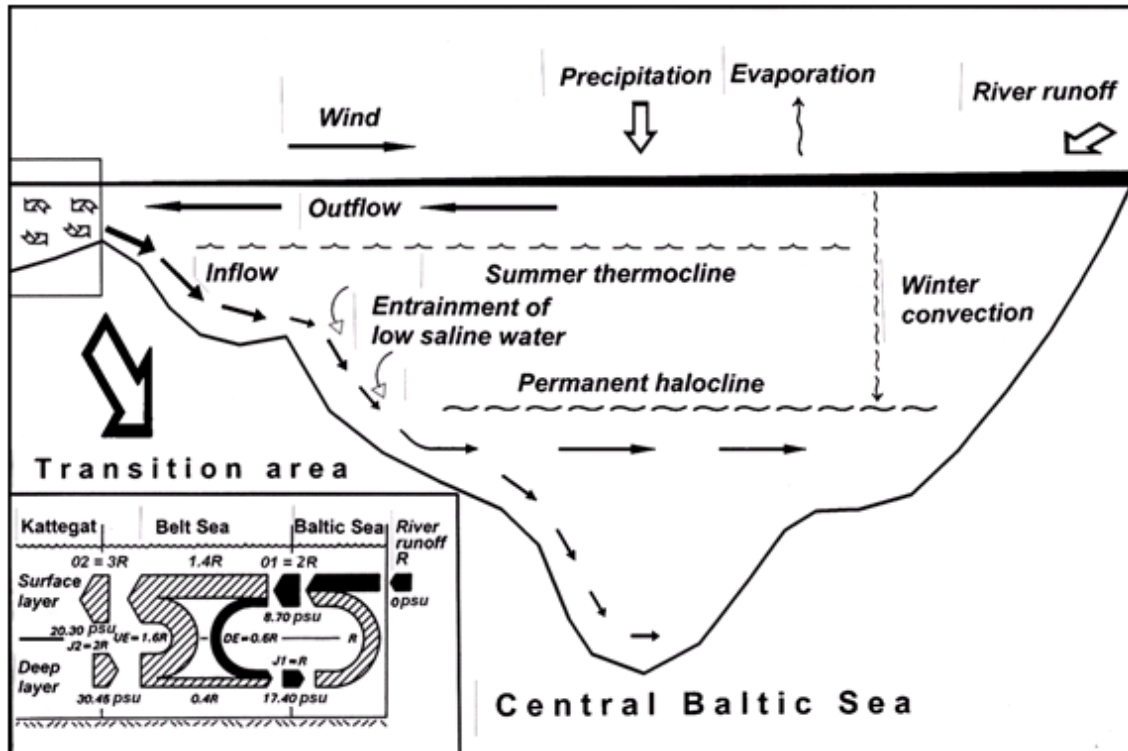


Fig. 3.11 Schematic picture of the water balance of the Baltic Sea, the water exchange with the North Sea and the transformation of water masses in the Belt Sea (bottom left, in river runoff units). Redrawn after (Lass and Matthäus 2008).

Table 3.3 Water and salt balance of the Baltic Sea after (Lass and Matthäus 2008). The table provides annual water mass ( $\text{km}^3$ ) and salt transports (Gt) for the relations shown in Fig. 1.1. Extending the above scheme we present the total fresh water input  $F=R+(P-E)$ , with river runoff  $R$ , and the budget of precipitation and evaporation ( $P-E$ ) derived from (Lindau 2002) for the period 1980-1995.  $R=446 \text{ km}^3$ ,  $P-E=25 \text{ km}^3$ .

	Kattegat	Belt Sea (+Sound)		Central Baltic Sea	
<b>Surface layer</b>	← $3F=1,413 \text{ km}^3$ 28.7 Gt	← $1.4F=659 \text{ km}^3$ 5.73 Gt	← $2F=942 \text{ km}^3$ 8.20 Gt	← $F=471 \text{ km}^3$ 0 Gt	
<b>Exchange</b>		↑ $1.6F=754 \text{ km}^3$ 23.0 Gt	↓ $0.6F=283 \text{ km}^3$ 2.46 Gt	↑ $1F=471 \text{ km}^3$ 8.20 Gt	
<b>Bottom layer</b>		→ $2F=942 \text{ km}^3$ 28.7 Gt	→ $0.4F=188 \text{ km}^3$ 5.74 Gt		



### **3.3.1 Regional distribution of salinity**

Salinity in the Baltic decreases eastward from the Belt Sea to the Baltic Proper and reaches its lowest values in the Bay of Bothnia. In the main basins the mean circulation is counter-clockwise and therefore salinity is usually higher in the eastern parts of basins than in the western areas.

#### ***Kattegat***

In the eastern Kattegat a clear two-layer stratification is given with a permanent halocline at depths of about 15 m. Surface salinity varies from 18‰ to 26‰ while bottom salinity may reach up to 34‰ (Leppäranta & Myrberg 2009). In contrast to this, the western part features average depths of only 10 m which is shallower than the upper layer's thickness in the east. Therefore a well-mixed estuary is normally found in the western Kattegat (Bo Pedersen and Møller 1981).

#### ***Belt Sea and Sound***

In the Belt Sea a two-layer structure is generally found like in the Kattegat. As of today, the upper layer consists of outflowing Baltic Sea water with salinities between 8 psu and 12 psu showing a high intraannual variability (cf. Fig. 3.10 and Fig. 3.12) whereas the bottom water originates from the Kattegat or the North Sea respectively. Bottom salinity in the northern Belt Sea can reach 34 psu while it is already diluted to below 28 psu in the Fehmarnbelt due to internal mixing and entrainment of fresher surface water. A historical analysis by Wittig (1953) reports slightly higher surface values though, referring to annual means between 10‰ and 17‰ for the period of 1876-1892 (see Fig. 3.13). These data were however collected with less refined methods compared to today's measurements. Although currents in the Fehmarnbelt show a high variability, salinity is more inert. Early in the year one will observe isohaline waters that slowly develop into a proper stratification. A salinity maximum is found in summer due to the absence of strong wind-induced mixing. With the onset of autumnal winds barotropic outflow increases and thus bottom salinity decreases again (König 2004).

In the Sound, three water masses can be found: surface water from the Arkona Sea (7-8 psu), Kattegat surface water (18-26 psu) and bottom water from the Kattegat with salinities between 32 psu and 34 psu.

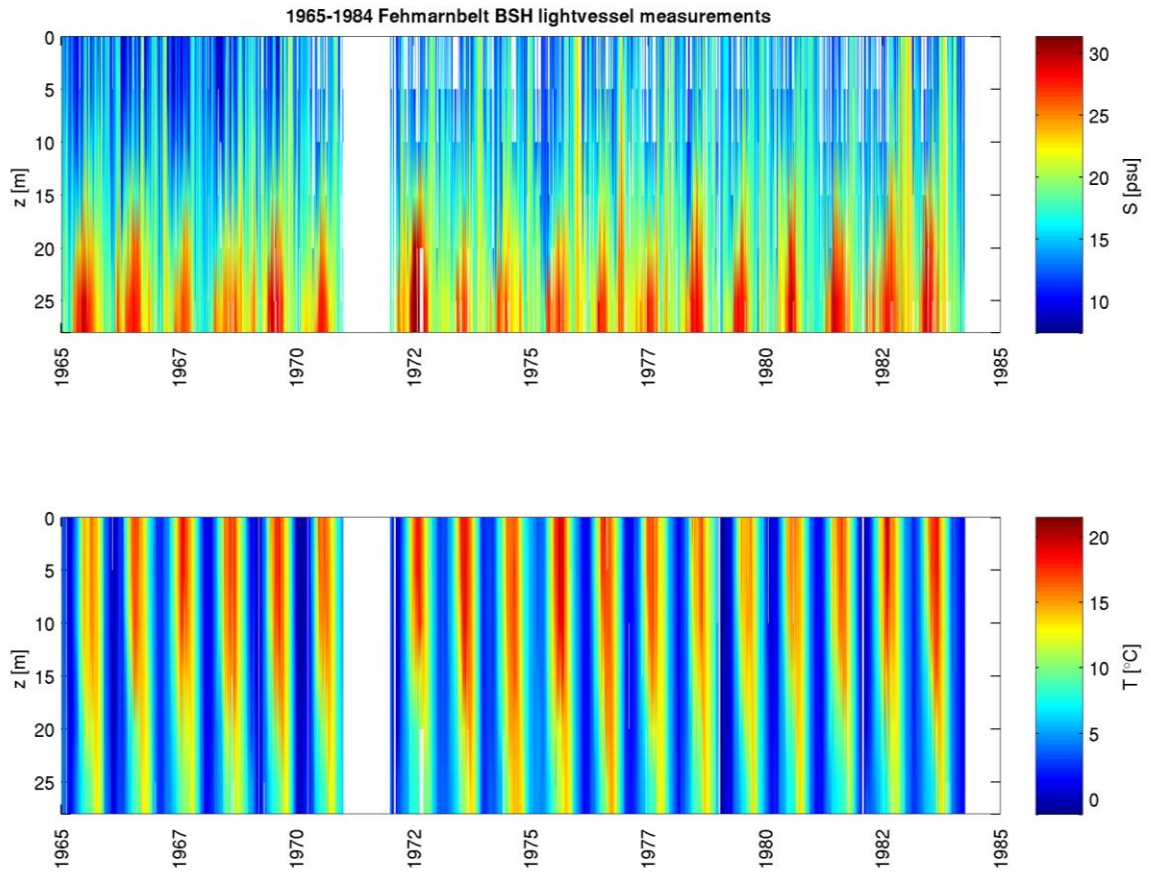


Fig. 3.12 Time series of daily salinity (upper panel) and temperature (lower panel) profiles from the Fehmarnbelt lightvessel position, 1965-1984 (based on BSH data). Note the cyclic nature of bottom salinity with infrequent inflows of saline North Sea water.

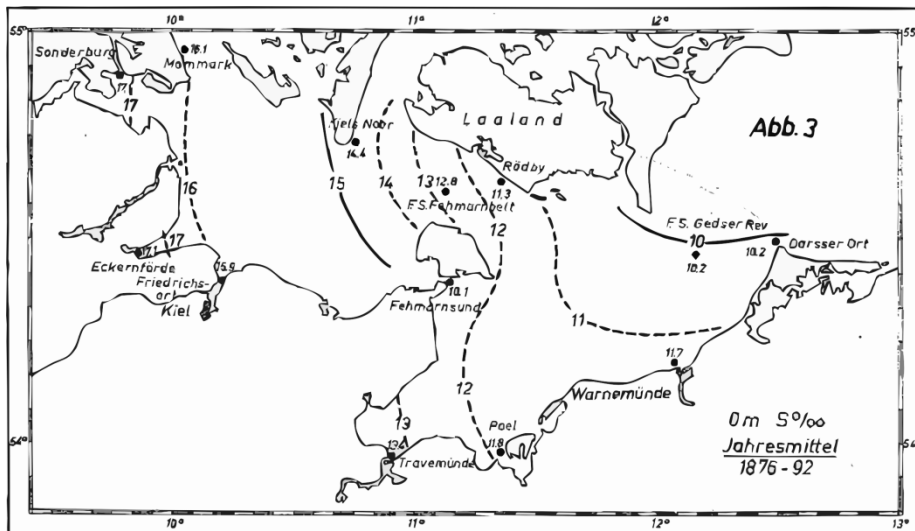


Fig. 3.13 Annual mean surface salinity in the Kiel Bight and Mecklenburg Bight from 1876-1892, from (Wittig 1953).



### **Arkona Basin**

In the Arkona Basin, the surface salinity is around 8 psu, the halocline is situated between 20 m and 30 m, indicating a maximum thickness of the mixed layer of 2/3 of the entire water column. Bottom salinity can reach 22 psu. A typical distribution of water masses with surface salinities between 8 psu and 10 psu is shown in Fig. 3.16.

### **Bornholm Basin**

Here, the surface salinity varies between 7 psu and 8 psu (observations from ICES, 2010 show up to 9 psu) with an upper layer thickness of up to 60 m. The salinity of the lower layer can reach 13 – 17 psu depending on strong saline inflows. It is a measure for the impact of weak inflows on the central Baltic deep water. During stagnant periods of weak inflows, salinity and thus density decreases in the deep zones of the Bornholm Basin. Depending on the intensity of the occasional inflows that are below the strength of a major Baltic inflow, incoming bottom water may pool in the Bornholm Basin and does not pass across the sill into the Słupsk Channel and on into the Gotland Basin. Only when the Bornholm Basin is filled up with dense water, weak inflows of saline, oxygenated water can pass the basin at about 55 m depth. This water propagates into the central Baltic just below the halocline of the Bornholm Sea (Matthäus et al. 2008).

### **Gotland Sea**

The Eastern and Western Gotland Basins comprise about half of the Baltic Sea's water mass (Leppäranta & Myrberg 2009); see also Table 2.1. In the eastern part the halocline is found at 60 m to 80 m with an upper layer salinity of 6.5 psu - 8 psu. Below the halocline there is an almost linear increase in salinity to 9 psu - 12 psu at 100 m and 11 psu - 13 psu at 200 m depth in the deep basins (cf. Fig. 3.14 and Fig. 3.15). Interdecadal cycles with periods of 20-30 years exist in surface salinity but standard deviation is very small ( $\sigma = 0.28$  psu). Bottom salinity of the last 50 years shows a slightly greater standard deviation ( $\sigma = 0.43$  psu) due to the stagnation period from the mid-1980s to mid-1990s. Coastal areas though show a somewhat lower salinity due to river runoff. In the northern part of the Gotland Sea, surface salinity is lower than in the east because of the cyclonic Gotland gyre: Gotland basin surface water mixes with water from the Gulf of Finland and the Bothnian Sea which results in surface salinities of 6 psu - 7 psu and a bottom salinity of about 11 psu. The intense stratification in the deep Gotland basins causes oxygen depletion in bottom water, which in turn can only be ventilated by major inflows of dense, oxygenated North Sea water.

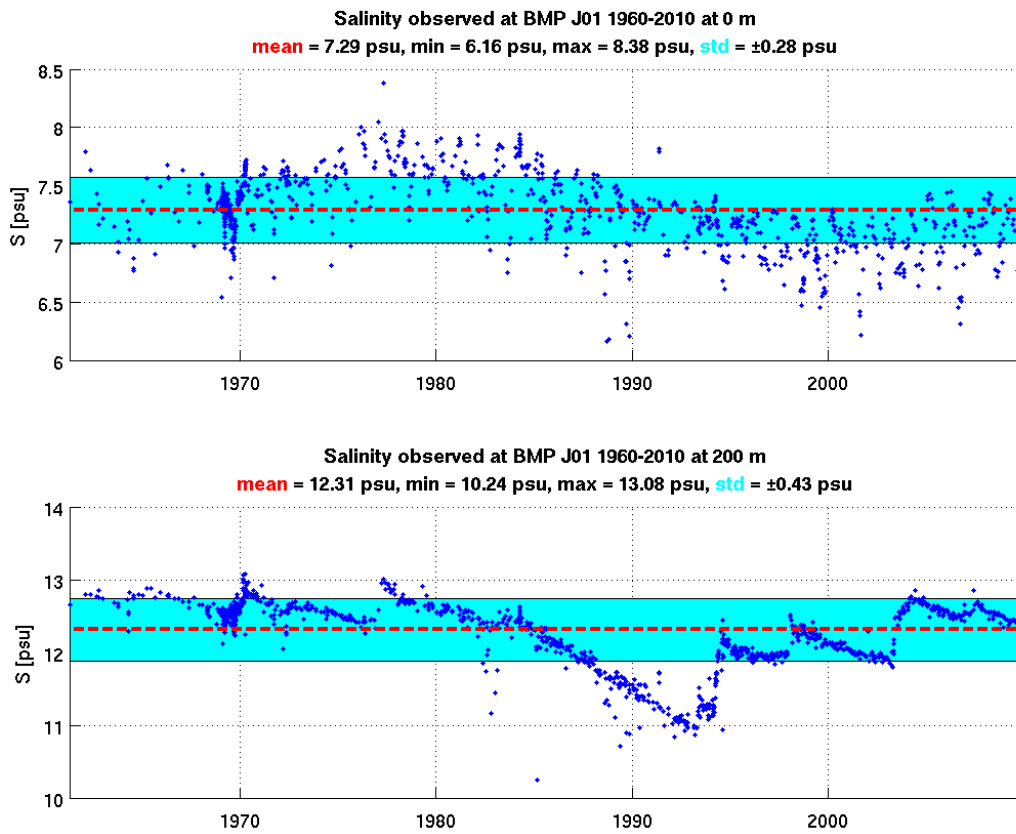
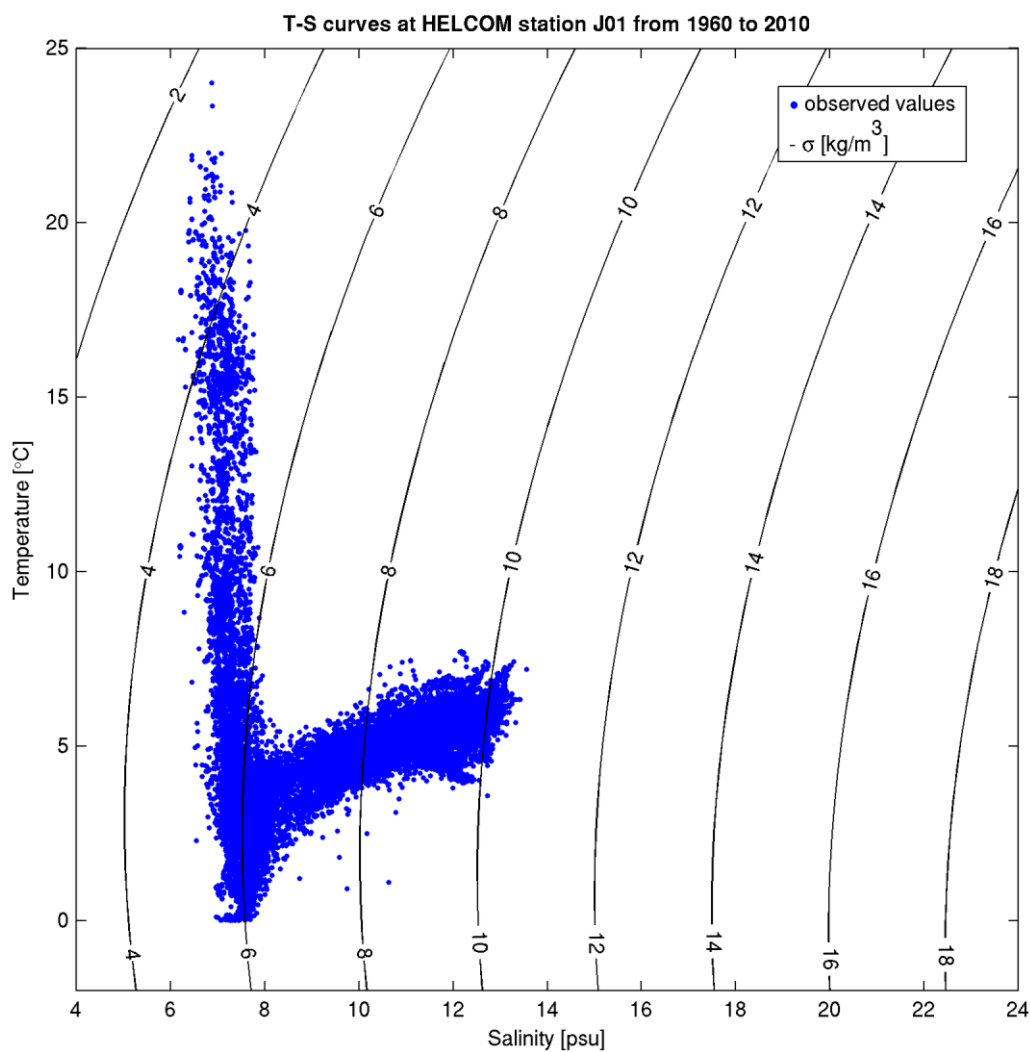


Fig. 3.14 Observed salinity at 0 m (upper panel) and 200 m (lower panel) at station BMP J01 in the Eastern Gotland Basin (ICES, 2010).



*Fig. 3.15 T-S diagram of measurements in the central Baltic (Eastern Gotland Basin) showing temperature plotted over salinity. Curved black lines mark the oceanographic density  $\sigma$ , i.e. density minus  $1000 \text{ kg/m}^3$ . The surface layer is shown by the vertical plume of the blue graph, indicating the annual temperature range from  $0^\circ\text{C}$  to more than  $20^\circ\text{C}$ . Note the continuous stratification below the low-density surface water. Data from ICES.*



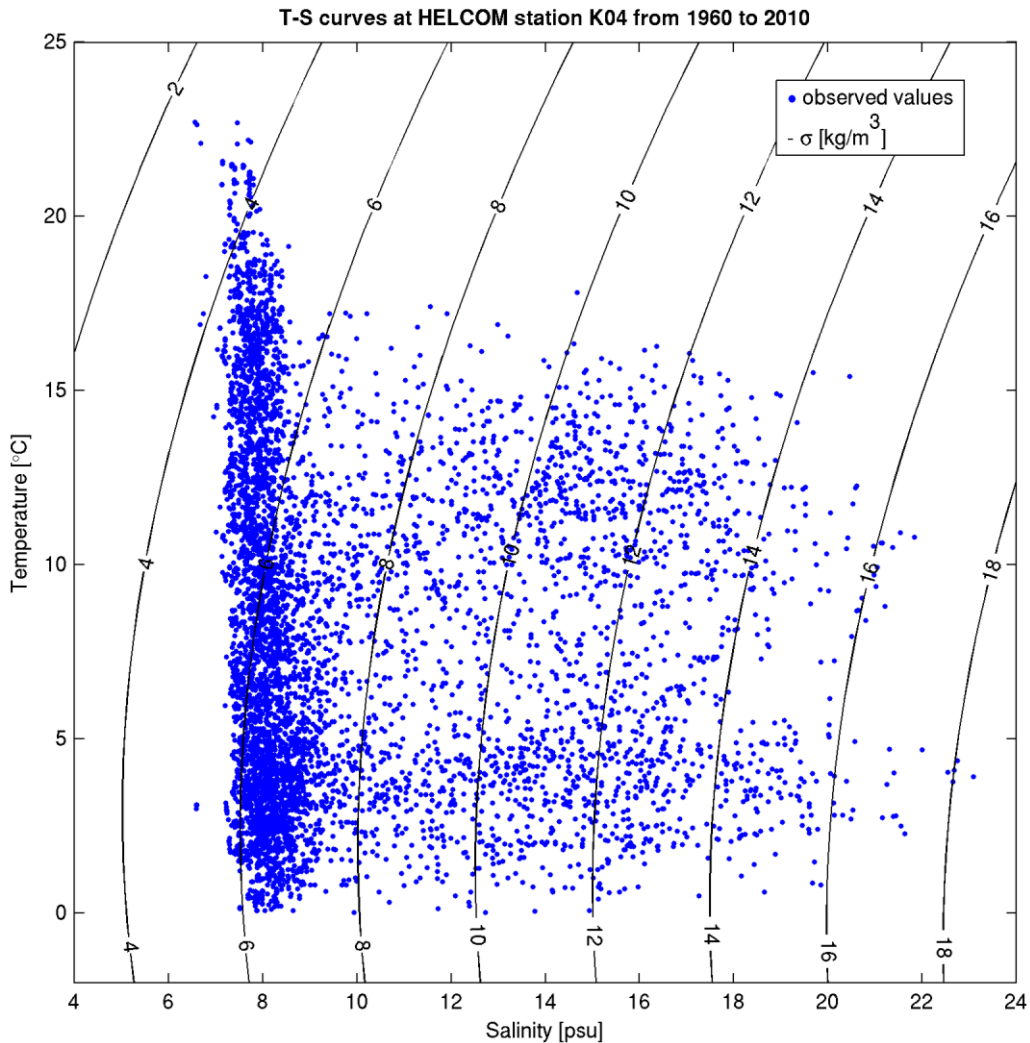
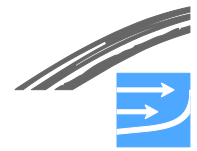


Fig. 3.16 *T-S diagram of measurements in the Arkona Basin. This water shows a distinct surface layer too but due to the relatively shallow depth it also shows seasonal effects below the surface, namely a wide range in temperature. Note the two pools of water with temperatures around 12°C and 4°C respectively. Data from ICES.*

### **Northeastern Gulfs**

The upper layer in the Gulf of Riga is comparably thin with a halocline depth of ca. 20 m - 30 m. The upper water mass with salinities of 4 psu – 5 psu originates from local river runoff while warm, saline surface water from the Eastern Gotland Basin forms the lower layer.

The Gulf of Finland has a partial two-layer structure. As no sill separates it from the Eastern Gotland Basin, bottom water can freely flow into this Gulf. The surface layer though is dominated by freshwater from the most voluminous river of the entire Baltic Sea catchment, the river Neva. Measurements have shown a runoff from this river of 2460 m<sup>3</sup>/s (Bergström & Carlsson 1994). This results in a continuous east-west gradient in the Gulf of Finland with salinities of 0 psu at the Neva mouth to 7 psu in the western Gulf. Also a halocline is only found in these parts of the Gulf of Finland, at depths of 60 m to 80 m. The bottom salinity amounts to 7 psu to 9 psu in the western parts, 5 psu to 8 psu in the central Gulf and 0 psu to 3 psu in the east at the mouth of the Neva. Anoxia at the bottom is common in summer due to



summer stratification and excess nutrient input. The eastern Gulf of Finland is covered with ice in winter, which can last into April.

The Gulf of Bothnia differs greatly in stratification. Water masses here are formed by exchange with the Northern Gotland Basin and by river runoff. The overall stratification is weak and thermohaline mixing reaches into the deep layers. Therefore, as the advection and subsequent mixing of surface water from the Gotland Sea tends to happen quite fast, lack of oxygen is uncommon in the Bothnian Bay. In deep zones though, stratification is strong enough to prevent autumnal deep convection and such bottom water can only be renewed by advection from the south. A weak halocline exists in the Bothnian Sea at depths of 60m to 80 m and in the Bay of Bothnia at 50 m to 60 m.

Salinity at the surface is 5 psu - 6 psu in the Åland Sea while bottom salinity typically varies between 7 psu and 7.5 psu. As in the Bothnian Sea, the lower layer in the Åland Sea is mostly formed by surface waters from the Gotland Basin that are stratified below the less dense local surface water, although a small portion of saline Gotland Basin deep water flows in over some sills and contribute to the deeper layer in the Åland Sea and eventually the Bothnian Sea. In exchange, an equivalent volume of surface water is transported into the Northern Gotland Basin. This mechanism strengthens stratification in the Bothnian Sea (Leppäranta & Myrberg 2009).

An overview of simulated mean surface and bottom salinities for the entire Baltic Sea is given in Fig. 3.17.

Table 1.4 shows the basic statistics of salinity at the sea surface and in the bottom layer in the main basins of the Baltic Sea (cf. Fig. 1.2). Derived from the climatology provided by (Feistel et al. 2008), the data were evaluated for subregions of 1 degree in longitude and latitude. Representative climatological grid cells have been chosen to characterize the Baltic Sea basins in the table. The minimum and maximum values describe the full range of salinity which was ever observed. Typical conditions are depicted by the mean values. The differences between surface and bottom salinity are a measure for the average strength of stratification. The variability is expressed by the standard deviation (STD) and more comprehensibly by the variation coefficient, which is the quotient of standard deviation and mean salinity as a percentage of change within the range of  $\pm 1$  standard deviation. This indicates the low salinities in the central and northern Baltic Sea, with a variation coefficient around  $\pm 3$ -7%. Only the salinity in Gulf of Finland and Gulf of Riga, which are subject to strong fresh water discharges, show salinity variation coefficients of  $\pm 10$ %. Higher bottom salinity in the Eastern Gotland Basin in comparison to the Western Gotland Sea reveal the long-term cyclonic circulation of inflowing saline water. The entrance pathway of inflows is also found in the increasing bottom salinities in Bornholm Basin and Arkona Basin, where the variability of the bottom salinity is highest, indicating the strong fluctuation of inflow pulses. Mean salinity is constantly increasing in Belt Sea, Sound and southern Kattegat from 12.7 psu to 19.5 psu at the surface to 20.8 psu to 33.9 psu at the bottom. The variability is high between 10-23% within the whole water column in the shallow Mecklenburg Bight and Kiel Bight. Outflowing brackish water causes also high variation in the surface layer of Great Belt, Sound and Kattegat, but the deeper layers are always filled with saline water.

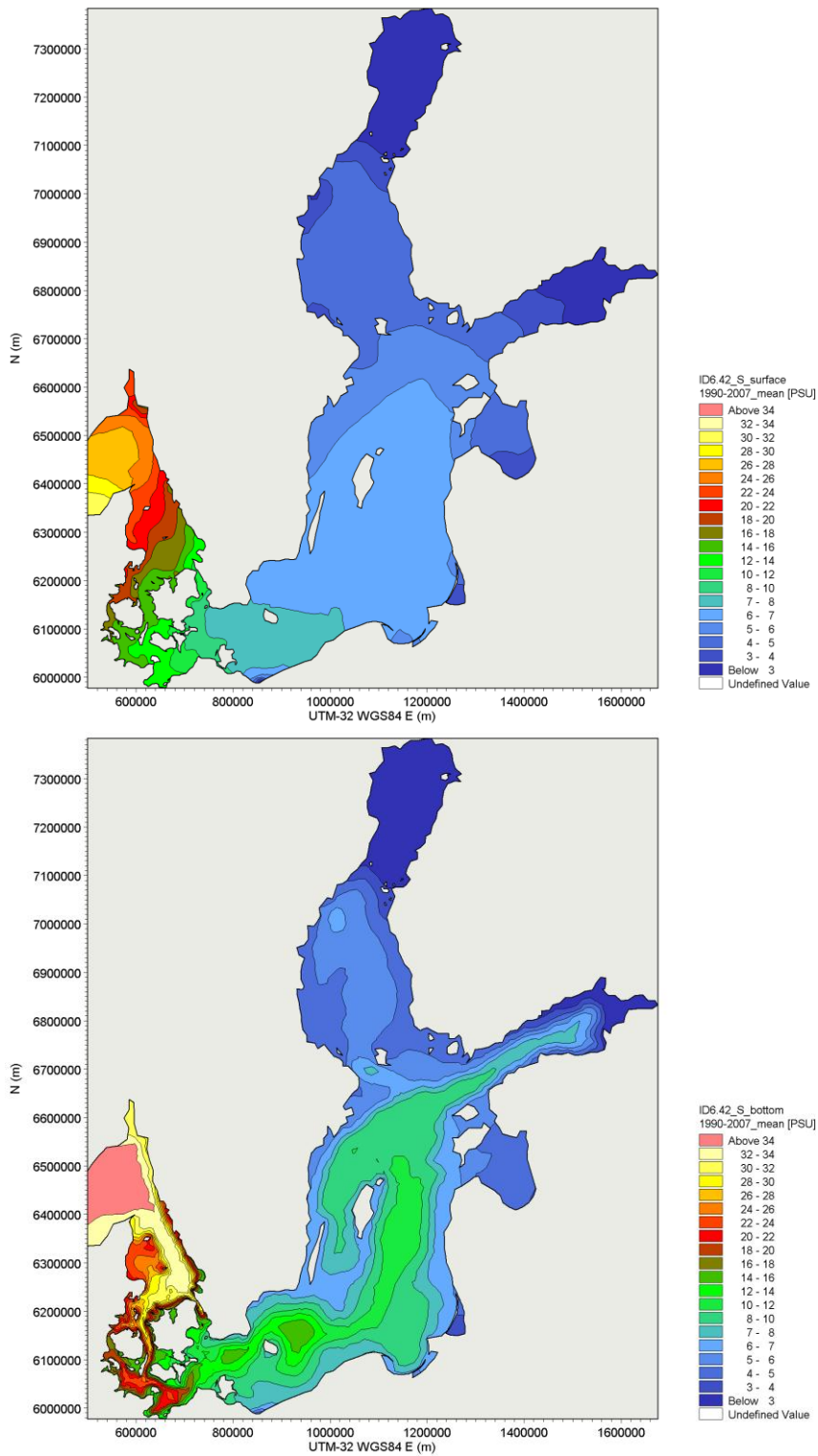


Fig. 3.17 Mean surface (upper panel) and bottom (lower panel) salinity (1990-2007) of the Baltic Sea simulated with the MIKE numerical model (FEHY, 2013c). A clear gradient between the northern Baltic Sea and the Kattegat is visible.



Table 3.4 Long-term statistics of surface and bottom salinity in Baltic Sea basins at the sea surface and in the bottom layer (after Feister et al., 2008). Potential outliers indicated by brackets.

Basin	Lon., lat.	Depth (m)	Min.	Max.	Mean	STD	Var. coeff. (%)	N
<b>Bothnian Bay</b>	22-23°E 64-65°N	0-10	2.6	4.5	<b>3.4</b>	0.22	<b>6</b>	2,029
		10-140	3.3	5.0	<b>4.2</b>	0.28	<b>7</b>	1,039
<b>Bothnian Sea</b>	19-20°E 61-62°N	0-10	3.4	6.2	<b>5.8</b>	0.25	<b>4</b>	1,825
		100-140	4.8	7.7	<b>6.6</b>	0.33	<b>5</b>	1,182
<b>Gulf of Finland</b>	25-26°E 59-60°N	0-10	3.0	8.4	<b>5.3</b>	0.60	<b>11</b>	3,174
		80-110	6.0	11.0	<b>9.1</b>	0.80	<b>9</b>	915
<b>Gulf of Riga</b>	23-24°E 57-58°N	0-10	1.4	7.4	<b>5.2</b>	0.54	<b>10</b>	1,382
		40-60	5.0	6.8	<b>5.8</b>	0.28	<b>5</b>	916
<b>Eastern Gotland Basin</b>	20-21°E 57-58°N	0-10	5.8	8.6	<b>7.0</b>	0.31	<b>4</b>	20,675
		230-240	9.5	13.7	<b>12.4</b>	0.46	<b>3</b>	3,538
<b>Karlsö Deep</b>	17-18°E 57-58°N	0-10	5.7	8.9	<b>6.9</b>	0.32	<b>5</b>	5,053
		130-200	8.3	11.0	<b>9.8</b>	0.62	<b>6</b>	1,317
<b>Bornholm Basin</b>	16-17°N 55-56°N	0-10	(3.1)	9.4	<b>7.4</b>	0.27	<b>4</b>	21,552
		80-90	8.9	20.5	<b>16.0</b>	1.41	<b>9</b>	1,426
<b>Arkona Basin</b>	13-14°E 55-56°N	0-10	6.0	21.5	<b>8.0</b>	0.51	<b>6</b>	17,417
		40-50	7.3	25.9	<b>15.1</b>	3.49	<b>23</b>	8,416
<b>Mecklenburg Bight</b>	11-12°E 54-55°N	0-10	(5.1)	26.8	<b>12.7</b>	2.96	<b>23</b>	39,742
		20-30	7.5	31.4	<b>20.8</b>	3.88	<b>19</b>	16,221
<b>Kiel Bight</b>	10-11°E 54-55°N	0-10	(5.0)	29.5	<b>15.8</b>	3.27	<b>21</b>	30,602
		30-60	9.0	34.1	<b>23.5</b>	2.30	<b>10</b>	7,115
<b>Great Belt</b>	10-11°E 55-56°N	0-10	7.4	33.3	<b>19.0</b>	4.03	<b>21</b>	74,991
		40-60	22.6	33.9	<b>30.5</b>	2.10	<b>7</b>	648
<b>Sound</b>	12-13°E 55-56°N	0-10	(4.8)	(35.7)	<b>12.7</b>	5.04	<b>40</b>	58,315
		40-60	21.7	35.2	<b>32.3</b>	1.85	<b>6</b>	13,282
<b>Southern Kattegat</b>	11-12°E 56-57°N	0-10	8.9	33.9	<b>19.5</b>	3.65	<b>19</b>	14,449
		50-110	32.3	35.0	<b>33.9</b>	0.57	<b>2</b>	1,004

### 3.3.2 Temperature

Water temperature in the Baltic Sea is also determined by the salinity-induced two-layer stratification. The upper layer experiences a strong annual cycle through air-sea interaction and solar radiation. This leads to the formation of a warm seasonal surface layer with a thermocline in summer. At the lower edge of this layer a dicothermal layer is formed when the water is heated from above but cooled by the colder bottom water, so-called "winter water", at the same time. This dicothermal water mass is referred to as "old winter water", it is a specific phenomenon of the Baltic Sea and other ice-covered seas.

The surface layer reaches its temperature maximum in August and a minimum in February and March (Siegel et al. 2008). After the ice-melt in spring, a thin layer at



the very surface is quickly heated by solar radiation and reaches a temperature of maximum density,  $T_m$ , of 1.5°C to 3°C (Leppäranta & Myrberg 2009). When the temperature rises above  $T_m$ , density decreases and convection is stopped which leads to the formation of a thermocline, separating the surface layer from the much colder bottom water. The depth of this thermocline is affected by wind mixing and solar radiation and therefore varies a lot. Typical thickness values are stated within 5 m – 100 m (Leppäranta & Myrberg 2009). The surface layer is not always homogenous though but may show several minor, internal thermoclines. Thus the definition of a well-mixed layer is often done by fixed vertical temperature gradients, e.g. 0.1°C/m. The depth of the summer thermocline is stated within 15 m - 30 m throughout the entire Baltic (Leppäranta & Myrberg 2009). Its formation begins in early May in the southern Baltic Sea and only one month later in the Bothnian Bay. In summer, the thermocline deepens somewhat due to wind-induced mixing, but its strong temperature gradient of up to 10°C prevents this mixing from influencing the bottom layer. With autumnal cooling, the thermocline deepens due to convection beginning in late August in the northern parts, while it takes a month for this effect to set in further south. All in all, the sea reacts slowly to atmospheric temperature changes because of its large thermal inertia. In winter, the upper layer is isothermal because of thermohaline convection and wind-induced mixing. In the central basins this convection usually cannot destroy the thermocline, but severe storms can well lead to the erosion of the thermocline anywhere in the Baltic and its reformation at lower depths (Krauss 1981).

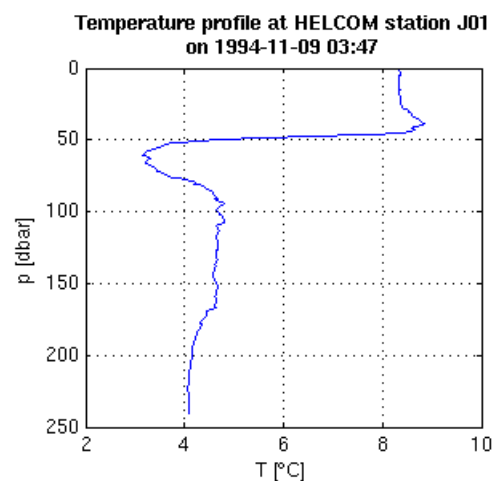
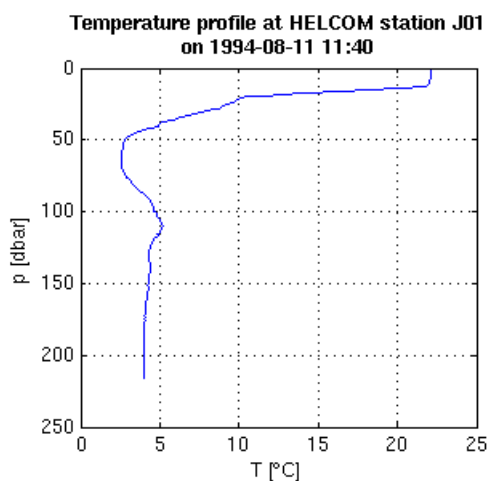
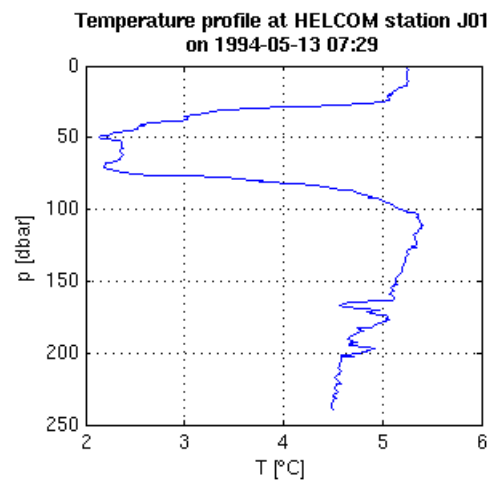
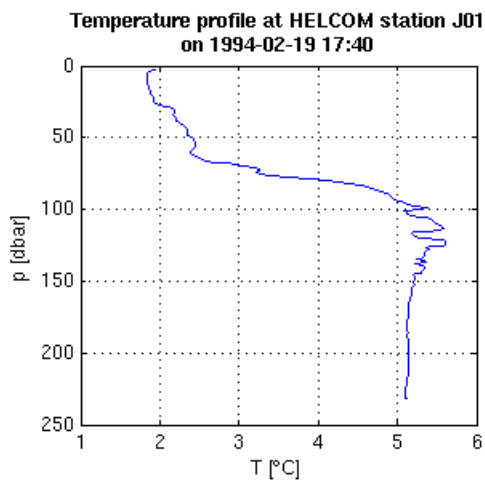




Fig. 3.18 Typical temperature profiles in the Eastern Gotland Basin in 1994 (data from ICES 2010). Upper left: winter, upper right: spring, lower left: summer, lower right: autumn.

As the lower layer is isolated from atmospheric effects, temperature changes here are due to advection of North Sea water and seasonal variations are very weak. Advection from the North Sea is seen strongest in the Belt Sea and the southern Baltic Sea. When such water masses flow northward, their higher density causes them to sink, so deep bottom waters are relatively warm. Typical bottom water temperatures range from 4°C to 6°C. In winter, an inverse thermocline occurs in the northern parts of the Baltic Sea, specifically in Bothnian Bay, where surface water reaches the freezing point and temperature increases with depth up to the density maximum's temperature, 2°C-3°C. That means "the difference between maximum density and the density at freezing point decreases with increasing salinity. The inverse thermocline is therefore more stable in freshwater than in brackish water" (Leppäranta & Myrberg 2009). While the permanent winter thermocline is normally located at the halocline, temperatures beneath the thermocline can be up to 5°C higher than in the upper layer due to advection.

### 3.3.3 Stratification

As indicated above, the stratification of the Baltic Sea is controlled by a combination of wind-driven and thermohaline circulations as well as by water exchange with the North Sea. Compared to other physical processes like the formation of sea ice, freshwater inflow and inflow of saline ocean water, stratification resulting from such processes has the strongest effects on the Baltic (Fennel et al. 2008). The halocline between the two layers is usually situated at 40 - 80 m but it is even shallower in the Belt Sea. The upper layer is homohaline while a continuous stratification occurs in the bottom layer.

During summer the upper layer is formed as warm, well-mixed water that is separated from the lower water body by its density. Additionally, spring and summer river runoff lowers the surface salinity. During spring, the surface salinity maximum is about 0.5‰ lower than the winter maximum, while a lag exists between the salinity minimum and the river runoff maximum (Leppäranta & Myrberg 2009). The stable stratification in summer causes a salinity maximum in the deep layer, whereas strong mixing during fall and winter reduces the salinity gradient between the two layers. Such effects are most common near coastlines where a halocline might not even exist at all.

The depth of the halocline depends on wind-driven and convective mixing, advection and the depth of sills. Except for the Belt Sea, the depth of the halocline is almost constant. In the belt Sea the stratification is different from the Baltic Proper because the halocline is tilted and moves back and forth depending on wind forcing. Under certain conditions, the halocline can also vanish completely, e.g. when wind-driven inflows into bay cause a hydrostatic outflow of saline bottom water in response or when strong wind-induced mixing occurs in the shallow western regions. The very eastern Gulf of Finland takes a special role as the runoff from the River Neva effects stratification in this shallow area. Here salinity increases nearly linearly from surface to bottom. The weakest halocline is found in the Bothnian Gulf of, but the salinity gradient between surface and bottom is still greater than 0.5‰ and thus prevents mixing of the entire water column (Leppäranta & Myrberg 2009).

### Ageing and renewal of water masses

Currently the stagnation periods where no major inflows of saline North Sea water occur are significantly longer than ever before, while the frequency of medium-scale baroclinic summer inflows has increased. During the last 30 years only six Major Baltic Inflows were recorded (Matthäus et al., 2008). As mixing between the lower and the upper layers in the central Baltic Sea through convection is normally





prevented due to strong haloclines, deep waters in the Baltic Sea tend to become anoxic and are thus even more dependent on renewal by advection of North Sea water. Major abundances of anoxic zones outside the seasonal effects in shallow coastal waters are in the deep parts of the Gotland Basin. The extent of bottom areas with hydrogen sulfide can be up to a third of the entire Baltic Sea (Leppäranta & Myrberg 2009). The Eastern Gotland Basin however is regularly supplied with saline water at intermediate depth levels between 80 m and 130 m, which explains why no  $H_2S$  is found above 140 m to 150 m, even during long stagnation periods.

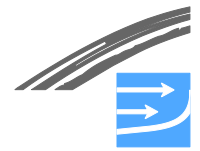
The residence time of deep waters within the Baltic Sea has been studied by a number of numerical simulations and from observed data. (Döös et al. 2004) used a three-dimensional circulation model with a Lagrangian approach. In this study times between 26 and 29 years were calculated, which is close to the traditional assumption of renewal times for the entire Baltic Sea of 30 years. Meyer et al. (2006) found in a numerical study that the mean age of bottom water was 1 year in the Bornholm Deep, 5 years in the Gotland Deep and 7 years in the Landsort Deep, the deepest point of the entire Baltic.

(Omstedt and Hansson 2006) found in a numerical study that salinity in the Baltic is non-linearly dependent and highly sensitive to changes in freshwater inflow. The time for a salinity-related water balance is about 33 years, which is close to the results of (Döös et al. (see above). The other important time scale for the Baltic Sea is the heat balance which is associated with a period of one year by (Omstedt and Hansson 2006). Changes in the Baltic Sea water temperature are highly dependent on air temperature, yet during climate warming. "the water and air temperatures may differ due to changes in the surface heat balance components" (Omstedt and Hansson 2006).

#### **3.3.4 Optical water types**

Incoming solar radiation is either reflected at the sea surface or it transcends into the water and is scattered or absorbed (i.e. thermalised) by the water and by dissolved and suspended matter. Another transformation of solar energy is the conversion into chemical energy by photosynthesis and re-emission as light by fluorescence and bioluminescence, all of which takes place in the upper, eutrophic layers. See also Chapter 5.2 for other factors determining phytoplankton. The bottom of this zone is commonly defined as the depth where the electromagnetic energy has fallen to 1% of the value directly below the surface (Apel 1988). Absorption and scattering in pure seawater are determined by the main chemical constituents of seawater, which are the following ions:  $Na^+$ ,  $Mg^{2+}$ ,  $K^+$ ,  $Ca^{2+}$ ,  $Sr^{2+}$ ,  $Cl^-$ ,  $Br^-$ ,  $F^-$ ,  $SO_4^{2-}$ ,  $HCO_3^-$ ,  $B(OH)_3$ . The main contribution comes from  $H_2O$ . A simple tool called a *Secchi disk* is used in observational oceanography to estimate the depth of total attenuation. It provides very approximate but still useful information about turbidity.

The knowledge about optical features of Baltic Sea water is largely based on irradiance data. A long time series (> 100 years) of Secchi depths exists and few records are available from water samples and in-situ soundings. Most optical research has been carried out in the southwestern Baltic Sea but more recently a number of programmes has been established in the Gulf of Finland. Depending on time and location, the present level of Secchi depths in the Baltic Sea varies from 5 m to 10 m. Coastal areas are generally more turbid than open basins, and turbidity there increases even during runoff peaks when large amounts of suspended matter is washed into the sea. As the Secchi depth is related to the scale of light attenuation, it can be used to infer physical properties of sea water. Mean Secchi depth in the Baltic has significantly decreased during the last 100 years due to anthropogenic influence. A major cause is eutrophication which has led to an increase of colored dissolved organic matter (CDOM) and chlorophyll in the Baltic Sea and in the lakes of its drainage (Leppäranta & Myrberg 2009).



A high content of CDOM and suspended matter which strongly influences light transfer is typical for Baltic Sea water masses. The inversion for optical measurements of water properties in such optically highly complex waters needs not be unique. The large amount of CDOM turns the Baltic Sea water brownish. In a 2004 study, Sipelglas et al. concluded that for variability of the attenuation coefficient, CDOM was the main optical component in their data set. Generally, chlorophyll is also a major factor in optical properties, not least due to its seasonal variability (cf. Chapter 5.4).

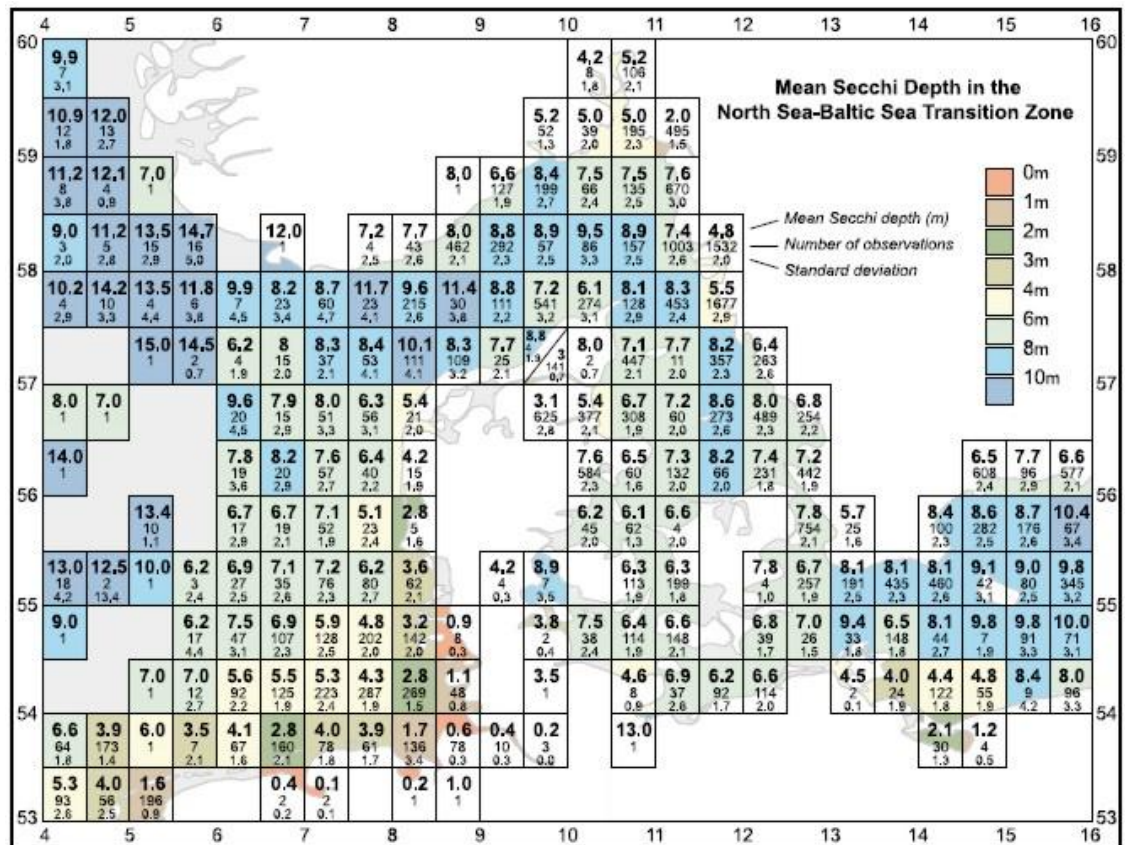


Fig. 3.19 Mean Secchi depth (top number), number of observations (middle number) and standard deviation (bottom number) for  $0.5^\circ \times 0.5^\circ$  squares for the transitional zone of the North Sea - Baltic Sea in the period 1902-1999; from (Aarup 2002). Most straits in the Belt Sea show a mean Secchi depth of 6 m while it increases to 8 m in the deeper parts of the Kattegat and also in the Arkona and Bornholm Sea. Reprinted from *Oceanologia*, Vol. 44, No. 4, Figure 2, p. 332, with the publisher's permission.

Ice and snow cover have as well a great impact on light transfer, depending on their wetness and layer thickness. Reflectance measurements show that in the early melting seasons the reflectance of snow becomes lower and has a weak minimum at 550 nm with an overall reflectance  $>0.4$ . In sea ice, the main optical impurities are made up by gas bubbles, included brine pockets and chlorophyll. Other studies showed that snow on sea ice causes a strong attenuation but a significant amount of light can pass into the water column once the ice is not covered by snow any more. Furthermore, the apparent optical properties of water below sea ice differ from those of ice-free water because incoming light is much more diffuse under an ice cover.



One of the most important applications in marine optics in the Baltic, especially remote sensing, is currently the mapping of harmful algae blooms. However it is not clear how to separate the signal of climatic change from local anthropogenic effects.

### **3.4 Estuarine Circulation**

#### **3.4.1 Long-term exchange**

The hydrographic state of the Baltic Sea can be understood as the results of a dynamical balance between freshwater input through rivers and precipitation and salt water inflows through the Danish Straits. These different water masses are transformed by small scale and mesoscale mixing, where the mixing processes are mainly driven by wind stress action and convective processes. The dense saline North Sea water, that flows through the Danish Straits as near bottom currents, has to overcome the sill areas (Darss Sill and Drogden Sill) and follows then basically the so-called 'Talweg' through the Arkona Basin (the path along the deepest points of topography) and reaches the Bornholm Basin through the Bornholm Channel. In the Bornholm Basin the dense bottom water has to exceed a certain height above the sea bottom to flow through the Stolpe Channel in the Gotland Basin. The bottom flow can be driven by its own gravity, as a down-slope propagating dense bottom flow, and it can be moved by the circulation driven by pressure gradients generated by wind forcing.

On its way to the Central Baltic (Baltic Proper), the dense saline water will be modified by mixing with ambient waters. The result is a relatively fresh body of surface water above the more saline deeper waters. Both waters are separated by the halocline. Thus the relatively stable general horizontal and vertical salinity gradients (halocline) are externally controlled by the saltwater and freshwater input and the outflow of a mixture of both water masses, the brackish waters that leave the Baltic Sea as surface current through the Danish Straits. Therefore, changes due to imbalances can be generated by variations of inflows of saline waters and/or freshwater, and by the meteorological processes that drive the mixing and transformation of the waters. An indication for such an imbalance can be seen in the salinity variations in the deep waters in the Baltic Proper. The typical saw-toothed profile (Fig. 3.20) shows clearly that the salinity decreases over a period of time until it is suddenly enhanced after an inflow event. In other words, the abovementioned balance is not perfect. The salinity of the bottom waters decreases for a couple of years until it suddenly increases in response to short but intense inflow events.

The delicate balance is affected if changes in the transition area modify the propagation of saline waters into the system, or if changes of freshwater discharge through diversion of rivers in the catchment area occur (Pedersen and Moller 1981). Although one might speculate that the construction of dams in Sweden could also have an impact on the frequency of inflow events, it appeared the seasons with higher river runoff have generally no effect on inflows. (Matthäus & Schinke, 1999).

On average, the net transport flows through Little Belt, Great Belt and Sound according to the relation 1:7:3 (Jacobsen 1980; Jakobsen and Trebuchet 2000). This has been derived from the long-term water budget of the Baltic Sea (HELCOM 1986) and was confirmed by current meter observations at Drogden Sill, Darss Sill and Little Belt. However, estimates of transport derived from single stations can only represent the magnitude of order of the flow through the entire cross-section.. Because of changes in stratification estimated salt transport are even more insecure. Reliable transports through cross-section can be calculated from numerical models which provide continuous data in space and time. Moreover the volume conservation of the models assures a realistic water budget of the Baltic Sea. The MIKE Regional model run ID6.42 yields the annual mass and salinity transports



shown in Table 3.5. The data show that the fluctuation in transport is regularly several times larger than the net transport. The salt transports are nearly balanced with a net flow less than 1 Gt/year. The small values given in the table correspond transient decrease in the Baltic Sea. The net flow of water shows the annual fresh-water excess from river runoff and precipitation in the order of 500 km<sup>3</sup>/year.

Table 3.5 Annual volume and salt transports across Drogden Sill, Darss Sill and Fehmarnbelt as simulated by the MIKE Regional Model (ID6.42) for the period 1990-2007 (FEHY 2013c).

	Volume inflow [km <sup>3</sup> ]	Volume outflow [km <sup>3</sup> ]	Net volume transport [km <sup>3</sup> ]	Salt inflow [Gt]	Salt outflow [Gt]	Net salt transp. [Gt]
<b>Drogden Sill</b>	564	-767	-203	7.8	-7.6	0.12
<b>Darss Sill</b>	1,283	-1616	-333	16.1	-16.4	-0.33
<b>Total Central Baltic</b>	1,847	-2,383	-536	23.8	-24.0	-0.21

### The Sound

The Sound is one of the three straits connecting the Central Baltic Sea to the Kattegat. In connection with the planning and construction of the Øresund Link numerous studies on the hydrography was carried out, see e.g. (ØL 1997). Some of the results are published in papers as for example (Jakobsen et al. 1997a), (Mattsson 1996), (Nielsen 2001) and (Green and Stigebrandt 2002). The specific investigations during the Øresund Link project lead to a more elaborated understanding of the local hydrography of the Sound region which gave decisive insights for achieving a "zero solution".

The Sound can for most purposes be considered a stratified channel, where the water discharge through the channel is driven by the water level difference between Kattegat and Arkona Basin. The water discharge is only to a minor extent driven by the local wind over the Sound and the density difference between the southern (towards Arkona Basin) and northern boundary (towards Kattegat). Still, the wind impacts the local flow in the numerous bays along the coastline.

Analyses of long-term data collected at the Drogden light-vessel in the Sound revealed that the flow in the Sound is northwards in 51.9% of time and southwards in 32.4% of time. The medium duration of northward flow is 3 days, while it is 2 days for southward flow.

The salinity at the northern boundary towards Kattegat is higher than at the southern boundary towards Arkona Basin. This difference drives a slow baroclinic exchange flow, which causes the water body to be stratified: high saline water flows in a lower layer southwards into the Sound; and low saline water flows in an upper layer northwards into the Sound. In average a salt water wedge starts just north of the narrow contraction at Helsingør-Helsingborg that ends at the shallow Drogden sill. The salt water wedge can be moved in the north-southwards direction by the barotropic flow and be more or less pronounced because of turbulent mixing of the water layers.

During southwards flow the high saline water from Kattegat can be lifted locally across the Drogden sill. And in general larger parts of the Drogden sill area are stratified during a south flowing current than during a north flowing current. The



size of the stratified areas during a south flowing current depends on the current speed near the bottom. If the velocity near the bottom during a south flowing current is high, the bottom generated turbulence can mix the two water masses into one layer. When large high saline water masses are transported across the sill they plunge south of the sill, whereby a front between the high saline water masses flowing across the sill and the low saline water masses in the Arkona Basin is created. The high saline water masses that have plunged south of the sill are trapped inside the Central Baltic Sea and can only be transported out of the Central Baltic Sea again by being entrained into the upper low saline layer. Details found in the investigations in connection with the planning and construction of the Øresund Link are:

- In the central part of the Sound during southwards flow less saline water is observed along the Swedish coast (also in the Lommabukten), in the separation zone north of Saltholm, in the lee zone south of Saltholm and in the southern part of the Sound. Upwelling of slightly higher saline water ( $\sim 1-3$  psu) along the coast of Amager may be forced by a westerly wind component. In the Drogden Channel on the sill an area of local high mixing is identified, while in the Flinten Channel the area stretches much further north than in the Drogden Channel.

During northwards flow the narrow contraction at Helsingør-Helsingborg can act as an internal hydraulic control on the flow and hence impact the extent of the salt water wedge. Details found in the hydrographic investigations in connection with the planning and construction of the Øresund Link is:

- In the central part of the Sound during northwards flow the salinity generally increases from east to west, except in the lee zone north of Saltholm, where more saline water is partly trapped in the beginning phase of northward flow. North of Saltholm in the region with less current the outflow spreads out. Along the coast of Amager a narrow upwelling of slightly higher saline water ( $\sim 1-3$  psu) may be identified.

Even though the density differences in the Sound are not important in driving the flow through the Sound, the stratification is still of importance for the flow and impacts the discharge through the Sound. It is because the stratification lubricates the flow, i.e. decreases the retarding friction on the flow. Hence the stratification in the Drogden Sill area decreases the contribution to the specific resistance of the Sound from the sill area. Because of the generally larger stratified areas with south flowing currents than with north flowing currents, the specific resistance of the Sound is determined to be  $210 \times 10^{-12} \text{ s}^2/\text{m}^5$  for south flowing currents and  $245 \times 10^{-12} \text{ s}^2/\text{m}^5$  for north flowing currents.

The design of the Øresund Link was optimised to reduce the blocking of the link. The initial design blocked the flow by 2.3%. By moving the artificial island into the lee zone south of Saltholm and by streamlining the island the blocking was decreased to be 0.5%. To obtain a "mathematical zero blocking solution" compensating dredging was carried out in the sill area. For the final Øresund Link including compensating dredging the blocking is  $0\% \pm 0.15\%$ .

### **3.4.2 Major Baltic Inflows**

The saline water from the North Sea enters the Baltic Sea through the Kattegat and the Danish Straits. There are basically two modes of inflow, a more or less permanent sequence of small amounts of saline water flowing over the sills and propagate slowly towards the Arkona Basin, and vigorous inflow events which are associated with substantial transports of salt water.





Fluctuations of the salinity in the northwestern European shelf seas were assumed to be one of the possible reasons for the occurrence of Major Baltic Inflows (MBI's), because they tend to coincide largely with these salinity variations (Dickson 1971).

However, it was found that certain meteorological conditions over Northern Europe and in particular over the Baltic are necessary for the generation of the inflows (Matthäus & Schinke, 1994). One of the necessary conditions linked to the major events in 1951 and 1993 is a lasting high wind speed from westerly directions over several weeks (Wyrтки, 1954a and Matthäus & Lass, 1995). To be classified as a Major Baltic Inflow, inflowing saline bottom water that has passed the sills at Darss and Drogden must fulfill the following criteria; (i) the inflow has to last for at least 5 consecutive days and (ii) the bottom salinity must be greater than 17‰ with very weak or no salinity stratification. These minimum criteria set the threshold of 0 in the intensity index. An inflow intensity of 100 corresponds to 30 consecutive days of inflow with a bottom salinity of 24‰ (Matthäus & Franck, 1992).

Major Baltic Inflows can renew the deep water in the central Baltic Sea, associated with an increase of the oxygen concentration of the waters below the permanent halocline. The entrainment of saline and cold water masses enhance the stability of stratification, and consequently decrease in vertical mixing of the deeper layers of water. These changes are essential for the distribution of the hydrographic, chemical and biotic conditions and affect the live of organisms that dwell in the deep and bottom water and at the seafloor.



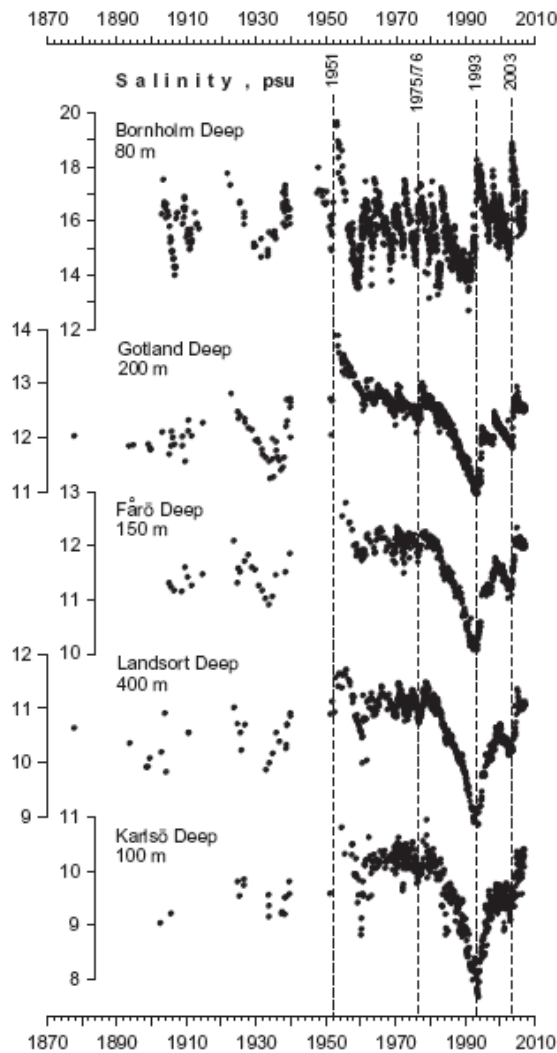


Fig. 3.20 Long-term variation of salinity in the central Baltic deep water (after Matthäus et al. 2008). The saw-toothed variations of the salinity is generated by major inflows and decreasing salinity between inflow event.

A general overview of the time distribution of all reported inflow events has been produced by Matthäus et al. (2008), using the indexing method developed by Matthäus and Franck in 1992. An example is shown in Fig. 3.21. As can be seen in Fig. 3.20, for the period between 1970 and 1990, there several salt water pulses in the deep water of the Bornholm Basin were detected, but only the vigorous inflow of 1976 reaches the deep waters of the Baltic Proper. This tells us two things: (i) the strong barotropic inflows in autumn or winter are the main events, (ii) there are also many less strong inflow event at almost every season, which do not replace the bottom waters in the deep parts of the central Baltic, but renew layers in the halocline (interleaving), provide a upward salt flow through replacing by pushing waters upward and give an important contribution to the overall salt budget. The smaller inflows are not as easy to detect as the big ones which are associated with extreme storms. But in since the 1990s a network of permanent stations has provided online information of inflow signals and increased the awareness of smaller events.

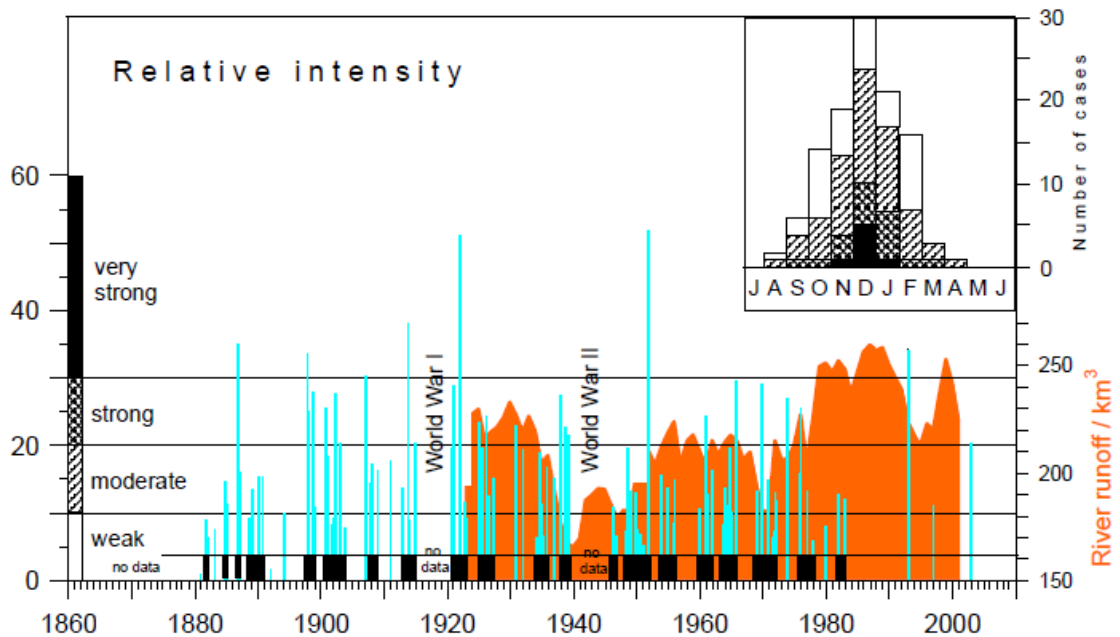


Fig. 3.21 Major Baltic Inflows (MBIs) between 1880 and 2007 and their seasonal distribution (upper right) shown in terms of their relative intensity and five year running means of river runoff to the Baltic Sea (inside the entrance sills) averaged from September to March (shaded). Black boxes on the time axis: MBIs arranged in clusters; from Matthäus et al. (2008).

The first time that a major inflow could be observed while it happened was in 1993, when the r/v A. v. Humboldt of the IOW was working sections across the Darss Sill and could produce a three dimensional figure of the event. One important aspect was the evidence that due to the strong mixing imposed by the strong winds, a substantial part of the inflowing waters was already mixed in the Arkona Sea and left entrained into the surface waters the Baltic Sea.

A quantification of the volume of the saline waters showed that a volume of about  $160 \text{ km}^3$  of the waters entered the Arkona Sea contributed to the renewal of the deep water in the central Baltic, which was quickly reached after about two weeks time (Matthäus & Lass, 1995). However, they could also show that a substantial part of the total volume of inflowing water was mixed in the Arkona Basin and pushed back across the Darss Sill as modified surface water. This indicates that the wind driven currents and mixing are not only an important prerequisite for the generation of a major inflow, but they can counteract the water renewal by providing water mass transformations.

### 3.5 Wind-Driven Currents

#### 3.5.1 Ekman current and transport

The response of the water currents to wind on the rotating earth is not intuitive. The wind drives waves which break and generate turbulent viscosities. These viscosities together with the action of the earth rotation, quantified by the Coriolis- or inertial frequency, ( $f=1.2 \cdot 10^{-4} \text{ s}^{-1}$  in the Baltic Sea area), generates a slow Ekman transport in the upper ocean layer moving towards the right to the wind direction (on the northern hemisphere). Only divergences or convergence of the Ekman transport, which can be generated by wind stress curls or by spatial structures such as coasts, give rise to vertical movements of the waters and can create pressure gradients. The flows driven by pressure gradients, which are usually in geostrophic balance, provide the strong currents. In contrast to the ocean though, no significant permanent vertical component of the wind stress curl exists at the surface of the



Baltic Sea since it is located entirely in one climate belt, namely the west wind belt (Lass et al. 2009). This implies that the wind cannot excite any permanent divergence of the Ekman transport in the open Baltic Sea and subsequently no up- or downwelling and hence no permanent geostrophic in the open Baltic Sea.

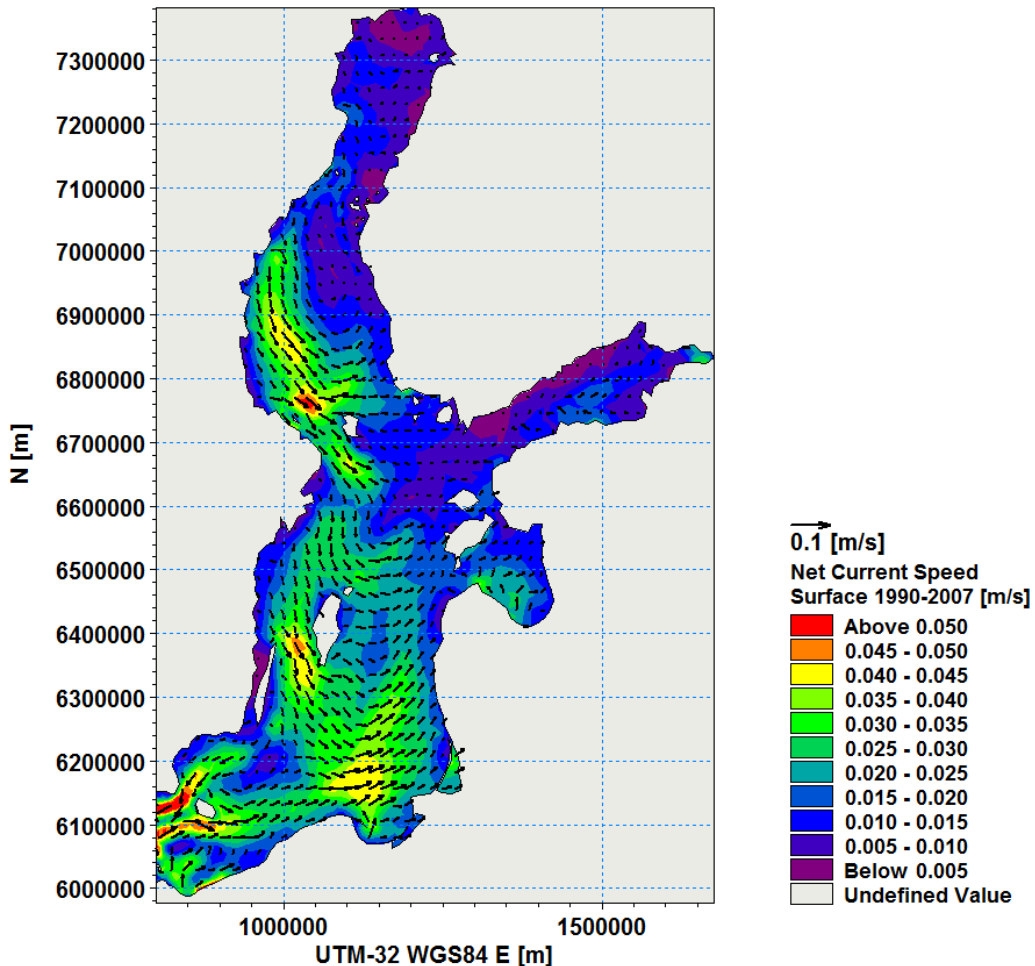


Fig. 3.22 1990-2007 mean surface circulation as simulated with the MIKE Regional numerical model (FEHY, 2013c). Colors indicate current speed while arrows show current velocity.

Currents may be caused by wind stress on short time scales such as 5-10 days but due to the high variability of wind, the long-term wind-driven mean circulation of the Baltic Sea is weak (Leppäranta & Myrberg 2008). This means that the resulting surface circulation of the Baltic Sea is a non-linear combination of a baroclinic mean background circulation that is independent of wind stress and the mean wind-driven circulation (Leppäranta & Myrberg 2008). An example of the long-term (1990-2007) mean surface circulation of the Baltic Sea simulated by FEHY (FEHY 2013c) is given in Fig. 3.22. It shows a large basin-wide cyclonal gyre around Gotland in the Baltic Proper and two smaller gyres in the Bothnian Sea and Bornholm Basin respectively. The mean current speeds in the Baltic Sea are in the order of one cm/s but the Belt Sea clearly shows a strong outflow with mean speeds of about 10 cm/s.

### 3.5.2 Upwelling, coastal jets and Kelvin waves

Owing to the high variability of the of the wind forces over the Baltic Sea, the wind generated current patterns last, as a rule, only for a few days. An important part of the water motion in the Baltic Sea is the generation of coastal currents. In an almost enclosed sea like the Baltic Sea, virtually all directions of wind have somewhere an alongshore component, which generates Ekman up- or downwelling. The



classical understanding of the forcing of upwelling is the following: an alongshore wind blowing in a direction with the coast to the right, an offshore Ekman transport is generated. Because of the condition that no flow can go through the coastal boundary, the Ekman transport must go to zero when approaching the coast. This implies a divergence of the cross shore current. The divergence is balanced by a vertical flow that lowers the sea level and rises the isopycnals (i.e. the density surfaces in the water body). As a result, barotropic and baroclinic pressure gradients are being generated, which drives a strong coastal current, the coastal jet, in downwind direction.

The upwelling events can be detected during the summer season, when the cold winter water replaces the warm water of the upper, wind mixed layer. Then the differences in temperature often span a range of 10°C. This signal can well be detected in infrared images, a review over upwelling in the Baltic Sea was recently given by (Myrberg et al. 2010).

Often the cold water cells are not extended along the coast where upwelling favorable winds act on the sea. We often find alongshore gradients in the temperature signals. This is the effect of coastal trapped waves, in particular Kelvin waves, which are excited by spatial and temporal changes of the wind forcing. These waves propagate alongshore with the coast to the right and stop the upwelling after their arrival. The specific extend and shape of cold water upwelling cell depends on the propagation properties of the Kelvin waves. If the upwelling is forced by wind pulses, the Kelvin waves can even generate downwelling where the local Ekman transport is still favoring upwelling (Fennel and Seifert 1995).

An example, where these effects are seen particularly clear is the upwelling off the east coast of Gotland Island (Fennel et al., submitted). Here upwelling shrinks to a cold water cell near the south eastern end of Gotland Island. For a circular island, the response is virtually the same for every wind direction and consists of up- and downwelling patterns that rotate around the island. For an elongated island like the Gotland island with narrow tips at the northern and southern ends, only alongshore southern or northern winds can create up- or downwelling. For example, southern wind pulses excite Kelvin at the northern tip, which propagate southward, diminish the upwelling and introduce even slight downwelling during their travel. Friction decreases the wave amplitudes during their travel and slackens the effect on the Ekman upwelling towards the south. Similarly, waves generated at the southern tip would ideally export the upwelling around the southern cape and along the west coast. Since the phase speed depends on the local stratification, water depth and coastal curvature, these waves propagate slowly and are trapped near the southern tip. Hence the upwelling cell nears the south eastern end are only weakly affected by the waves from the north, and the export of upwelling around the southern tip is hindered by the slow propagation due to the shallower depths, which reduce the propagation speed.

This mechanism explains why the formation of the upwelling cell typically occurs near the southern end of the east coast during southern winds that are favorable for upwelling. The examples also illustrate that upwelling cannot fully be understood without considering the coastal trapped waves.

Another remarkable effect of the Kelvin waves is that they introduce alongshore gradient of the pressure field and the alongshore current. Thus the coastal response is a three-dimensional problem. In particular, the Kelvin waves stop the acceleration of the coastal jet, which is arrested to the amplitude at the time of the arrival of the wave, and the pressure alongshore gradient drives an undercurrent.



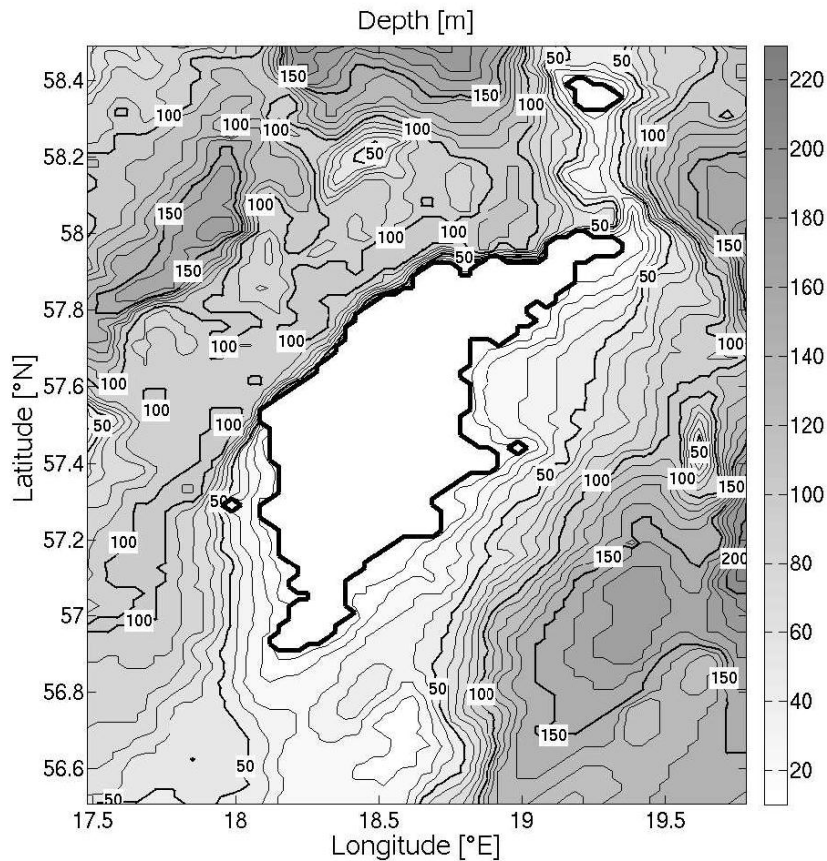


Fig. 3.23 Bathymetry around Gotland (central Baltic). From (Fennel et al. 2010, submitted).

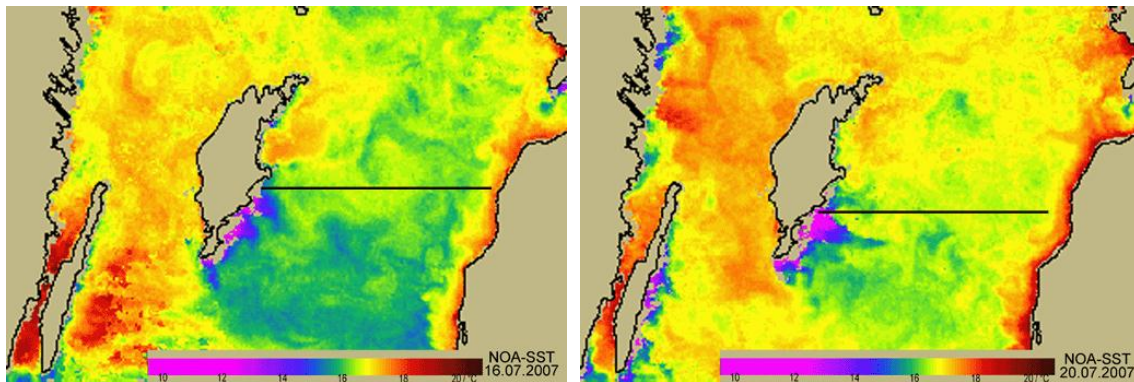


Fig. 3.24 Sea-surface temperature measured in July (dates as indicated) by NOAA AVHRR over the Gotland Basin from (Lass et al 2010); the horizontal line denotes a transect studied in that publication).

### 3.5.3 Interaction of the coastal zone and the open sea

If we look at a satellite image of the sea surface temperature (SST), for example Fig. 3.25, we usually see a lot of variability in the scale of several kilometres. Since the meteorological forcing has a much larger scale, which matches the scale of the basins, it is obvious that the mesoscale patterns are due to the internal dynamic of the ocean, i.e. in our case the Baltic Sea.

As required by basic laws of hydrodynamics, the pressure fields adjust largely to the bathymetry and geostrophic currents tend to flow parallel to isobaths. In such a stage, the communication between the open sea and the coastal zone would be weak. However, the main agents supporting a basin-wide interaction are, besides

the ageostrophic Ekman transport, the transients. The frequent adjustment to new forcing events supports cross-isobath motion, through instabilities of frontal zones and eddies.

If upwelling favourable wind blow long enough, the uplifted isopycnals may outcrop and moved offshore by the Ekman transport. This mechanism leads to the formation of so called upwelling fronts, which can create instabilities and support the generation of filaments and eddies that usually populate the open sea.

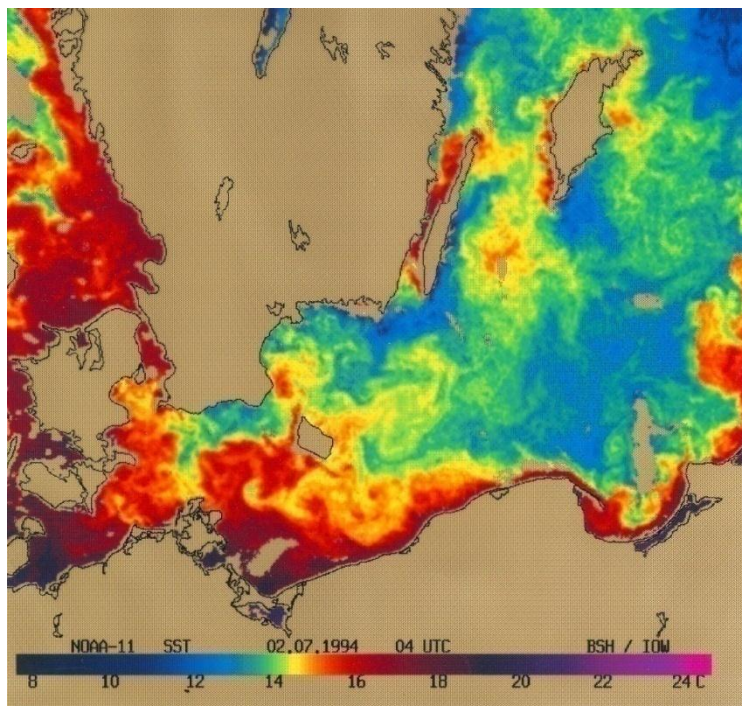


Fig. 3.25 Example of a satellite image of the Sea Surface Temperature (SST) of the Baltic Sea, showing a strong spatially variability (eddies, front and filaments) with scales of five to ten kilometres (courtesy H. Siegel, IOF).

### 3.6 Turbulence and mixing

The crucial role of mixing for the large-scale overturning circulation in the Baltic Sea is demonstrated by the following simple calculation. With a freshwater input of about 500 km<sup>3</sup>/year (net precipitation and river run-off) and a comparable export of brackish water with a salinity of about 8 g/kg through the Danish Straits, the Baltic Sea exports about 4 Gt of salt per year, and imports the same amount on the long-term average (Feistel and Feistel 2008a; Matthäus 2006). The imported water from the North Sea, however, is of higher salinity, thus requiring a diapycnal flux in order to transport the amount of 4 Gt of salt from medium saline to less saline water classes. With a cross-sectional area of about 130,000 km<sup>2</sup> at 60 m depth, this would correspond to a mean diapycnal salt transport rate of about  $J = 30 \text{ kg}/(\text{m}^2/\text{year})$ . Mixing is therefore a fundamental link in the basin-scale “conveyor belt” of the Baltic Sea.



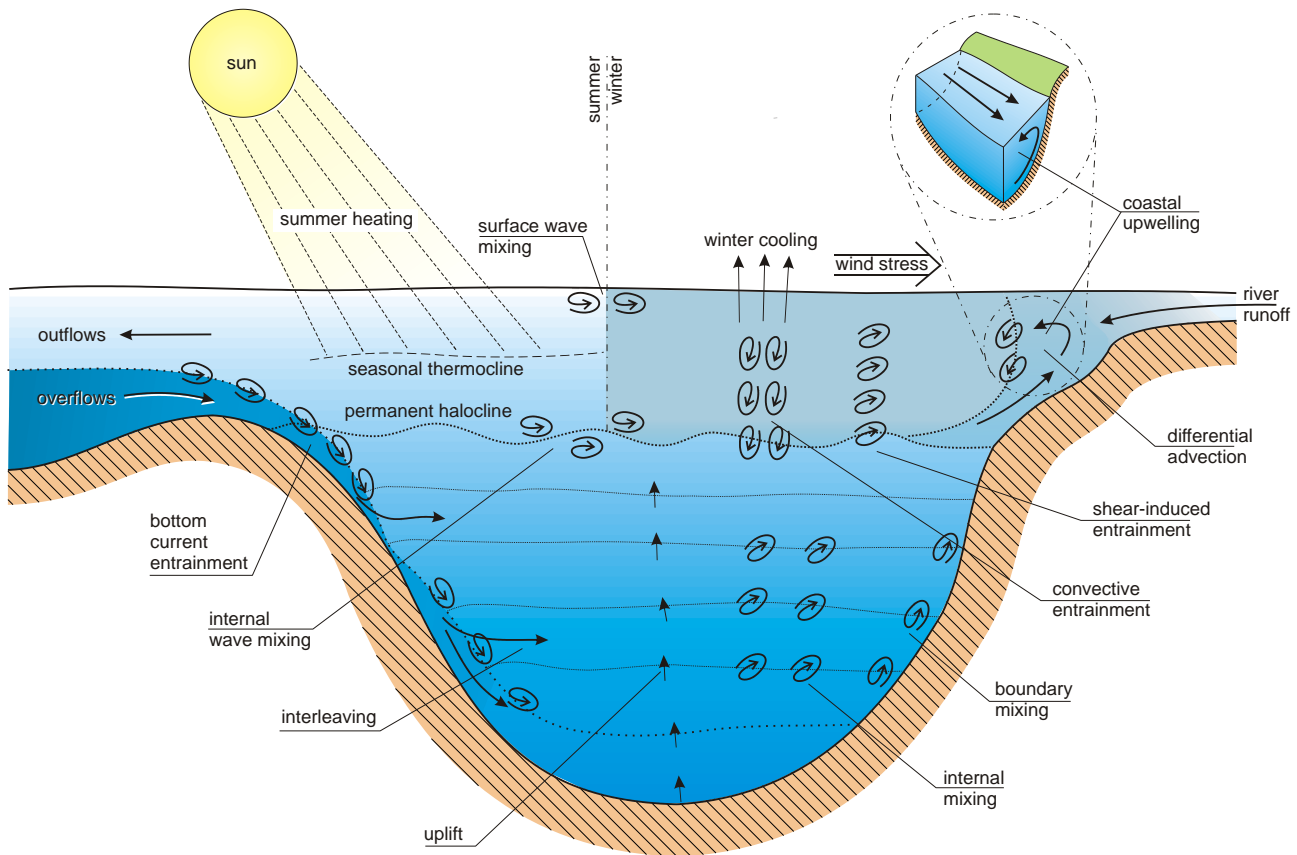
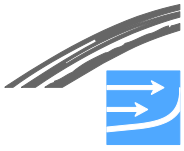


Fig. 3.26 Scheme of vertical mixing and transport processes in the Baltic Sea (from Reissmann et al. 2009).

### 3.6.1 Bulk estimates for basin-scale mixing

In a recent review, Reissmann et al. (2009) discussed a number of different mixing processes that could explain the transport rates inferred from basin-scale budgets as sketched above (Fig. 3.26). These authors suggested that the interplay between halocline erosion during wintertime (due to wind stirring and convection), and episodic uplifts of the halocline during inflow events form the two key components of the overall mixing process. This concept is briefly illustrated in the following with a computational example taken from (Reissmann et al. 2009).

A well-known feature observed in the Baltic Proper is a seasonal variation of the mixed layer salinity with a minimum during summer and a maximum during the cold season (Feistel et al. 2008). From the analysis of available data, Matthäus (1978) suggests that the mean salinity variation in the seasonal cycle is approximately  $\Delta S = 0.52$  g/kg. With the simplifying assumption that the increase in salinity during the cold season exclusively results from halocline erosion due to entrainment (i.e. ignoring all lateral transport processes), Reissmann et al. (2009) estimate an average salinity flux of  $J = \rho \Delta S H = 31$  kg/(m<sup>2</sup>/year) at the base of a mixed layer of thickness  $H = 60$  m. This value is comparable to the mean diapycnal transport rate estimated above, suggesting that halocline erosion is one of the key players in diapycnal mixing.

On the seasonal scale, the salt entrained into the mixed layer by halocline erosion is lost due to isopycnal advection of mixed-layer water out of the Baltic Proper towards the Danish Straits. A process is therefore required for restoring the vertical



salinity gradients in the halocline, thereby replenishing the pool of high-salinity waters at the mixed layer base for future entrainment. In order to explain this mechanism, Reissmann et al. (2009) pointed out that downward advection of high-salinity water by dense bottom gravity currents into the deeper parts of the central basins must be compensated by upwelling at other locations (Fig. 3.26), suggesting that the vertical advection associated with this upwelling leads to a restoration of the halocline.

As a rough estimate, (Reissmann et al. 2009) assumed that during a typical Major Baltic Inflow about  $100 \text{ km}^3$  of water transport 2 Gt of salt into the deep water below the permanent halocline. Independent of subsequent mixing processes, this intruding volume elevates the pycnocline by approximately 0.8 m on the basin-scale average (the horizontal cross-section is approximately  $130,000 \text{ km}^2$  at 60 m depth). Assuming that a representative isohaline with  $S = 10$  psu is lifted by this distance, and eroded by vertical mixing during the following winter(s), 1 Gt of salt becomes entrained into the mixed layer. The resulting increase in surface-layer salinity is less than  $\Delta S = 0.1$  psu on the average if a mixed-layer volume of  $15,000 \text{ km}^3$  is assumed, and thus substantially smaller than the observed seasonal increase (see above). It is, however, likely that the halocline uplift and the associated mixing are more pronounced along the pathway of the inflowing water masses, resulting in a locally enhanced signal of the seasonal salinity increase in the Baltic Proper. From changes in the oxygen distribution in the deep water of the Eastern Gotland Basin during the Major Baltic Inflow 2003, Reissmann et al. (2009) infer e.g. a pycnocline lift of approximately 30 m. They finally conclude that deep-water uplift during inflow events and subsequent pycnocline erosion is by far the dominating vertical transport mechanism in the Baltic Sea on the long-term average.

### **3.6.2 Mixing processes**

While the interplay between halocline uplift and erosion explains the observed basin-scale mixing rates *on the long-term average*, other mixing processes may be crucial for the determination of local water properties in the deepest layers, in particular during stagnation periods. The above computations do, for example, not distinguish between inflows with different intrusions depths (as long as these occur below the halocline), although the actual intrusion depth is crucial for the deep-water ventilation. Any mixing process occurring along the inflow pathway will lead to a modification of the final intrusion depth. It is important to point out that the impact of mixing on the (only sporadically occurring) densest water classes in the Western Baltic is of particular importance since the maximum densities determine the maximum depth that can be ventilated by inflows. This argument illustrates why the effect of man-made constructions on mixing during inflows in the Western Baltic Sea deserves special attention.

Even in the absence of inflow activity, deep-water diapycnal mixing is essential for the upward transport of nutrients (e.g. phosphate released from the sediments) towards the surface mixed layer, and thus for the timing and evolution of some of the most important ecosystem reactions. The state of the art of our understanding of these processes will be briefly outlined below, with a more detailed description of mixing processes in the Belt Sea deferred to a separate report on the Fehmarnbelt link region. This includes measurements and model studies focusing on the effect of man-made constructions in the pathway of inflows.

### **3.6.3 Entrainment in buoyancy-driven inflows**

Entrainment and mixing play an important role in modifying water mass properties and intrusion depths of dense water inflows, underlining their essential importance to the ventilation of the deep layers of the Baltic Sea, e.g. (Stigebrandt 1987). This fact has motivated numerous investigations with the main results briefly summarized below.



(Köuts and Omstedt 1993) located regions of increased mixing along the pathway of dense bottom currents, and inferred the volume increase of inflow water due to entrainment for each of these regions from salinity and temperature observations over approximately two decades. From this analysis, they suggested a volume increase of 79 percent for the Belt Sea, 53 percent for the Arkona Sea and 28 percent for the Stolpe Channel. For the Bornholm Channel and the Bornholm Sea mixing was identified as negligible. In a more detailed and process-oriented investigation (Lass and Mohrholz 2003) identified three major mixing mechanisms: (i) wind mixing in the vicinity of sills, (ii) differential advection in the head region of the dense bottom currents, and (iii) shear-induced entrainment of ambient water into dense bottom currents.

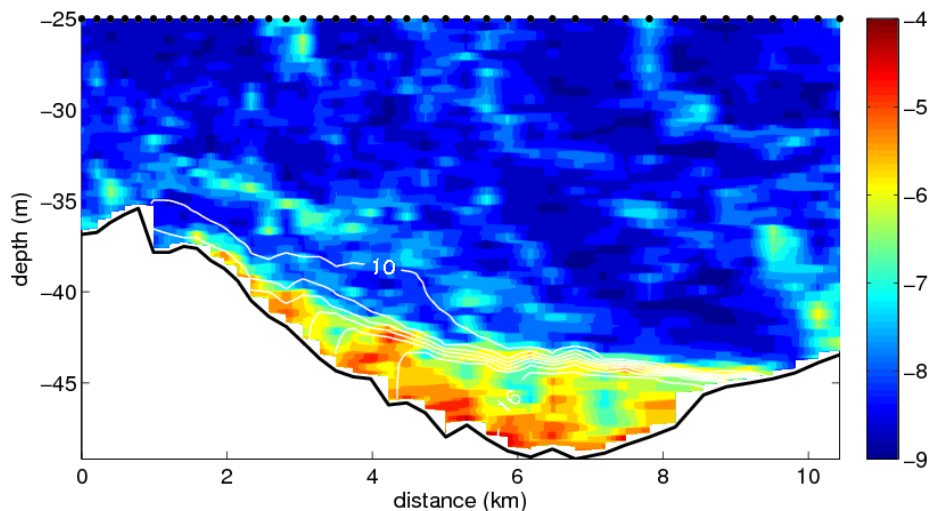


Fig. 3.27 Transect through the Bornholm Channel from 19 November 2005 between 10:20 h and 12:30 h UTC, south-east is to the left and north-west is to the right. The salinity contours are drawn at intervals of 1 g/kg here. The upper 25 m are not shown for clarity. Figure taken from (Reissmann et al. 2009).

While these results are entirely based on indirect evidence of mixing from hydrographic observations, an extensive data set including *direct* measurements of turbulence and mixing parameters in bottom gravity currents has recently become available (Umlauf & Arneborg 2009a; Umlauf et al. 2007; Sellschopp et al. 2006). In contradiction to the results by Köuts and Omstedt (1993), these data indicate that substantial entrainment also occurs when the gravity currents descend into the Arkona Basin, and in the Bornholm Channel connecting the Arkona and the Bornholm Basins (Reissmann et al. 2009). Fig. 3.27 illustrates the elevated turbulence levels associated with the passage of the gravity current through the Bornholm Channel, where the interesting asymmetry observed in the density structure has been subject to a number of recent theoretical investigations (Umlauf et al. 2010; Umlauf and Arneborg 2009a, b). A number of modeling studies supporting these findings have been discussed by (Arneborg et al. 2007) and (Burchard et al. 2009).

Support for another conclusion of (Köuts and Omstedt 1993) that the Stolpe Channel is likely to be a location of strong mixing and entrainment comes from a recent (unpublished) data set from cruise POS373 with R/V Poseidon in September 2008. Data from a turbulence microstructure transect across the furrow reveal strong turbulence and mixing on the steep southern slope of the channel (see Fig. 3.28). The distorted isopycnal structure and the transient nature of the mixing patches (not shown) suggests that, here, turbulence is generated by breaking internal waves; a more detailed analysis is subject of ongoing work at IOW, conducted in the framework of the "International Graduate School on Internal Waves in the Atmosphere

and Ocean" (ILWAO). Substantial mixing and an asymmetric cross-channel density structure, similar to that discussed above, had already been reported before for the gravity currents passing the Stolpe Stolpe Channel, however, without any direct turbulence measurements available (Paka et al. 1998, 2006, Piechura & Beszczynska-Möller 2004). It is worth pointing out that strong entrainment in the Stolpe Channel is also consistent with the fact that the near-bottom areas in this region are almost always well ventilated with oxygen while the water masses are mostly poor in oxygen at the same depths in the Bornholm Sea (Feistel et al. 2006a). This can be explained by oxygen-rich surface water being entrained into the oxygen depleted dense bottom currents during the passage over the Stolpe Sill, with underlines the importance of entrainment for the ventilation of the Baltic Sea deep waters.

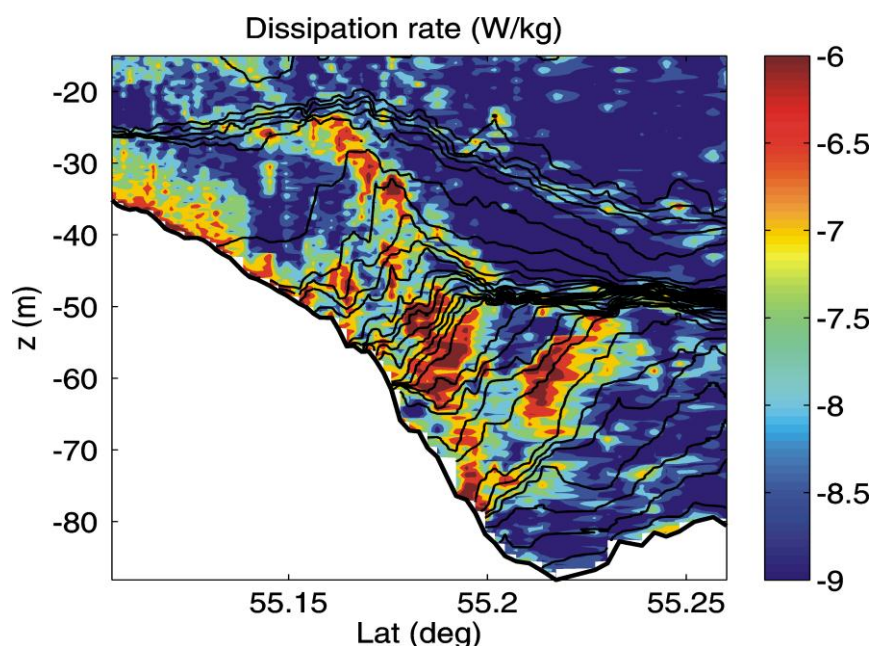


Fig. 3.28 Northward transect down the steep southern slope of the Stolpe Channel, obtained on 25 September 2008 during POS373 with R/V Poseidon (Longitude was 17.00E). Shown in colors is the dissipation rate. Black contour lines correspond to isopycnals.

### 3.6.4 Internal wave mixing

The observations of (Lass et al. 2003) suggest the existence of a turbulence regime embedded between the surface and bottom boundary layers where mixing is dominated by internal-wave interaction. Turbulence in this regime occurs in intermittent patches due to pelagic disintegration of internal waves. The general view has been that non-linear internal-wave interaction cascades energy to small scales and ultimately to turbulence via shear instabilities. This can be quantified in different ways depending on the assumptions made about the internal-wave field and the nature of the non-linear interactions (Gregg 1989; Polzin et al. 1995).

From turbulence observations in the Eastern Gotland Basin, (Lass et al. 2003) found evidence for a relationship of the form

$$\varepsilon = \alpha (E_{kin} + E_{pot}) N \quad (3.2)$$

where  $\varepsilon$  is the dissipation rate of turbulent kinetic energy,  $N$  the buoyancy frequency, and  $E_{kin}$  and  $E_{pot}$  the kinetic and potential energies of the internal wave field, respectively. The measurements of (Lass et al. 2003) suggested  $\alpha = 0.001$  for the dimensionless constant appearing in (3.2). Assuming a constant mixing efficiency  $\Gamma = 0.2$  (Osborn 1980), the model in (3.2) yields



$$k_v = \Gamma \frac{\varepsilon}{N^2} = \frac{a}{N} \quad (3.3)$$

for the vertical turbulent diffusivity, where the new constant  $a$  linearly depends on  $E_{kin}$  and  $E_{pot}$ . This result suggests that the rate of dissipation of kinetic energy in stratified layers varies in space and time along with the variation of the total energy of the internal wave field. Numerical studies with models of different complexity computed consistent mixing rates when employing the functional dependency in (3.3) with values of the order of  $a = 10^{-7} \text{ m}^2/\text{s}^2$  (Axell 2002; Meier 2001; Stigebrandt 1987).

Dissipation rate measurements in the Eastern Gotland Basin were performed by (Lass et al. 2003) during winter stratification in April 1999, from which vertical profiles of the turbulent diffusivity were computed according to (3.3). This method suggested values of the order of  $k_v = 10^{-6} \text{ m}^2/\text{s}$  for the deep-water region below the halocline, i.e. somewhat smaller than the values obtained by other authors from basin-scale budgets (Fig. 3.29). It is thus likely that other processes like boundary mixing and upwelling contribute to the irreversible vertical transport. Furthermore, for logistical reasons, ship-based turbulence measurements tend to have a bias towards lower wind speeds, whereas much of the mixing may occur as a result of elevated internal-wave energy during storm events.

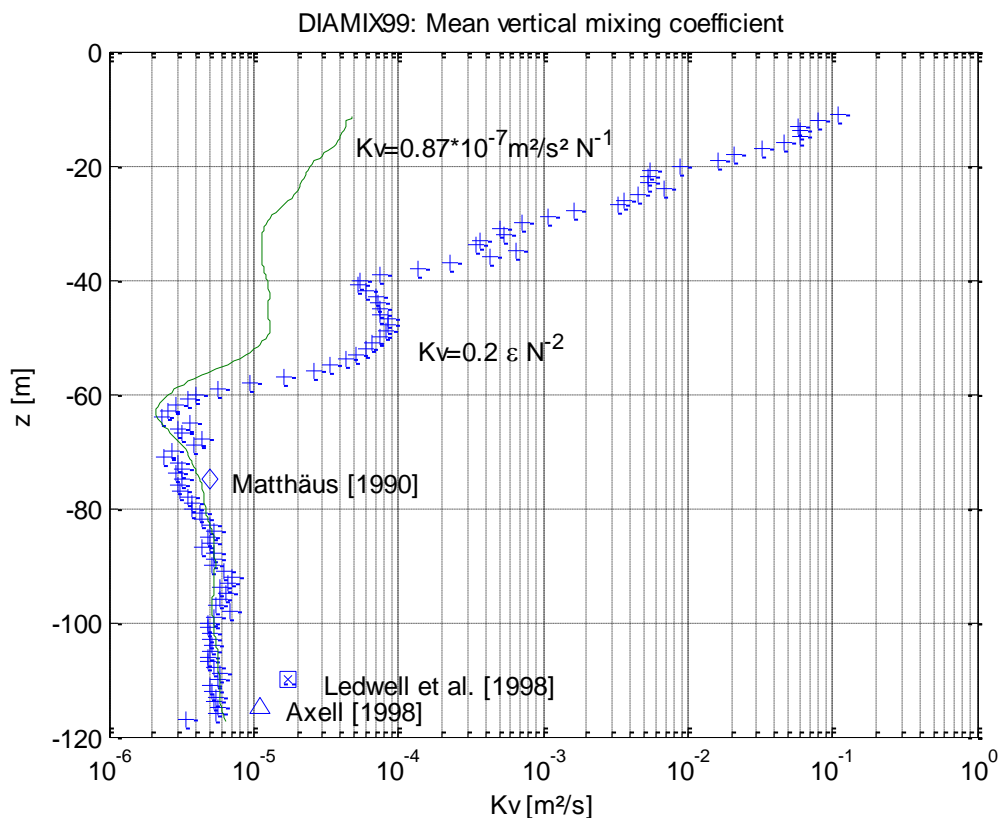


Fig. 3.29 Averaged turbulent vertical diffusivities computed from equation (3.2), compared to other estimates by Matthäus (1990) at 75 m depth and by (Axell 1998) at 115 m depth. Also included are the values found by Ledwell et al. (1998) for the ocean thermocline from a tracer release experiment from (Lass et al. 2003).

### 3.6.5 Upwelling and mixing

Coastal upwelling has been identified as an important vertical transport mechanism for nutrients in nearly all regions of the Baltic Sea because of its potential in by-





passing the blocking effect of the thermocline during summer stratification. The subject has been reviewed by (Lehmann et al. 2002); Myrberg and Andrejev 2003), and (Lehmann and Myrberg 2008).

(Lass et al. 2010) found evidence for the impact of coastal upwelling as a mechanism supporting cyanobacteria blooms in the Baltic Proper. During several wind events from south-west, upwelling of cold waters on the south-eastern coast of the island of Gotland was observed (cf. Fig. 3.24), where the upwelling front is seen to disintegrate into thin filaments that were shown to lead to a quicker cross-basin dispersion of water properties compared to classical Ekman transport (Lass et al. 2010; Zhurbas et al. 2008). The ecological importance of upwelling during summer time is evident from the fact that the upwelled water is poor in nitrate but rich in phosphate, which promotes the evolution of nitrogen-fixating cyanobacteria blooms if the mixed-layer water is depleted of nutrients.

In spite of numerous observations of upwelling events in the Baltic Sea, in particular from remote sensing, until today a robust estimate for the contribution of coastal upwelling to the overall vertical transport does not exist (Lehmann and Myrberg 2008). It is also important to note that upwelling only affects the transport of heat, salt, and matter across the thermocline region located in the upper part of the water column. Upwelling rarely reaches the upper halocline, and never the deep-water regions, pointing at the importance of other vertical transport mechanisms for the communication between sediment, deep-water and the halocline and thermocline regions. As outlined above, internal-wave mixing was identified as one of them; other potentially important mechanisms are reviewed in the following.

### **3.6.6 Other mixing processes**

Meso-scale Baltic Sea eddies ("Beddies") are another potentially important source of mixing, at least inside and below the halocline region. Individual Beddies were observed during all seasons and in various regions of the Baltic Sea, some covering the whole water column but most of them detected inside the permanent halocline (e.g. Lass & Mohrholz 2003; Stigebrandt et al. 2002; Zhurbas and Paka 1997, 1999; Aitsam et al. 1984). Diameters between 10 and 20 km and vertical scales ranging between a few meters and the entire water depth were reported. For the Beddies located inside the halocline, vertical extensions of the order of magnitude of the halocline thickness itself were found, typically around 20 m depending on the region considered. Beddies drift with velocities of a few cm/s, and spin with maximum rotational speeds between 20 and 30 cm/s in geostrophic balance. In addition to these observations of individual beddies, Reissmann (2002, 2005, 2006) used an objective pattern recognition algorithm to automatically detect Beddies as anomalies in three-dimensional hydrographic data fields. These investigations cover the Arkona Basin (AB), the Bornholm Basin (BB), the Stolpe Channel (SF), and the Eastern Gotland Basin (EGB) during both summer and winter situations, and suggest that Beddies cover a constant fraction of about 12% of the total volume (Fig. 3.30).



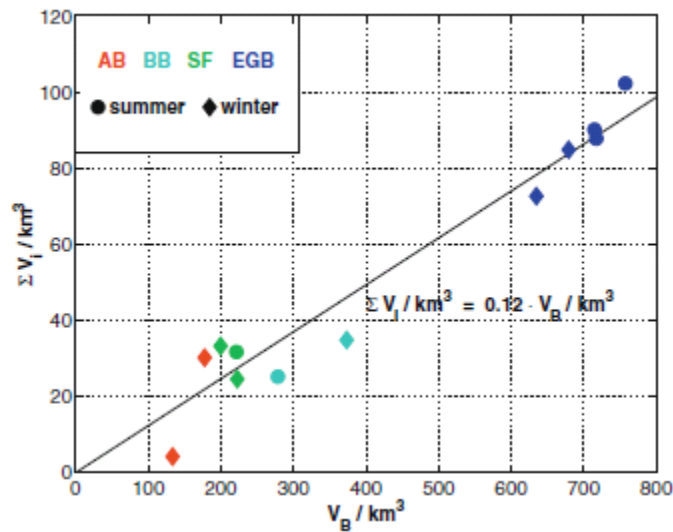


Fig. 3.30 The total volume fraction  $\Sigma V_i$  occupied by Beddies detected in different sub-basins of volume  $V_B$  for 12 data fields from the AB, the BB, the SF, and the EGB (from Reissmann et al. 2009)

In spite of numerous observations confirming the existence of Beddies in different parts of the Baltic Sea, in the absence direct observations of turbulence parameters the quantification of their contribution to basin-scale mixing has proven to be notoriously difficult. In an attempt to quantify Beddy-mixing from hydrographic observations alone, (Reissmann 2002, 2005) notes that the available potential energy in the Beddy field exceeds 20 percent (i.e. a significant fraction) of the potential energy required to mix the halocline in about half of the data fields from the AB and BB during winter situations, and from the SF during all seasons. Only in the Eastern Gotland Basin, the fraction of Beddies was found to be negligible for all data fields. From this, (Reissmann 2002, 2005) argues that the full conversion of available potential energy associated with the Beddies into turbulence would result in a significant reduction of stratification due to mixing. This argument, however, ignores the fact that the energetic pathway from available potential energy to irreversible mixing involves the conversion into mean kinetic energy, and only then into turbulent kinetic energy. It is well-known that most of this energy (80 percent is a typical value according to (Osborn 1980) is dissipated into heat during this conversion process, and only a small fraction is available for mixing. Taking this aspect of mixing into account, it is unlikely that mixing due to Beddies has a significant effect in the Baltic. This does, however, not exclude Beddies as ecological relevant flow features since effects other than mixing (e.g. the isolation of distinct water masses for extended time periods) may play a role.

Besides Beddies, long-term current and temperature records in the Eastern Gotland Basin have revealed the existence of a permanent cyclonic rim current and a strong temporal variability of velocity and temperature fluctuations (Reissman et al. 2009). Spectral analysis of has demonstrated a number of pronounced peaks in the sub-inertial and near-inertial frequency bands, the latter clearly dominating the daily variances. Both the rim current and the daily variances were shown to strongly increase during inflow events with a clear correlation between mean and near-inertial currents observed at a mooring located on the north-eastern rim of the basin (Hagen and Feistel 2001).

In addition to mixing associated with near-inertial waves (see above), the rim current and the sub-inertial fluctuations may be related to mixing through the generation of near-bottom turbulence due to current shear (Reissman et al. 2009). Even



though order-of-magnitude estimates of the energy dissipated in the bottom-boundary layer due to these motions can be computed (e.g. from a cubic relation between dissipation rate and near-bottom speed), the mixing associated with these currents is much more difficult to determine. The major unknown in this problem is the mixing efficiency that is likely to be substantially decreased compared to the canonical value of 20 percent, since stratification in the bottom boundary layer is usually weak.

To improve the current understanding of the deep-water mixing processes in the Eastern Gotland Basin, the Baltic Sea Tacer Release Experiment (BaTRE) was started in September 2007 with the release of an inert tracer in about 200 m depth. The spreading of the tracer cloud and a combination of long-term moored instrumentation and ship-born turbulence measurements are expected lead to new insights into the mixing processes in this important region of the Baltic Proper (Umlauf et al. 2008).

### **3.7 Sea ice**

Sea ice is a factor that has two main impacts on the Baltic Sea. On the one hand it poses a risk to navigation, fishery, and offshore operations. Ice may considerably obstruct navigation and sometimes it poses a severe threat to shipping. Both smaller ships, which may be affected by relatively thin new ice and also high powered vessels that are suitable for navigation in ice covered waters may be damaged by heavy ice and may require special assistance for navigating through sea ice. Port operations and facilities may as well be affected by ice.

On the other hand, ice plays a key role in influencing interactions between the sea and the atmosphere. Therefore the knowledge of ice conditions in the Baltic Sea is also required in order to understand the Baltic Sea as an ecological system. Therefore the frequency and extent of ice occurrence are of major importance. The degree of ice coverage significantly influences light conditions, levels of oxygen dissolved in water, salinity, water temperatures and, consequently, the whole spectrum of biological conditions in the Baltic Sea. Despite its importance, a detailed quantitative understanding of the relation between the degree of ice coverage and the above-mentioned factors is an open problem in Baltic Sea oceanography (Schmelzer et al. 2008).

#### **3.7.1 Baltic Sea**

In general the probability of sea ice is lower in deeper and open sea areas than in shallower and semi-enclosed areas. It is also true for the Baltic Sea.

Average sea ice extent in the Baltic Sea during mild-, normal- and severe winters are shown in Fig. 3.31:

- During mild winters only the northeastern part of the Baltic Sea is ice covered, i.e. the Bothnian Bay and the innermost parts of the Gulf of Finland;
- During normal winters the ice cover expands further to the southwest and covers also the Bothnian Sea, all of the Gulf of Finland, the Gulf of Riga and stretches along coast in the Baltic Proper; and
- During severe winters the Baltic Sea is completely ice covered except for a minor area in the deepest central part of the Baltic Proper.

Average day of freezing and break-up of sea ice are shown in Fig. 3.32 and Fig. 3.33 respectively. The build-up of sea ice starts:



- Earlier in the northeastern part of the Baltic Sea than in the southwestern part of the Baltic Sea; and
- Earlier in shallow areas close to land than in deeper areas further from land.

The reversed picture is seen for break-up of sea ice.

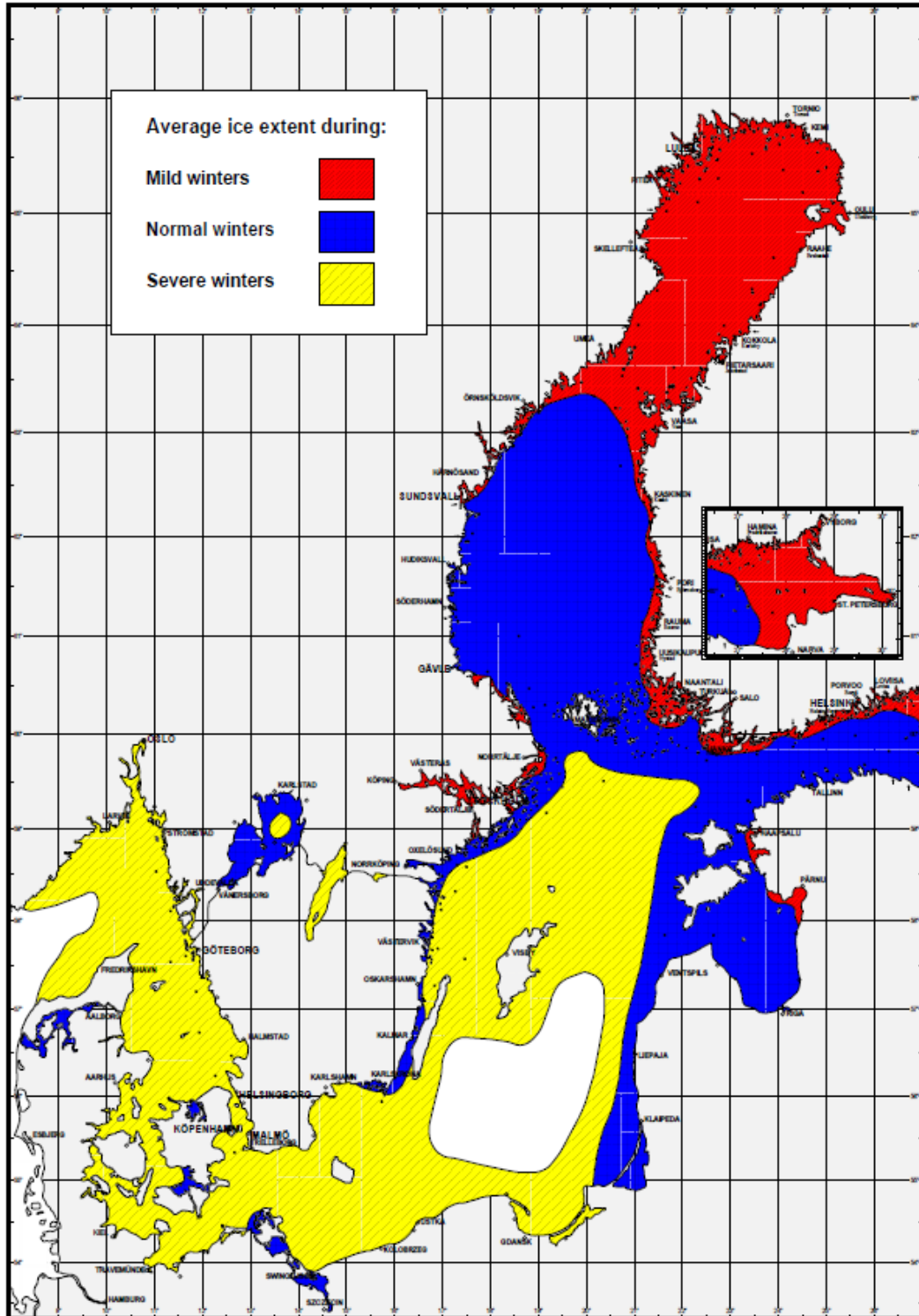


Fig. 3.31 Average sea ice extent during mild-, normal- and severe winters (SMHI & FIMR 1982).

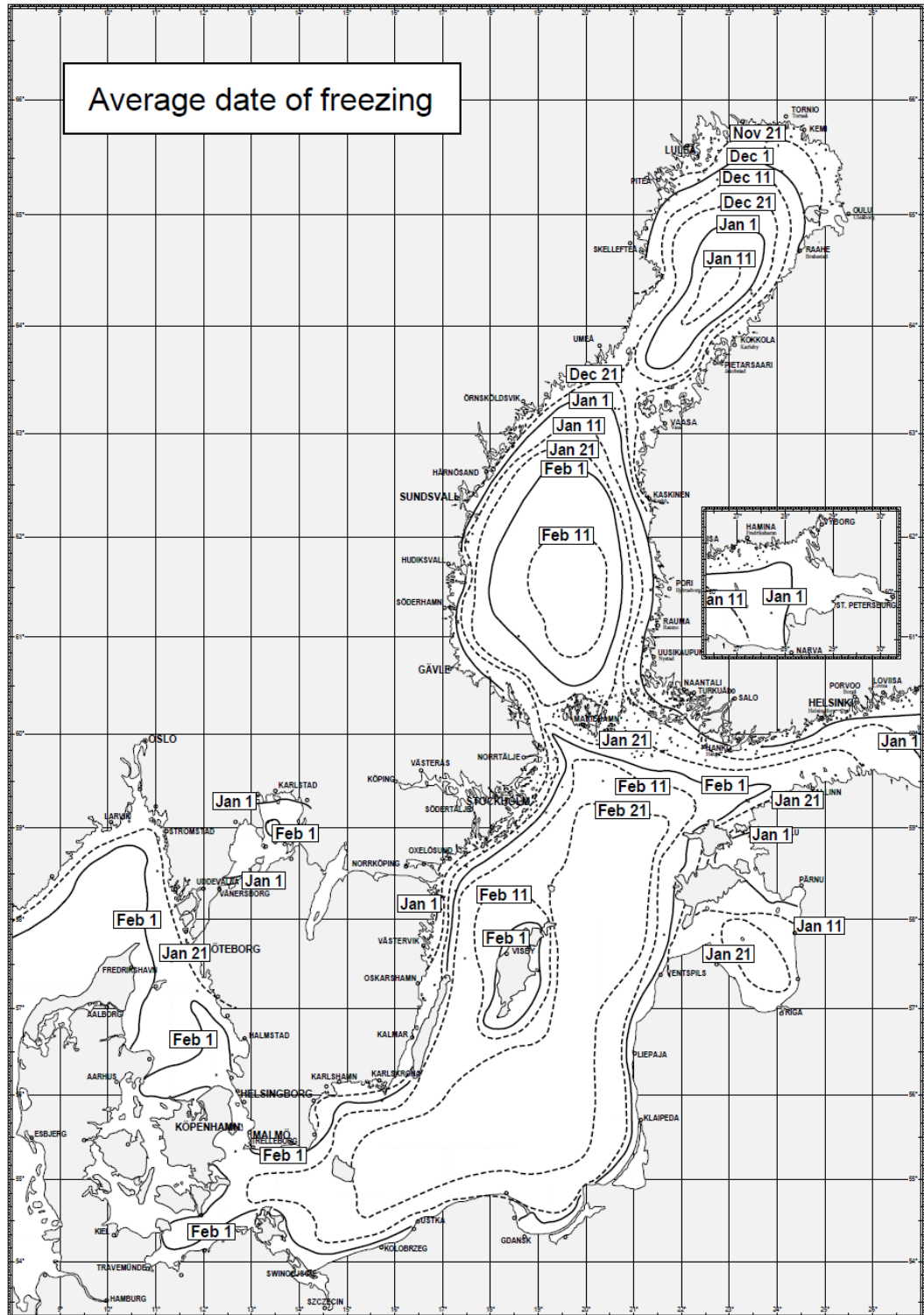


Fig. 3.32 Average date of freezing (SMHI & FIMR 1982).

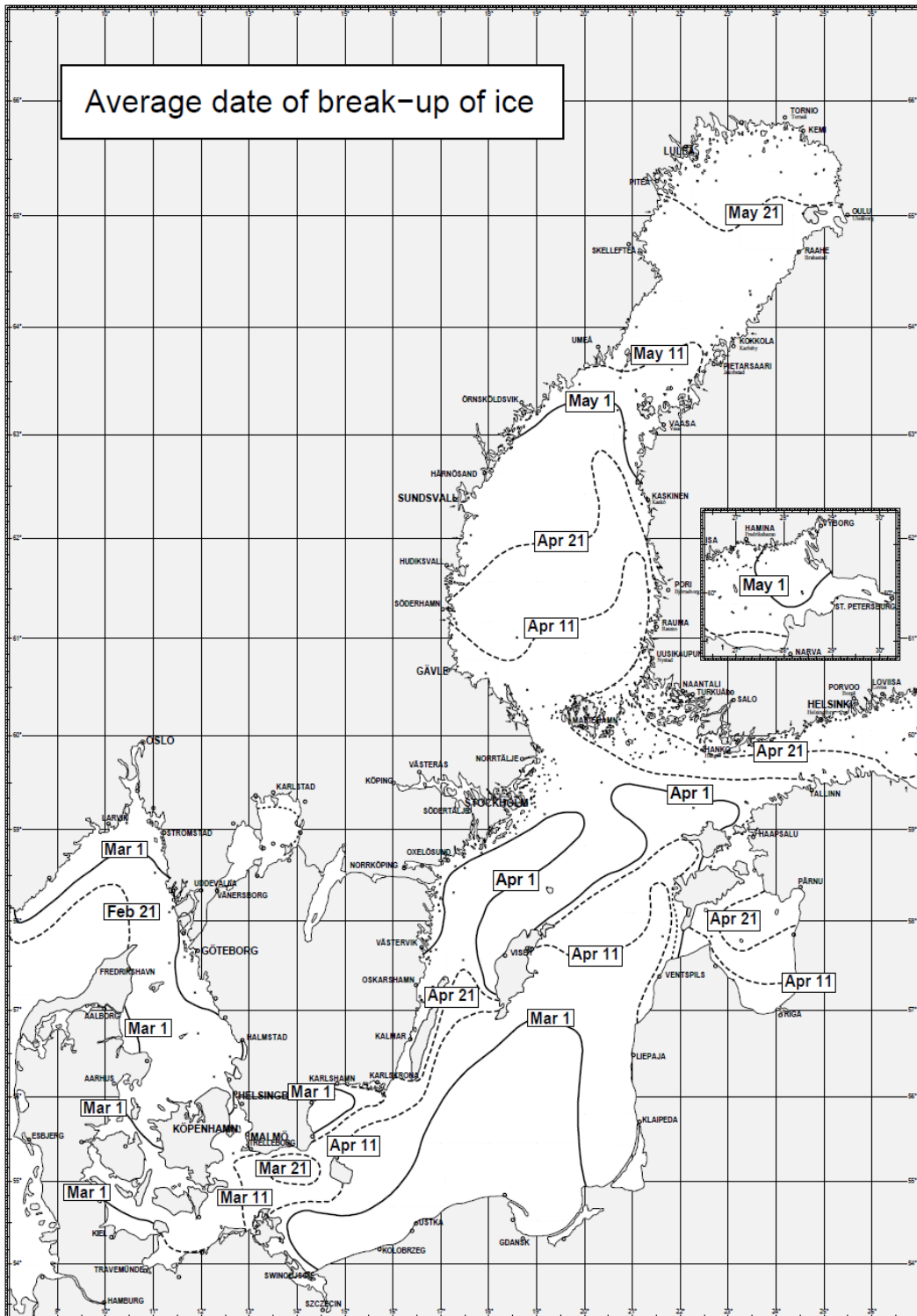


Fig. 3.33 Average date of break-up of sea ice (SMHI & FIMR 1982).



## **4 NUTRIENTS AND OXYGEN IN THE BALTIC SEA**

### **4.1 Nutrients**

#### **4.1.1 Seasonal nutrient cycles**

The distribution of inorganic nutrients in the surface layer of the Baltic Sea is characterized by a pronounced seasonality with reaching high concentrations in winter, the seasons with lowest biological activity, and a decrease to around the detection limit during the period of high biological productivity which is beginning in early spring and ending in late summer (Nausch and Nehring 1996; Nausch & Lysiak-Pastuszek 2002). An example is shown in Fig. 4.1 for the Arkona Sea. Mineralization of organic matter during autumn and winter accompanied by deep reaching vertical convection cause an enrichment of phosphate and nitrate in the surface layer. Due to the long-lasting winter in the central Baltic Sea a typical homogenous nutrient level between early February and end of March/beginning of April is formed. Trend analysis can be performed only during this period (Nehring and Matthäus 1991). In the Arkona Basin and especially in the western Baltic Sea the spring bloom starts much earlier, often already at the beginning of March or in the second half of February. Therefore, the winter plateau is quite often more peak like. In the years 2008 and 2009 winter concentrations of phosphate (0.60  $\mu\text{mol/l}$ ) and nitrate (2.7 – 2.8  $\mu\text{mol/l}$ ) are on a similar level. In both years it is obvious that the nitrate reservoir is completely exhausted already at the beginning of March. Thus, nitrogen limitation causes the breakdown of the spring phytoplankton bloom. In contrast, around 0.20  $\mu\text{mol/l}$  phosphate are still available at the end of April. During the further course of the year, phosphate concentrations decrease and reach often the detection limit, especially if huge cyanobacteria blooms develop. However, the detection limit is reached before the mass development of heterocystous cyanobacteria starts. Consequently, the intensive nitrogen-fixing blooms are mainly based on regenerated phosphate, changes in the internal phosphorus pool and (Nausch et al., 2004) on additional phosphorus supply by upwelling processes (Nausch et al. 2009; Lass et al. 2010). During autumn, first phosphate and later also nitrate concentrations start to increase due to the intensification of decomposition processes. In February of the following year, again typical winter concentrations are reached.

The reason for the different seasonal cycles of phosphate and nitrate is a disturbed Redfield ratio (Table 4.1). Phytoplankton incorporates carbon, nitrogen and phosphorus in a molar ratio of around 106:16:1 (Redfield et al. 1963). When primary production is limited by light, a similar ratio is found in seawater caused by the mineralization of organic matter. In the Baltic Sea, denitrification in suboxic water layers and at the sediment surface is thought to be responsible for this anomaly. First measurements at the end of the 1950/beginning of 1960s give also a molar N/P ratio of 7-10.



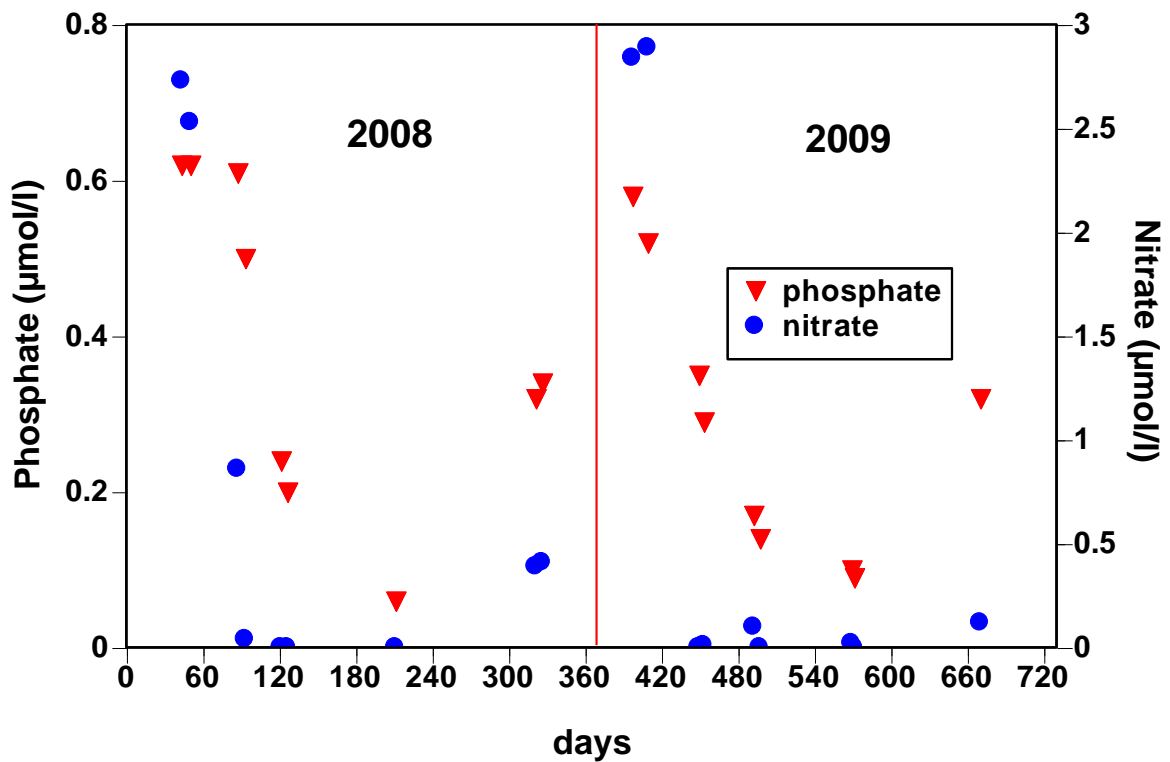


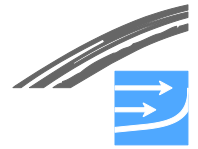
Fig. 4.1 Annual cycle of phosphate and nitrate 2008 and 2009 in the surface layer (0 – 5 m) in the Arkona Sea (measurements at station 113/BMP K05).

Table 4.1 Molar N/P ratios in the winter surface layer (February, 0 – 10 m) between 1990 and 2000, including SMHI data for 2000 (Matthäus et al. 2001). See Fig. 2.1 for locations of sub-basins.

Station/ year	113 (Arkona Sea)	213 (Bornholm Sea)	271 (Gotland Deep)	286 (Fårö Deep)	284 (Landsort Deep)	245 (Karlsö Deep)
1990	7.3	4.9	6.1	6.5	no data	4.9
1991	7.1	7.2	7.7	8.2	no data	no data
1992	7.5	6.9	6.6	7.6	no data	6.2
1993	7.5	7.3	7.1	7.9	7.9	6.7
1994	9.3	8.3	8.1	8.8	no data	7.9
1995	11.7	10.2	7.9	8.5	9.8	7.3
1996	12.5	9.6	9.8	8.1	8.1	7.9
1997	11.6	8.8	8.8	10.3	9.0	7.0
1998	8.2	7.2	8.0	8.0	10.2	7.2
1999	10.0	7.7	9.8	8.9	10.3	6.9
2000	8.2	5.8	7.0	8.4	7.6	6.3
<b>Mean</b>	<b>9.2</b>	<b>7.6</b>	<b>7.9</b>	<b>8.3</b>	<b>9.0</b>	<b>6.8</b>
<b>s. d.</b>	<b>2.0</b>	<b>1.6</b>	<b>1.2</b>	<b>0.9</b>	<b>1.1</b>	<b>0.9</b>

#### 4.1.2 Long-term trends

As already described before, winter values are used for trend analysis. Fig. 4.2 demonstrates these trends for the Eastern Gotland Basin. At the beginning of the time series, before regular monitoring cruises started, only few data, especially for nitrate + nitrite are available. In (Nausch et al. 2008) data are summarized for 5 (10) year periods. In the Bornholm Basin and the eastern Gotland Basin phosphate



concentrations are similar for the period 1958/68 and 1969/1973. They are ranging between 0.21 and 0.34  $\mu\text{mol/l}$ . In contrast to coastal areas where eutrophication is an already long-lasting phenomenon the open seas seems not to be affected strongly at that time. Thus, so-called background concentrations of 0.25 -0.30  $\mu\text{mol/l}$  seem to be most reliable. For nitrate, rare data of the periods 1958/68 and 1969/73 differ, but it is generally accepted that background concentrations are in the range of 2.0 – 2.5  $\mu\text{mol/l}$  (Nausch et al. 2008).

During the 1979s phosphate as well as nitrate concentrations started to increase and remain on a high level with larger fluctuations since the 1980s due to mainly internal processes. The phosphate winter concentrations recently observed are nearly twice as high as the background concentrations. The same holds for the inorganic nitrogen compounds. These results are clear signs of eutrophication.

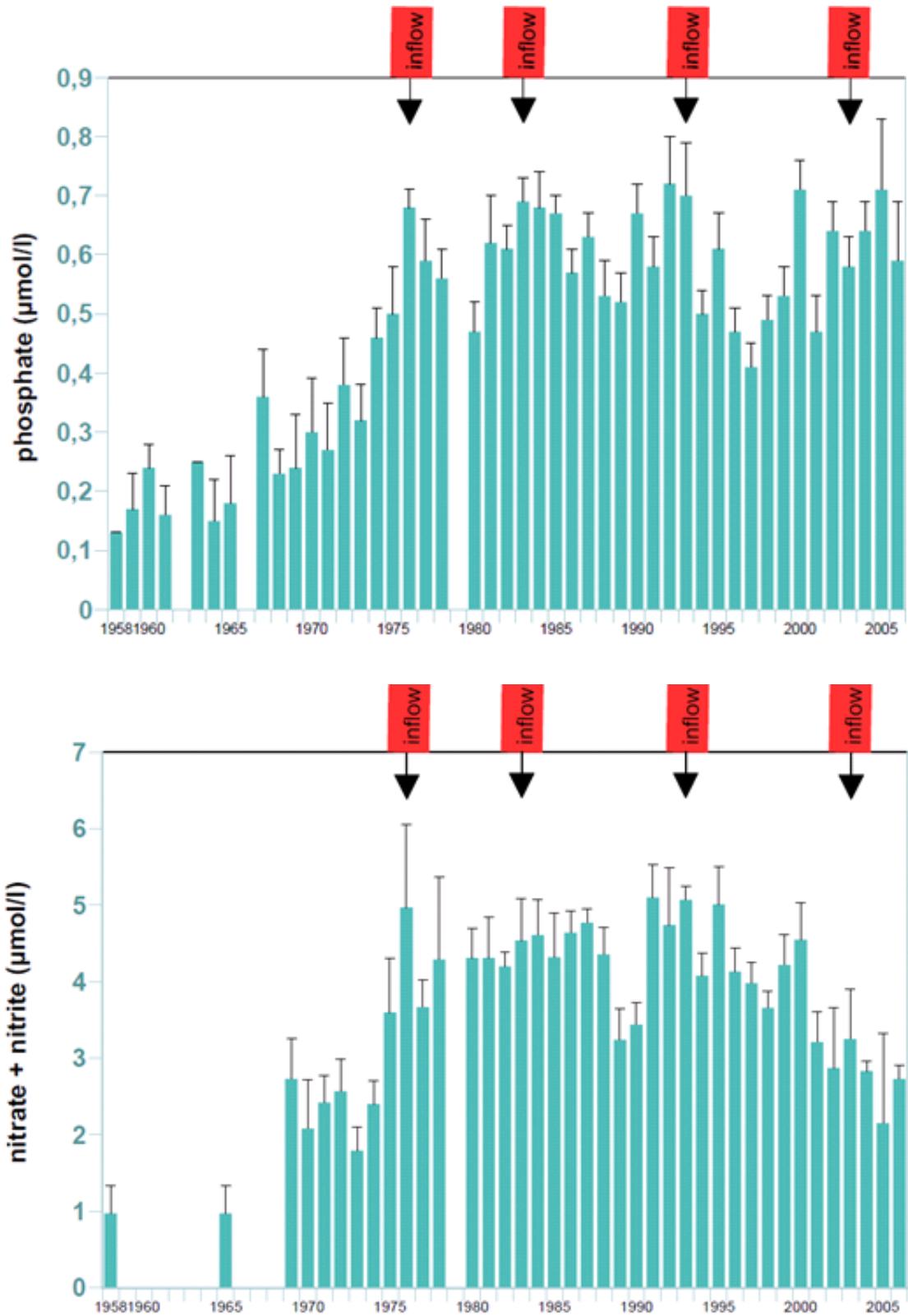


Fig. 4.2 Mean phosphate and nitrate+nitrite concentrations in the mixed winter surface layer (0 – 10 m) pooling five stations in the eastern Gotland Basin from 1958 to date (1962, 1966, and 1979 no data). Major Baltic Inflows are marked by red tags. Figures taken from (Nausch et al. 2008).

### 4.1.3 Inorganic nutrients in the depth

Nutrient concentrations in the deep basins of the central Baltic Sea are closely correlated with the hydrographic regime governed by the alternation between Major Baltic Inflows and stagnation periods. A detailed analysis of these processes is summarized in (Matthäus et al. 2008). In the presence of oxygen, phosphate is partly bound in the sediments and onto settling particles in the form of an iron-III-hydroxophosphate complex. If the system turns from oxic to anoxic conditions, this complex is reduced by hydrogen sulphide (Hille et al. 2005). Phosphate and iron (II) ions are liberated leading to an increase in phosphate.

Also in the presence of oxygen, phosphate is partly bound in the sediments and onto settling particles in the form of an iron-III-hydroxophosphate complex. If the system turns from oxic to anoxic conditions, this complex is reduced by hydrogen sulphide (Hille et al. 2005). Phosphate and iron (II) ions are liberated leading to an increase in phosphate.

This can be demonstrated for the eastern Gotland Basin for the period 2003 to 2005 (Fig. 4.3 and Fig. 4.4). The last MBI from January 2003 reached the eastern Gotland Basin in April /May 2003. The oxygen rich inflow near to the bottom caused an elevation of the stagnant water below the pycnocline by almost 30 m. This old stagnant bottom water had high phosphate concentrations, partly > 4  $\mu\text{mol/l}$  whereas the newly ventilated water below had only 2.0 – 2.5  $\mu\text{mol/l}$ . With the beginning of a new stagnation period in the mid of 2004, reestablishment of anoxic conditions started at the bottom. The hydrogen sulphide containing layer arose more and more. In parallel, also the phosphate concentrations increase whereas the layer is free of nitrate (not shown). Ammonium enrichment can be observed also with in this oxygen free layer.

A detailed description of the nutrient situation in the Baltic Sea can be found in the annually published assessments of the Baltic Sea (e.g. the latest report by (Nausch et al. 2009).

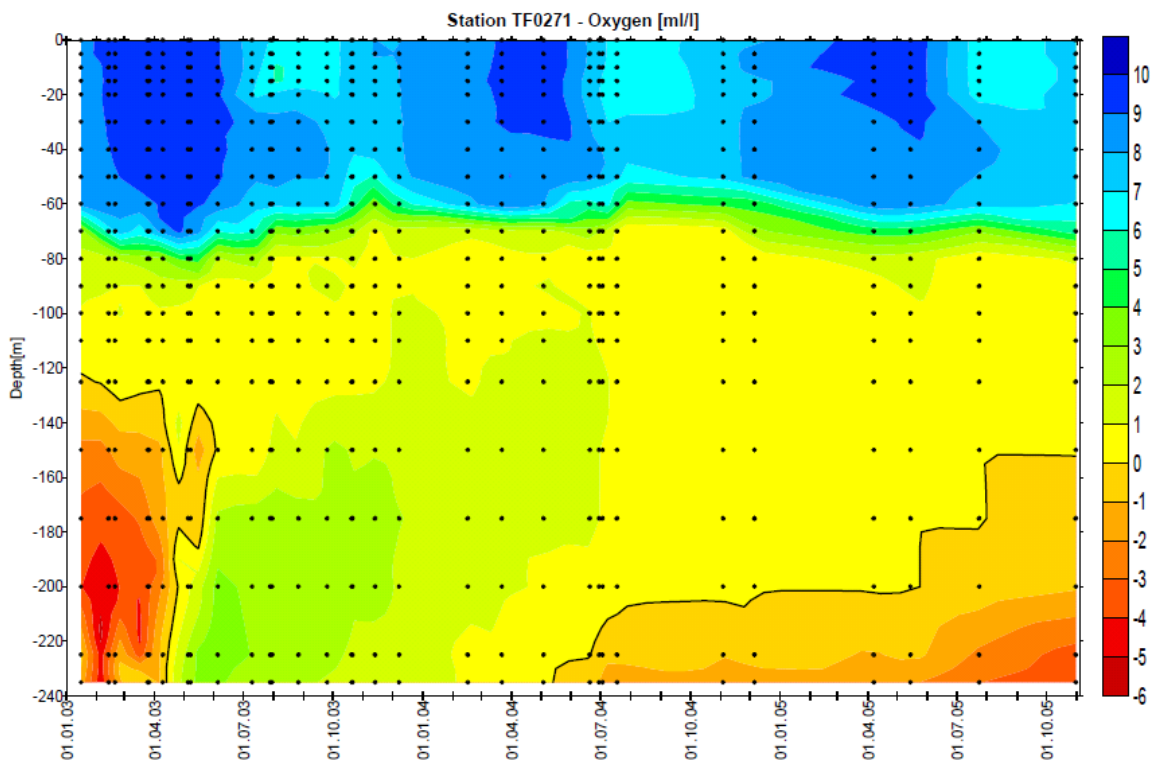


Fig. 4.3 Vertical distribution of oxygen and hydrogen sulphide (shown as negative oxygen equivalents) in the Gotland Deep (BMP J01) between 2003 and 2005 (from Nausch et al 2008).

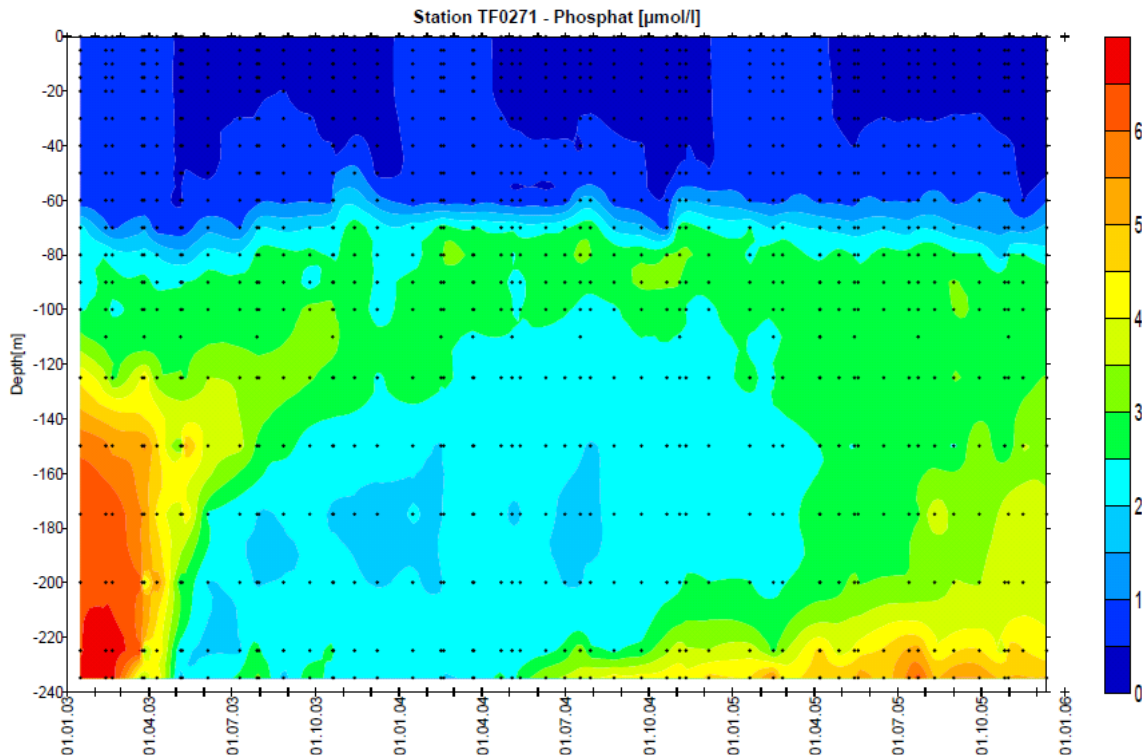


Fig. 4.4 Vertical distribution of phosphate in the Gotland Deep (BMP J01) between 2003 and 2005 (from Nausch et al. 2008).

## 4.2 Oxygen conditions

### 4.2.1 Introduction

The oxygen budget of the sea is characterized by the input from the atmosphere and through primary production of algae and submerged vegetation and by the consumption through respiration, decomposition of organic matter and loss to the atmosphere. Consequently, the oxygen budget is negative since oxygen input through the surface and by photosynthetic activity is lesser than consumption through the metabolism of heterotrophic organisms (Schwoerbel 1984). Additionally, temperature and salinity caused stratification, vertical circulation, advection and convection can influence the oxygen content.

Therefore, the oxygen situation in the surface layer is normally good. Changes in the oxygen content are mainly caused through the annual cycles of temperature and salinity and the seasonally differing production and consumption processes. Below permanent or temporarily occurring pycnoclines, however, a significant loss of oxygen can take place because in these water layers the absence of light prevents production processes and only oxygen consumption is relevant. The oxygen consumption can be so intensive that anaerobic conditions occur and the formation of hydrogen sulphide starts as in the deep basins of the central Baltic Sea. These different features can be seen in a transect from the Darss Sill to the northern Gotland Basin (Fig. 4.5).

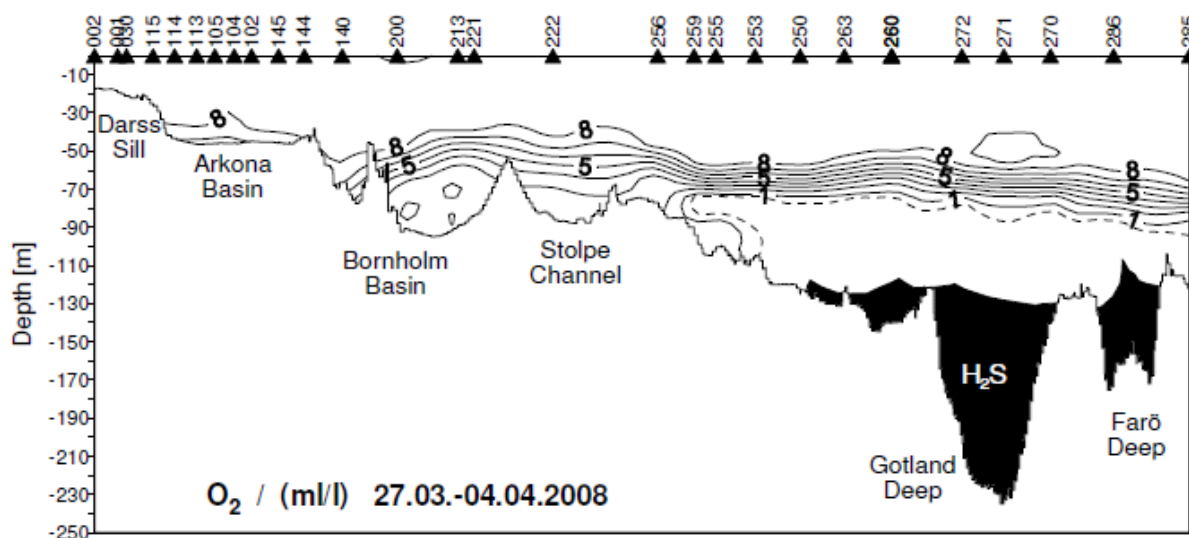


Fig. 4.5 Vertical distribution of oxygen resp. hydrogen sulphide between Darss Sill and northern Gotland Basin in March/April 2008 (from Nausch et al. 2009).

#### 4.2.2 Surface layer

In the mixed surface layer, a typical annual cycle of oxygen can be observed (Matthäus 1978; Nausch et al. 2009) as can be shown for the Gotland Sea (Fig. 4.6). Mainly, temperature and the primary production of phytoplankton are responsible for this cycle. Low temperature in winter causes high solubility of oxygen, but productivity is minor. In spring, temperature still remains on a low level, but the spring bloom of phytoplankton generates an additional oxygen supply. The rapid temperature increase, starting mid-May, diminishes oxygen solubility. During summer only 6 – 7 ml/l can be measured. Autumnal cooling leads to an increase of the oxygen content in the surface layer.



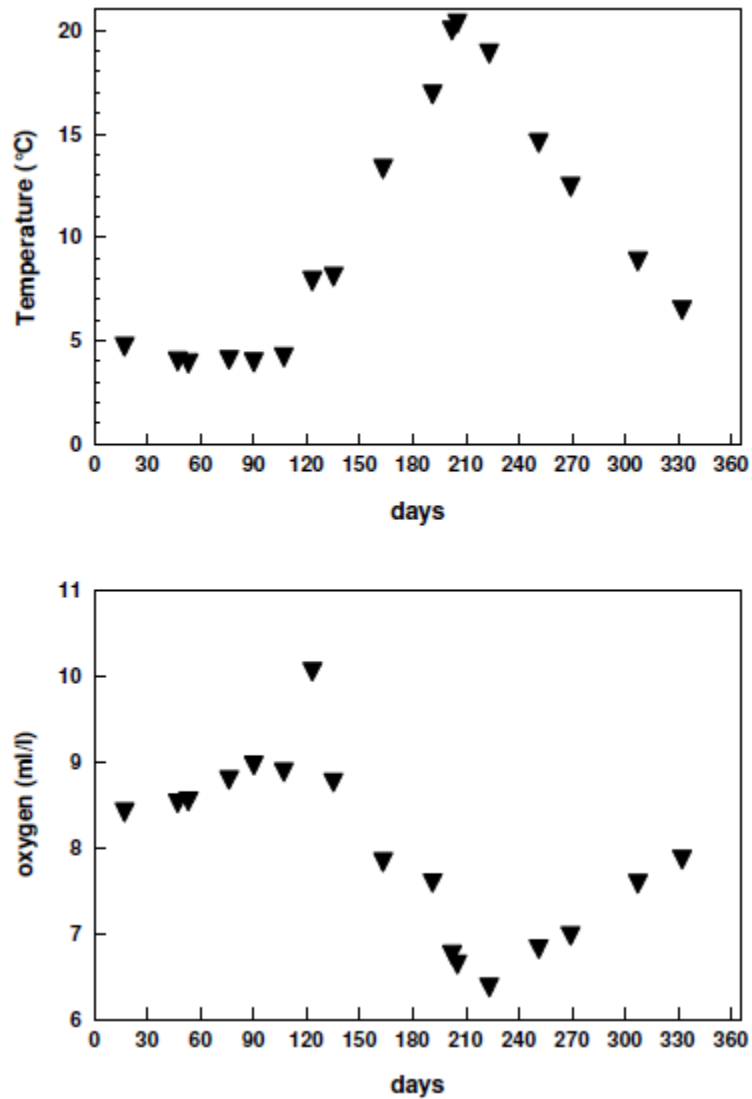


Fig. 4.6 Annual cycle of temperature and oxygen in the surface layer (0 – 10 m) in the Eastern Gotland Basin in 2007 (based on IOW and SMHI data, from (Nausch et al. 2008))

The strong influence of temperature and also salinity hampers however the comparability of data. Therefore, quite often oxygen saturation is favored because here the influence of temperature and salinity is eliminated. Fig. 4.7 summarizes the oxygen saturation values in the surface layer of the Baltic Sea in 2007. 34 stations from the western Baltic Sea to the eastern Gotland Basin were used. The typical annual cycle is obvious. In February and October, a slight under saturation is observed due to the dominance of oxygen consuming processes. The quite uniform distribution is found throughout the whole area of investigation. The oxygen saturation values are  $94.1 \pm 1.8\%$  and  $95.3 \pm 1.0\%$  for February and October respectively. With the onset of the spring phytoplankton bloom, the oxygen content increases and saturation values rise over 100%. The bloom starts in the western Baltic and proceeds, depending from the weather situation, into the central Baltic Sea. Thus, in March  $107.3 \pm 2.4\%$  were measured in the western Baltic whereas in the Bornholm Sea and the eastern Gotland Sea only around 102% were found. At the beginning of May, the spring phytoplankton bloom is already terminated in the western Baltic ( $103.7 \pm 0.7\%$ ), in the Bornholm and Gotland Sea it is in full operation ( $107.8 \pm 0.5\%$  and  $107.4 \pm 4.0\%$ , respectively). The intensity of cyanobacteria blooms in summer influences the oxygen saturation to a high degree. In 2007, no

huge mass occurrence of heterocystous cyanobacteria was observed. Thus oxygen saturation remains relatively low.

The above described annual cycles of oxygen content and saturation are typical for all the recent years. Generally, the fluctuation range is relatively low what can be seen as an indication of a healthy oxygen budget of the surface water of the Baltic Sea (Nausch et al. 2009).

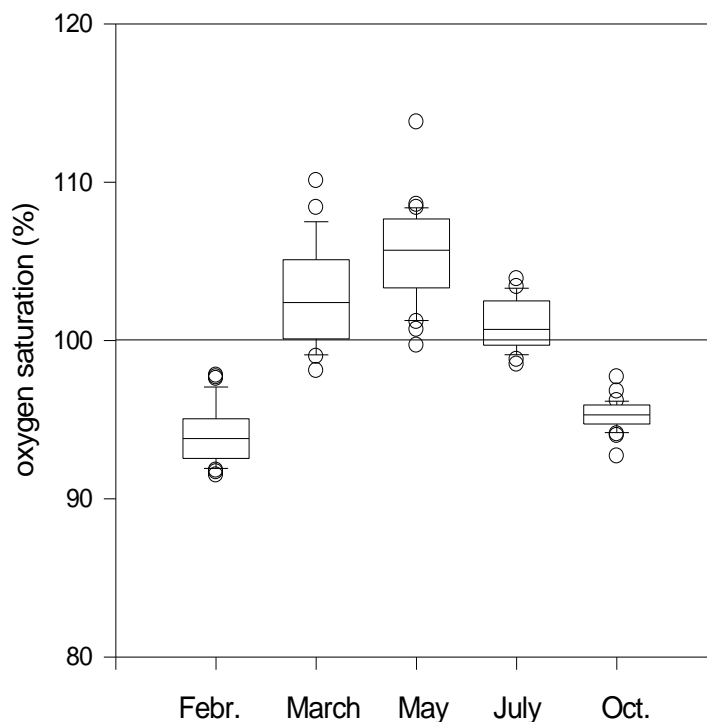


Fig. 4.7 Box-whisker-plots of the oxygen saturation (%) in 2007 in the surface layer (0 - 10 m) between western Baltic Sea and the Eastern Gotland Basin. Circles indicate outliers.

#### 4.2.3 Deep water conditions

In the shallow western Baltic Sea and in the Arkona Basin (max. depth 47 m), also in the bottom near layer an annual cycle can be observed. During winter time, vertical mixing takes place down to the bottom. Additionally, frequent inflow processes cause water renewing. Thus, the bottom water is relatively well supplied during winter and spring. The development of the thermocline in late spring/winter prevents deep reaching vertical convection. Together with the increased mineralization of organic substances, the oxygen saturation decreases in summer and autumn. Intensified cooling of the surface waters and storm events in autumn dissolve the thermocline, leading again to mixing down to the bottom in winter. Due to the importance of these processes in the Fehmarnbelt region they are described more in detail in the special Fehmarnbelt Baseline Report (FEHY 2013a).

In the more eastern basins of the Baltic Sea, a permanent halocline exists (see Chapter 3.3.1) preventing vertical mixing down to the bottom. Therefore, the oxygen situation is coined through the occurrence or absence of barotropic or baroclinic inflow events. These processes are described in detail in Chapter 3.4.2.

Not only major Baltic Inflows (MBIs) of highly saline water, but also regular inflows of lower volumes of water frequently penetrate across the Darss and Drogden Sills, pass the Arkona Basin, and are trapped in the deep water of the Bornholm Basin causing a high variability in temperature, salinity and oxygen concentration (Mat-



thäus et al., 2008). The Bornholm Basin deep water is relatively often ventilated. For example, the MBIs in 1993 and 2003 resulted in the highest oxygen concentrations on record in the 80 m level of the Bornholm Deep in May 1993 (8.4 ml/l) and February 2003 (7.7 ml/l) (Matthäus et al., 2008). These maximal concentrations were followed by a rapid oxygen decrease and the formation of hydrogen sulphide. Already in May 2005 a hydrogen sulphide concentration of -3.1 ml/l (oxygen equivalent) was reported (Aneer and Höglander 2005).

In contrast to the Bornholm Deep, no regular seasonal variations can be observed in the Gotland Deep, Farö Deep, Landsort and Karlsö Deep. The effects of MBIs can be clearly identified whereby the eastern Gotland Basin is the best integrator for these processes. The strongest MBI observed so far took place in November-December 1951 causing the highest salinities in the central Baltic deep water (13.86 psu at 200 m depth in the Gotland Deep). Despite salinity decreased during the following 40 years, frequently MBIs were detected (Matthäus et al., 2008). The deep water oxygen regime reacted accordingly. Oxygen concentrations fluctuated around zero. Partly, hydrogen sulphide was found, but the MBIs repeatedly supplied the system with new pulses of oxygen (Fig. 4.8). From the mid 1970s onwards, the frequency of MBIs decreased drastically. The strong MBI in December 1975/January 1976 was the beginning of the most significant stagnation period in the eastern Gotland Basin, lasting 16 years. Due to the absence of inflows, oxygen disappeared in the depth of this basin and huge amounts of hydrogen sulphide were formed. In the Gotland Deep it decreased from 2 ml/l oxygen in March 1977 to -7.6 ml/l hydrogen sulphide (negative oxygen equivalents) in November 1992. The western Gotland Basin (Landsort and Karlsö Deep) remained oxygenated during this period. Most probably this was due to increasing advection of oxygenated water passing the stagnating deep water of the eastern Gotland Basin immediately below the halocline. Also decreasing stability of the stratification which favoured vertical mixing can be seen as a reason (Matthäus et al. 2008). The long stagnation period was terminated by an MBI in January 1993. As a result, oxygen concentrations of 3.3-3.4 ml/l were measured in May – July 1994. These concentrations were comparable to the values in the 1930s (Fig. 4.8). Afterwards, again a rapid decrease in the oxygen content was observed, probably supported by an intensified microbial mineralization at high temperatures in the depth. The so far latest MBI was detected in January 2003 followed by a stagnation period which continues until today. The oxygen system reacted as described before. From 1993 onwards, stagnation effects were observed also in the western Gotland Basin. The 2003 inflow had only small effects on the oxygen conditions there (Nausch et al., 2005, 2006) owing to the high salinity in the deep water which caused a higher stability of stratification and hampering vertical exchange.

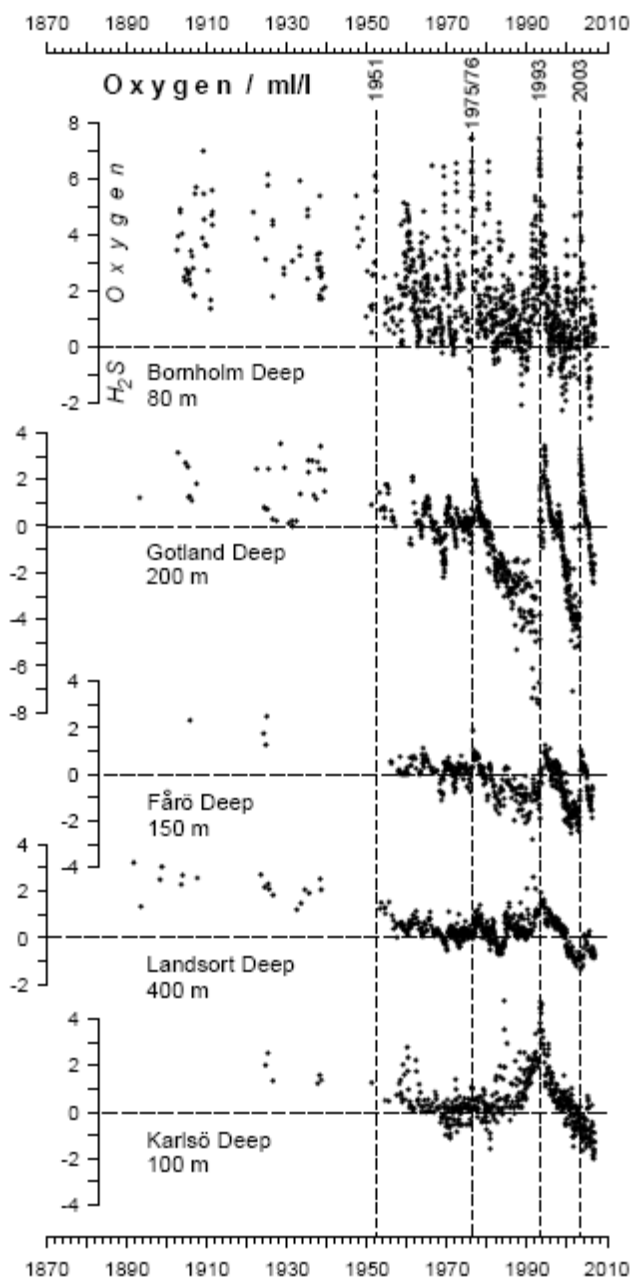


Fig. 4.8 Long-term variations of oxygen and hydrogen sulphide concentrations in the Central Baltic deep water (hydrogen sulphide converted into negative oxygen equivalents after (Fonselius 1969), from (Matthäus et al. 2008).

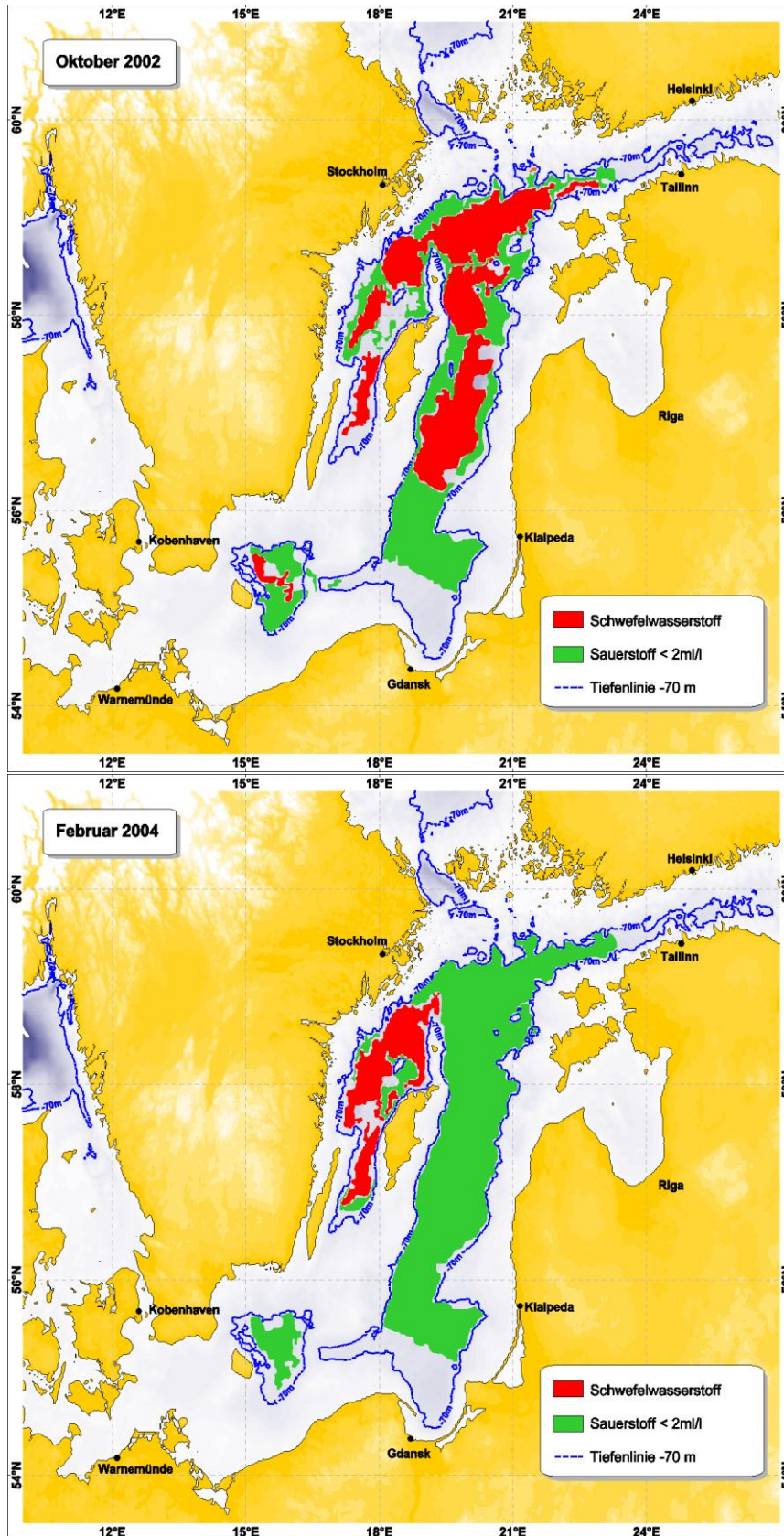


Fig. 4.9 Suboxic (green) and anoxic (red) in the near bottom areas in the Central Baltic Sea. Figures taken from (Feistel 2010).

The effects of the MBI of January 2003 can be seen clearly in Fig. 4.9. In October 2002 huge areas in the depth were free of oxygen. The inflow event ventilated first the Bornholm Basin. In February 2004 the whole eastern Gotland basin was free of



hydrogen sulphide. As describe above, the effects in the western Gotland Basin were minor. The present stagnation period had increased the anoxic zones again. According to Swedish data (SMHI, 2010) at present around 40,000 km<sup>2</sup> corresponding to 10% of the Baltic Sea area are free of oxygen near to the bottom.

A simulated long-term mean (1990-2007) of minimum bottom oxygen is shown in Fig. 4.10. It reveals that anoxia is common at the bottom of all major sub-basins of the Baltic Sea.

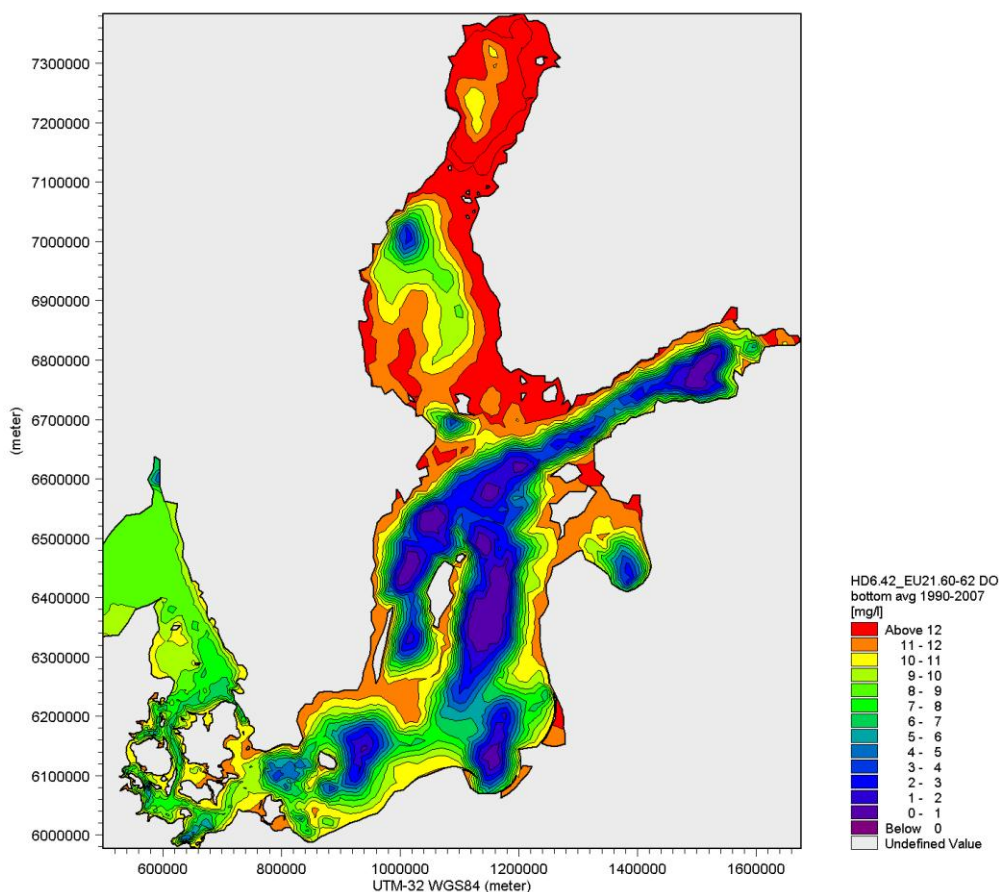


Fig. 4.10 Long-term mean (1990-2007) bottom oxygen content in the Baltic Sea simulated with the MIKE numerical model (FEHY, 2013c). Anoxic areas are marked as values <0.





## **5 CYANOBACTERIA AND PHYTOPLANKTON IN THE BALTIC SEA**

Phytoplankton is the principal primary producer that provides the energy base for all higher components of the food web in marine and coastal ecosystems.

Because phytoplankton responds rapidly and directly to changes in nutrient availability, by changing the species composition and abundance and biomass, it is one of the key parameters for defining the water quality, especially for the assessment of eutrophication. Within the European Union, eutrophication has often been defined as: "the enrichment of water by nutrients, especially nitrogen and/or phosphorus, causing an accelerated growth of algae and higher forms of plant life to produce an undesirable disturbance to the balance of organisms present in the water and to the quality of water concerned" (EC 1991).

Another more general definition is given by Nixon (1995): "Eutrophication is defined as an increase in the rate of supply of organic matter in an ecosystem."

However, the marine phytoplankton itself influences a cascade of biological and hydrological parameters, especially during the eutrophication process: increasing nutrient input goes along with increasing phytoplankton biomass and leads to decreasing light penetration, which hampers the growth of macrophytes and higher plants. The loss of macrophyte cover changes the structure of the benthic habitat with negative consequences for benthic diversity and fish breeding. In addition, excessive blooms of plankton lead to increasing oxygen consumption and finally oxygen depletion. Increasing nutrient supply results in an increase of duration and frequency of algal blooms. Potential toxic blooms during warm and calm summer periods are important socio-economic factors, because such blooms affected not only the aquatic ecosystem, but also the touristic and economic management of the coastal zones (Schernewski 2002).

### **5.1 Data basis**

Time series analysed in this report were obtained from the German HELCOM monitoring programme covering different periods between 1998-2008 at various stations along the salinity gradient of the Baltic Sea (Fig. 5.1). All data sets are based on harmonized and quality assured methods of the HELCOM-combine manual (HELCOM 2007a). For historical chl-a concentration the updated long-term data set of Wasmund et al. (2006) was used, because the authors have already compiled data from several national and international institutions to get a quality assured homogeneous data set for long-term trend analyses (described in Wasmund & Siegel, 2008).

The seasonal phytoplankton development is characterized by spring, summer and autumn blooms of different algal groups. As the timing of the blooms differs among areas, the definition recommended by (HELCOM 1996) of the relevant seasons in the Baltic Sea has been adapted for data analyses (Table 5.1).

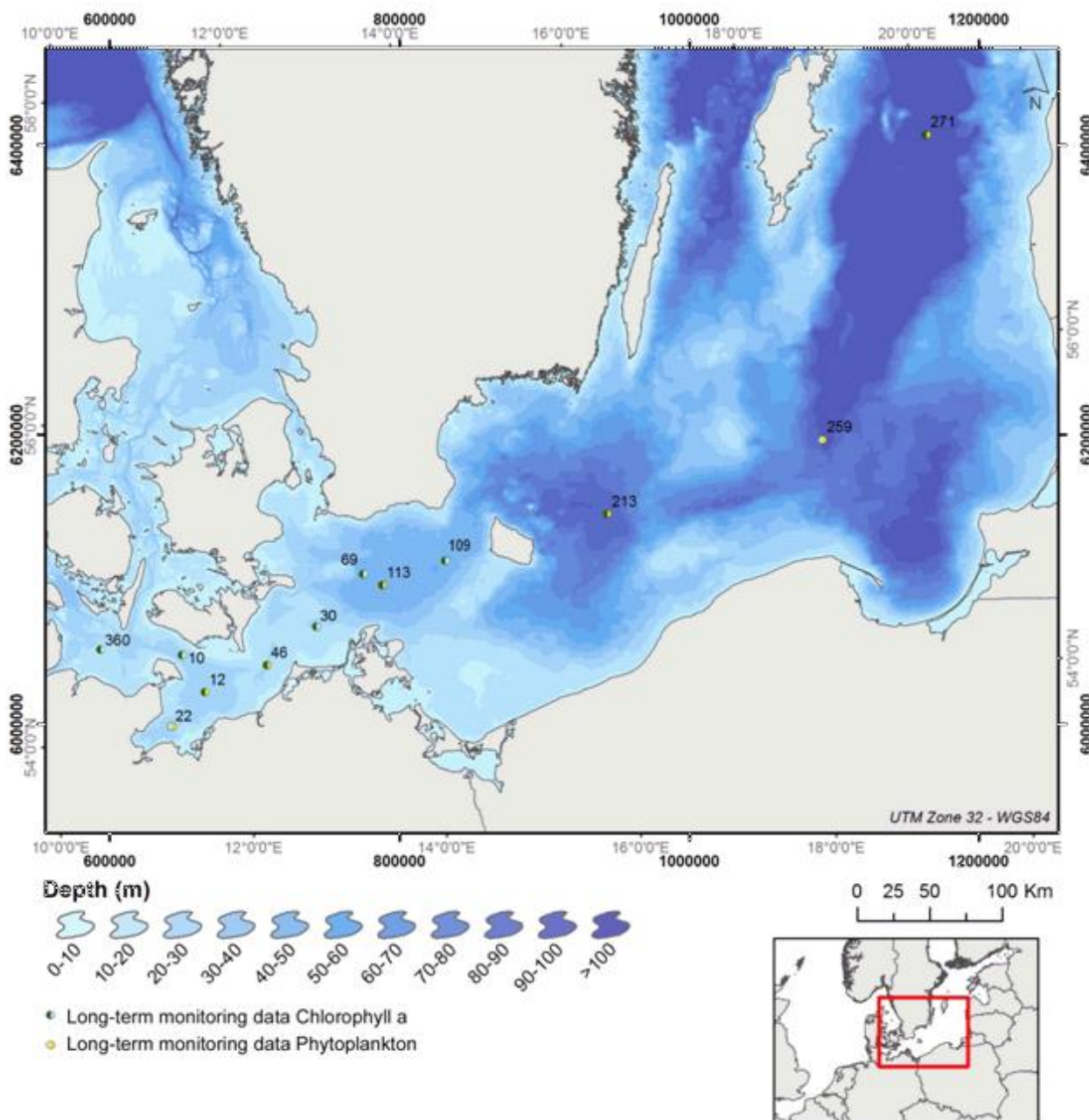


Fig. 5.1 Geographical position of long-term phytoplankton stations. Numbers correspond to IOW internal notation.

Table 5.1 Characterization of seasons according to the HELCOM recommendations (HELCOM 1996).

<b>Baltic area</b>	Belt Sea	Baltic proper
<b>Spring</b>	February-April	March-May
<b>Summer</b>	May-August	June- September
<b>Autumn</b>	September-November	October-December



## 5.2 Factors determining phytoplankton

Nutrients are one of the most important factors for phytoplankton growth. Increasing nutrients lead to increasing biomass. In the south-western parts of the Baltic Sea (Belt Sea area and Kattegat), as well as in the Baltic Proper, nitrogen is generally the limiting factor, but limitation or co-limitation by phosphorus may occur, e.g. (Graneli et al. 1990; Moisander 2003). According to (Nausch et al. 2004) short-term phosphate limitation could be observed when heterocystous cyanobacteria were abundant. In general, phosphorus limitation mainly occurs in coastal zones (Elmgren and Larsson 1997), estuaries and river plumes and has been documented in large parts of the Bothnian Bay (Andersson et al. 1996). Resulting from anthropogenic eutrophication, changes in nutrient stoichiometry and supply have been observed in the last decades in all Baltic areas, which have probably lead to changes in species composition and increasing amounts of species promoted by special nutrient conditions (e.g. Cyanobacteria in the Baltic proper (Laamanen and Kuosa 2005; Wasmund 1997), Prasinophyceae in the northern parts of the Baltic Sea (Vahtera et al. 2005)).

Light is another basic requirement for photosynthesis in autotrophic organisms. Low light intensities, during winter, night and at greater depths limit the development of biomass. On the other hand, high light conditions at noon, during summer or near the surface inhibit or can even damage the photosynthetic reaction centres. Changes in light intensity are associated with diurnal and seasonal changes and, moreover, with short-term changes in seconds and minutes due to weather and wave conditions (Schubert et al., 2001). Long-term changes in general under-water light supply are associated primarily with water transparency (see Chapter 3.3.4), which is determined by various parameters, particularly by light attenuation by suspended particles (e.g., planktonic microalgae) and humic substances. Long-term changes in light intensity are much smaller than diurnal, seasonal and depth dependent variations and, therefore are of minor influence for productivity. Decreasing trends in radiation have been reported by (Russak (1994) between 1955 and 1992. However, the main factor for reduced under water light supply in the Baltic Sea is reduced water transparency (Sanden & Hakansson, 1996; Leppäranta & Myrberg 2009); see also Chapter 3.1.4 induced by increasing algal biomass itself.

Temperature (see Chapter 3.3.2) affects algal physiology directly but has a much higher effect on algal biomass and species composition by indirect impacts (Wasmund & Siegel, 2008). Beside individual temperature optimums, temperature affects primarily the seasonal succession (in combination with light supply), (Gasiunaitė et al. 2005). The water temperature influences the stratification of the water column, which in turn influences the species composition (Wasmund and Siegel 2008). Some species prefer stable water conditions and other species a mixed water column. Additionally, the stratification has impact on the light conditions in and the nutrient supply to the upper water layers.

Salinity is of special importance in brackish waters. Irrespective of the vertical gradients, the marine west-east and south-north, as well the estuarine gradients (see also Chapter 3.4) play an important role for spatial distribution of biomass and species composition (see Chapter 5.3).

Beside these main factors the phytoplankton communities are influenced by grazing pressure, carbon and trace metals, as well as other factors that are not be addressed here.

### 5.3 Spatial distribution

Phytoplankton is irregularly distributed in the water body. Physical and biological processes are the main regulatory determinants. In general the vertical gradients of phytoplankton are more pronounced than the horizontal gradients. They depend mainly on light penetration and stratification.

The horizontal distribution is associated with the main gradients in the Baltic Sea (Wasmund & Siegel, 2008):

- estuarine gradients (trophic conditions and salinity),
- upwelling gradients (nutrient availability, temperature and salinity)
- large scale marine gradients of decreasing salinity from Kattegat to the Bothnian Sea.

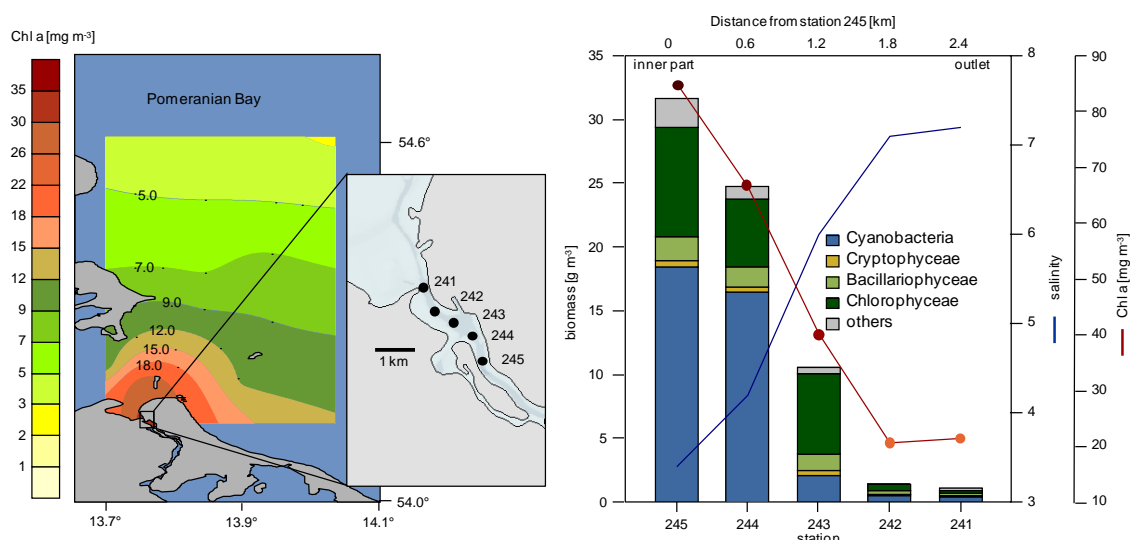


Fig. 5.2 Estuarine gradient for chl-a distribution and phytoplankton biomass using the example of Pomeranian Bay (left) and Peenestrom(right) in September 1995. Left: chl-a concentration in surface water (1m depth). The stations marked a short distance estuarine gradient (2.5 km) shown in the right figure. Right: Phytoplankton composition and chl-a concentration in relation to salinity in the surface water for the short distance transect between stations 245 and 241 (modified from Wasmund et al., 1999).

An estuarine gradient is shown in Fig. 5.2 using the example of a short distance transect within the inner coastal waters of Pomeranian Bay (Wasmund et al., 1999 and Wasmund & Siegel, 2008). In general the phytoplankton biomass expressed as species specific biomass and chl-a concentration decreased from the mouth of the outlet to more open coastal waters (Wasmund & Siegel 2008). In addition the taxonomic composition changed in the same gradient. These changes were not only based on dilution effects, because the various taxa groups disappeared in different proportions with increasing salinity Fig. 5.2, (Wasmund et al., 1999).

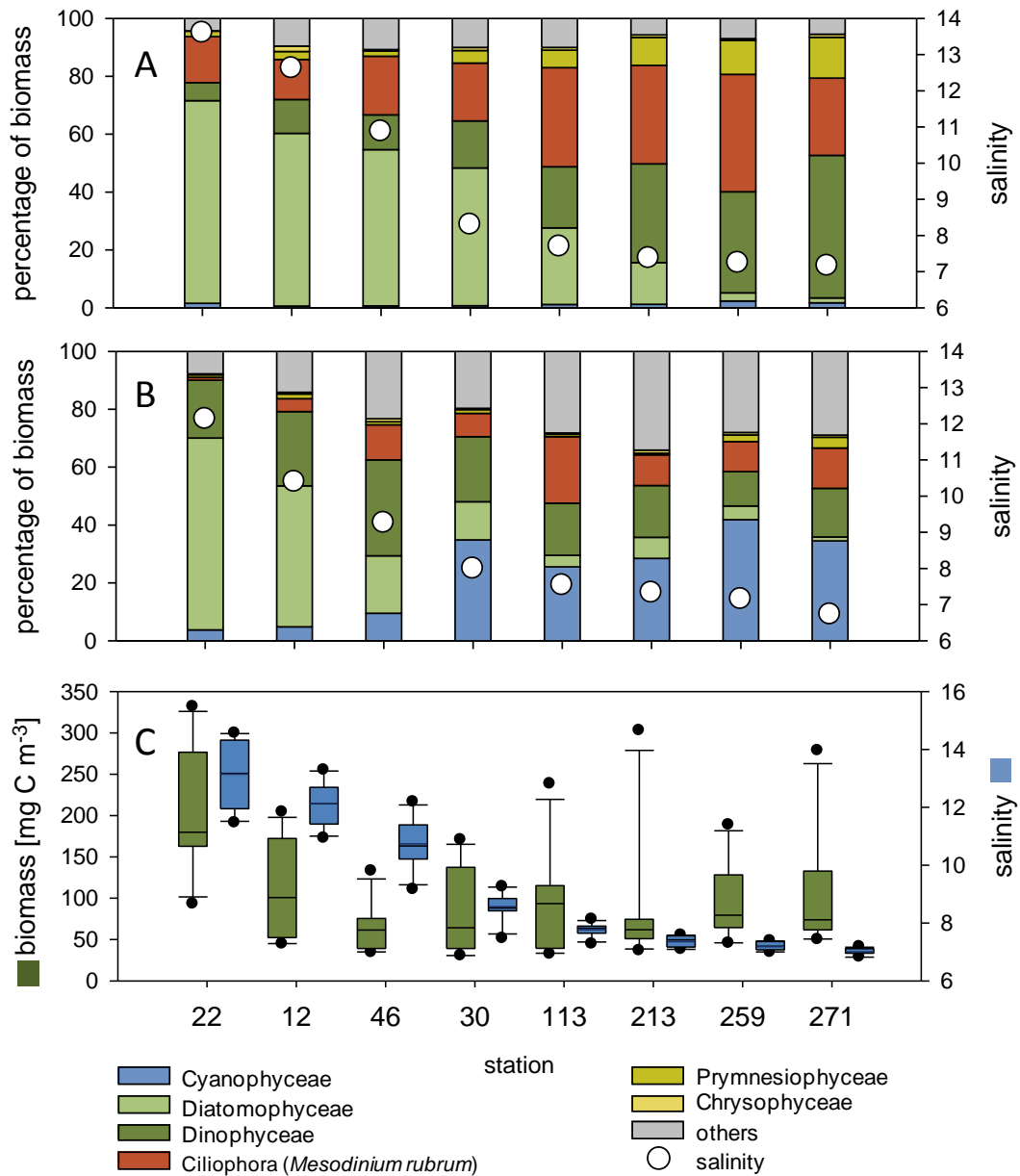


Fig. 5.3 Seasonal variation of phytoplankton biomass (determined in integrated samples of 0-10 m depth), split into main taxonomical groups, along the large marine gradient of the Baltic Sea. Fig. A: Spring season: Data represent mean values from 1998-2008. Fig. B: Summer season: Data represent mean values from 1998-2008. Fig. C: Biomass (green) and surface salinity (blue) data based on yearly means, excluding winter values, for the time period 1998-2008. Stations: 22 - Mecklenburg Bight (inner part), 12 - BMP M02, Mecklenburg Bight (outer part), 46 - Kadet Channel, 30 - BMP K08, Darss Sill, 113 - Arkona Basin, 213 - BMP K02, Bornholm Basin, 259 - BMP K01, southern Baltic Proper, 271 -BMP J01, Eastern Gotland Basin.



Table 5.2 Seasonal mean of chlorophyll a concentration of surface water (mean value of 1-10 m depth). The characterization of seasons follows the HELCOM recommendations (HELCOM 1996).

Year	Kiel Bight	Mecklenb. Bight	Kadet Channel	Arkona Basin	Bornholm Basin	Gotland Basin
Station No.	360	12	46	109,113,69	213	271
<b>Spring</b>						
2000	3.61	2.45	2.29	2.94	2.13	2.70
2001	3.27	1.99	2.77	3.35	3.79	1.95
2002	11.66	2.81	0.92	4.40	2.41	2.80
2003	3.78	1.99	1.50	1.75	3.98	3.27
2004	4.06	2.90	2.25	3.49	2.51	3.29
2005	2.06	2.93	2.54	2.77	3.26	4.56
2006	no data	1.62	1.25	3.41	2.39	2.50
2007	1.15	0.98	2.81	2.35	3.46	2.76
2008	2.12	1.96	2.21	4.82	8.57	11.09
2009	2.01	2.27	1.91	5.48	3.63	2.47
<b>Summer</b>						
2000	1.23	1.18	0.84	1.63	1.61	2.69
2001	1.52	1.54	1.37	1.57	2.13	2.18
2002	1.83	2.27	1.69	2.50	1.38	2.05
2003	0.95	1.53	1.17	1.76	2.10	2.95
2004	1.87	2.96	1.51	2.21	1.51	3.16
2005	3.15	2.86	1.79	1.43	1.60	5.77
2006	1.99	1.89	1.53	1.27	1.30	2.68
2007	2.16	2.63	1.85	2.83	2.54	3.60
2008	2.28	1.61	2.96	5.32	5.17	4.21
2009	2.61	2.06	2.02	3.06	no data	no data
<b>Autumn</b>						
2000	3.23	3.79	2.33	3.56	2.28	3.39
2001		3.41	2.10	2.96	1.68	1.89
2002	4.32	3.71	2.20	1.89	0.92	1.55
2003	4.70	3.41	2.30	1.89	1.37	2.49
2004	3.84	4.04	2.50	2.46	2.89	2.26
2005	3.39	3.09	2.56	2.44	2.53	2.21
2006	4.64	3.29	2.58	3.65	4.67	1.59
2007	2.97	4.68	3.27	2.91	2.54	4.70
2008	4.33	2.84	1.59	2.10	no data	no data
2009	2.00	2.91	2.90	4.86	no data	no data

In estuarine gradients, the phytoplankton biomass is determined mainly by the nutrient gradient while the species composition is formed by the salinity gradient. The large-scale marine gradient is formed by salinity conditions. In addition, the overall biomass development and species composition is determined by geographical position (latitude), due to shorter vegetation periods. According to (Kahru et al. 1982) the variability in the phytoplankton biomass is often caused by differences in the time when seasonal blooms commence. Therefore a clear discrimination of the interact parameters is often impossible, and phytoplankton community composition becomes unpredictable at much smaller spatial scales than the overall plankton distribution, and tend to be more mosaic than a smoothly varying continuum (Kononen 1992).

Within the west-northeast gradient the regional species composition was found to change both in terms of main taxonomical classes (Fig. 5.3), as well as individual taxa (Wasmund & Siegel 2008). According to Wasmund & Siegel (2008) the diversi-





ty seems to be lowest in the Bornholm and Gotland Basins due to unfavourable salinity conditions of approximately 5-8 PSU for both, marine and limnetic species (horohalinicum).

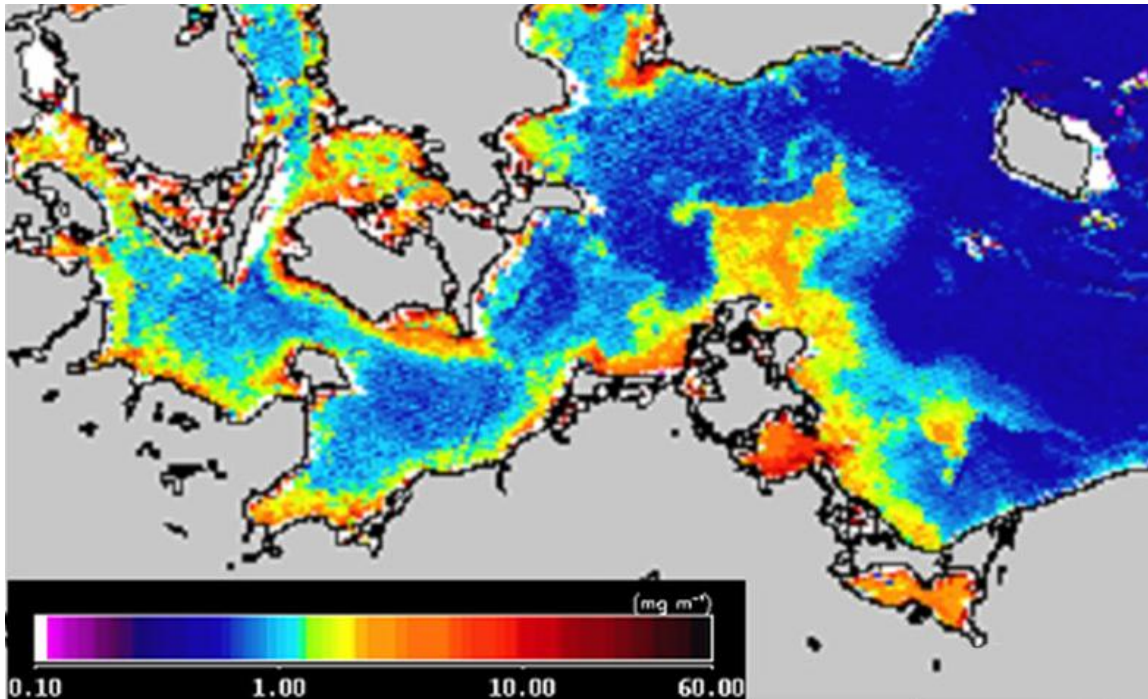


Fig. 5.4 Surface chl-a distribution in April 2003 in the western Baltic Sea derived from SeaWiFS (figure from Wasmund & Siegel, 2008)

As shown in Fig. 5.3, for the spring season, diatoms decreased along the gradient towards lower salinities, whereas the autotrophic ciliate *Mesodinium rubrum*, cryptophytes and dinophytes increased. Also in summer the proportion of diatoms is higher in the western, higher saline, parts of the Baltic, whereas the bloom forming cyanobacteria normally represents the main phytoplankton group during summer in the eastern and northern parts. Especially the diazotrophic (N-fixing) potential harmful species, like *Nodularia spumigena* and *Aphanizomenon* spp. are adapted to the conditions in the Baltic proper, but have rarely been observed in the Kattegat and the northern Gulf of Bothnia (Kahru et al. 1994; Wasmund 1997).

The horizontal distribution of chl-a concentration is similar to that of phytoplankton biomass, as discussed above, with higher chl-a concentration in the coastal zones (Fig. 5.4). The mean chl-a values per season along the marine gradient are shown in Table 5.2 for the last decade.

#### 5.4 Seasonal succession

Phytoplankton develops in dependency of the environmental conditions changing over the annual cycle. Accordingly, different seasonal stages of phytoplankton biomass and composition could be identified. These are in general the spring, summer, and autumnal blooms, besides the minimum in winter. In the western and southern parts of the Baltic Sea a late spring bloom (also "post-spring bloom") may occur (Wasmund et al. 2009), whereby a "bloom" is defined here as temporary increase in biomass and chlorophyll a, as a result of strong growth under changing environmental conditions. Usually, all seasonal stages are initiated by changes in the physical environment.



In winter, the growth is limited by light, i.e. photosynthetically active radiation (PAR). With the ice melt continuous phytoplankton growth is enabled. This spring bloom occurs in the western parts of the Baltic Sea between February and April, in the central Basin in April or even May (Fig. 5.5). In the Bothnian Sea the spring bloom peaks in May. This retard in spring bloom timing is caused by retarded stabilization of the water column, which is determined by the combined effect of vertical temperature and salinity gradients (see Wasmund & Siegel 2008) for a more detailed description).

The spring bloom is usually dominated by diatoms with a possible succession to dinoflagellates and is terminated by nutrient limitation. In most Baltic areas the biomass declined after the spring bloom. For Kiel Bight and the Kattegat region post-spring blooms have been described (e.g. Wasmund et al., 1998) with an increase of small dinoflagellates. Whereas the spring bloom disappears by quick sedimentation, the post spring bloom is usually finished by the grazing pressure of zooplankton. The post spring bloom in the western parts is often dominated by *Dictyocha speculum* in its naked form (Jochem and Babenerd 1989; Wasmund et al. 2007; Wasmund and Siegel 2008).

During summer, a diverse community establishes that is mainly based on regenerated nutrients. According to Wasmund & Siegel (2008) in the Kiel Bight nutrients may become available by upwelling processes and may give an increase in diatom biomass. Cyanobacteria increase or flourish in upwelling water only after warming and under stratified conditions. Diazotrophic (N-fixing) cyanobacteria are advantaged in the Baltic Proper (Fig. 5.5) due to relatively lower N:P ratios in this area (compare Fig. 5.3). Large blooms occur there regularly between July and August if the water temperature exceeds 16°C and wind speed is lower than 6 m/s (Wasmund, 1997).

After the disappearance of the thermocline, upward transport of nutrients enables new algal growth in autumn. In the western Baltic the autumn bloom is dominated by dinoflagellates, particularly *Ceratium* species, which grow slowly during summer and bloom after autumn mixing. In the eastern parts and the Baltic Proper the autumn bloom is often dominated by the diatom *Coscinodiscus granii*. In the transition area between Belt Sea and Baltic Proper the currents may be responsible for the dominance of the respective species.

The relationship between chl-a and biomass depends on abiotic conditions, like nutrient status and light availability, and on the composition of the phytoplankton community. Especially in summer, when picoplankton occurred in higher amounts, the relationship varied strongly. The same could be observed during blooms under strongly light-limited conditions or when plankton with greater biovolumes (e.g. diatoms and dinoflagellates in autumn) dominated the community (Falkowski & Raven, 1987). However, chl-a is a widely used and well accepted proxy for phytoplankton biomass which reflects the seasonal pattern of phytoplankton biomass (Fig. 5.6).

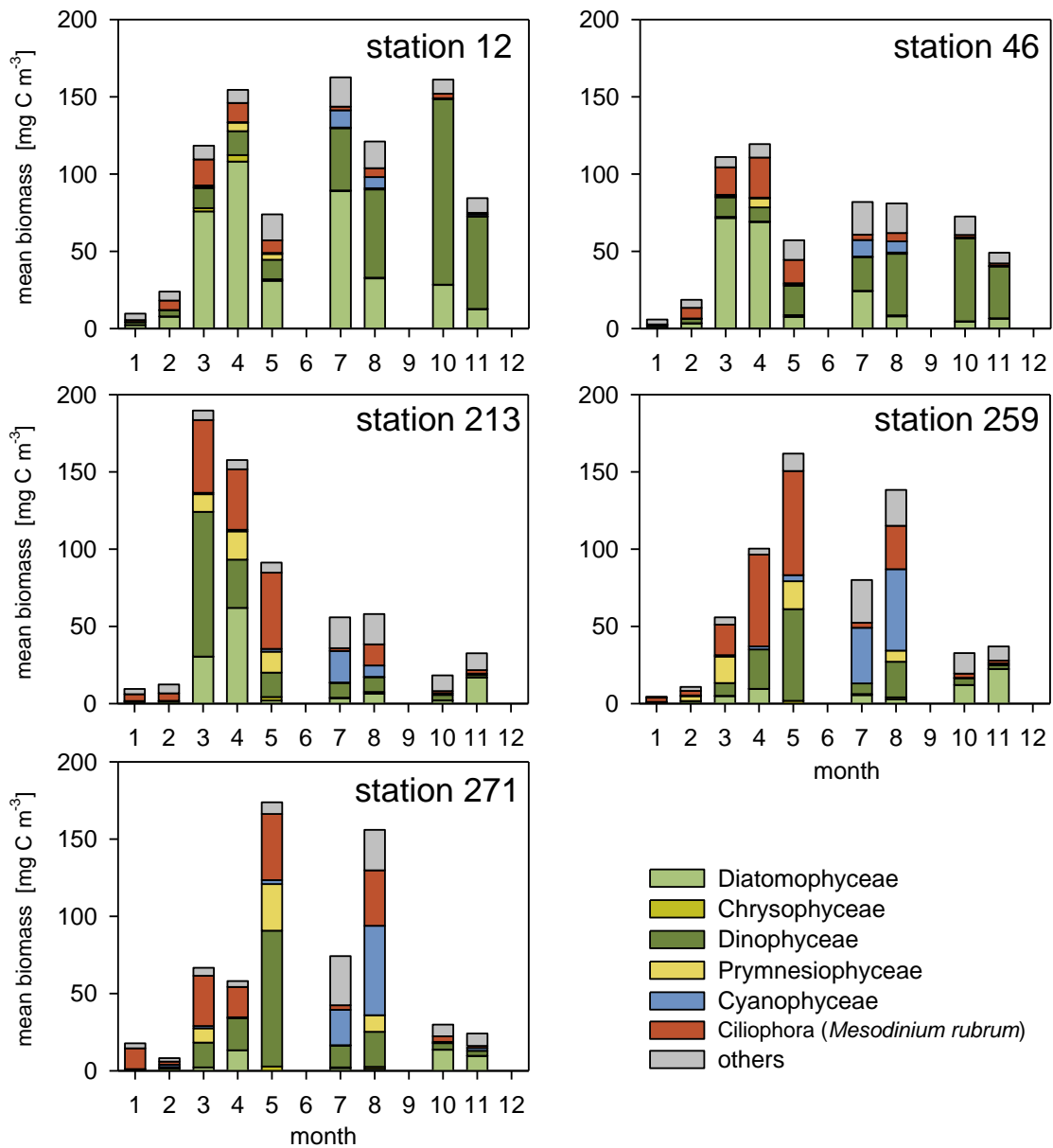


Fig. 5.5 Seasonal patterns of phytoplankton biomass (determined in integrated samples of 0-10 m depth) as mean values for the time period 1999-2008. The figure is based on the comprehensive HELCOM data set. See Fig. 5.1 for position of stations.

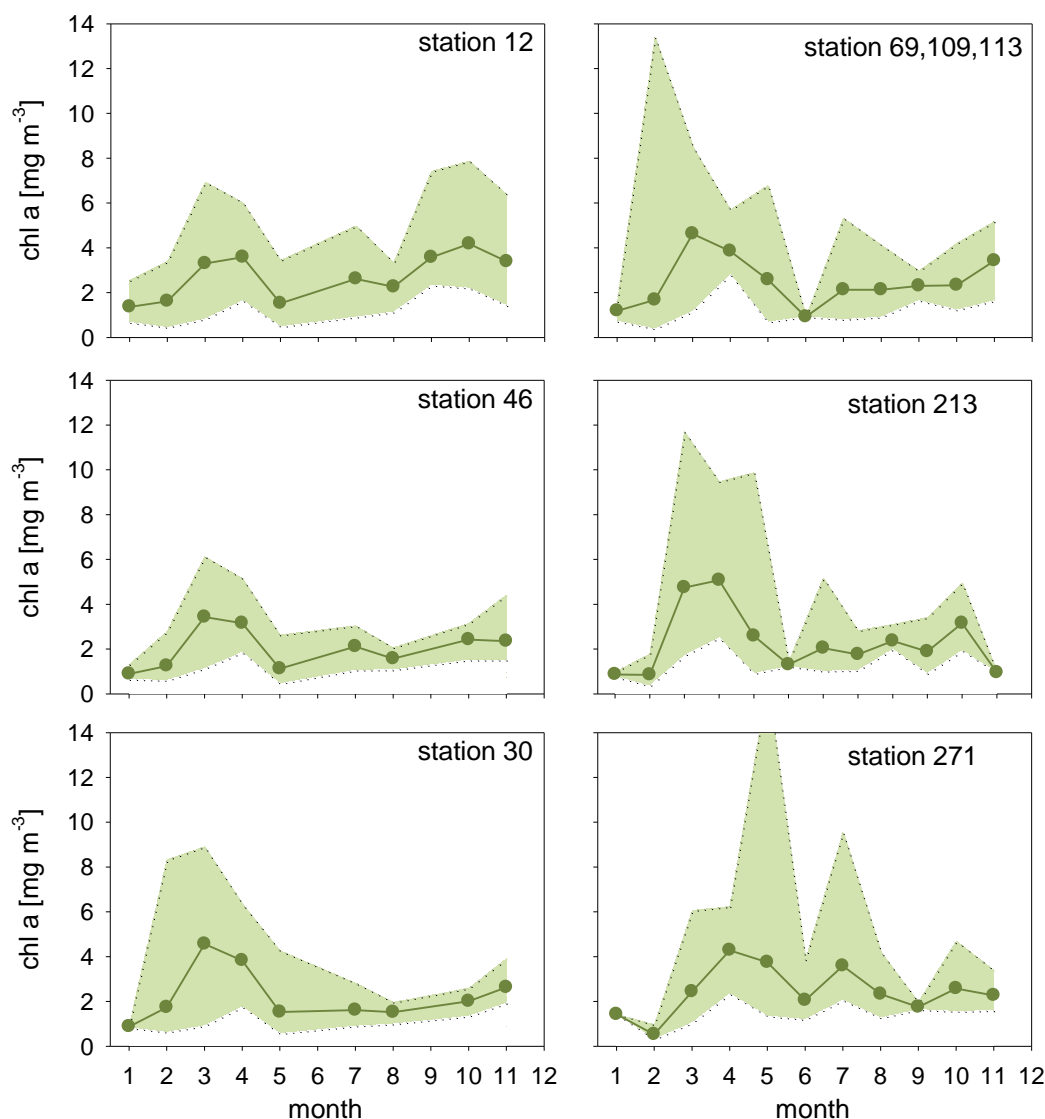


Fig. 5.6 Seasonal patterns of chl-a concentration (mean of 0-10 m depth) averaged for the time period 1999-2009. The upper line denoted maximum values, the lower line minimum values, respectively. The figure is based on the comprehensive HELCOM data set. See Fig. 5.1 for position of stations.

## 5.5 Primary production

Primary production rates are strongly associated with phytoplankton biomass and chlorophyll concentration in the water column, and follow the spatial and temporal changes of phytoplankton biomass. However, the photosynthesis itself depends mainly on light conditions, as well as on temperature, nutrient conditions and not least on the physiological status of the species building up the community.

According to the light depending of photosynthesis, the primary production rates declined strong with water depth. In coastal waters the complete primary production is almost concentrated on the upper 10 m (Zalewski et al. 2005). In less turbid open waters the primary production reaches much deeper, according to comprehensiveness of the euphotic zone (probably up to 20 m, Wasmund and Siegel 2008). In general primary production, normalized per unit area, is higher in river plumes in comparison with open sea areas (Wasmund et al. 2001), due to higher



nutrient supply and higher plankton biomass. However, in high eutrophicated waters the primary production could be diminished according to decreasing light availability by increasing suspended humic substances and biomass itself. The typical annual primary production data in the large sea areas of the Baltic Sea are compiled in Table 5.3.

Table 5.3 *Phytoplankton primary production in the different sea areas. Data are compiled from various literatures by Wasmund & Siegel (2008) and Wasmund et al. (2001).*

Baltic Sea region	Annual total primary production [g C m <sup>-2</sup> y <sup>-1</sup> ]	Time period of measurement
Kattegat/Belt Sea	190	1984-1993
Arkona Basin	190	1993-1997
Bornholm Basin	193	1993-1997
Eastern Gotland Basin	208	1993-1997
Oder plume	422	1993-1997
Vistula plume	283	1993-1997
Western Gotland Sea/ Baltic Proper	200	1970-ies
Gulf of Riga	261	1993-1997
Gulf of Finland	82	1985
Bothnian Sea	48	1998*
Bothnian Bay	17	1970s

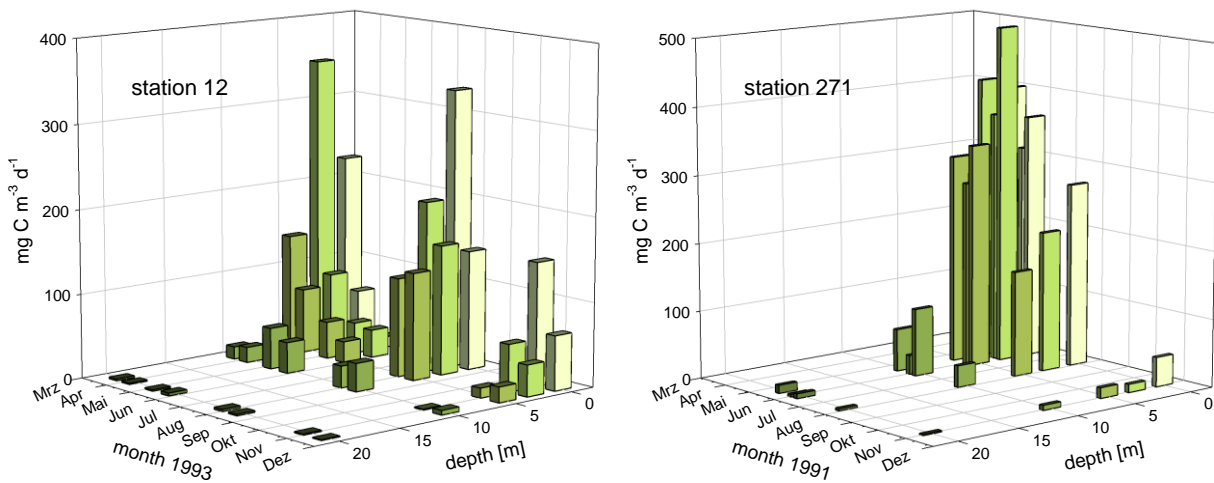


Fig. 5.7 *Seasonal variation and depth dependence of phytoplankton primary production at station 12 (BMP M02, Mecklenburg Bight) in 1993 and station 271 (BMP J01, Eastern Gotland Sea) in 1991.*

## 5.6 Long-term trends

Changes in phytoplankton composition and biomass are indicators for changes in the marine environment. The anthropogenically induced eutrophication and changes in climate conditions could be considered as major forces for system alteration.



Due to high natural variation in time and space, the detection of statistical trends in phytoplankton is not simple. Especially the inflexible and sparse HELCOM monitoring programme is often unable to register bloom events and seasonal stages, as can be seen in (ICES 2010) data. However, (Wasmund & Uhlig 2003) and (Wasmund and Siegel 2008) could present trends for main taxa groups and chl-a concentration in spring and summer seasons. The main results for the Baltic Sea long-term investigation can be summarised as follows.

### 5.6.1 Species composition

#### Spring bloom

A significant reduction in diatoms was observed for many areas in the northern Baltic Proper, Gotland Sea, Belt Sea and Kattegat. For the southern Baltic Sea this trend is not significant. A shift from diatoms to dinoflagellates is proposed for the northern parts of the Baltic Sea (HELCOM 1996). In the Baltic Proper and the Belt Sea upward trends were found in all seasons for dinoflagellate (Dinophyceae) abundance, whereas downward trends were found in the Kattegat and Sound. Shift in species composition have been investigated in detail for the Kiel Bight (Wasmund et al. 2007). The authors documented a disappearance of the diatom *Skeletonema* sp. summer blooms coupled with a shift of this genus to the spring season. This shift may relate to a species shift of various *Skeletonema* species, which are not detectable by the microscopy method used for monitoring (Utermöhl 1958). In addition species like *Chaetoceros* spp., *Ceratium longipes*, *Heterocapsa triquetra* and others declined. On the other hand species like *Cerataulina pelagica*, *Ceratium furca*, *Dictyocha speculum*, *Prorocentrum minimum* and others, see for detailed information (Wasmund et al. 2007) prospered in the Kiel Bight.

#### Summer bloom

Due to their potential toxicity, diazotrophic cyanobacteria blooms are of special interest in the Baltic Sea. The question if cyanobacteria bloom intensity increased has been intensively discussed. Cyanobacteria blooms have been reported from the open Baltic Sea already in the 19th century, but their intensity and frequency seem to increase (Finni et al., 2001). (Hübel and Hübel 1980) and (Melvasalo and Viljamaa 1987) observed intensive blooms in the Baltic proper since 1969, while (Postel 2000) found high biomass of cyanobacteria in the western Baltic Sea in 1972/1973, 1983 and 1992. Large blooms were detected by satellite also in 1982–1984 and 1991–1993 (Kahru et al. 1994). In the Tvärminne area at the entrance to the Gulf of Finland, (Kononen 1992) observed a cyanobacteria biomass  $>100 \text{ mg C m}^{-3}$  in 1979, 1983, 1986 and 1987. In Gdansk Basin, cyanobacteria seem to decrease from 1979 to 1993 (Wrzolek 1996). During the last decade intensive blooms were detected by satellite imaging in 1999 (not shown), 2003, 2005 and 2006, Fig. 5.8, (Hansson and Öberg 2009). Apparently, cyanobacterial blooms are more variable than those of diatoms and dinoflagellates, and it is difficult to deduce steady trends.



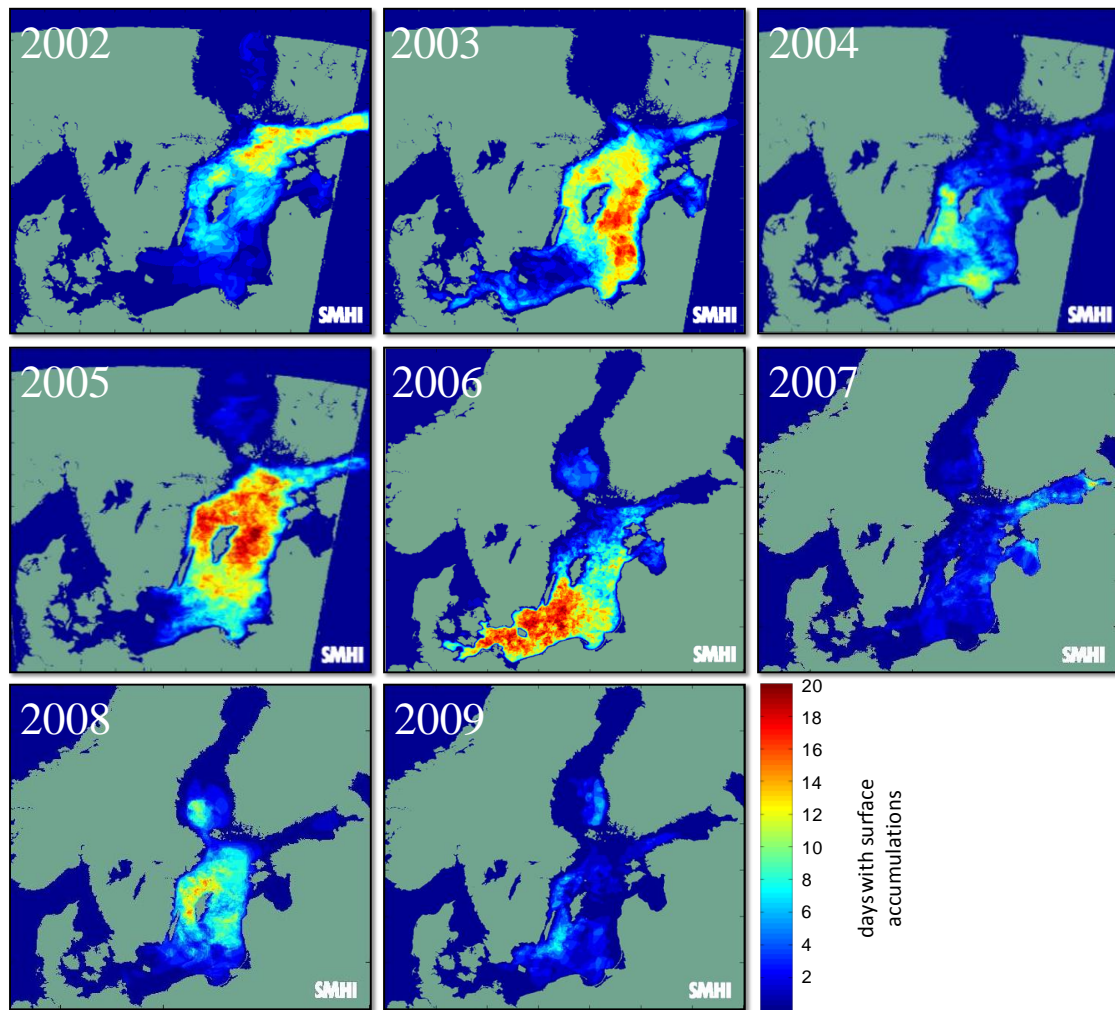


Fig. 5.8 Number of days with surface accumulations of cyanobacteria. Figure was redrawn from HELCOM indicator factsheets 2004-2009 (Hansson 2004-2008; Hansson and Öberg 2009).

For the Baltic Proper (Wasmund and Uhlig 2003) reported downward trends with high biomasses in 1979-1981, 1985-1986, 1991-1993 and 1998. The decreasing trend is confirmed when one considers more recent data from HELCOM monitoring (Fig. 5.8, Fig. 5.9) for most Baltic Sea areas by (Jaanus et al. 2007), with exception of the northern Baltic regions, where increasing trends are reported (Suikkanen et al., 2007). The driving forces behind the increase or decrease are not fully understood yet. Main parameters are changes in nutrient availability and nutrient ratios, due to increasing anthropogenic eutrophication, and changed climatic conditions or large scale cycles.

**Autumn bloom**

The autumn bloom is most prominent in the western parts of the Baltic. *Ceratium* blooms constitute the most abundant part. This situation has not changed in the last century (Wasmund et al., 2007). On the other hand, upward trends for Diatoms were found in autumn in the western Gotland Basin, Belt Sea and Kattegat (Wasmund et al. 2007).

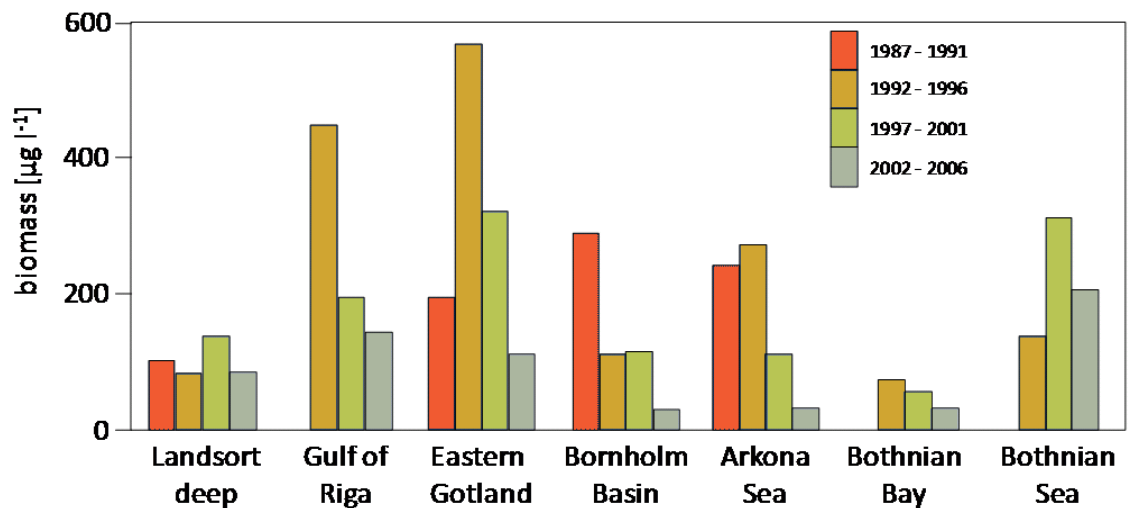


Fig. 5.9 Biomass of cyanobacteria (0-10m integration depth) averaged by 5-year-periods in selected sub-basins of the Baltic Sea. Graphs represent only areas where statistically significant changes have taken place between different time-periods. Modified from (Jaanus et al. 2007). Data source: Estonian, Latvian, Lithuanian, German and Swedish phytoplankton monitoring programs. Description of data: Annual weighted summer (June-September) average of phytoplankton group biomasses. (Jaanus et al. 2007)

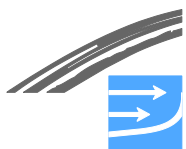
### 5.6.2 Non-indigenous species

According to (Olenina et al. 2009), nine phytoplankton species are identified as non-native ones in the Baltic Sea region (5 diatoms: *Coscinodiscus wailesii*, *Odonotella sinensis*, *Pleurosigma simonsenii*, *Pleurosira leavis f. polymorpha* and *Thalassiosira punctigera*; 4 dinoflagellates: *Alexandrium tamarense*, *Gymnodinium catenatum*, *Karenia (Gyrodinium) mikimotoi* and *Prorocentrum minimum*). Only the dinoflagellate *Prorocentrum minimum* (Pavillard) Schiller can be categorized as an invasive species, which is spreading and causing significant impacts on plankton community, habitat and ecosystem functioning. HELCOM estimated the impact of this species at level 3 on a five level-scale, characterizing a strong biopollution impact.

### 5.6.3 Chlorophyll and total biomass

According to (Wasmund et al. 2007) in Kiel Bight the phytoplankton biomass increased in the last century from approximately 55 mg C m<sup>-3</sup> (postulated for the time period 1905-1950) up to 83-216 mg C m<sup>-3</sup> (annual means, 2001-2003). The largest increase was observed up to the 1960s of the last century, followed by more or less stable biomass values since the 1970s. This was confirmed by unchanged chl-a values since 1970 (Wasmund et al. 2007).

Discrete seasonal chl-a data (mean of 0-10m depth) from HELCOM monitoring, supplemented by other national and international data sets (Wasmund & Siegel, 2008), are presented in Fig. 5.10 and Fig. 5.11. Because chl-a can be determined easier and with higher precision than phytoplankton biomass determined by microscopy, most trend analyses use this proxy. Significant trends could be observed only in the spring season (Fig. 5.10). While significant downward trends in chl-a concentration occurred at stations 12 (Mecklenburg Bight) and 46 (Darss Sill), a slight but significant increase was observed for the Arkona Basin and the Bornholm Sea (Wasmund & Siegel 2008). The increase in chl-a in open waters of the Baltic Sea, with exception of Bothnian Sea and Northern Baltic proper, has also been confirmed by (Jaanus et al. 2007) for summer values in the period 1992-2006. However, trend analyses by (HELCOM 2009b) showed increasing chl-a values for the Bothnian Sea, too.



In the Gdansk Bay and the southeastern Gotland Basin no trends could be observed for annual chl-a concentrations between 1980 and 2005, compare (HELCOM 2009b), whereas a slowly downward trend could be found for the Baltic proper from 1974 up to 2008 (Håkansson & Lindgren 2008). For the Kattegat decreasing trends were reported from (HELCOM 2009a).

#### 5.6.4 Primary production

Long-term data sets of primary production are rare for the Baltic Sea. Often the data sets show a large spatial and temporal variability (HELCOM 2009b). (Rydberg et al. 2006) reported for the last 50 years increasing trends in daily mean summer production from the various areas in the Western Baltic (Kattegat, Little Belt, Sound and Great Belt) with observed doubling of values during summer. Increasing trends were also reported from the Gulf of Gdansk (1970-88) and the Bornholm Sea, compare (Wasmund and Siegel 2008), Table 5.3.

Table 5.4 *Phytoplankton primary production in the different Sea areas in the 1970s and the 1990s. Table originates from (Wasmund & Siegel 2008). The values represent in situ measurements except for "Total Baltic" calculate d by (Wasmund et al. 2010).*

<b>Baltic Sea region</b>	<b>1970s annual total primary production [g C m<sup>-2</sup>y<sup>-1</sup>] (Kaiser et al. 1981)</b>	<b>1990s annual total primary production [g C m<sup>-2</sup>y<sup>-1</sup>] (Wasmund et al. 2001)</b>
Kattegat/Belt Sea	90-120	190
Baltic Proper	90-125	200
Gulf of Riga	80-100 (assumed)	261
Gulf of Finland	70	82
Bothnian Sea	70	48
Bothnian Bay	18	17

(Wasmund et al. 2001) compared two data sets from the 1970s (Kaiser et al. 1981; Elmgren 1984) with measurements from the end of the last century (Table 5.4) and calculated annual phytoplankton primary production values of 34.8, 49.8 and 62.1 10<sup>6</sup>t C per year, respectively, in the total Baltic Sea. The data in Table 5.4 suggested more or less a doubling of primary production in the last two decades of the last century, especially in the southern and western parts of the Baltic. An increase in primary production by a factor of 1.3-1.7 was estimated already by (Elmgren 1989) for the first 80 years of the last century.

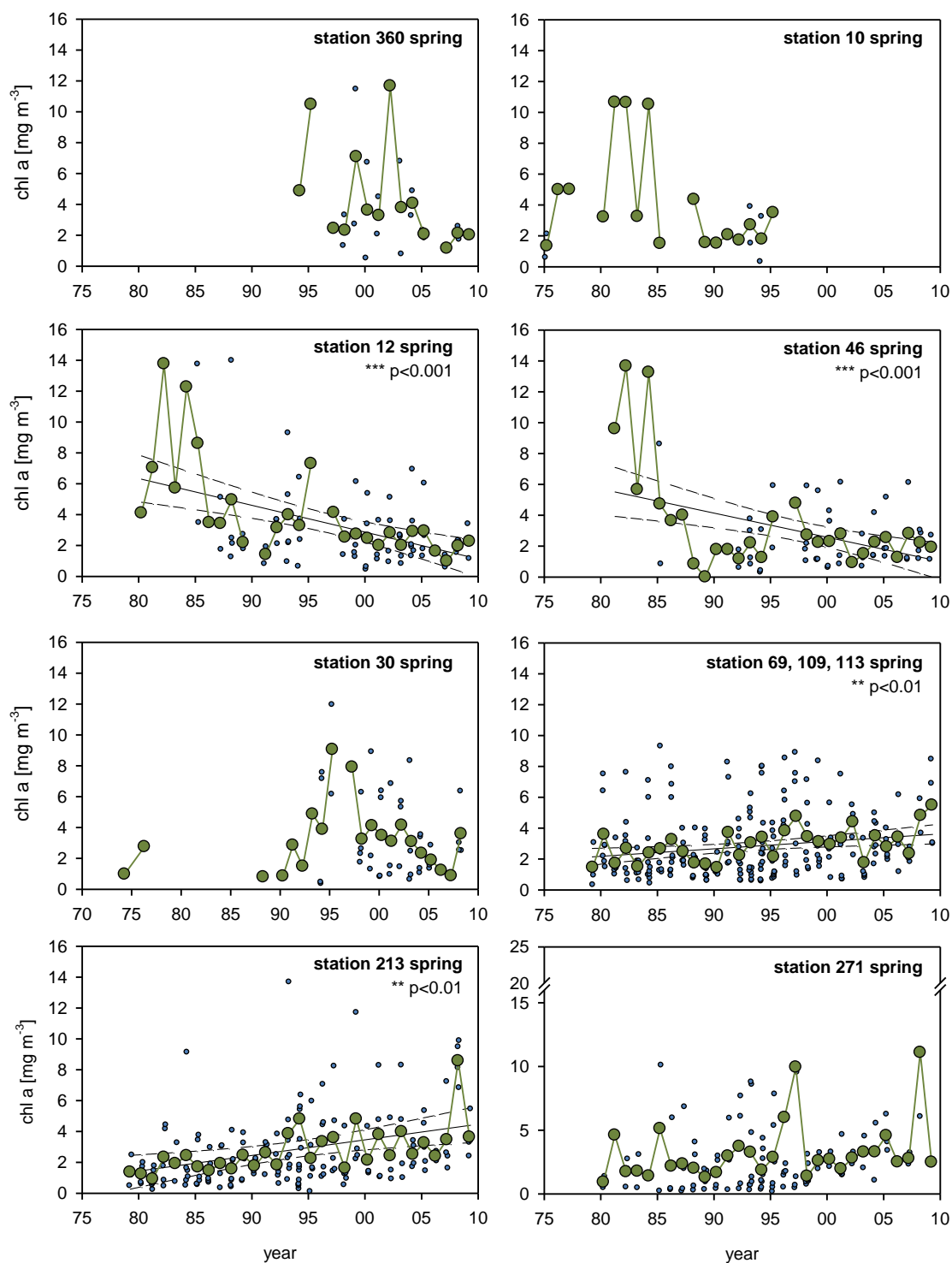


Fig. 5.10 Long-term investigation of chl-a concentration (mean of 0-10 m depth), both for seasonal means (green circles) and original data (blue circles) for the spring season. Updated data series of (Wasmund and Uhlig 2003) and (Wasmund et al. 2009). Lines represent linear regression and 95% confidence intervals for original data sets (blue). See Fig 5.1 for position of stations.

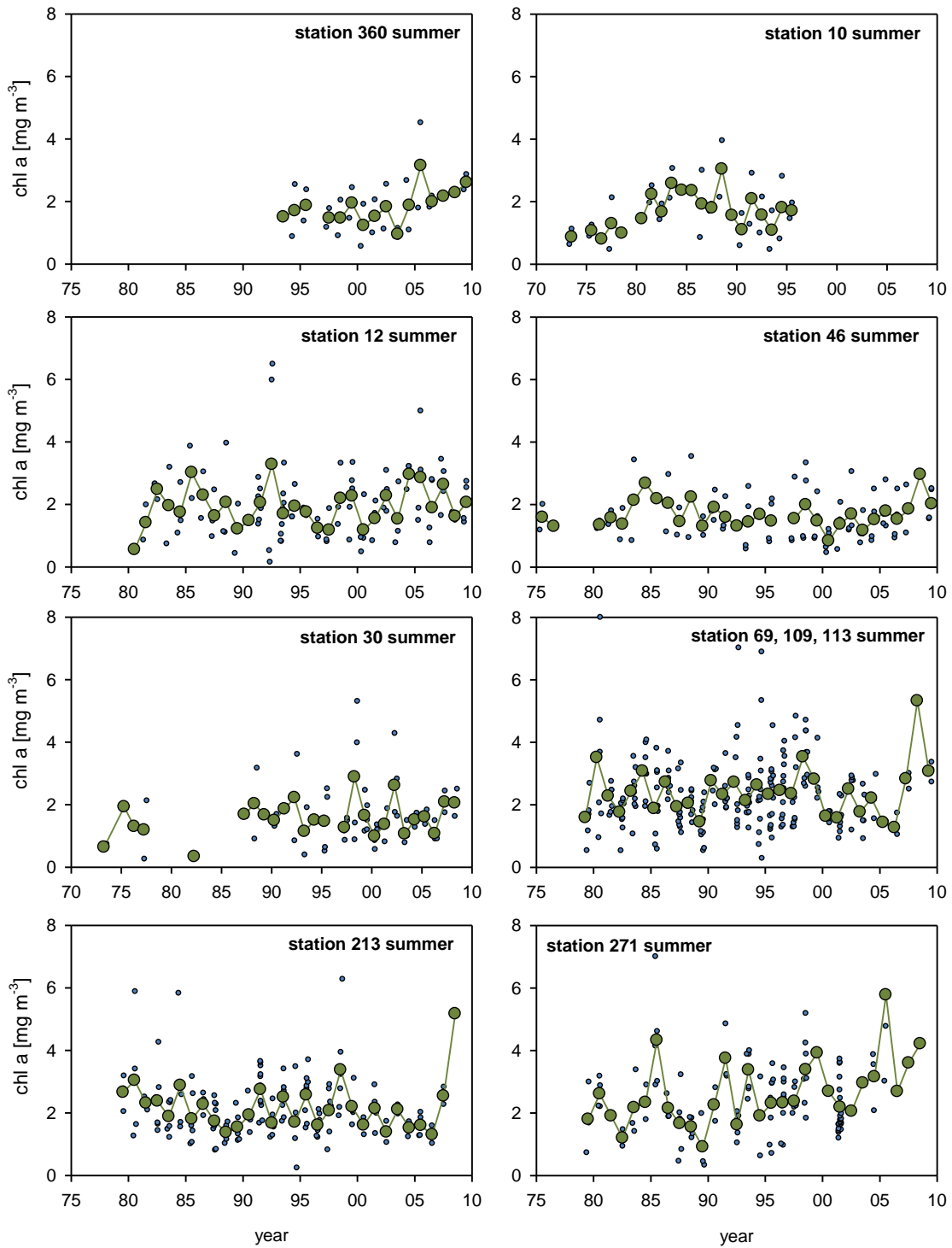


Fig. 5.11 Long-term investigation of chl-a concentration (mean of 0-10 m depth), both for seasonal means (green circles) and original data (blue circles) for summer season. Updated data series of (Wasmund and Uhlig 2003) and (Wasmund et al. 2009). See Fig. 5.1 for position of stations.



## **6 PRESENT PRESSURES**

### **6.1 Major constructions**

The most prominent constructions with regard to general infrastructure and local environmental impact around the Baltic Sea have been the St. Petersburg dam, oil terminals, nuclear power stations and a number of bridges across the Danish Straits. Of these examples, only oil terminals are known to have indirectly affected the Baltic Sea in general due to increased shipping activity of tankers (see Chapter 6.2.2 below). Apart from that, oil terminals pose the risk of local oil spills causing environmental pollution.

Power stations on the coastline are point sources of warm water from their cooling systems. The discharged water may contain contaminants (Macqueen 1980), especially chlorine from anti-fouling treatment (Rajamohan et al. 2007). The discharge of cooling water from nuclear plants into isolated bays of the Baltic Sea leads to locally raised sea surface temperatures, giving rise to increased production of cyanobacteria, while power plants that discharge their water to the open sea show considerably less effects (Gorny et al. 2000).

As sea level variations during severe floods in the St. Petersburg area can reach up to four meters above the mean in the city waterfront, which was erected on low-level marshland (Leppäranta and Myrberg 2008), a flood protection barrier has been constructed in the 1970s. (Rukhovets 1982) states that comparisons between simulations without and with a dam show a considerable difference in water transports across the dam compared to natural conditions. Stagnant zones in the Neva Bay and associated allocation of pollution by waste water became more extensive with a dam in place (Leppäranta and Myrberg 2008). (Voltzinger et al 1990) conclude that the dam has no influence on the general pattern of water transport but there are marked changes in the vicinity of the dam.

The bridges across the Danish Straits are hydrographically implemented as zero solutions, designed to not affect the Baltic Sea after their implementation.

Offshore wind farms have been constructed in Danish waters and a number of locations along the German coastline has been approved by German authorities for the construction of further wind farms. It has been shown in the QuantAS study that the effect on the hydrography and ecology of the Baltic Sea of all offshore wind farms that were planned or had been applied for permission as of 2009 is negligible in shallow waters (HELCOM 2009d). It is however expected that the number of offshore wind farms as well as their size will considerably increase during the next decades. While an offshore wind farm in 2002 consisted of some 20 wind turbines, it is estimated that by 2020 a single wind farm may have 1,000 individual turbines. With increasing capacity of the turbines (3-5 MW) there comes also the need for bigger foundations (Tillessen 2010). The impact of such massive installations on the Baltic Sea is not yet clear.

### **6.2 Ship traffic and its effects**

#### **6.2.1 High-speed traffic**

The increase in high-speed ship traffic in the Baltic Sea has led to a number of environmental impacts. Especially the Gulf of Finland and the Archipelago Sea around Åland has seen a strong increase in fast-ferry traffic within the last ten years (Leppäranta & Myrberg 2008). E.g. the Helsinki-Tallinn ferry line with a daily frequency of up to 70 crossings during the high season sails in the transcritical velocity range, i.e. within 15% of the maximum phase speed of shallow-water waves,





$\sqrt{gH}$ . Wave systems at such speeds may contain so-called solitonic waves that are very different from waves induced by conventional ships (Soomere 2006). Studies by (Erm and Soomere 2004, 2006) have shown local resuspension of light sediments in the wakes of fast ferries sailing in water depths that range from about 2 m to 15 m. In connection with coastal currents resuspension may contribute to sediment transports. A rough estimate suggests that ca. 1 ton of sediments per meter of affected coastline may annually be relocated by ship wakes in Tallinn Bay (Erm and Soomere 2006).

The waves caused by conventional ships and hydrofoils have typical heights of 20 cm to 30 cm with periods of 3.5–4 s, and can hardly be distinguished from the natural background (Soomere and Rannat 2003). Wake waves from large high-speed vessels though frequently have heights of ca. 1 m and periods of 10–15 s, characteristics that seldom occur naturally in the Tallinn Bay. While the leading waves in the wake group of high-speed vessels are usually the highest ones, the third wave group may produce the highest waves in remote areas with heights up to 70 cm in a distance of 8 km to 10 km from the ship lane (Soomere and Rannat 2003).

### **6.2.2 Oil spill**

Oil leakage from ships and especially from tankers that have been damaged by collision or grounding poses a severe threat to the Baltic Sea's ecosystem since the natural overall renewal of deep water masses in the Baltic is very limited and happens only on a scale of decades (see chapter 3.3.3).

The Baltic Sea contains some of the most frequented shipping routes in the world. The Kiel Canal, which is the world's busiest artificial waterway, connects the Baltic Sea to the North Sea and also the Danish Straits experience a high volume of ship traffic. Although current nautical regulations include safety measures such as Traffic Separation Schemes, a number of ships has been grounded in the shallow straits across the Darss Sill in recent years. It is also the depth of these shallow waters that limits the size of vessels to enter the Baltic Sea from the Kattegat. Vessels with a draught greater than 15.4 m will not be able to navigate the Danish Straits, which restricts tank ships to the so-called "Aframax" maximum size of less than 150,000 dead weight tons. Another restriction that limits and endangers ship traffic is sea ice, especially in the northern Baltic Sea (Liukkonen 2006).

The number of tankers navigating the Great Belt has nevertheless risen in past years and it is expected that even the large class of tanker vessels will see an even more increased traffic in the future (HELCOM 2009e), see also Fig. 6.1. In the course of this, the Fehmarnbelt as a part of the Great Belt transit route will also experience this increase in tanker traffic. In 2006 alone, a number of 9,000 tankers navigated the Kadet Furrow across the Darss Sill, which poses the next obstruction in the transit from Great Belt, and the transit shipping lanes of the entire Baltic Sea registered a tanker traffic of 12,300 vessels (Schleswig-Holstein Ministry of Science, Economic Affairs and Transport 2007).

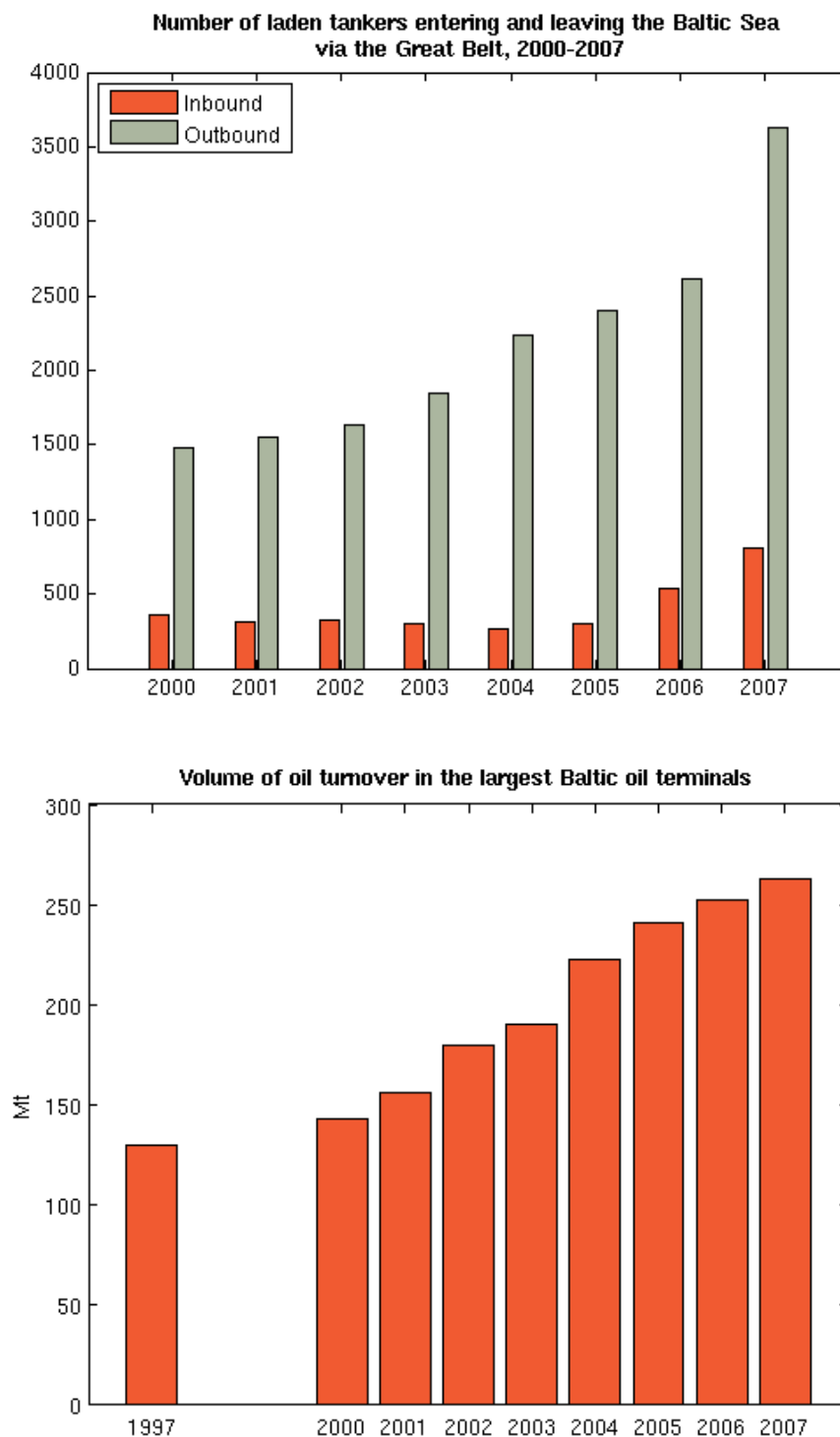


*Fig. 6.1 Upper panel: number of laden tankers entering and leaving the Baltic Sea via the Great Belt. Figure redrawn with data from (HELCOM 2009e). Lower panel: amount of oil transported (million tons) via the 17 largest oil terminals in the Baltic Sea area (Fredericia, Kalundborg, Muuga, Porvoo, Naantali, Rostock, Ventspils, Riga, Klaipeda, Butinge, Gdansk, Primorsk, St Petersburg, Kaliningrad, Gothenburg, Brofjorden, and Vysotsk) during 1997-2007. Figure redrawn with data from (HELCOM 2009c).*

It is moreover expected that oil turnover in the Baltic will further increase by 30% until 2015, based on 2007 figures. This may mean a number of 14,000 tanker vessels on Baltic Sea transit routes (Schleswig-Holstein Ministry of Science, Economic



Affairs and Transport, 2007, citing HELCOM). Another upcoming tanker project is the construction of a Liquefied Natural Gas (LNG) terminal at the Polish port of Świnoujście. This will bring about an increased ship traffic south of Bornholm and increase the risk of collisions (Hajduk 2009). The shipping from oil terminals in Russia is likewise increasing and the turnover of oil in the harbour of Primorsk has risen very much stronger since 1997 than in all other major Baltic oil terminals (HELCOM 2009c).

## **6.3 Eutrophication and hazardous substances**

### **6.3.1 Eutrophication**

In 2009, the Helsinki Commission published for the first time a consistent classification of eutrophication. This classification is based on three elements: available background concentrations, a defined acceptable deviation from these background concentrations and the status data for the period 2001-2006 (HELCOM 2009a). Different parameters like loads, winter nutrient concentration, Secchi depth, chlorophyll a concentrations, depths of submerged vegetation and others were used given that the above mentioned three elements are available in a reasonable quality. All in all 189 sea areas were classified, among them 172 coastal areas and 17 open sea areas (Fig. 6.2). Only the open waters of the Bothnian Bay and the Swedish parts of the northeastern Kattegat are classified as "areas not affected by eutrophication". It is commonly accepted that the open parts of the Bothnian Bay are close to pristine and that the northeastern Kattegat is influenced by Atlantic waters. In the coastal zone, 161 areas show signs of eutrophication, only 11 have a good ecological status. Consequently, HELCOM comes to the conclusion that eutrophication is still a major concern despite measure undertaken so far. There the so-called "Baltic Sea Action Plan" which was adopted 2007 by all Contracting Parties of the Helsinki Commission, is aimed to reduce nutrient inputs further. The annual input of phosphorus should be reduced by 15,250 t, the nitrogen input has to be decreased annually by 135,000 t. The over-arching goal is a Baltic Sea free of eutrophication.

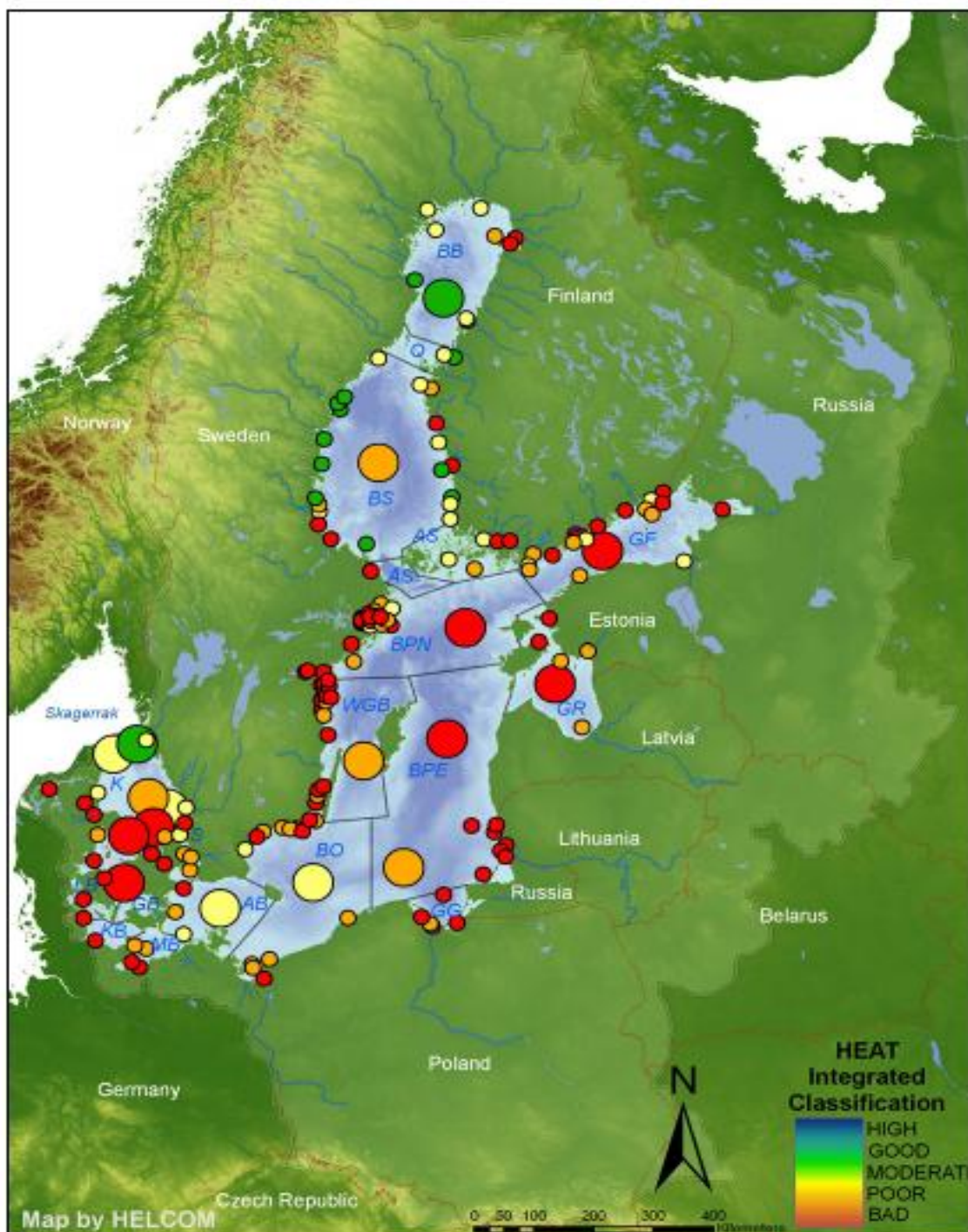


Fig. 6.2 Integrated classification of the eutrophication status of the Baltic Sea. Large circles represent open sea areas, small circles show coastal areas. Very good status (blue), not existing, good status (green) describes "areas not affected by eutrophication" while moderate (yellow), poor (orange) and bad (red) are equivalents to "areas affected by eutrophication" (HELCOM 2009a).

### 6.3.2 Hazardous substances

Since the beginning of the industrialization of the region in the late 19<sup>th</sup> century, the Baltic Sea has been exposed to an extensive use of chemicals and its marine environment has a long history of contamination; therefore the Baltic Sea has often been referred to as the most polluted sea in the world (HELCOM 2010c). Hazardous substances, also known as pollutants, can accumulate in the marine food web up to



levels which are toxic to marine organisms, particularly predators. They may also represent a health risk for people, e.g. by consumption of contaminated sea food. Once they are released into the Baltic Sea, hazardous substances can remain in the water for very long periods.

Certain contaminants may be hazardous because of their effects on hormone and immune systems, as well as their toxicity, persistence and bio-accumulating properties. Conditions in the different sub-regions of the Baltic Sea vary depending on salinity, flora and fauna, and on the characteristics of the seabed; these conditions influence the distribution of contaminants and their fate. (HELCOM 2010c) defines substances as hazardous if they are toxic, persistent and bioaccumulate, or very persistent and very bioaccumulating. Substances that affect hormone and immune systems are also considered hazardous.

According to (HELCOM 2010c), hazardous substances enter the Baltic Sea ecosystem by four main routes:

1. point-sources of pollution situated on the coast or inland in the catchment areas including industries and municipal wastewater plants;
2. land-based diffuse sources such as runoff from agricultural land, forests, and other land uses;
3. activities taking place at sea such as shipping, dredging or operation of oil platforms;
4. atmospheric deposition of contaminants from all types of combustion sources as well as volatile chemicals (e.g., pesticides) from many other uses; some of these contaminants have been transported long distances in the air.

HELCOM has conducted an integrated thematic assessment of hazardous substances in the Baltic Sea using data from 1999–2007 on concentrations of hazardous substances in biota, sediments or seawater and measurements of biological effects at a total of 144 assessment units in the Baltic Sea; 104 of the assessment units were coastal sites or areas, while the remaining 40 were open-sea areas. 137 out of the 144 areas assessed were classified as “moderate”, “poor” or “bad” and were therefore classified as being “disturbed by hazardous substances” (Fig. 6.3). This indicates that the entire Baltic Sea was an area with a high contamination level from 1999–2007. With the exception of the northwestern Kattegat, all open-sea areas of the Baltic Sea were classified as being “disturbed by hazardous substances” (HELCOM 2010c). 98 of the 104 coastal assessment units were classified as being “disturbed by hazardous substances”. So, for the entire Baltic Sea, only seven units were assessed as “undisturbed by hazardous substances”.



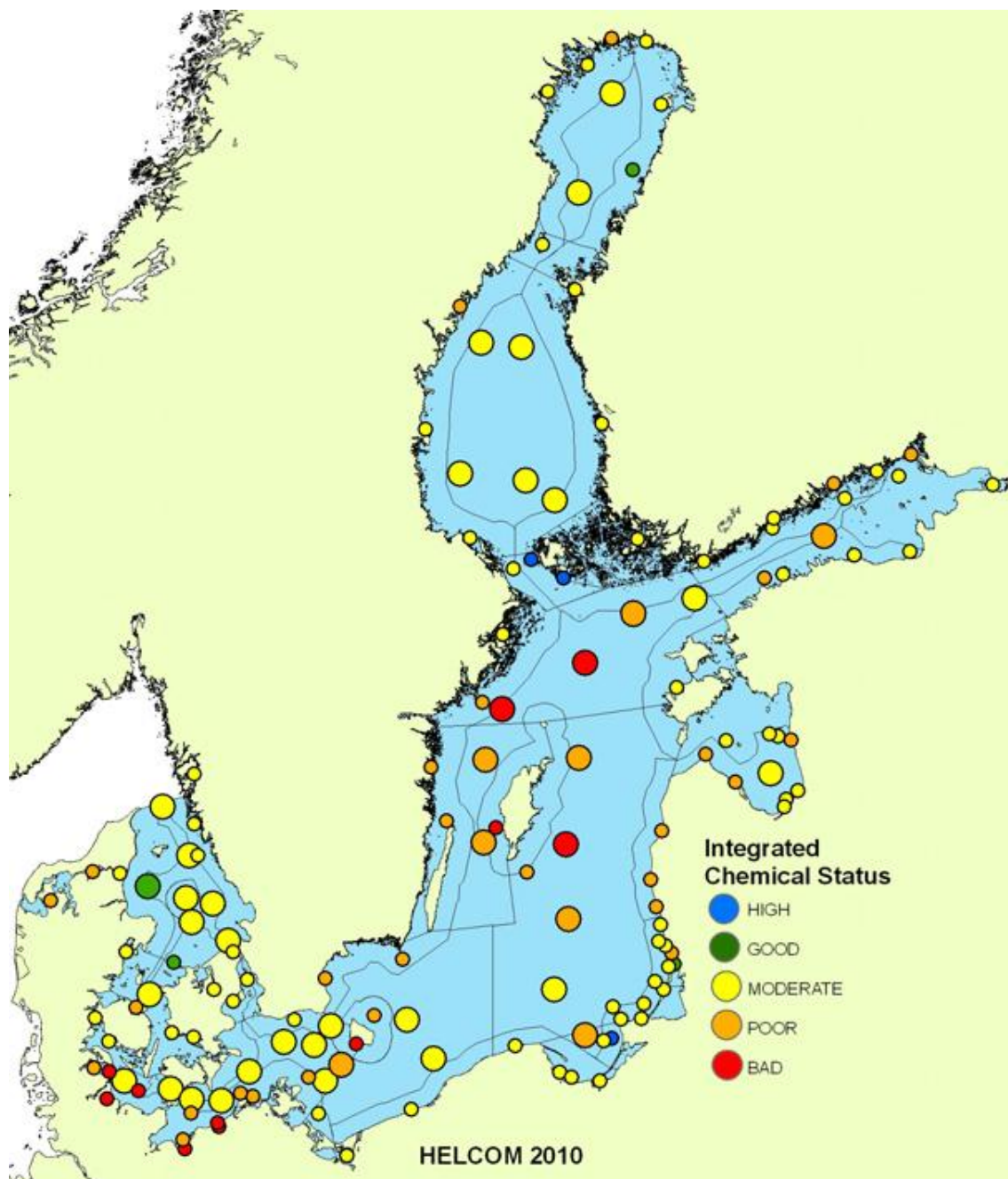
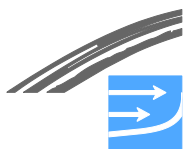


Fig. 6.3 Integrated classification of the hazardous substances status in the 144 assessment units. Blue = high status, green = good, yellow = moderate, orange = poor, and red = bad status. High and good status are equivalent to "areas not disturbed by hazardous substances", while moderate, poor, and bad status are equivalent to "areas disturbed by hazardous substances". Large dots represent assessment units of the open basins; small dots represent coastal assessment units which are mainly located in the territorial waters delimited by the grey line. Other grey lines represent the divisions between the sub-basins (cf. Fig. 6.2). Ecological objectives that were assessed using CHASE included all HELCOM objectives: "Concentrations of hazardous substances close to natural levels", "All fish safe to eat", "Healthy wildlife" and "Radioactivity at pre-Chernobyl levels". From (HELCOM 2010c).

The highest contamination ratios were reported for polychlorinated biphenyls (PCBs) and benz[a]anthracene (). Other substances with high contamination ratios include tributyltin (TBT), mercury, DDE (a metabolite of DDT), and dioxins. The





open-sea areas in the Bothnia Gulf and Gulf of Riga, the Arkona and Bornholm Basins, and the Danish open waters were mainly classified as being in “moderate” status, while the northwestern Kattegat received a status classification of “good”.

Table 6.1 Distribution of the substances with the highest concentrations in relation to target levels (i.e., the highest Contamination Ratio, CR) in the 137 assessment units classified as “areas disturbed by hazardous substances” in the different sub-basins of the Baltic Sea. Numbers in parentheses indicate the number of times the substance was found having the highest CR in the assessment units of the basin (HELCOM 2010c).

Baltic Sea sub-basin	Substances
<b>Bothnian Bay</b>	Cadmium, cesium 137 (3), BDE, DDE, DEHP and PCB
<b>Bothnian Sea</b>	Cadmium, cesium-137, DDE (2), dioxins (2), HCHs, lead and mercury (2)
<b>Åland Sea and Archipelago Sea</b>	Cesium-137 and PCB
<b>Northern Baltic Proper</b>	BDE*, cadmium, DDE*, lead, octylphenol, PCB (2) and TBT
<b>Gulf of Finland</b>	Cadmium, cesium-137, copper, DDT, lead, mercury (6), TBT and zinc (2)
<b>Gulf of Riga</b>	DDT (2), lead (4), PCB (3) and zinc
<b>Eastern Baltic Proper</b>	Anthracene, benz[a]anthracene (8), benzo[k]fluoranthene (1), cesium-137 (2), DDE (2), dioxins, mercury (3) and TBT (3)
<b>Western Gotland Basin</b>	DDE, dioxins, nickel and PCB (2)
<b>Gdansk Depression</b>	Benz[a]anthracene, cesium-137, mercury and PCB
<b>Bornholm Basin</b>	Cadmium, cesium-137, DDE (2), lead, PCB (2), TBT and zinc
<b>Arkona Basin</b>	Benzo[g,h,i]perylene, cadmium (2), cesium-137, DDE, lead (2), mercury, PCB (3) and TBT
<b>Bight of Mecklenburg and Kiel Bight</b>	Cesium-137, HCHs, lead (3), PAH-metabolites and PCB (7)
<b>Belt Sea and the Sound</b>	Arsenic, DEHP, nonylphenol (3), PCB (2), VDSI and TBT
<b>Kattegat</b>	Arsenic, BDE, fluorene, nickel, nonylphenol, octylphenol, PCB (3), TBT (3) and VDSI (2)

\*) The substances had equal weight at the site.

BDE = brominated diphenylether; DDE = 1,1-dichloro-2,2-bis(chlorophenyl)ethylene; DDT = 1,1,1-trichloro-2,2-di(4-chlorophenyl)ethane; DEHP = bis(2-ethylhexyl)phthalate; HCH = hexachlorocyclohexane; PCBs = polychlorinated biphenyls; TBT = tributyltin; VDSI = van der Meer sequence index.

According to (HELCOM 2010c), the assessment of hazardous substances shows that the goal of the Baltic Sea Action Plan to attain a “Baltic Sea with life undisturbed by hazardous substances” has not been reached. There are however encouraging signs of decreasing trends of certain substances and an improvement in the health status of some top predators.



## 6.4 **Fishery**

Fish play an important role in the Baltic Sea ecosystem. Not only do they consume plankton and benthic invertebrates, they also serve as food for marine top predators may substantially facilitate pelagic-benthic coupling.

Roughly one hundred fish species inhabit the brackish waters of the Baltic Sea (HELCOM 2008a). As their distribution is mainly governed by salinity, composition of fish communities varies in different regions of the Baltic Sea in relation to different habitat characteristics like salinity, water temperature, oxygen content and availability of nutrients.

(HELCOM 2008a) states that “fish populations of the Baltic Sea are affected by fishing, eutrophication, oxygen depletion and high levels of hazardous substances, as well as by natural stresses such as cold winter temperatures and varying levels of salinity”. For the purpose of this report we will exemplarily provide a brief overview of pressures due to commercial fishing.

### 6.4.1 **Commercial fishing**

Between 1950 and 1970 new fishing methods, new nylon net materials, open sea fishery and trawling were developed and in the course of that Baltic Sea fish catches increased rapidly. The peak in cod fishery was achieved in the middle of the 1980s (HELCOM 2008b). A resulting collapse of Baltic cod stock beginning in the 1980s caused economic difficulties for small fishing communities and fish refining industry in the southern Baltic countries. Catches of clupeids (herring and sprat), cod and flatfish from 1909 to 2005 are shown in Fig. 6.4 below.

The number and size of trawlers has gradually increased in the Baltic Sea since the mid 20<sup>th</sup> century. More effective vessels using different techniques meant a less laborious and cost-effective fishery. With the decline in cod stock the number of Baltic fishing vessels and professional fishermen has continuously been decreasing since the 1990s, but retrieving and handling of ever bigger catches in the Baltic Sea is common due to more effective gear, bigger trawlers and tankers (HELCOM 2008b). The present annual level of total catch is approximately 700,000 t, about 90% of this total fish catch consist of herring, sprat, cod and flounder (HELCOM 2008c).

While the population structure for major commercial fish (cod, herring, sprat and salmon) is quite well studied and distinct stocks are identified, very little information is available for fish which are managed at national levels. Information on genetic population structure for most fish species is still lacking in the Baltic Sea, which hampers biologically sustainable use of the Baltic fish communities (HELCOM 2008c). To prevent a further decline of commercial stocks and enable a recovery of the populations, the European Commission has introduced catch quota, so-called Total Allowable Catches (TAC).

Fishing affects mainly the commercially important fish stocks, but it affects also the communities of benthic invertebrates and fish, marine mammals, seabirds and the abiotic environment. The main ecological effect of fishery is the removal of large quantities of target species (Helcom 2008d). Fishing decreases the density and stock biomass of target species and changes interactions of predators and prey. It removes bigger individuals which increases the survival and growth of the smaller individuals of the population.

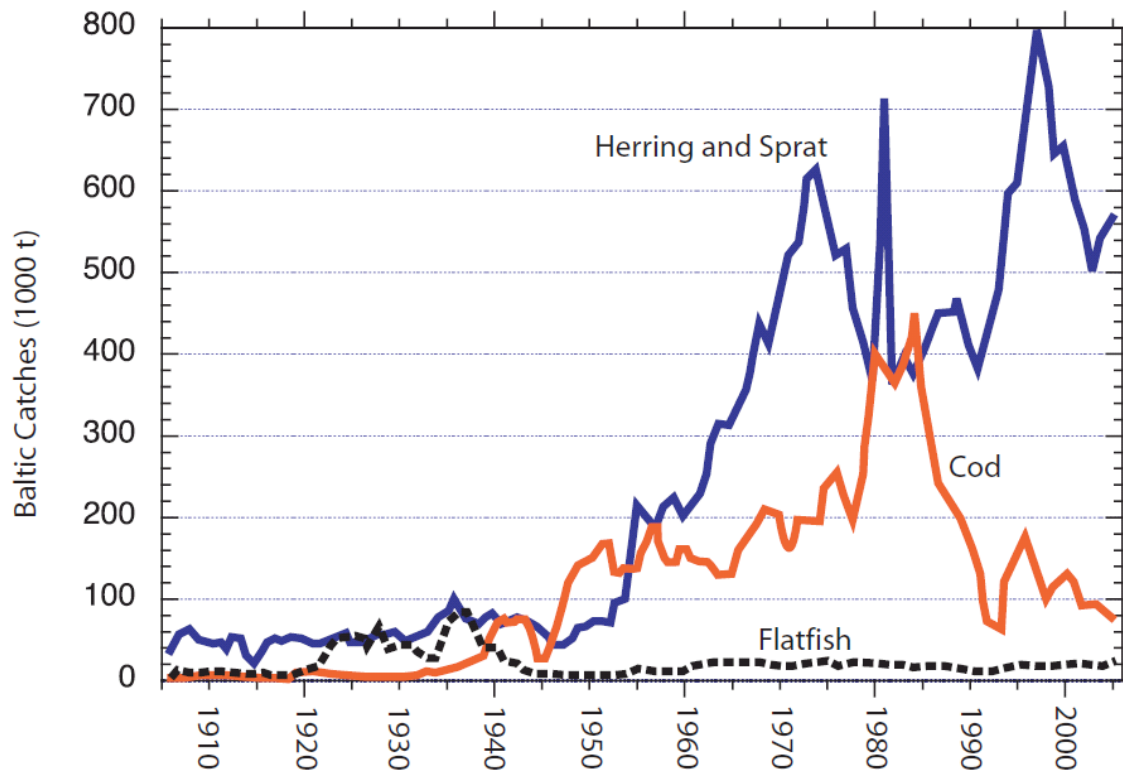


Fig. 6.4 Reported catches of clupeids (sprat and herring), cod and flatfish from 1909-2005 in kilotons, comprising catches from the Baltic Sea including Belt Sea catches in most cases. From (Hammer et al. 2008).

Bottom trawls are especially affecting marine biota (HELCOM 2008d): they reduce structural biota, alter the relative abundance of species and change the structure and ecology of the seabed and biota by dragging their nets and gear across the sea bottom. Only few studies are available in the Baltic Sea region on bottom trawling impacts on the marine ecosystem. (Rumohr and Krost 1991) documented that bottom trawling may cause damage to several species of thin-shelled bivalves and starfish. On the other hand, solid shelled bivalves or even more fragile *Macoma baltica* suffer little or survive well.

According to (HELCOM 2008d), unwanted by-catch is one of the main environmental effects of fishing. In March 2007 the European Commission issued a "Communication on a policy to reduce unwanted by-catch and eliminate discards in European fisheries" (EC 2007). It states that the rates of discards and by-catch of fish in the Baltic Sea fisheries is presently unknown, but studies indicate that the major Baltic commercial fisheries for cod, herring, and sprat have low discards and by-catch rate compared to other areas e.g. the North Sea. Estimates of discard for the two Baltic cod stocks are available since 1996 when the sampling was commenced. In the period 1996-2007, the western and eastern cod discards have fluctuated between 5.0-26.6 and 3.7-23.3 million of mainly juvenile cod individuals, respectively (Helcom 2008d). These estimates are however relatively uncertain (ICES 2008). The HELCOM Baltic Sea Action Plan urges that all caught species and by-catch which can not be released alive or without injuries should be landed and reported by 2012.



## **7 EXPECTED CLIMATE CHANGE**

### **7.1 Overview**

The Baltic Sea area is subject to global influences, such as those related to atmospheric circulation and temperature. In particular global emissions of greenhouse gases since the middle of the 20<sup>th</sup> century have been shown to account for a significant proportion of global warming during the past century. For this trend the term “climate change” has become common. However, climate change does not refer only to anthropogenic climate change, but is a broader term which includes any change in climate over time whether due to natural variability or as a result of human activity.

The Baltic Sea climate is embedded in the general atmospheric circulation system of the Northern hemisphere with mean westerly air flow of annually varying intensity. The strong westerly air flow provides maritime, humid air transport into the southwestern and southern parts of the Baltic Sea basin, while in the eastern and northern parts the maritime westerly air flow is weakened, providing continental climate conditions. There is a permanent exchange of air masses of different features resulting in a great variability of weather. The air pressure system formed by low pressure near Iceland and high pressure around the Azores Islands is known to affect the weather and circulation in the Baltic Sea basin. Furthermore, high/low pressure systems over Russia may influence the climate and circulation in the Baltic Sea basin, in particular in the north-eastern parts. These systems show a distinct annual cycle. In the autumn and winter season southwesterly air flow intensifies due to the amplifying Icelandic low pressure. During spring and summer Azores High extends into mid-Europe and the southwesterly air flow weakens.

The strength of the surface air pressure difference between the Icelandic Low and the Azores High, the North Atlantic Oscillation (NAO), has often been used to characterize circulation pattern and climatic variability over Northern Europe. It has been shown that the wintertime NAO is correlated with weather and circulation in the Baltic Sea basin, while the summertime NAO mostly not influences Baltic Sea weather.

The variability of the NAO has been quite large and irregularly over the last century. In Fig. 7.1 the winter NAO index (WNAOI) is shown. The WNAOI is the difference of the sea level pressure anomalies at Iceland and the Azores Islands in wintertime normalized by the standard deviations of the long term means. A high WNAOI refers to an enhanced pressure gradient and therefore to an accelerated westerly air flow to the Baltic Sea basin and vice versa. Consequently, a high WNAOI is correlated with mild and wet winter. A low WNAOI in 1950-1980 was associated with cold temperatures in the Baltic Sea basin; while an increasing NAO from 1990 results in mild winters (see Fig. 7.2).

The air temperature distribution over the Baltic Sea basin reflects the general circulation regimes, with a north-south temperature gradient controlled by the contrast of maritime and continental climate influence. The mean annual temperature differs by more than 10°C with the coldest regions in northeast Finland and the upper regions of Scandinavian mountains.

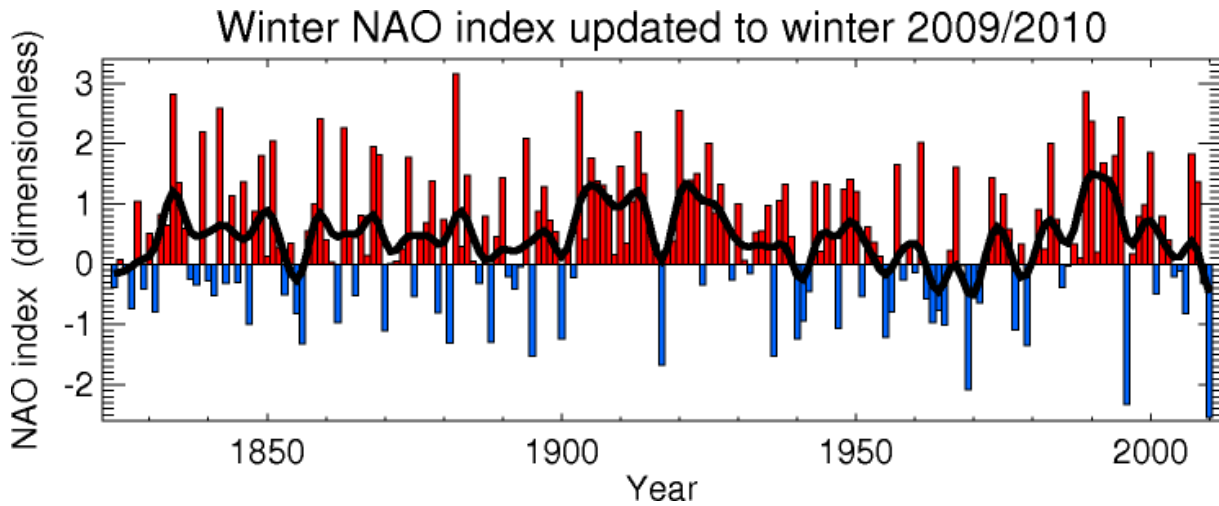
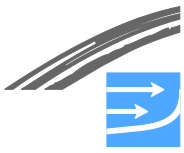


Fig. 7.1 Wintertime NAO index from 1820 to 2010. (Source: <http://www.cru.uea.ac.uk/~timo/datapages/naoi.htm>)

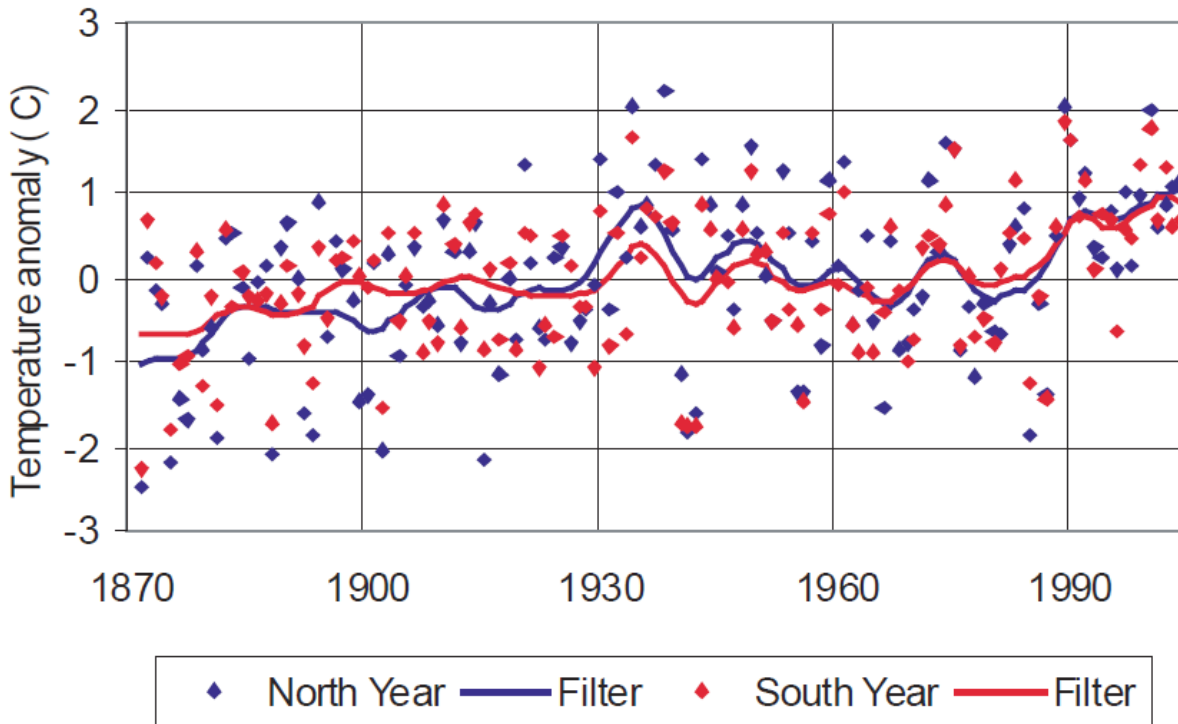
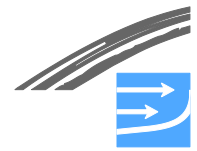


Fig. 7.2 Annual mean 2-m air temperature anomalies for the Baltic Sea 1871-2000, based on land stations. Blue colour relates to the area north of 60°N, and the red colour to the area south of that latitude. Dots represent individual years, while the smoothed curves highlight variability on a longer time scale. (Source: (HELCOM 2007b; BSEP No. 111))

The warming trend for the Baltic Sea basin in the last century is in the order of 0.08°C /decade (Fig. 7.2) and therefore larger than the global trend of 0.05°C /decade. A pronounced warming started around 1990 which is related to the accelerating global warming trend.

Climate change in the Baltic Sea basin is related to global climate change. Possible future development, climate projections, in the Baltic Sea basin are based on global models, scenarios, and data. Changes in the global climate can be driven by natural variability and as a response to anthropogenic forcing. Natural variability is due to



solar variability, volcano eruptions, and associated with internal dynamics of the earth's system. The most important anthropogenic force is the emission of greenhouse gases, and hence an increasing concentration of greenhouse gases in the atmosphere. Relevant anthropogenic greenhouse gases are carbon dioxide, methane, and nitrous oxide. Greenhouse gases reduce the transparency of the atmosphere for infrared (thermal) radiation, and as a result the heat budget of the earth's system changes with increasing temperature of the lower atmosphere. Estimates of different factors influencing the global climate suggest that the largest contribution to the observed warming in the last century is attributed to an increase in greenhouse gas concentration.

## 7.2 Future development

For the assessment of a future climate development global climate models together with emission scenarios are used. Different emission scenarios (SRES: IPCC special report on emission scenarios) have been developed by the IPCC (Intergovernmental Panel on Climate Change). The SRES scenarios follow four storylines, each based on different assumptions concerning the factors that might drive the development of human society during the next 100 years. The storylines A1 and A2 rely on a world where people strive after personal wealth rather than environmental quality, while for storylines B1 and B2 a sustainable development is assumed. Based on these storylines a number of emission scenarios have been developed which were be used by IPCC to force the global climate models.

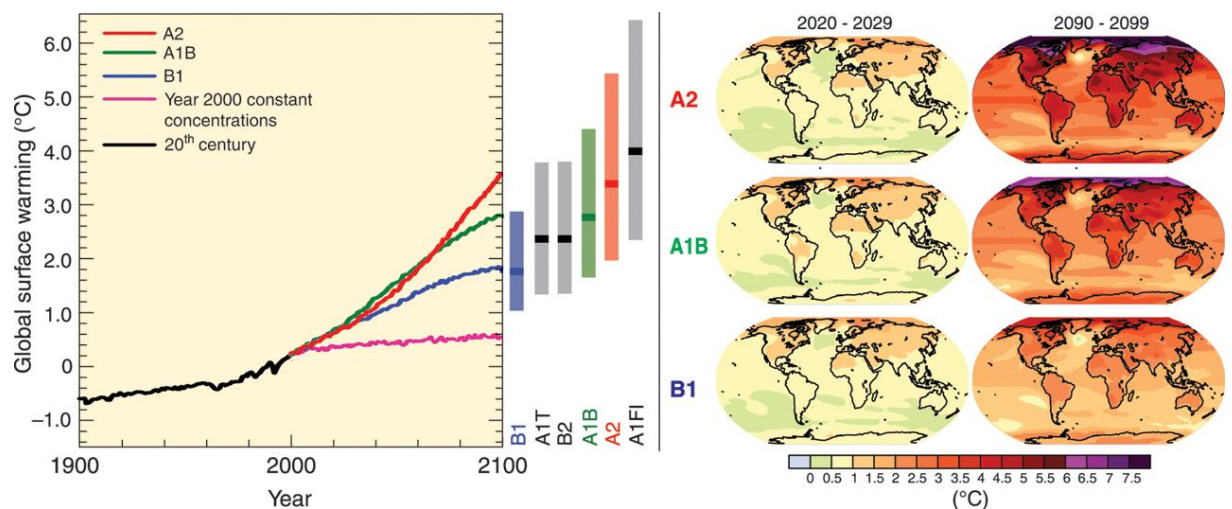


Fig. 7.3 Left panel: Multi-model global averages of surface warming (relative to 1980-1999) for SRES scenarios A2, A1B and B1. The orange line is for an experiment where concentrations were held constant at year 2000 values. Right panel: Projected surface temperature changes for the early and late 21th century relative to the period 1980-1999. (Source: IPCC Synthesis Report 2007)

Multi-model simulations of different SRES scenarios show an expected global warming of 2-4°C at the end of the century (Fig. 7.3). Scenarios of A1 and A2 storylines show a stronger warming than scenarios of B1 and B2 storylines. However, a changing climate will be felt at a regional scale and strategies for adaption and protection have to be based on regional climate. Regional climate will not necessarily scale with climate projections from global models due to the coarse spatial resolution (250 km) of today's global climate models. For this reason regional climate models (RCM) are used to assess regional climate change. These models cover a limited area of the globe and have a spatial resolution less than 20 km. At their boundaries they are driven by a global model and in the interior an own dynamics can develop.





In order to establish a basis for design of the Fixed Link across Fehmarnbelt between Denmark and Germany, Femern Bælt A/S decided moreover to engage the Danish Meteorological Institute (DMI) and Risø DTU representing Fehmarnbelt Hydrography Consortium (FEHY) and invite to a workshop on different aspects of climate change relevant for the design and operation of the Fixed Link, for details see (FEHY 2009).

For the Baltic Sea basin RCM simulations show a positive temperature trend of a little more than 1°C over the last century, in agreement with observations (FEHY 2009). In winter and spring the temperature increase is stronger compared to summertime in the northeastern part of the Baltic Sea basin and in the southwestern part the increase is stronger in summer. Furthermore, daily maximum temperature in summer will increase from 3°C up to 10°C. For precipitation the simulations show an increase in winter, while in summer projections show an increase in the northern part and a decrease in the southern part. Extreme precipitation events generally show an increase in winter.

Consequently, RCMs have been used to drive ocean models of the Baltic Sea. The sea ice season will decrease by 1-2 months in the northern part and 2-3 months in the central part of the Baltic Sea. The sea surface temperature will increase by 2-4°C and the increase would be strongest in May and June and in the southern and central basins.

In "Assesment of Climate Change for the Baltic Sea Basin" (The BACC Author Team 2008) it is stated that an increased winter runoff outweighs the drier summer periods, and recirculation is an issue in the projection runs discussed there. E.g. Meier et al. are cited with a 2006 study of 16 model runs where salinity changes range from +4% to -45% but the positive trend is not statistically significant. Overall salinity in the Baltic Sea is therefore projected to lower in the order of 2 g/kg (2 psu) (BACC 2008). On the other hand it is also said in that book that "the assumed projected future anthropogenic climate changed provide the greatest source of uncertainty for projected future hydrological changes" (BACC 2008). The FEHY workshop also found that a decrease in salinity is likely (FEHY 2009). But if one considers a projected rise in sea level of up to 1 m without changes in net freshwater input and wind signals, the hydraulic resistance in the Belt Sea will be lowered, so saline inflows at the bottom are increased. It is therefore not yet clear how the overall salinity of the Baltic Sea will develop due to anthropogenic climate change.

RCM based studies on climate change e.g. (BACC 2008) are based on time slice experiments. That means that RCMs are forced for limited time slices only, mainly a reference period 1970-1999 and a projection period 2070-2100. A reason for time slice experiments is the tremendous computational capacity necessary for running RCMs. Recently, transient RCM simulations became available covering the period 1960-2100 and can be used to force Baltic Sea models. Advantages of transient simulations are that they provide the development in time and (unknown) initial conditions for e.g. 2070 are not needed.

An example for a transient simulation is shown in Fig. 7.4. It depicts the development of sea ice coverage in the Baltic Sea based on two emission scenarios.

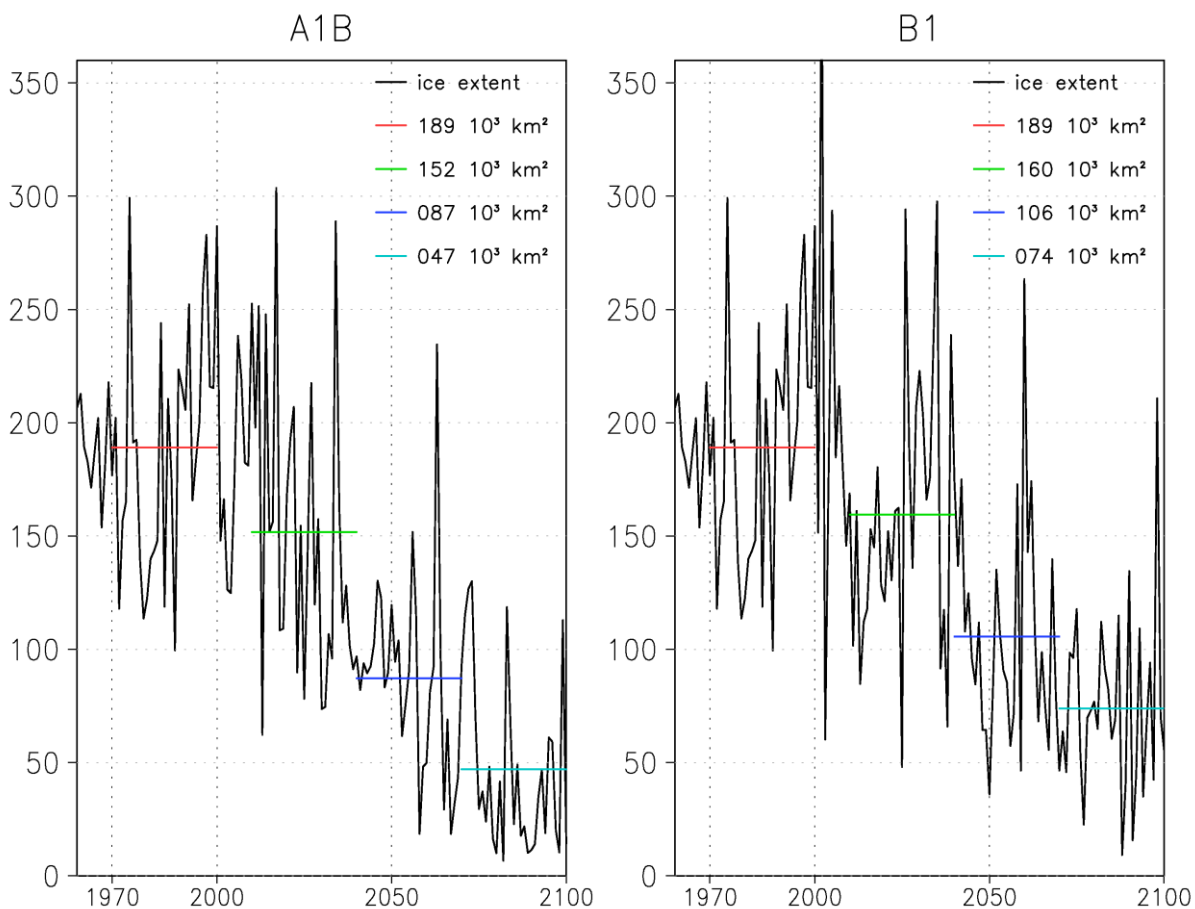


Fig. 7.4 Simulated maximum sea ice extent in the Baltic Sea for SRES scenarios A1B and B1. The black line is the annual maximum sea ice extent and colored lines show the 30 years mean. From (Neumann 2010).

Both scenarios show a decreasing sea ice extent with about 30% sea ice coverage of today's extent at the end of the century due to increasing temperature. Figure 7.5 shows the sea surface temperature (SST) trend in the Baltic Sea for scenarios A1B and B1 for different seasons. The warming is in the order of 2-3°C. Winter SST shows a tendency for stronger warming and SST in scenario B1 seems to stabilize at the end of the century.

Changes in sea surface salinity (SSS) are shown in Fig. 7.6. Both scenarios show a clear trend towards decreasing salinities in the order of 1.5–2 psu. Main reason for salinity decrease is an increasing freshwater supply. To a minor degree increased wind speed also contributes to decreasing salinity. Differences between emission scenarios A1B and B1 are small due to the freshwater changes in both scenarios do not differ significantly. The winter season shows a stronger signal caused by an enhanced runoff in winter in a warmer climate. However, absolute numbers of a SSS decrease are relatively uncertain because the freshwater budget in climate simulations bears a wide spread.

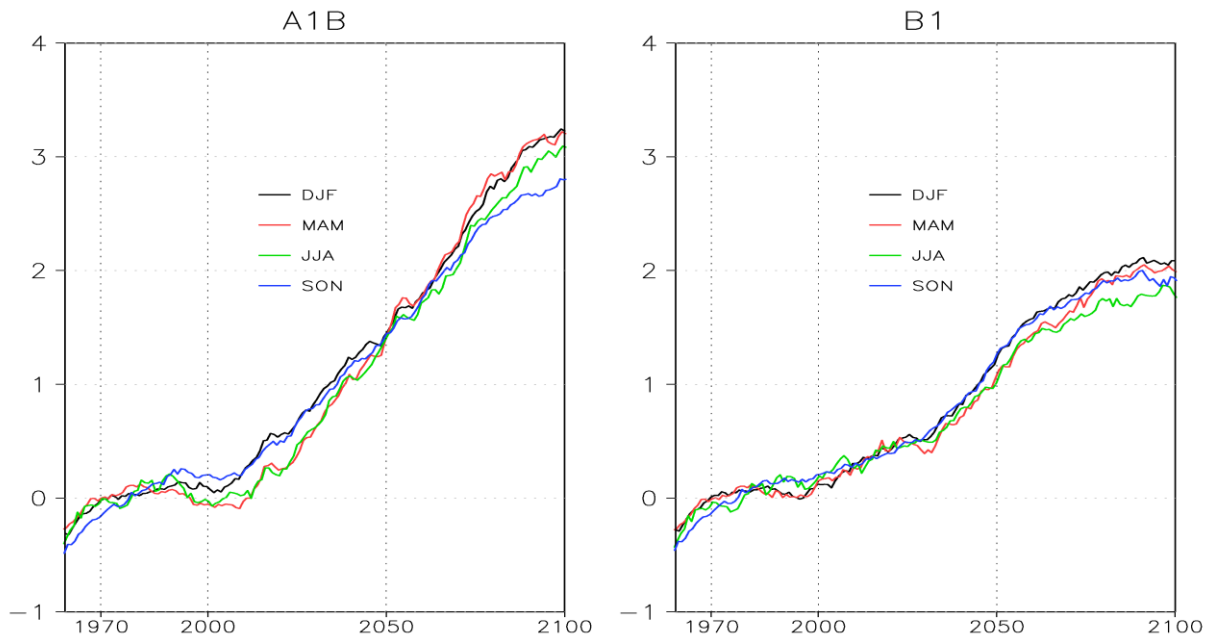


Fig. 7.5 SST (sea surface temperature) warming [K] in the Baltic Sea for emission scenarios A1B and B1. Shown is horizontally averaged SST for winter (DJF), spring (MAM), summer (JJA) and fall (SON) seasons smoothed with a 30 years running mean. From (Neumann 2010).

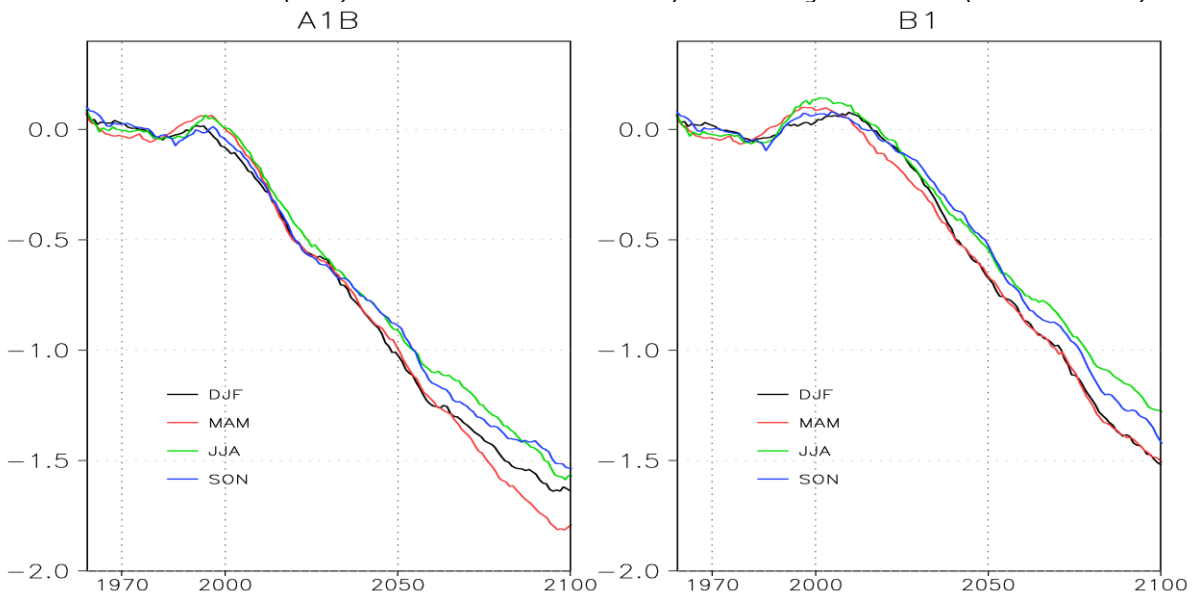


Fig. 7.6 SSS (sea surface salinity) change [g/kg] in the Baltic Sea for emission scenarios A1B and B1. Shown is horizontally averaged SSS for winter (DJF), spring (MAM), summer (JJA) and autumn (SON) seasons smoothed with a 30 years running mean. From (Neumann 2010).

Changes in the environmental conditions like temperature and salinity will impact the habitat conditions for many species in the Baltic Sea. This may result in changing distribution patterns and abundances. Details of these simulations are presented in (Neumann 2010).

However, uncertainties in climate projections are large. A main reason is that the development of the human society bears much insecurity (IPCC storylines). Another source of uncertainties are the models itself which mainly differ in parameterization details and resolution. Consequently, more simulations are needed to increase the number of ensemble members to provide a sound probabilistic approach.



Most of the above projections for climate change are also assumed representative for the outer part of the Baltic Sea, including Fehmarnbelt and the rest of the Belt Sea area. However, the impact to salinity may be reduced due to the closer proximity to the ocean, where the salinity not is expected to change.



## 8 REFERENCES

### 8.1 Literature

- Aarup T. (2002): Transparency of the North Sea and Baltic Sea – a Secchi depth data mining study. *Oceanologia*, **44** (3), 323–337.
- Aertjeberg G., Andersen J.H., Hansen O.S. (2003): Nutrients and eutrophication in Danish marine waters. – Ministry of Environment. National Environmental Research Institute, 126pp.
- Aitsam A., Hansen H.-P., Elken J., Kahru M., Laanemets J., Pajuste M., Pavelson J., Talpsepp L. (1984): Physical and chemical variability of the Baltic Sea: a joint experiment in the Gotland Basin. *Continental Shelf Research*, **3** (3), 291-310.
- Alenius A., Myrberg K., Nekrasov A. (1998): The physical oceanography of the Gulf of Finland: a review. *Boreal Environment Research*, **3**, 97-125.
- Andersson A., Hajdu S., Haecky P., Kuparinen J., Wikner J. (1996): Succession and growth limitation of phytoplankton in the Gulf of Bothnia (Baltic Sea). *Marine Biology*, **126**, 791-801.
- Aneer G., Höglander H. (2005): Report on the conditions of the coastal and offshore waters of the Baltic Proper. Information Office for the Baltic Proper, County Administrative Board of Stockholm, 7 September 2005, Information 9/05.
- Apel J.R. (1988): *Principles of Ocean Physics*. 5<sup>th</sup> ed., Academic Press.
- Arneborg L., Fiekas V., Umlauf L., Burchard H. (2007): Gravity current dynamics and entrainment - a process study based on observations in the Arkona Basin, *Journal of Physical Oceanography*, **37**, 2094-2113.
- Axell L.B. (1998): On the variability of the Baltic Sea deepwater mixing. *Journal of Geophysical Research*, **103** (C10), 21667-21682.
- Axell L.B. (2002): Wind-driven internal waves and Langmuir circulations in a numerical ocean model of the southern Baltic Sea. *Journal of Geophysical Research*, **107** (C11).
- The BACC Author Team (2008): *Assessment of Climate Change for the Baltic Sea Basin*. Springer, Berlin
- Bartnicki J., Gusev A., Aas W., Fagerli H. (2007): Atmospheric Supply of Nitrogen, Lead, Cadmium, Mercury and Dioxines/Furanes to the Baltic Sea in 2005. In: EMEP Centres Joint Report for HELCOM, [http://www.helcom.fi/stc/files/environment/EMEP\\_2005/Chapter3\\_nitrogen.pdf](http://www.helcom.fi/stc/files/environment/EMEP_2005/Chapter3_nitrogen.pdf)
- Bartnicki J., Valiyaveetil S. (2008): Estimation of atmospheric nitrogen deposition to the Baltic Sea in the periods 1997-2003 and 2000-2006. Summary report for HELCOM, Meteorological Synthesizing Centre-West (MSC-W) of EMEP, Oslo, 1-80.
- Bartnicki J. (2009): Atmospheric nitrogen depositions to the Baltic Sea during 1995-2007. HELCOM indicator fact sheet. [http://www.helcom.fi/environment2/ifs/ifs2009/en\\_GB/n\\_deposition/](http://www.helcom.fi/environment2/ifs/ifs2009/en_GB/n_deposition/)



- Bebber W.J. van (1891): Die Zugstraßen der barometrischen Minima nach den Bahnenkarten der Deutschen Seewarte für den Zeitraum 1875-1890. Meteorologische Zeitschrift, **8**, 361-366.
- Bergström S. (1976): Development and application of a conceptual runoff model for Scandinavian catchments. Doctoral thesis, Department of Water Resources Engineering, Lund Institute of Technology, Lund University, Lund, Sweden, 134pp.
- Bergström S., Carlsson B. (1993): Hydrology of the Baltic Basin – Inflow of fresh water from rivers and land for the period 1950-1990. SMHI Reports Hydrology, **7**, 21 pp.
- Bergström S., Carlsson B. (1994): River Runoff to the Baltic Sea 1950-1990. Ambio, **23** (4-5), 180-287.
- Björck S. (1995): A Review of the History of the Baltic Sea, 13.0-8.0 ka BP. Quaternary International, **27**, 19-40.
- Bo Pedersen F., Møller J.S. (1981): Diversion of the river Neva. Nordic Hydrology, **12**, 1-20.
- Bruns E. (1955): Handbuch der Wellen der Meere und Ozeane. VEB Deutscher Verlag der Wissenschaften, Berlin, 255 pp.
- Bruns, E. (1963): Forschungen und theoretische Berechnungen zur Ausarbeitung von Methoden der Seegangs- und Wellenvorhersage für die westliche Ostsee und die Küstengebiete der DDR, IfM Warnemünde, 36 pp., unpublished.
- Burchard H., Janssen F., Bolding K., Umlauf L., Rennau H. (2009): Model simulations of dense bottom currents in the Western Baltic Sea, Continental Shelf Research, **29** (1), 205-220.
- Carlsson B., Sanner H. (1994): Influence of river regulation on runoff to the Gulf of Bothnia. SMHI Reports Hydrology, 9, 30 pp.
- Christensen F.T., Skourup J. (1991): Extreme Ice Properties. ASCE Journal of Cold Regions Engineering, **5** (2), 51-68.
- Colding A. (1881) Nogle Undersøgelser over Stormen over Nord- og Mellem-Europa af 12te-14te November 1872 og over den derved fremkaldte Vandflod i Østersøen. Bianco Lunos Kgl. Hof-Bogtrykkeri, Copenhagen.
- Dickson R.R. (1971): A recurrent and persistent pressure anomaly pattern as the principle cause of intermediate scale hydrographic variation in the European shelf seas. Deutsche Hydrographische Zeitschrift, **24**, 97-119.
- Döös K., Meier H.E.M., Döscher R. (2004): The Baltic Haline Conveyor Belt or The Overturning Circulation and Mixing in the Baltic. Ambio, **33** (4-5), 261-266.
- EC (1991): Council Directive of 21 May 1991 concerning urban waste water treatment (91/271/EEC). Official Journal L 135.
- EC (2007): A policy to reduce unwanted by-catches and eliminate discards in European fisheries. European Commission, COM(2007) 136 final.





- Elmgren R. (1984): Trophic dynamics in the enclosed, brackish Baltic Sea. *Rapports et Procès-verbaux des Reunions. Conseil International pour l'Exploration de la Mer*, **183**, 152-169.
- Elmgren R. (1989): Man's impact on the ecosystem of the Baltic Sea: Energy flows today and at the turn of the century. *Ambio* 18: 326-332.
- Elmgren R., Larsson U. (1997): Himmerfjärden: changes of a nutrient-enriched coastal ecosystem in the Baltic Sea, Swedish Environmental Protection agency. Report 4565 (1997), 197 pp.
- Erm A., Soomere T. (2004): Influence of fast ship waves on optical properties of sea water in Tallinn Bay, Baltic Sea. *Proceedings of the Estonian Academy of Sciences. Biology, Ecology*, **53**, 161-178.
- Erm A., Soomere T. (2006): The impact of fast ferry traffic on underwater optics and sediment resuspension. *Oceanologia*, **48** (S), 283-301.
- EUTROSYM (1976): UNEP-Symposium on eutrophication and restoration of surface waters. Karl-Marx-Stadt, 20.-25.09.1976, Vol. 1, Part 1.2.
- FEHY (2009): Climate Change and the Fehmarnbelt Fixed Link. DHI/IOW Consortium in association with LICEngineering, Bolding & Burchard and Risø DTU.
- FEHY (2013a): Fehmarnbelt Fixed Link. Marine Water- Baseline. Hydrography of the Fehmarnbelt Area. Report No. E1TR0057 Vol II. DHI/IOW Consortium in association with LICEngineering, Bolding & Burchard and Risø DTU.
- FEHY (2013b): Fehmarnbelt Fixed Link. Marine Water- Impact Assessment. Hydrography of the Fehmarnbelt Area. Report No. E1TR0059 Vol II. DHI/IOW Consortium in association with LICEngineering, Bolding & Burchard and Risø DTU.
- FEHY (2013c): Fehmarnbelt Fixed Link. Marine Water- Impact Assessment. Hydrography, Water Quality and Plankton of the Baltic Sea. Report No. E1TR0058 Vol I. DHI/IOW Consortium in association with LICEngineering, Bolding & Burchard and Risø DTU.
- Feistel R., Nausch G., Mohrholz V., Lysiak-Pastuszek E., Seifert T., Matthäus W., Krüger S., Sehested Hansen I. (2003a): Warm waters of summer 2002 in the deep Baltic Proper. *Oceanologia*, **45** (4), 571–592.
- Feistel R., Matthäus W. (2003b): Temporal and spatial evolution of the Baltic deep water renewal in spring 2003. *Oceanologia*, **45** (4), 623–642.
- Feistel R., Nausch G., Hagen E. (2006): Unusual Baltic inflow activity in 2002-2003 and varying deep-water properties. *Oceanologia*, **48** (S), 21-35.
- Feistel R., Nausch G., Wasmund N. (Eds., 2008): State and evolution of the Baltic Sea, 1925-2005. John Wiley & Sons.
- Feistel R., Feistel S., Nausch G., Szaron J., Łysiak-Pastuszek E., Ærtebjerg G. (2008a): BALTIC: Monthly time series 1900 – 2005. In: Feistel R., Nausch G., Wasmund N. (Eds.): State and evolution of the Baltic Sea, 1925-2005. John Wiley & Sons, 311-336.



- Feistel R. (2010): Faktenblatt zur Sauerstoffsituation am Boden der Ostsee. IOW, <http://www.io-warnemuende.de/sauerstoff.html>
- Fennel W., Seifert T., Kayser B. (1991): Rossby radii and phase speeds in the Baltic Sea. *Continental Shelf Research*, **11**, 23-36.
- Fennel W., Sturm M. (1992): Dynamics of the western Baltic. *Journal of Marine Systems*, **3** (1-2), 183–205.
- Fennel W., Seifert T. (1995): Kelvin wave controlled upwelling in the western Baltic. *Journal of Marine Systems*, **6**, 289-300.
- Fennel W., Mutzke A. (1997); The initial evolution of a buoyant plume. *Journal of Marine Systems*, **12**, (1-4), 53-68.
- Fennel W., Gilbert D., Jilan S. (2008): Physical Processes in Semi-Enclosed Marine Systems. In: Urban E.R. Jr., Sundby B., Malanotte-Rizzoli P., Melillo J.M. (2008): *Watersheds, Bays and Bounded Seas*. Island Press, Scientific Committee on Problems of the Environment (SCOPE) Series, **70**.
- Fennel W., Radtke H., Schmidt M., Neumann T. (2010): Transient upwelling in the central Baltic Sea. *Continental Shelf Research*, submitted.
- FEMA (2010): Plankton flora and fauna of the Greater Fehmarnbelt: Preliminary Baseline Analysis. Fehmarnbelt Fixed Link Marine Biology Service.
- Feser F., Weisse R., von Storch H. (2001): Multidecadal atmospheric modelling for Europe yields multi-purpose data. *EOS*, **82**, 305-310.
- Finni T., Kononen K., Olsonen R., Wallström K. (2001): The history of cyanobacterial blooms in the Baltic Sea. *Ambio*, **30**, 172–178.
- Fonselius S. (1969): Hydrography of the Baltic deep basins. III. Fishery Board of Sweden, *Hydrography* 23, 1-97.
- Gasiunaite Z.R., Cardoso A.C., Heiskanen A-S., Henriksen P., , Kauppila P., Olenina I., Pilkaityte R., Purina I., Razinkovas A., Sagert S., Schubert H., Wasmund N. (2005): Seasonality of coastal phytoplankton in the Baltic Sea: Influence of salinity and eutrophication. *Estuarine, Coastal and Shelf Science*, **65**, 239-252.
- Gerstengarbe F.-W., Werner P.C. (2005): catalog der Grosswetterlagen Europas (1881-2004). PIK Report No. 100, Potsdam Institute for Climate Impact Research, 148 pp.
- Gibbard P.L., Rose J., Bridgland D.R. (1988): The History of the Great Northwest European Rivers During the Past Three Million Years [and Discussion]. *Philosophical Transactions of the Royal Society*, **318**, 559-602.
- Gorny V.I., Kritsuk S.G, Latypov I.Sh., Tronin A.A., Shilin B.V. (2000): Estimation of nuclear power plants influence on the Baltic Sea thermal state by using infrared thermal satellite data. *International Journal of Remote Sensing*, **21** (12), 2479-2496
- Graham P. (2000): Large-scale hydrologic modeling in the Baltic Basin. Doctoral thesis, Division of Hydraulic Engineering, Department of Civil and Environmen-



tal Engineering, Royal Institute of Technology, Stockholm, Sweden, 55 pp. and 5 reprinted papers.

- Graneli E., Wallström K., Larsson U., Graneli W., Elmgren R. (1990): Nutrient limitation of primary production in the Baltic Sea area. *Ambio* 19, 142–151.
- Green, M., Stigebrandt, A. (2002): Instrument-induced linear flow resistance in Öresund. *Continental Shelf Research*, **22** (3), 435-444.
- Gregg M.C. (1989): Scaling turbulent dissipation in the thermocline. *Journal of Geophysical Research*, **94** (C7), 9686-9698.
- Håkansson L., Lindgren D. (2008): On regime shifts in the Baltic Proper – evaluations based on extensive data between 1974 and 2005. *Journal of Coastal Research*, **24** (3), 246-260.
- Hagen E., Feistel R. (2001): Spreading of Baltic Deep Water: A Case Study for the Winter 1997–1998. *Meereswissenschaftliche Berichte*, **45**, 99-133.
- Hagen E., Feistel R. (2004): Observation of low-frequency current fluctuations in deep water of the Eastern Gotland Basin/Baltic Sea. *Journal of Geophysical Research*, **109** (C03044).
- Hagen E., Feistel R. (2007): Synoptic changes in the deep rim current during stagnant hydrographic conditions in the Eastern Gotland Basin, Baltic Sea. *Oceanologia*, **49** (2), 185–208.
- Hajduk J. (2009): Shipping Routes in the Southern Baltic and Vessel Traffic Safety. *Marine Traffic Engineering Conference*, Malmö, 19-22 November 2009.
- Hammer C., von Dorrien C., Ernst P., Gröhsler T., Köster F., MacKenzie B., Möllmann C., Wegner G., Zimmermann C. (2008): Fish Stock Development under Hydrographic and Hydrochemical Aspects, the History of Baltic Sea Fisheries and its Management. In: Feistel R., Nausch G., Wasmund N. (Eds.): *State and evolution of the Baltic Sea, 1925-2005*. John Wiley & Sons, 543-573.
- Hansson, M. (2004-2008): Cyanobacterial blooms in the Baltic Sea. HELCOM Indicator Fact Sheets 2004-2008. Online.  
[http://www.helcom.fi/environment2/ifs/en\\_GB/cover/](http://www.helcom.fi/environment2/ifs/en_GB/cover/)
- Hansson, M., Öberg, J. (2009): Cyanobacterial blooms in the Baltic Sea. HELCOM Indicator Fact Sheets 2009. Online.  
[http://www.helcom.fi/environment2/ifs/en\\_GB/cover/](http://www.helcom.fi/environment2/ifs/en_GB/cover/)
- HELCOM (1986): Water balance of the Baltic Sea. *Baltic Sea Environment Proceedings* No.16.
- HELCOM (1996): Third periodic assessment of the state of the marine environment of the Baltic Sea, 1989-1993; background document. *Baltic Sea Environment Proceedings* No. 64B, 1-252.
- HELCOM (2002): Environment of the Baltic Sea area 1994-1998. *Baltic Sea Environment Proceedings* No. 82B, 218pp.



- HELCOM (2006): Division of the Baltic and adjacent waters. Manual for Marine Monitoring in the COMBINE Programme of HELCOM, Part A.  
[http://www.helcom.fi/groups/monas/CombineManual/PartA/en\\_GB/main/](http://www.helcom.fi/groups/monas/CombineManual/PartA/en_GB/main/)
- HELCOM (2007a): Manual for Marine Monitoring in the COMBINE Programme of HELCOM Annex C-6 last update 2007,  
[http://www.HELCOM.fi/groups/monas/CombineManual/AnnexesC/en\\_GB/annex6](http://www.HELCOM.fi/groups/monas/CombineManual/AnnexesC/en_GB/annex6)
- HELCOM (2007b) Climate Change in the Baltic Sea Area – HELCOM Thematic Assessment in 2007. Baltic Sea Environment Proceedings No. 111.
- HELCOM (2008a): Introduction to fish and fisheries in the Baltic Sea.  
[http://www.helcom.fi/environment2/biodiv/fish/en\\_GB/intro/](http://www.helcom.fi/environment2/biodiv/fish/en_GB/intro/) Last updated: 3 December 2008
- HELCOM (2008b): A historic view of Baltic fisheries.  
[http://www.helcom.fi/environment2/biodiv/fish/en\\_GB/history/](http://www.helcom.fi/environment2/biodiv/fish/en_GB/history/) Last updated: 4 December 2008
- HELCOM (2008c): Commercial Fisheries and the management of the Baltic stock.  
[http://www.helcom.fi/environment2/biodiv/fish/en\\_GB/commercial\\_fisheries/](http://www.helcom.fi/environment2/biodiv/fish/en_GB/commercial_fisheries/) Last updated: 10 December 2008
- HELCOM (2008d): Fisheries effects on the Baltic ecosystem.  
[http://www.helcom.fi/environment2/biodiv/fish/en\\_GB/effects/](http://www.helcom.fi/environment2/biodiv/fish/en_GB/effects/) Last updated: 4 December 2008
- HELCOM (2009a): Eutrophication in the Baltic Sea – An integrated assessment of the effects of nutrient enrichment in the Baltic Sea region. Executive Summary. Baltic Sea Environmental Proceedings, No. 115A.
- HELCOM (2009b): Eutrophication in the Baltic Sea – An integrated assessment of the effects of nutrient enrichment in the Baltic Sea region. Baltic Sea Environment Proceedings, No. 115B.
- HELCOM (2009c): Total and regional Runoff to the Baltic Sea. HELCOM Indicator Fact Sheets,  
[http://www.helcom.fi/BSAP\\_assessment/ifs/ifs2009/en\\_GB/Runoff](http://www.helcom.fi/BSAP_assessment/ifs/ifs2009/en_GB/Runoff).
- HELCOM (2009d): QuantAS Consortium presents its research findings: Offshore wind farms have no relevant impact on the water exchange between North Sea and Baltic Sea. IOW Press release, 12 October 2009.  
[http://www.helcom.fi/press\\_office/news\\_baltic/en\\_GB/BalticNews380902/](http://www.helcom.fi/press_office/news_baltic/en_GB/BalticNews380902/)
- HELCOM (2009e): Overview of the Shipping Traffic in the Baltic Sea.  
[http://www.helcom.fi/stc/files/shipping/Overview%20of%20ships%20traffic\\_updateApril2009.pdf](http://www.helcom.fi/stc/files/shipping/Overview%20of%20ships%20traffic_updateApril2009.pdf)
- HELCOM (2009f): Atmospheric nitrogen depositions to the Baltic Sea during 1995-2007. HELCOM Indicator Fact Sheets 2009,  
[http://www.helcom.fi/environment2/ifs/en\\_GB/cover/](http://www.helcom.fi/environment2/ifs/en_GB/cover/).
- HELCOM (2010a): Ecosystem health of the Baltic Sea in 2003–2007 – HELCOM Initial Holistic Assessment. Baltic Sea Environment Proceedings, No. 122.



- HELCOM: (2010b): Fifth pollution load compilation. Baltic Sea Environment Proceedings, in press.
- HELCOM (2010c): Hazardous substances in the Baltic Sea - An integrated thematic assessment of hazardous substances in the Baltic Sea. Executive Summary. Baltic Sea Environment Proceedings, No. 120A
- HELCOM (2010d): The nature of the Baltic Sea.  
[http://www.helcom.fi/environment2/nature/en\\_GB/nature/](http://www.helcom.fi/environment2/nature/en_GB/nature/)
- HELCOM (2010e): Fifth Baltic Sea Pollution Load Compilation 5 (PLC-5). In preparation. [http://www.helcom.fi/projects/on\\_going/en\\_GB/plc-5/](http://www.helcom.fi/projects/on_going/en_GB/plc-5/)
- Heney E.S. , Wright J., Flatte S.M. (1986): Energy and action through the internal wave field: an eikonal approach. *Journal of Geophysical Research*, **91** (C7), 8487-8495
- Hille S., Nausch G., Leipe T. (2005): Sedimentary deposition and reflux of phosphorus (P) in the eastern Gotland Basin and their coupling with the water column P concentrations. *Oceanologia*, **47**, 1-17.
- Högländer H., Larsson U., Hajdu S. (2004): Vertical distribution and settling of spring phytoplankton in the offshore NW Baltic Sea proper. *Marine Ecology Progress Series*, 283, 15-27
- Hübel H., Hübel M. (1995): Blaualgen-Wasserblüten in der Ostsee: Ursachen - Ausmaß - Folgen. *Deutsche Hydrographische Zeitschrift*, Suppl. 2, 151-158.
- ICES (2008). Overview report on Baltic Sea.  
<http://www.ices.dk/committe/acom/comwork/report/2008/2008/8%201-8%202%20Baltic%20ecosystem%20overview.pdf>
- ICES (2010): HELCOM data. ICES Oceanographic Database and Services, <http://www.ices.dk/Ocean/index.asp>
- ICOADS (2010): International Comprehensive Ocean-Atmosphere Data Set. <http://dss.ucar.edu/datasets/ds540.0>
- IPCC, Intergovernmental Panel on Climate Change (2007): Climate Change 2007: Synthesis Report.  
[http://www.ipcc.ch/pdf/assessment-report/ar4/syr/ar4\\_syr.pdf](http://www.ipcc.ch/pdf/assessment-report/ar4/syr/ar4_syr.pdf).
- Jaanus A., Andersson A., Hajdu S., Huseby S., Jurgensone I., Olenina, I., Wasmund N., Toming K. (2007): Shifts in the Baltic Sea summer phytoplankton communities in 1992-2006. HELCOM Indicator Fact Sheets 2007, [http://www.helcom.fi/BSAP\\_assessment/ifs/archive/ifs2007/en\\_GB/Phytoplankton/](http://www.helcom.fi/BSAP_assessment/ifs/archive/ifs2007/en_GB/Phytoplankton/)
- Jacobsen T.S. (1980): Sea water exchange of the Baltic, measurements and methods. The Belt project. The National agency of Environmental Protection, Denmark, 106 pp.
- Jakobsen Fl. (1995). The Major Inflow to the Baltic Sea during January 1993. *Journal of Marine Systems*, **6** (3), 227-240.
- Jakobsen Fl. (1996): The dense water exchange of the Bornholm Basin in the Baltic Sea. *German Journal of Hydrography*, **48** (2), 133-145.



- Jakobsen Fl. (1997): Hydrographic investigation of the Northern Kattegat front. *Continental Shelf Research*, **17** (5), 533-554.
- Jakobsen Fl. (2000). The wind influence on the Jutland Coastal Current interpreted on the basis of some observations. *Nordic Hydrology*, **31** (2), 127-148.
- Jakobsen Fl., Petersen N.H., Petersen H.M., Møller J.S., Schmidt T., Seifert T. (1996): Hydrographic investigations in the Fehmarn Belt in connection with the planning of the Fehmarn Belt link. In: Proceedings of the Baltic Marine Science Conference 1996 (Rønne, Denmark), 10 pp. Published in ICES Cooperative Research Report 257, 2003, 179-189.
- Jakobsen Fl., Lintrup M.J., Møller J.S. (1997a): Observations of the specific resistance in Øresund. *Nordic Hydrology*, **28** (3), 217-232.
- Jakobsen Fl., Ottavi J. (1997b). Transport through the contraction area in the Little Belt. *Estuarine, Coastal and Shelf Science*, **45** (6), 759-767.
- Jakobsen Fl., Trébuchet C. (2000): Observations of the transport through the Belt Sea and an investigation of the momentum balance. *Continental Shelf Research*, **20**, 293-311.
- Jakobsen Fl., Hansen I.S., Hansen N.-E.O., Østrup-Rasmussen F. (2010): Flow resistance in the Great Belt, the biggest strait between the North Sea and The Baltic Sea. *Estuarine, Coastal and Shelf Science*, **87**, 325-332.
- Jansson B.O., Dahlberg K. (1999): The environmental status of the Baltic Sea in the 1940s, today and in future. *Ambio*, **28**, 312-319.
- Jerlov N.G. (1976): *Marine Optics*, Elsevier.
- Jochem F., Babenerd B. (1989): Naked *Dictyocha speculum* - a new type of phytoplankton bloom in the Western Baltic. *Marine Biology*, **103**, 373-379.
- Kahru M., Horstmann U., Rud O. (1994): Satellite detection of increased cyanobacteria blooms in the Baltic Sea: natural fluctuations or ecosystem change? *Ambio*, **23**, 469-472.
- Kahru M., Aitsam A., Elken J. (1982): Spatio-temporal dynamics of chlorophyll in the open Baltic Sea. *Journal of Plankton Research*, **4**, 779-790.
- Kaiser W., Renk H., Schulz S. (1981): *Die Primärproduktion der Ostsee*. Geodätische und Geophysikalische Veröffentlichungen, IV **33**, 27-52.
- König J. (2004): Wassermassenaustausch durch den Fehmarnbelt. Diploma thesis, University of Kiel, unpublished.
- Kononen K. (1992): *Dynamics of the toxic cyanobacterial blooms in the Baltic Sea*. Finnish Marine Research, **261**, 3-36.
- Köuts T., Omstedt A. (1993): Deep water exchange in the Baltic Proper. *Tellus*, **45** (4), 311-324.
- Krauss W. (1981): The Erosion of a Thermocline, *Journal of Physical Oceanography*, **11**, 415-433.





- Krauss W., Brüggge B. (1991): Wind-Produced Water Exchange between the Deep Basins of the Baltic Sea. *Journal of Physical Oceanography*, **21**, 373-384.
- Kronsell J, Andersson P. (2010): Total and regional Runoff to the Baltic Sea. HELCOM Indicator Fact Sheets 2010. [http://www.helcom.fi/BSAP\\_assessment/ifs/ifs2010/en\\_GB/Runoff/](http://www.helcom.fi/BSAP_assessment/ifs/ifs2010/en_GB/Runoff/)
- Laamanen M., Kuosa H. (2005): Annual variability of biomass and heterocysts of the N<sub>2</sub>-fixing cyanobacterium *Aphanizomenon flos-aquae* in the Baltic Sea with reference to *Anabaena* sp and *Nodularia spumigena*. *Boreal Environment Research*, **10** (1), 19-30.
- Larsson U., Elmgren R., Wulff F. (1985): Eutrophication and the Baltic Sea: causes and consequences. *Ambio*, **14**, 9-14.
- Lass H.U., Schwabe R., Matthäus W., Francke E., (1987). On the dynamics of water exchange between Baltic and North Sea. *Beiträge zur Meereskunde*, **56**, 27-49.
- Lass H.U., Mohrholz V. (2003): On dynamics and mixing of inflowing saltwater in the Arkona Sea. *Journal of Geophysical Research*, **108** (C2), 3042-3057.
- Lass H.U., Mohrholz V., Seifert T. (2005): On pathways and residence time of salt-water plumes in the Arkona Sea. *Journal of Geophysical Research*, **110** (C11019).
- Lass H.U., Matthäus W. (2008): General Oceanography of the Baltic Sea. In: Feistel R., Nausch G., Wasmund N. (Eds.): *State and evolution of the Baltic Sea, 1925-2005*. John Wiley & Sons, 5-43.
- Lass H.U., Mohrholz V., Knoll M., Prandke H. (2008): Enhanced mixing downstream of a pile in an estuarine flow. *Journal of Marine Systems*, **74** (1-2), 505-527.
- Lass H.U., Mohrholz V., Nausch G., Siegel H. (2010): On phosphate pumping into the surface layer of the eastern Gotland Basin by upwelling. *Journal of Marine Systems*, **80**, 71-89.
- Lehmann A., Krauss W., Hinrichsen H.-H. (2002): Effects of remote and local atmospheric forcing on circulation and upwelling in the Baltic Sea. *Tellus*, **54** (A), 299-316.
- Lehmann A., Myrberg K. (2008): Upwelling in the Baltic Sea - a review. *Journal of Marine Systems*, **74** (S1), S3-S12.
- Leppäranta M., Myrberg K. (2009): *Physical Oceanography of the Baltic Sea*. Springer.
- Lindau R. (2002): Energy and water balance of the Baltic Sea derived from merchant ship observations. *Boreal Environment Research*, **7**, 417-424.
- Lintrup M.J., Jakobsen F. (1999). The importance of Öresund and the Drogden Sill for Baltic inflow. *Journal of Marine Systems*, **18** (4), 345-354.
- Lisitzin E. (1943): Die Gezeiten des Bottnischen Meerbusens. *Fennia*, **67** (4), 1-47.
- Lisitzin E. (1944): Die Gezeiten des Bottnischen Meerbusens. *Fennia*, **68** (2), 3-19.



- Macqueen J.F. (1980): Concentration of contaminants discharged with power station cooling water. *Advances in Water Resources*, **3**, 165-172.
- Magaard L., Krauss W. (1966): Spektren der Wasserstandsschwankungen der Ostsee im Jahre 1958. *Kieler Meeresforschungen*, **22**, 155-162.
- Matthäus W. (1978): Zur mittleren jahreszeitlichen Veränderlichkeit im Sauerstoffgehalt der offenen Ostsee. *Beiträge zur Meereskunde*, **41**, 61-94.
- Matthäus W., Schinke H. (1994): Mean atmospheric circulation patterns associated with major Baltic inflows. *Deutsche Hydrographische Zeitschrift*, **46**, 321-339.
- Matthäus W., Lass H.U. (1995): The recent salt inflow into the Baltic Sea. *Journal of Physical Oceanography*, **25**, 280-286.
- Matthäus W., Schinke H. (1999): The influence of river runoff on deep water conditions of the Baltic Sea. *Hydrobiologia*, **393** (1), 1-10.
- Matthäus W., Nausch G., Lass H.-U., Nagel K., Siegel H. (2001): hydrographisch-chemische Zustandeinschätzung der Ostsee 2000. – *Meereswissenschaftliche Berichte Warnemünde*, **45**, 27-88.
- Matthäus W., Nehring D., Feistel R., Nausch G., Mohrholz V., Lass H.U. (2008): The Inflow of Highly Saline Water into the Baltic Sea. In: Feistel R., Nausch G., Wasmund N. (Eds.): *State and evolution of the Baltic Sea, 1925-2005*. John Wiley & Sons, 265-309.
- Mattsson, J. (1996): Some comments on the barotropic flow through the Danish Straits and the division of the flow between the Belt Sea and the Öresund. *Tellus*, **48A**, 456-464.
- Meier H.E.M., Döscher R., Broman B., Piechura J. (2004): The major Baltic inflow in January 2003 and preconditioning by smaller inflows in summer/autumn 2002: a model study. *Oceanologia*, **46** (4), 557-579.
- Meier H.E.M. (2007): Modeling the pathways and ages of inflowing salt- and freshwater in the Baltic Sea. *Estuarine, Coastal and Shelf Science*, **74** (4), 610-627.
- Meier H.E.M., Feistel R., Piechura J., Arneborg L., Burchard H., Fiekas V., Golenko N., Kuzmina N., Mohrholz V., Nohr C., Taka V.T., Sellschopp J., Stips A., Zhurbas V. (2006): Ventilation of the Baltic Sea deep water: A brief review of present knowledge from observations and models. *Oceanologia*, **48** (S), 133-164.
- Melvasalo T., Viljamaa H. (1987): Coastal pollution and seasonal fluctuations in heterocystous blue-green algae in the northern part of the Gulf of Finland. *Proceedings of the Fourth Symposium of the Baltic Marine Biologists Gdansk 1975*, Sea Fisheries Institute, 107-114.
- Miętus M. (1998): *The Climate of the Baltic Sea Basin*. World Meteorological Organization, Report No. 41, 64 pp.
- Mikulski Z. (1970): Inflow of river waters to the Baltic Sea in 1961-1970. *Nordic Hydrology*, **4**, pp.216-227



- Mikulski Z. (1982): River inflow to the Baltic Sea. Polish Academy of Sciences, Polish National Committee of the IHP, University of Warsaw, Faculty of Geography and Regional Studies.
- Moisander P.H., Steppe T.F., Hall N.S., Kuparinen J., Paerl H.W. (2003): Variability in nitrogen and phosphorus limitation for Baltic Sea phytoplankton during nitrogen-fixing cyanobacterial blooms. *Marine Ecology Progress Series*, **262**, 81-95.
- Myrberg K., Andrejev O. (2003): Main upwelling regions in the Baltic Sea - a statistical analysis based on three-dimensional modelling. *Boreal Environment Research*, **8**, 97-112.
- Myrberg K., Andrejev O., Lehmann A., (2010): Dynamic features of successive upwelling events in the Baltic Sea, *Oceanologia*, **52** (1), 77-99.
- Nausch G., Nehring D. (1996): Baltic Proper, Hydrochemistry. In: Third Periodic Assessment of the Marine Environment of the Baltic Sea, 1989-1993. *Baltic Sea Environmental Proceedings*, **64b**, 80-85.
- Nausch G., Lysiak-Pastuszek E. (2002): Eutrophication and related fields: Baltic Proper, Hydrochemistry. In: Fourth Periodic Assessment of the State of the Marine Environment of the Baltic Area, 1994-1998. *Baltic Sea Environmental Proceedings*, **85B**, 42-45.
- Nausch G., Feistel R., Lass H.U., Nagel K., Siegel H. (2005): Hydrographisch-chemische Zustandseinschätzung der Ostsee 2004. *Meereswissenschaftliche Berichte*, 62, 1-78.
- Nausch G., Feistel R., Lass H.U., Nagel K., Siegel H. (2006): Hydrographisch-chemische Zustandseinschätzung der Ostsee 2005. *Meereswissenschaftliche Berichte*, 66, 1-82.
- Nausch G., Nehring D., Nagel K. (2008): Nutrient concentrations, trends and their relation to eutrophication. In: Feistel R., Nausch G., Wasmund N. (Eds.): *State and evolution of the Baltic Sea, 1925-2005*. John Wiley & Sons, 337-366.
- Nausch G., Feistel R., Umlauf L., Nagel K. Siegel H. (2009): hydrographisch-chemische Zustandseinschätzung der Ostsee 2008. *Meereswissenschaftliche Berichte*, 77, 1-99.
- Nausch M., Nausch G., Wasmund N. (2004): Phosphorus dynamics during the transition from nitrogen to phosphate limitation in the central baltic Sea. *Marine Ecology Progress Series*, **266**, 15-25.
- Nausch, M., Nausch, G., Lass, H.-U., Mohrholz, V., Nagel, K., Siegel, H., Wasmund, N. (2009): Phosphorus input by upwelling in the eastern Gotland Basin (Baltic Sea) in summer and its effects on filamentous cyanobacteria. *Estuarine, Coastal and Shelf Science*, **63**, 434-442.
- Nehring, D., Matthäus, W. (1991): Current trends in hydrographic and chemical parameters and eutrophication in the Baltic Sea. *Internationale Revue der gesamten Hydrobiologie*, **76**, 297-316.
- Neumann T. (2010): Climate-change effects on the Baltic Sea ecosystem: A model study. *Journal of Marine Systems*, **81**, 213-224.



- Nielsen, M.H. (2001): Evidence for internal hydraulic control in the northern Öresund. *Journal of Geophysical Research*, **106 C7**, 14055-14068.
- Nixon, S. A. (1995): Coastal marine eutrophication: a definition, social causes, and future concerns. *Ophelia*, **41**, 199-219.
- Olenina I., Hajdu S., Wasmund N., Jurgensone I., Gromisz S., Kownacka J., Toming K., Olenin S. (2009): Impacts of invasive phytoplankton species on the Baltic Sea ecosystem in 1980-2008, HELCOM Indicator Fact Sheets 2009, [http://www.helcom.fi/BSAP\\_assessment/ifs/ifs2009/en\\_GB/InvasivePhytoplanktonSpecies/](http://www.helcom.fi/BSAP_assessment/ifs/ifs2009/en_GB/InvasivePhytoplanktonSpecies/)
- Omstedt A., Axell L.B. (1998): Modeling seasonal, interannual and long-term variations of salinity and temperature in the Baltic Proper. *Tellus*, **50A** (4), 637-652.
- Omstedt A., Hansson D. (2006): The Baltic Sea ocean climate system memory and response to changes in the water and heat balance components. *Continental Shelf Research*, **26**, 236-251.
- Osborn T.R. (1980): Estimates of the local rate of vertical diffusion from dissipation measurements. *Journal of Physical Oceanography*, **10** (1), 83-89.
- Overeem I., Weltje G.J., Bishop-Kay C., Kroonenberg S.G. (2002): The Late Cenozoic Eridanos delta system in the Southern North Sea Basin: a climate signal in sediment supply? *Basin Research*, **13** (3), 293-312.
- Piechura J., Beszczynska-Möller A. (2004). Inflow waters in the deep regions of the southern Baltic Sea-transport and transformations. *Oceanologia*, **46** (1), 113-141.
- Polzin K.L., Toole J.M., Schmitt R.W. (1995): Finescale Parameterizations of Turbulent Dissipation, *Journal of Physical Oceanography*, **25** (3), 306-328.
- Postel L. (2000): Interannual variations of the amount of herring in relation to plankton biomass and activity, temperature and cloud coverage in the Baltic Sea. *ICES CM 2000/M*, 16.
- Quandt, H. (1980): Besondere Seegangerscheinungen im Schelfgebiet und ihre Berücksichtigung in der Schiffsführung. Dissertation, Ingenieurhochschule für Seefahrt Warnemünde/Wustrow.
- Rajamohan R., Vinnitha E., Venugopalan V.P., Narasimhan S.V. (2007): Chlorination byproducts and their discharge from the cooling water system of a coastal electric plant. *Current Science*, **93** (11), 1608-1612.
- Redfield, A.C., Ketchum, B.H., Richards, F.A. (1963): The influence of organisms on the composition of sea water. In: Hill, M.N. (Ed.), *The Sea*, **2**, Wiley, New York.
- Registrar of the USSR (1974). Beter I Volny v okeanakh I moryakh. 1974, Chast II. Spravochnye dannye po rezhimu vetrov i volneniya na moryakh, **1 Baltijskoe More**, 79-85.
- Reißmann J.H. (2002): Integrale Eigenschaften von mesoskaligen Wirbelstrukturen in den tiefen Becken der Ostsee. *Meereswissenschaftliche Berichte*, **52**, 149 pp.



- Reißmann, J.H. (2005): An algorithm to detect isolated anomalies in three-dimensional stratified data fields with an application to density fields from four deep basins of the Baltic Sea. *Journal of Geophysical Research*, **110**.
- Reissmann, J. H. (2006): On the representation of regional characteristics by hydrographic measurements at central stations in four deep basins of the Baltic Sea. *Ocean Science*, **2**, 71-86.
- Reissmann J.H., Burchard H., Feistel R., Hgen E., Lass H.-U., Mohrholz V., Nausch G., Umlauf L., Wiczorek G. (2009): Vertical mixing in the Baltic Sea and consequences for eutrophication – A review. *Progress in Oceanography*, **82**, 47-80.
- Rolff C., Elmgren R., Voss M. (2008): Deposition of nitrogen and phosphorus on the Baltic Sea: seasonal patterns and nitrogen isotope composition. *Biogeosciences*, **5**, 1657-1667.
- Rosenberg, R., Elmgren, R., Fleischer, S., Jonsson, P., Persson, G., Dahlin, H. (1990): Marine eutrophication case studies in Sweden. *Ambio*, **19**, 102-108.
- Rukhovets L.A. (1982): Mathematical Simulation of Water exchange and Pollutant Dispersion in the Neva Bay. *Meteorologiya i Hidrologiya*, 7/1982, 78-87 (in Russian).
- Rumohr H., Krost P. (1991): Experimental evidence of damage to benthos by bottom trawling, with special reference to *Arctica islandica*. *Helgoländer Meer- esuntersuchungen*, **33**, 340–345.
- Rydberg L., Ærtebjerg G., Edler L. (2006): Fifty years of primary production measurements in the Baltic entrance region, trends and variability in relation to land-based input of nutrients. *Journal of Sea Research*, **56**, 1–16.
- Sanden P., Hakansson B. (1996): Long-term trends in Secchi depth in the Baltic Sea. *Limnology and Oceanography*, **41**, 346–351.
- Schernewski G., Neumann T. (2002): Perspectives on eutrophication abatement in the Baltic Sea. In: Ass E.-P. (Ed.): *Littoral 2002: 6<sup>th</sup> International Symposium*, proceedings, University of Porto, 2, 503-511.
- Schernewski, G., Neumann, T. (2005): The trophic state of the Baltic Sea a century ago: a model simulation study. *Journal of Marine Systems*, **53**, 109-124.
- Schleswig-Holstein Ministry of Science, Economic Affairs and Transport (2007): Kleine Anfrage des Abgeordneten Dr. Heiner Garg (FDP) und Antwort der Landesregierung – Minister für Wissenschaft, Wirtschaft und Verkehr. In: *Drucksache 16/1334*, Diet of Schleswig-Holstein, 24 April 2007.
- Schmager G., Fröhle P., Schrader D., Weisse R., Müller-Navarra S. (2008): Sea State, Tides. In: Feistel R., Nausch G., Wasmund N. (Eds.): *State and evolution of the Baltic Sea, 1925-2005*. John Wiley & Sons, 143-198.
- Schmelzer N., Seinä A., Lundqvist J.-E., Sztobryn M. (2008): Ice. In: Feistel R., Nausch G., Wasmund N. (Eds.): *State and evolution of the Baltic Sea, 1925-2005*. John Wiley & Sons, 199-240.



- Schmidt M., Fennel W., Neumann T., Seifert T. (2008): Description of the Baltic Sea with Numerical Models. In: Feistel R., Nausch G., Wasmund N. (Eds.): State and evolution of the Baltic Sea, 1925-2005. John Wiley & Sons, 583-624.
- Schubert H., Sagert S., Forster R.M. (2001): Evaluation of the different levels of variability in the underwater light field of a shallow estuary. *Helgoland Marine Research*, **55**, 12-22.
- Sellschopp J., Arneborg L., Knoll M., Fiekas V., Gerdes F., Burchard H., Lass H. U., Mohrholz V., and Umlauf L. (2006): Direct observations of a medium-intensity inflow into the Baltic Sea, *Continental Shelf Research*, **26**, 2393-2414.
- Seifert T., Tauber F., Kayser B. (2001): A high resolution spherical grid topography of the Baltic Sea - 2nd edition. Baltic Sea Science Congress, Stockholm 25-29 November 2001, Poster #147, <http://www.io-warnemuende.de/iowtopo>.
- Siegel H., Gerth M., Mutzke A. (1999): Dynamics of the Oder river plume in the southern Baltic Sea: Satellite data and numerical modeling, *Continental Shelf Research*. **18**, 1143-1159.
- Siegel H., Gerth M., Tschersich G. (2008): Satellite-derived Sea Surface Temperature for the period 1990–2005. In: Feistel R., Nausch G., Wasmund N. (Eds.): State and evolution of the Baltic Sea, 1925-2005. John Wiley & Sons, 241-264.
- Sipelglas L., Arst H., Raudsepp U., Kõuts T., Lindfors A. (2004): Optical properties of coastal waters of northwestern Estonia: In situ measurements. *Boreal Environment Research*, **9**, 447-456.
- SMHI, FIMR (1982): Climatological Ice Atlas for the Baltic Sea, Kattegat, Skagerrak and Lake Vänern (1963-1979). Sjöfartsvärket, 220 pp.
- SMHI (2010): Oxygen Indicator Factsheet. Presentation at the 2<sup>nd</sup> HELCOM workshop to develop a core set of eutrophication indicators, Helsinki, 2010-02-04.
- Soomere T., Rannat K. (2003): An experimental study of wind waves and ship wakes in Tallinn Bay. *Proceedings of the Estonian Academy of Sciences. Engineering*, **9** (3), 157-184.
- Soomere T. (2006): Nonlinear ship wake waves as a model of rogue waves and a source of danger to coastal environment. *Oceanologia*, **48** (S), 185-202.
- Spethmann H. (1912): *Der Wasserhaushalt der Ostsee*. Zeitschrift der Gesellschaft für Erdkunde. Berlin.
- Stålnacke P., Grimvall A., Sundblad K., Tonderski A. (1999): Estimation of riverine loads of Nitrogen and Phosphorus to the Baltic Sea, 1970-1993. *Environmental Monitoring and Assessment*, **58**, 173-200.
- Stigebrandt A. (1979): Observational evidence for vertical diffusion driven by internal waves of tidal origin in the Oslofjord. *Journal of Physical Oceanography*, **9** (2), 435-441.
- Stigebrandt A., Lass H.-U., Liljebladh B., Alenius P., Piechura J., Hietala R., Beszczyńska A. (2002): DIAMIX – an experimental study of diapycnal deep-water mixing in the virtually tideless Baltic Sea. *Boreal Environment Research*, **7** (4), 363–369.





- Stips A., Prandke H., Neumann T. (1998): The structure and dynamics of the bottom boundary layer in shallow sea areas without tidal influence: an experimental approach. *Progress in Oceanography*, **41** (4), 383-453.
- Stips A., Burchard H., Bolding K., Prandke H., Wüst A. (2005): Measurement and simulation of viscous dissipation rates in the wave affected surface layer. *Deep Sea Research II*, **52** (9-10), 1133-1155.
- Suikkanen S., Laamanen M., Huttunen M. (2007): Long-term changes in summer phytoplankton communities of the open northern Baltic Sea. *Estuarine, Coastal and Shelf Science*, **71**, 580-592.
- Schwoerbel J. (1984): Einführung in die Limnologie. VEB Gustav Fischer Verlag, Jena, 1-233.
- Sverdrup H., Munk W. (1947): Wind, sea and swell; theory of relations for forecasting. U. S. Navy, Washington. HO Publication No. 601.
- Thiel G. (1943): Einiges über die Ergebnisse von Strombeobachtungen in der westlichen Ostsee. *Annalen der Hydrographie und Maritimen Meteorologie*, **71**, 226-231.
- Thorade H. (1943): Über den Gezeitenstrom im Fehmarnbelt. *Annalen der Hydrographie und Maritimen Meteorologie*, **71**, 231-236.
- Tiesel R. (2008): Weather of the Baltic Sea. In: Feistel R., Nausch G., Wasmund N. (Eds.): State and evolution of the Baltic Sea, 1925-2005. John Wiley & Sons, 65-92.
- Tillessen T. (2010): High demand for wind farm installation vessels. *Hansa International Maritime Journal*, **147**, 170-171.
- Umlauf L., Tanhua T., Waniek J., Schmale O., Holtermann P., Rehder G. (2008): Hunting a new oceanic tracer. *Eos*, **89** (43), 419-420.
- Umlauf L., Arneborg L. (2009a): Vertical mixing in the Baltic Sea and consequences for eutrophication – A review. *Journal of Physical Oceanography*, **39**, 2385-2401.
- Umlauf L., Arneborg L. (2009b): Dynamics of Rotating Shallow Gravity Currents Passing through a Channel. Part II: Analysis. *Journal of Physical Oceanography*, **39**, 2402-2416.
- Umlauf L., Arneborg L., Hofmeister R., Burchard H. (2010): Entrainment in shallow rotating gravity currents: A modeling study. *Journal of Physical Oceanography*, accepted.
- Utermöhl H. (1958): Zur Vervollkommnung der quantitativen Phytoplankton-Methodik. *Mitteilungen Internationale Vereinigung für theoretische und angewandte Limnologie*, **9**, 1-38.
- Vahteraa E., Laanemets J., Pavelson J., Huttunen M., Kononen K. (2005): Effect of upwelling on the pelagic environment and bloom-forming cyanobacteria in the western Gulf of Finland. *Baltic Sea Journal of Marine Systems*, **58** (1-2), 67-82.



- Voltsinger N.E., Zolnikov A.V., Klevanny K.A., Preobrazhensky L.Yu. (1990): Calculation of the Hydrological Regime of the Neva Inlet. *Meteorologiya i Gidrologiya*, 1/1990, 70-77 (in Russian).
- Wasmund N. (1997): Occurrence of cyanobacterial blooms in the Baltic Sea in relation to environmental conditions. *Internationale Revue der gesamten Hydrobiologie*, **82**, 169-184.
- Wasmund N., Nausch G., Matthäus W. (1998): Phytoplankton spring blooms in the southern Baltic Sea - spatio-temporal development and long-term trends. *Journal of Plankton Research*, **20**, 1099-1117.
- Wasmund N., Zalewski M., Busch S. (1999): Phytoplankton in large river plumes in the Baltic Sea. *ICES Journal of Marine Science*, **56** (S), 23-32.
- Wasmund N., Andrushaitis A., Lysiak-Pastuszek E., Müller-Karulis B., Nausch G., Neumann T., Ojaveer H., Olenina I., Postel L., Witek Z. (2001): Trophic status of the south-eastern Baltic Sea: a comparison of coastal and open areas. *Estuarine, Coastal and Shelf Science*, **53**, 849-864.
- Wasmund N., Uhlig S. (2003): Phytoplankton trends in the Baltic Sea. *ICES Journal of Marine Science*, **60** (2), 177-186.
- Wasmund N., Pollehne F., Postel L., Siegel H., Zettler M. L. (2006): Biologische Zustandseinschätzung der Ostsee im Jahr 2005, *Meereswissenschaftliche Berichte*, **69**, 1-78.
- Wasmund N., Göbel J., von Bodungen B. (2007): 100-years-changes in the phytoplankton community of Kiel Bight (Baltic Sea). *Journal of Marine Systems*, **73**, 300-322.
- Wasmund N., Siegel H. (2008): Phytoplankton. In: Feistel R., Nausch G., Wasmund N. (Eds.): *State and evolution of the Baltic Sea, 1925-2005*. John Wiley & Sons, 441-481.
- Wasmund N., Pollehne F., Postel L., Siegel H., Zettler M. L. (2009): Biologische Zustandseinschätzung der Ostsee im Jahr 2008. *Meereswissenschaftliche Berichte*, **78**, 1-91.
- Weisse R., von Storch H., Feser F. (2005): Northeast Atlantic and North Sea storminess as simulated by a regional climate model 1958-2001 and comparison with observations. *Journal of Climate*, **18**, 465-479.
- Weisse R. (2007): A Sea State Hindcast for the Baltic Sea 1992–2002. Unpublished manuscript, cited in Schmager et al., 2009.
- Wessel P., Smith W.H.F. (1996): A Global, Self-consistent, Hierarchical, High-Resolution Shoreline Database, *Journal of Geophysical Research*, **101**, 8741-8743.
- Wittig H. (1953): Der mittlere jährliche Gang des Salzgehaltes in der Kieler und Mecklenburger Bucht. *Kieler Meeresforschungen*, **9** (2), 171-175.
- Witting R. (1911): Tidvattnen i Östersjön och Finska Viken. *Fennia*, **29**, 1-84.
- Wrzolek L. (1996): Phytoplankton in the Gdansk Basin in 1979–1993. *Oceanological Studies*, 1–2, 87–100.



- Wübber C.H., Krauss W. (1979). The two-dimensional seiches of the Baltic Sea. *Oceanologica Acta*, **2**, 435–446.
- Wyrтки K. (1954a): Der große Salzeinbruch in die Ostsee im November und Dezember 1951. *Kieler Meeresforschungen*, **10** (1), 19-25.
- Wyrтки K. (1954b): Die Dynamik der Wasserbewegungen im Fehmarnbelt II. *Kieler Meeresforschungen*, **10** (1), 162-181.
- Zhurbas V.M., Paka V.T. (1997): Mesoscale thermohaline variability in the Eastern Gotland Basin following the 1993 major Baltic inflow. *Journal of Geophysical Research*, **102** (C9), 20917–20926.
- Zhurbas V.M., Paka V.T. (1999): What drives thermohaline intrusions in the Baltic Sea? *Journal of Marine Systems*, **21** (1-4), 229-241.
- Zhurbas V., Laanemets J. (2008): Modeling of the mesoscale structure of coupled upwelling/downwelling events and the related input of nutrients to the upper mixed layer in the Gulf of Finland, Baltic Sea. *Journal of Geophysical Research*, **113** (C05004).
- ØL (1997): The Øresund Link. Basic Hydrographic Monitoring: February 1992 – February 1997. Report prepared in May 1997 for Øresundskonsortiet.

## **8.2 Computer code**

- Grindsted A. (2008): Tidal fitting toolbox. The MathWorks, <http://www.mathworks.com/matlabcentral/fileexchange/19099-tidal-fitting-toolbox>.



## 9 GLOSSARY

- BAAC: BALTEX Assessment of Climate Change for the Baltic Sea Basin
- BALTEX: The Baltic Sea Experiment, a Regional Hydroclimate Project of the Coordinated Energy and Water Cycle Observations Project within the Global Energy and Water Cycle Experiment of the World Climate Research Programme  
<http://www.baltex-research.eu/>
- BSH: Bundesamt für Seeschifffahrt und Hydrographie, German Federal Shipping and Hydrography Authority  
<http://www.bsh.de/en/index.jsp>
- CDOM: Colored dissolved organic matter
- DHI: DHI Water Environment Health  
<http://www.dhigroup.com/>
- DWD: Deutscher Wetterdienst, German Meteorological Service
- EC: European Commission
- EMEP: European Monitoring and Evaluation Programme  
<http://www.emep.int/index.html>
- EUTROSYM: Internationales Symposium über die Eutrophierung und Sanierung von Oberflächengewässern, UNEP-Symposium on eutrophication and restoration of surface waters, *Karl-Marx-Stadt 1976*
- FEMA: Fehmarnbelt Fixed Link Marine Biology Service
- FIMR: Merentutkimoslaitos/Havsforskningsinstitutet, Finnish Institute of Marine Research
- HELCOM: Helsinki Commission, the governing body of the "Convention on the Protection of the Marine Environment of the Baltic Sea Area"  
<http://www.helcom.fi/>
- ICES: International Council for the Exploration of the Sea  
<http://www.ices.dk/indexfla.asp>
- IOW: Leibniz-Institut für Ostseeforschung Warnemünde, Leibniz Institute for Baltic Sea Research Warnemünde  
[http://www.io-warnemuende.de/en\\_index.html](http://www.io-warnemuende.de/en_index.html)
- SII: Statens isbrydnings- og ismeldetjeneste. Danish ice breaking and ice warning service, transferred to Danish Naval Forces Operational Command in 1996.
- SMHI: Sveriges meteorologiska och hydrologiska institut, Swedish Meteorological and Hydrological Institute, <http://www.smhi.se/en>



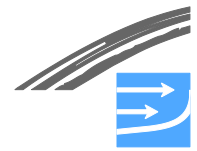


## Table of figures

Fig. 1.1	Sketch of water exchange in the Baltic Sea (redrawn after (Lass and Matthäus 2008)).....	1
Fig. 1.2	Bathymetry and geographical structures of the Baltic Sea. Water depths refer to (Seifert et al. 2001). Water depth is cut off at 200m. Acronyms indicate some basins and connecting channels: Arkona Basin (AB), Bornholm Channel (BC), Bornholm Basin (BB), Stolpe Channel (SC, also called Slupsk Furrow), Gdansk Depression (GD), Eastern Gotland Basin (EGB), Landsort Deep (LD), Fårö Deep (FD), Karlsö Deep (KD) and Aland Deep (AD).....	3
Fig. 1.3	Major rivers contributing to the Baltic Sea water budget. Dark blue arrows indicate specific river runoff, light blue arrows show accumulated diffuse sources. The Göta älv is shown for although it empties into the Kattegat. Torneälv and Kemijoki have been summed up as their mouths are located only 15 km apart. Values from (Mikulski 1970) and (Bergström & Carlsson 1994).....	5
Fig. 1.4	Cross-section showing simulated longitudinal salinity distribution as monthly means from Great Belt through Fehmarnbelt and into the Baltic Proper, where the vertical line shows the position of the planned link (FEHY MOM model, version v06_r01).....	8
Fig. 1.5	Major Baltic inflows between 1880 and 2007 and their seasonal distribution (upper right) shown in terms of their relative intensity and five year running means of river runoff to the Baltic Sea (inside the entrance sills) averaged from September to March (shaded). Black boxes on the time axis: major inflows arranged in clusters (Matthäus et al. 2008). Intensities: 0 equals an inflow of 5 days duration with $S=17\text{‰}$ (17 psu), 100 equals an inflow of 30 days duration with $S=24\text{‰}$ .....	10
Fig. 1.6	Mean surface (upper panel) and bottom (lower panel) salinity (1990-2007) of the Baltic Sea simulated with the MIKE numerical model (FEHY, 2010/b). A clear gradient between the northern Baltic Sea and the Kattegat is visible. ....	13
Fig. 1.7	Observed salinity at 0 m (upper panel) and 200 m (lower panel) at station BMP J01 in the Eastern Gotland Basin (ICES, 2010).....	15
Fig. 1.8	Mean water level (1990-2007) of the Baltic Sea simulated with the MOM numerical model (FEHY, 2013c). A clear gradient between the northern Baltic Sea and the Kattegat is visible. Local depressions due to large gyres exist in sub-basins like the Bornholm Basin or the Bothnian Sea. ....	18
Fig. 1.9	Mean Secchi depth (top number), number of observations (middle number) and standard deviation (bottom number) for $0.5^\circ \times 0.5^\circ$ squares for the transitional zone of the North Sea - Baltic Sea in the period 1902-1999; from (Aarup 2002). Most straits in the Belt Sea show a mean Secchi depth of 6 m while it increases to 8 m in the deeper parts of the Kattegat and also in the Arkona and Bornholm Sea. Reprinted from Oceanologia, Vol. 44, No. 4, Figure 2, p. 332, with the publisher's permission.....	19
Fig. 1.10	Conceptual model of nutrient input sources to the Baltic Sea (HELCOM 2010a – holistic assessment). ....	20
Fig. 1.11	Annual cycle of phosphate and nitrate 2008 and 2009 in the surface layer (0 – 5 m) in the Arkona Sea (measurements at station 113/BMP K05),( ICES 2010). ....	22
Fig. 1.12	Mean phosphate and nitrate+nitrite concentrations in the mixed winter surface layer (0 – 10 m) pooling five stations in the eastern Gotland Basin from 1958 to date (1962, 1966, and 1979 no data). Major Baltic Inflows are marked with red tags. Figures taken from (Nausch et al. 2008). ....	23
Fig. 1.13	Vertical distribution of oxygen resp. hydrogen sulphide between Darss Sill and northern Gotland Basin in March/April 2008 (from Nausch et al., 2009).....	24
Fig. 1.14	Proportion of Cyanophyceae on total biomass (integrated sample of 0-10 m depth) for summer long-term data in various Baltic Sea areas (see Fig. 5.1 for station positions). To assure comparable data, summer was defined as mean values for July and August in all investigated areas. ....	26
Fig. 1.15	Long-term investigation of chl-a concentration (mean of 0-10 m depth), both for seasonal means (green circles) and original data (blue circles) for the spring season. Updated data series of (Wasmund and Uhlig 2003) and (Wasmund et al. 2009). Lines represent linear	





	regression and 95% confidence intervals for original data sets (blue). See Fig. 5.1 for position of stations.....	27
Fig. 1.16	Number of laden tankers entering and leaving the Baltic Sea via the Great Belt. Figure redrawn with data from (HELCOM 2009e). .....	29
Fig. 1.17	Integrated classification of the eutrophication status of the Baltic Sea. Large circles represent open sea areas, small circles show coastal areas. Very good status (blue, not existent, good status (green) describes "areas not affected by eutrophication" while moderate (yellow), poor (orange) and bad (red) are equivalents to "areas affected by eutrophication" (HELCOM 2009a).....	30
Fig. 2.1	Bathymetry and geographical structures of the Baltic Sea. Water depths refer to Seifert et al. (2001). Water depth is cut off at 200 m. Acronyms indicate some basins and connecting channels: Arkona Basin (AB), Bornholm Channel (BC), Bornholm Basin (BB), Stolpe Channel (SC, also called Slupsk Furrow), Gdansk Depression (GD), Eastern Gotland Basin (EGB), Landsort Deep (LD), Fårö Deep (FD), Karlsö Deep (KD) and Åland Deep (AD).....	34
Fig. 2.2	Number of water depth samples per grid cell (see Eq. 2.1) used for IOW Baltic Sea bathymetry.....	35
Fig. 2.3	Relation between the gradient of the sea bottom and the range of variation of water depth samples.....	36
Fig. 2.4	Relative frequency of occurrence of sea bottom gradients in bins of 1m/km derived from the 2 km Baltic Sea grid Eq. (2.1).....	37
Fig. 2.5	Open sea surface (km <sup>2</sup> , green curves) and enclosed water volume (km <sup>3</sup> , blue curves) in dependence on water depth (left panel) and relative errors (right panel) for an assumed variation of sea level of ±1 m. The black curve corresponds to number of open grid cells and the red curve shows the 95% confidence range of volume. Note that Baltic Sea includes Belt Sea and Kattegat. ....	38
Fig. 2.6	Regional masks of main sub-basins of the Baltic Sea. Colors and numbers indicate the regional masks. 1: Skagerrak (not part of Baltic Sea), 2: Kattegat, 3: Little Belt, 4: Great Belt, 5: Sound, 6: Kiel Bight, 7: Mecklenburg Bight, 8: Arkona Basin, 9: Bornholm Basin 10: Southern Gotland Basin, 11: Western Gotland Basin, 12: Eastern Gotland Basin, 13: Northern Baltic Proper, 14: Gulf of Riga, 15: Gulf of Finland, 16: Åland Sea, 17: Bothnian Sea, 18: Bothnian Bay. ....	40
Fig. 2.7	Cumulative frequency of occurrence of water depth derived from the IOW Baltic Sea bathymetry providing partial areas within depth intervals, see Fig. 2.6 for regional sub-divisions. ....	42
Fig. 2.8	Bathymetry of Stolpe Channel connecting Bornholm Basin to the west with Baltic Proper to the east. Bold isoline indicates closing water depth of 70 m (data from Seifert et al., 2001). ....	44
Fig. 2.9	Bathymetry of the central Baltic Proper showing the Gotland Depression (below -100 m water depth) and the Eastern Gotland Basin, which is enclosed below -140 m (bold black line). Data from (Seifert et al. 2001).....	45
Fig. 2.10	Sketch of the drainage area of the Baltic Sea sub-divided into Bothnian Bay (BoB), Bothnian Sea (BoS), Gulf of Finland (GoF), Gulf of Riga (GoR), Baltic Proper (BPr), Belt Sea (BSe), and Kattegat (Kat), taken from the Baltic Environmental Atlas ( <a href="http://maps.grida.no/baltic">http://maps.grida.no/baltic</a> ). ....	49
Fig. 2.11	Major rivers contributing to the Baltic Sea water budget. Dark blue arrows indicate specific river runoffs, light blue arrows show accumulated diffuse sources. The Göta älv is shown for although it empties into the Kattegat. Torneälv and Kemijoki have been summed up as their mouths are located only 15 km apart. Values from Mikulski (1970) and Bergström and Carlsson (1994).....	51
Fig. 2.12	Total river discharge (m <sup>3</sup> /s) into the Baltic Sea (excluding transition area) derived from FEHY data set. The bold black lines indicate the long-term mean runoff, and thin lines the range of variation by one standard deviation. ....	54
Fig. 2.13	Inter-annual variation of yearly river discharge (km <sup>3</sup> ) to the Baltic Sea. (HELCOM 2010) refers to (Kronsell and Andersson 2010).....	55

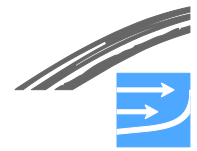
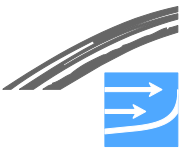


Fig. 2.14	Contribution of Baltic sub-basins to the yearly river runoff according to (Kronsell and Andersson 2010). .....	56
Fig. 2.15	The annual cycle of river runoff (m <sup>3</sup> /s) shown by climatological monthly means.....	57
Fig. 2.16	Conceptual model of nutrient input sources to the Baltic Sea (HELCOM 2010a – holistic assessment). .....	58
Fig. 2.17	Proportion of different nitrogen sources to the Baltic Sea. Point sources include both coastal and inland point sources Transboundary inputs have not been divided into point or diffuse sources (redrawn from HELCOM 2010a/b). .....	59
Fig. 2.18	Proportion of different phosphorus sources to the Baltic Sea. Point sources include both coastal and inland point sources Transboundary inputs have not been divided into point or diffuse sources (redrawn from HELCOM 2010 a/b). .....	60
Fig. 2.19	Annual mean riverine input of nitrogen (kt) to the Baltic Sea and its sub-basins. Coloured lines represent: Gulf of Bothnia (magenta), Gulf of Finland (green), Gulf of Riga (blue), Baltic Proper (red), and Belt Sea (black). The bold black line with symbols denotes the total yearly input to the Baltic, straight lines indicate the long-term average and the variation by one standard deviation (dashed). Source: FEHY compilation data. ....	62
Fig. 2.20	Riverine and direct source inputs of total nitrogen into the Baltic sea for 1994-2006 taken from (HELCOM 2009b). .....	62
Fig. 2.21	Annual mean river input of phosphorus (kt) to the Baltic Sea and its sub-basins. Coloured lines represent: Gulf of Bothnia (magenta), Gulf of Finland (green), Gulf of Riga (blue), Baltic Proper (red), and Belt Sea (black). The bold black line with symbols denotes the total yearly input to the Baltic, straight lines indicate the long-term average and the variation by one standard deviation (dashed).Source: FEHY compilation data. ....	63
Fig. 2.22	Regional distribution of atmospheric nitrogen deposition divided into oxidized (NO <sub>x</sub> ) and reduced (NH <sub>y</sub> ) fractions taken from (HELCOM 2009f), see Table 2.8 below for explanation of regional acronyms.....	65
Fig. 2.23	Number of wind speed samples from voluntary ships compiled for ICOADS by Miętus (1998). Red symbols indicate location of meteorological station from west to east: Warnemünde, Darss Sill, Greifswald, Arkona Basin, Swinoujście, Eastern Gotland Basin, Utö, and Kem, see Table 2.9. (Heligoland in North Sea not shown.) .....	69
Fig. 2.24	A typical cyclonic weather pattern over Europe taken from the classification of Deutscher Wetterdienst (DWD) by (Gerstengarbe and Werner 2005). .....	70
Fig. 2.25	The cyclonic weather pattern of 8 Nov. 1991 simulated by SN-REMO, compare to Fig. 2.24. Note different area and map projection. ....	70
Fig. 2.26	Seasonal wind over the Baltic Sea. Colours depict the seasonal mean of absolute wind speed (m/s) and unit arrows indicate the direction of the mean wind vector (note vector length independent of wind speed). .....	71
Fig. 2.27	Rosette plot of daily mean wind vectors observed at Arkona station. Classification into 16 directional bins reveals frequent occurrence of westerly to southwesterly winds. ....	72
Fig. 2.28	Climatological monthly means of air temperature (isolines in °C) over seasonal mean relative humidity (%). (JAJO) refers to the central months of the seasons: January, April, July, and October. ....	73
Fig. 2.29	Mean seasonal sum of precipitation (colours in mm) and average cloudiness indicated in 5% steps by isolines as predicted by SN-REMO for 1947-2007. ....	74
Fig. 2.30	Daily mean air pressure (hPa) observed in 2009 at buoy station in Arkona Basin. Horizontal black lines indicate seasonal averages.....	76
Fig. 2.31	SN-REMO model prediction of yearly mean air temperature (left panel) and wind speed (right panel) over the Baltic Proper. ....	77
Fig. 3.1	Low air pressure field over the North Sea – Baltic Sea system (from 24 December 1977 at 12:00). .....	80
Fig. 3.2	Mean water level (1990-2007) of the Baltic Sea simulated with the MOM numerical model (FEHY, 2013c). A clear gradient between the northern Baltic Sea and the Kattegat is visible.	



	Local depressions due to large gyres exist in sub-basins like the Bornhom Basin or the Bothnian Sea. ....	81
Fig. 3.3	Storm surge in the Baltic Sea on the 13 November 1872 at 14:00. From (Colding 1881). ....	83
Fig. 3.4	Schematic diagram of wind sea and swell (from Schmager et al., 2009). While the initial wind-induced sea state shows superpositions of high frequencies, dispersion of surface waves leads to swell with longer periods.....	85
Fig. 3.5	Baltic Sea wave diagram (from Schmager et al., 2009).To use the diagram, fetch and wind speed (knots) must be known, so one can follow the the path indicated by the black arrows from a known point in the lower right panel. The arrows given represent values listed in Table 3.1 below .....	86
Fig. 3.6	Frequency Distribution of the wave height H3% in the Baltic Sea east of 15°E and south of 60°N (redrawn with data from Registrar of the USSR, 1974).....	87
Fig. 3.7	Computed phases of the M2 partial tide in the Baltic referred to the passage of the moon through the Greenwich meridian; figure by Müller-Navarra in (Schmager et al. 2008). ....	89
Fig. 3.8	Form number (O1+K1)/(M2+S2) indicating dominance of diurnal, semi-diurnal, and mixed tides; figure by Müller-Navarra in (Schmager et al. 2008).....	91
Fig. 3.9	Intensity coefficient (mm) of the four leading tides in the Baltic Sea (M2+S2+K1+O1), figure by Müller-Navarra in Schmager et al. (2008).....	91
Fig. 3.10	Hourly salinity time series in the summer of 2005 at different depth levels from a fixed monitoring station at the Darss Sill, position: 54° 42' N, 12° 42' E (IOW data, own work). Note the generally high variability in salinity below 7 m depth, especially at 19 m on July 28. ....	95
Fig. 3.11	Schematic picture of the water balance of the Baltic Sea, the water exchange with the North Sea and the transformation of water masses in the Belt Sea (bottom left, in river runoff units). Redrawn after (Lass and Matthäus 2008). ....	96
Fig. 3.12	Time series of daily salinity (upper panel) and temperature (lower panel) profiles from the Fehmarnbelt lightvessel position, 1965-1984 (based on BSH data). Note the cyclic nature of bottom salinity with infrequent inflows of saline North Sea water. ....	98
Fig. 3.13	Annual mean surface salinity in the Kiel Bight and Mecklenburg Bight from 1876-1892, from (Wittig 1953).....	98
Fig. 3.14	Observed salinity at 0 m (upper panel) and 200 m (lower panel) at station BMP J01 in the Eastern Gotland Basin (ICES, 2010).....	100
Fig. 3.15	T-S diagram of measurements in the central Baltic (Eastern Gotland Basin) showing temperature plotted over salinity. Curved black lines mark the oceanographic density $\sigma$ , i.e. density minus 1000 kg/m <sup>3</sup> . The surface layer is shown by the vertical plume of the blue graph, indicating the annual temperature range from 0°C to more than 20°C. Note the continuous stratification below the low-density surface water. Data from ICES. ....	101
Fig. 3.16	T-S diagram of measurements in the Arkona Basin. This water shows a distinct surface layer too but due to the relatively shallow depth it also shows seasonal effects below the surface, namely a wide range in temperature. Note the two pools of water with temperatures around 12°C and 4°C respectively. Data from ICES.....	102
Fig. 3.17	Mean surface (upper panel) and bottom (lower panel) salinity (1990-2007) of the Baltic Sea simulated with the MIKE numerical model (FEHY, 2013c). A clear gradient between the northern Baltic Sea and the Kattegat is visible.....	104
Fig. 3.18	Typical temperature profiles in the Eastern Gotland Basin in 1994 (data from ICES 2010). Upper left: winter, upper right: spring, lower left: summer, lower right: autumn. ....	107
Fig. 3.19	Mean Secchi depth (top number), number of observations (middle number) and standard deviation (bottom number) for 0.5° x 0.5° squares for the transitional zone of the North Sea - Baltic Sea in the period 1902-1999; from (Aarup 2002). Most straits in the Belt Sea show a mean Secchi depth of 6 m while it increases to 8 m in the deeper parts of the Kattegat and also in the Arkona and Bornholm Sea. Reprinted from Oceanologia, Vol. 44, No. 4, Figure 2, p. 332, with the publisher's permission.....	109



Fig. 3.20	Long-term variation of salinity in the central Baltic deep water (after Matthäus et al. 2008). The saw-toothed variations of the salinity is generated by major inflows and decreasing salinity between inflow event. ....	114
Fig. 3.21	Major Baltic Inflows (MBIs) between 1880 and 2007 and their seasonal distribution (upper right) shown in terms of their relative intensity and five year running means of river runoff to the Baltic Sea (inside the entrance sills) averaged from September to March (shaded). Black boxes on the time axis: MBIs arranged in clusters; from Matthäus et al. (2008)....	115
Fig. 3.22	1990-2007 mean surface circulation as simulated with the MIKE Regional numerical model (FEHY, 2013c). Colors indicate current speed while arrows show current velocity. ....	116
Fig. 3.23	Bathymetry around Gotland (central Baltic). From (Fennel et al. 2010, submitted). ....	118
Fig. 3.24	Sea-surface temperature measured in July (dates as indicated) by NOAA AVHRR over the Gotland Basin from (Lass et al 2010); the horizontal line denotes a transect studied in that publication). ....	118
Fig. 3.25	Example of a satellite image of the Sea Surface Temperature (SST) of the Baltic Sea, showing a strong spatial variability (eddies, front and filaments) with scales of five to ten kilometres (courtesy H. Siegel, IOW). ....	119
Fig. 3.26	Scheme of vertical mixing and transport processes in the Baltic Sea (from Reissmann et al. 2009).....	120
Fig. 3.27	Transect through the Bornholm Channel from 19 November 2005 between 10:20 h and 12:30 h UTC, south-east is to the left and north-west is to the right. The salinity contours are drawn at intervals of 1 g/kg here. The upper 25 m are not shown for clarity. Figure taken from (Reissmann et al. 2009).....	122
Fig. 3.28	Northward transect down the steep southern slope of the Stolpe Channel, obtained on 25 September 2008 during POS373 with R/V Poseidon (Longitude was 17.00E). Shown in colors is the dissipation rate. Black contour lines correspond to isopycnals.....	123
Fig. 3.29	Averaged turbulent vertical diffusivities computed from equation (3.2), compared to other estimates by Matthäus (1990) at 75 m depth and by (Axell 1998) at 115 m depth. Also included are the values found by Ledwell et al. (1998) for the ocean thermocline from a tracer release experiment from (Lass et al. 2003).....	124
Fig. 3.30	The total volume fraction $\Sigma V_i$ occupied by Beddies detected in different sub-basins of volume $V_B$ for 12 data fields from the AB, the BB, the SF, and the EGB (from Reissmann et al. 2009) .....	126
Fig. 3.31	Average sea ice extent during mild-, normal- and severe winters (SMHI & FIMR 1982). .	128
Fig. 3.32	Average date of freezing (SMHI & FIMR 1982).....	129
Fig. 3.33	Average date of break-up of sea ice (SMHI & FIMR 1982).....	130
Fig. 4.1	Annual cycle of phosphate and nitrate 2008 and 2009 in the surface layer (0 – 5 m) in the Arkona Sea (measurements at station 113/BMP K05).....	132
Fig. 4.2	Mean phosphate and nitrate+nitrite concentrations in the mixed winter surface layer (0 – 10 m) pooling five stations in the eastern Gotland Basin from 1958 to date (1962, 1966, and 1979 no data). Major Baltic Inflows are marked by red tags. Figures taken from (Nausch et al. 2008). ....	134
Fig. 4.3	Vertical distribution of oxygen and hydrogen sulphide (shown as negative oxygen equivalents) in the Gotland Deep (BMP J01) between 2003 and 2005 (from Nausch et al 2008).....	135
Fig. 4.4	Vertical distribution of phosphate in the Gotland Deep (BMP J01) between 2003 and 2005 (from Nausch et al. 2008).....	136
Fig. 4.5	Vertical distribution of oxygen resp. hydrogen sulphide between Darss Sill and northern Gotland Basin in March/April 2008 (from Nausch et al. 2009).....	137
Fig. 4.6	Annual cycle of temperature and oxygen in the surface layer (0 – 10 m) in the Eastern Gotland Basin in 2007 (based on IOW and SMHI data, from (Nausch et al. 2008) .....	138
Fig. 4.7	Box-whisker-plots of the oxygen saturation (%) in 2007 in the surface layer (0 – 10 m) between western Baltic Sea and the Eastern Gotland Basin. Circles indicate outliers. ....	139



Fig. 4.8 Long-term variations of oxygen and hydrogen sulphide concentrations in the Central Baltic deep water (hydrogen sulphide converted into negative oxygen equivalents after (Fonselius 1969), from (Matthäus et al. 2008).....141

Fig. 4.9 Suboxic (green) and anoxic (red) in the near bottom areas in the Central Baltic Sea. Figures taken from (Feistel 2010). .....142

Fig. 4.10 Long-term mean (1990-2007) bottom oxygen content in the Baltic Sea simulated with the MIKE numerical model (FEHY, 2013c). Anoxic areas are marked as values <0.....143

Fig. 5.1 Geographical position of long-term phytoplankton stations. Numbers correspond to IOW internal notation. ....145

Fig. 5.2 Estuarine gradient for chl-a distribution and phytoplankton biomass using the example of Pomeranian Bay (left) and Peenestrom(right) in September 1995. Left: chl-a concentration in surface water (1m depth). The stations marked a short distance estuarine gradient (2.5 km) shown in the right figure. Right: Phytoplankton composition and chl-a concentration in relation to salinity in the surface water for the short distance transect between stations 245 and 241 (modified from Wasmund et al., 1999). .....147

Fig. 5.3 Seasonal variation of phytoplankton biomass (determined in integrated samples of 0-10 m depth), split into main taxonomical groups, along the large marine gradient of the Baltic Sea. Fig. A: Spring season: Data represent mean values from 1998-2008. Fig. B: Summer season: Data represent mean values from 1998-2008. Fig. C: Biomass (green) and surface salinity (blue) data based on yearly means, excluding winter values, for the time period 1998-2008. Stations: 22 – Mecklenburg Bight (inner part), 12 – BMP M02, Mecklenburg Bight (outer part), 46 – Kadet Channel, 30 – BMP K08, Darss Sill, 113 – Arkona Basin, 213 – BMP K02, Bornholm Basin, 259 – BMP K01, southern Baltic Proper, 271 –BMP J01, Eastern Gotland Basin. ....148

Fig. 5.4 Surface chl-a distribution in April 2003 in the western Baltic Sea derived from SeaWiFS (figure from Wasmund & Siegel, 2008).....150

Fig. 5.5 Seasonal patterns of phytoplankton biomass (determined in integrated samples of 0-10 m depth) as mean values for the time period 1999-2008. The figure is based on the comprehensive HELCOM data set. See Fig. 5.1 for position of stations.....152

Fig. 5.6 Seasonal patterns of chl-a concentration (mean of 0-10 m depth) averaged for the time period 1999-2009. The upper line denoted maximum values, the lower line minimum values, respectively. The figure is based on the comprehensive HELCOM data set. See Fig. 5.1 for position of stations. ....153

Fig. 5.7 Seasonal variation and depth dependence of phytoplankton primary production at station 12 (BMP M02, Mecklenburg Bight) in 1993 and station 271 (BMP J01, Eastern Gotland Sea) in 1991. ....154

Fig. 5.8 Number of days with surface accumulations of cyanobacteria. Figure was redrawn from HELCOM indicator factsheets 2004-2009 (Hansson 2004-2008; Hansson and Öberg 2009). ....156

Fig. 5.9 Biomass of cyanobacteria (0-10m integration depth) averaged by 5-year-periods in selected sub-basins of the Baltic Sea. Graphs represent only areas where statistically significant changes have taken place between different time-periods. Modified from (Jaanus et al. 2007). Data source: Estonian, Latvian, Lithuanian, German and Swedish phytoplankton monitoring programs. Description of data: Annual weighted summer (June-September) average of phytoplankton group biomasses. (Jaanus et al. 2007) .....157

Fig. 5.10 Long-term investigation of chl-a concentration (mean of 0-10 m depth), both for seasonal means (green circles) and original data (blue circles) for the spring season. Updated data series of (Wasmund and Uhlig 2003) and (Wasmund et al. 2009). Lines represent linear regression and 95% confidence intervals for original data sets (blue). See Fig 5.1 for position of stations.....159

Fig. 5.11 Long-term investigation of chl-a concentration (mean of 0-10 m depth), both for seasonal means (green circles) and original data (blue circles) for summer season. Updated data series of (Wasmund and Uhlig 2003) and (Wasmund et al. 2009). See Fig. 5.1 for position of stations. ....160



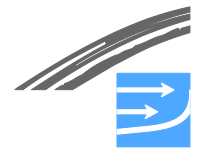
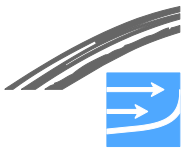


Fig. 6.1	Upper panel: number of laden tankers entering and leaving the Baltic Sea via the Great Belt. Figure redrawn with data from (HELCOM 2009e). Lower panel: amount of oil transported (million tons) via the 17 largest oil terminals in the Baltic Sea area (Fredericia, Kalundborg, Muuga, Porvoo, Naantali, Rostock, Ventspils, Riga, Klaipeda, Butinge, Gdansk, Primorsk, St Petersburg, Kaliningrad, Gothenburg, Brofjorden, and Vysotsk) during 1997-2007. Figure redrawn with data from (HELCOM 2009c). .....	163
Fig. 6.2	Integrated classification of the eutrophication status of the Baltic Sea. Large circles represent open sea areas, small circles show coastal areas. Very good status (blue), not existing, good status (green) describes "areas not affected by eutrophication" while moderate (yellow), poor (orange) and bad (red) are equivalents to "areas affected by eutrophication" (HELCOM 2009a).....	165
Fig. 6.3	Integrated classification of the hazardous substances status in the 144 assessment units. Blue = high status, green = good, yellow = moderate, orange = poor, and red = bad status. High and good status are equivalent to "areas not disturbed by hazardous substances", while moderate, poor, and bad status are equivalent to "areas disturbed by hazardous substances". Large dots represent assessment units of the open basins; small dots represent coastal assessment units which are mainly located in the territorial waters delimited by the grey line. Other grey lines represent the divisions between the sub-basins (cf. Fig. 6.2). Ecological objectives that were assessed using CHASE included all HELCOM objectives: "Concentrations of hazardous substances close to natural levels", "All fish safe to eat", "Healthy wildlife" and "Radioactivity at pre-Chernobyl levels".From (HELCOM 2010c). .....	167
Fig. 6.4	Reported catches of clupeids (sprat and herring), cod and flatfish from 1909-2005 in kilotons, comprising catches from the Baltic Sea including Belt Sea catches in most cases. From (Hammer et al. 2008). .....	170
Fig. 7.1	Wintertime NAO index from 1820 to 2010. (Source: <a href="http://www.cru.uea.ac.uk/~timo/datapages/naoi.htm">http://www.cru.uea.ac.uk/~timo/datapages/naoi.htm</a> ) .....	172
Fig. 7.2	Annual mean 2-m air temperature anomalies for the Baltic Sea 1871-2000, based on land stations. Blue colour relates to the area north of 60°N, and the red colour to the area south of that latitude. Dots represent individual years, while the smoothed curves highlight variability on a longer time scale. (Source: (HELCOM 2007b; BSEP No. 111) .....	172
Fig. 7.3	Left panel: Multi-model global averages of surface warming (relative to 1980-1999) for SRES scenarios A2, A1B and B1. The orange line is for an experiment where concentrations were held constant at year 2000 values. Right panel: Projected surface temperature changes for the early and late 21th century relative to the period 1980-1999. (Source: IPCC Synthesis Report 2007) .....	173
Fig. 7.4	Simulated maximum sea ice extent in the Baltic Sea for SRES scenarios A1B and B1. The black line is the annual maximum sea ice extent and colored lines show the 30 years mean. From (Neumann 2010). .....	175
Fig. 7.5	SST (sea surface temperature) warming [K] in the Baltic Sea for emission scenarios A1B and B1. Shown is horizontally averaged SST for winter (DJF), spring (MAM), summer (JJA) and fall (SON) seasons smoothed with a 30 years running mean. From (Neumann 2010). .....	176
Fig. 7.6	SSS (sea surface salinity) change [g/kg] in the Baltic Sea for emission scenarios A1B and B1. Shown is horizontally averaged SSS for winter (DJF), spring (MAM), summer (JJA) and autumn (SON) seasons smoothed with a 30 years running mean. From (Neumann 2010). .....	176





## List of tables

Table 1.1	Water and salt balance of the Baltic Sea after (Lass and Matthäus 2008). The table provides annual water mass (km <sup>3</sup> ) and salt transports (Gt) for the relations shown in Fig. 1.1. Extending the above scheme we present the total fresh water input $F=R+(P-E)$ , with river runoff R, and precipitation and evaporation (P-E) derived from (Lindau 2002) for the period 1980-1995. $R=446$ km <sup>3</sup> , $P-E=25$ km <sup>3</sup> . .....	2
Table 1.2	The ten largest rivers of the Baltic Sea system, including the Belt Sea, Sound and Kattegat, their approximate drainage area and mean annual runoff 1950-1999 (Bergström and Carlsson 1994) .....	5
Table 1.3	Annual volume and salt transports across Drogden Sill, Darss Sill and Fehmarnbelt as simulated by the MIKE Regional Model (ID6.42) for the period 1990-2007. ....	9
Table 1.4	Long-term statistics of surface and bottom salinity in Baltic Sea basins at the sea surface and in the bottom layer (after Feister et al. 2008). Potential outliers indicated by brackets. ....	16
Table 1.5	Estimated total nitrogen and phosphorus inputs (tons/year) into the Baltic Sea during the 1980s and before the beginning of the 20th century (Larsson et al. 1985). ....	21
Table 1.6	Phytoplankton primary production in the different sea areas (values from the 1990s). Data are compiled from various literatures by Wasmund & Siegel (2008). ....	26
Table 2.1	Area, volume, and mean water depth derived from IOW gridded bathymetry compared to (HELCOM 2002). The sub-division of the Gulf of Bothnia refers to (Leppäranta & Myrberg 2009), statistics for sub-divisions of the Baltic Proper are not specified in (HELCOM 2002). Sub-basin figures in italics. ....	39
Table 2.2	Closing depth and enclosed volume of bottom water in main basins and connecting channels of the Baltic Sea (excluding transition area) derived from the IOW bathymetric data set. ....	42
Table 2.3	The ten largest rivers of the Baltic Sea system, including the Belt Sea, Sound and Kattegat, their approximate drainage area and mean annual runoff 1950-1999 (Bergström & Carlsson, 1994) .....	50
Table 2.4	Characteristics of the main Baltic sub-basins in relation to river discharge. Mean river runoff and drainage area after (Bergström and Carlsson 1993), sea surface and water volume taken from (HELCOM 2002). ....	52
Table 2.5	Estimated total nitrogen and phosphorus inputs (tons/year) into the Baltic Sea during the 1980s and before the beginning of the 20th century (Larsson et al. 1985) .....	60
Table 2.6	Yearly mean riverine inputs of nutrients to the Baltic Sea (total amounts of nitrogen (N) and phosphorus (P) in kt). ....	61
Table 2.7	Regional distribution of riverine nutrient inputs (absolute amounts in kt and area specific loads in t/km <sup>2</sup> ). (HELCOM 2009a) data refer to 2006 and FEHY compilation data are averaged over the period 1970-2009. ....	64
Table 2.8	Average atmospheric deposition of total nitrogen in 1995-2009 after (HELCOM 2009f) in relation to nitrogen riverine loads in 2006 after (HELCOM 2009a) and to sea surface according to (HELCOM 2002). Regional acronyms refer to Fig. 2.22. ....	66
Table 2.9	List of meteorological stations for which data of air pressure (P), air temperature (T), wind (W), cloudiness (C), relative humidity (R) and precipitation (N) were available. Frequency denotes basic time resolution. DWD refers to German Weather Service. The data record for Eastern Gotland Basin is derived from Miętus (1998). Tables of climatological monthly means at Swinoujscie, Utö, and Kemi, were taken from (Leppäranta and Myrberg 2009). ....	68
Table 2.10	Regional contribution of precipitation minus evaporation (P-E), 1980-1995, after Lindau 2002) in relation to annual mean river runoff (HELCOM 2009c) in 1950-2008. ....	75
Table 3.1	Sea state parameters determined from the wave diagram in Fig. 3.5. ....	86
Table 3.2	Tidal fitting of the sea level elevation recorded at gauge stations. Daily refers to partial tides $M2+S2+K1+O1$ , yearly to the annual cycle and its sub-harmonics, and all comprises	



the major 37 tidal constituents plus the yearly contributions, see text. The tidal contribution to the observed rms of sea level is given in relative (%) and absolute (cm) units. .... 93

Table 3.3 Water and salt balance of the Baltic Sea after (Lass and Matthäus 2008). The table provides annual water mass (km<sup>3</sup>) and salt transports (Gt) for the relations shown in Fig. 1.1. Extending the above scheme we present the total fresh water input  $F=R+(P-E)$ , with river runoff R, and the budget of precipitation and evaporation (P-E) derived from (Lindau 2002) for the period 1980-1995. R=446 km<sup>3</sup>, P-E=25 km<sup>3</sup>. .... 96

Table 3.4 Long-term statistics of surface and bottom salinity in Baltic Sea basins at the sea surface and in the bottom layer (after Feister et al., 2008). Potential outliers indicated by brackets. .... 105

Table 3.5 Annual volume and salt transports across Drogden Sill, Darss Sill and Fehmarnbelt as simulated by the MIKE Regional Model (ID6.42) for the period 1990-2007 (FEHY 2013c). .... 111

Table 4.1 Molar N/P ratios in the winter surface layer (February, 0 – 10 m) between 1990 and 2000, including SMHI data for 2000 (Matthäus et al. 2001). See Fig. 2.1 for locations of sub-basins. .... 132

Table 5.1 Characterization of seasons according to the HELCOM recommendations (HELCOM 1996). .... 145

Table 5.2 Seasonal mean of chlorophyll a concentration of surface water (mean value of 1-10 m depth). The characterization of seasons follows the HELCOM recommendations (HELCOM 1996)..... 149

Table 5.3 Phytoplankton primary production in the different sea areas. Data are compiled from various literatures by Wasmund & Siegel (2008) and Wasmund et al. (2001)..... 154

Table 5.4 Phytoplankton primary production in the different Sea areas in the 1970s and the 1990s. Table originates from (Wasmund & Siegel 2008). The values represent in situ measurements except for "Total Baltic" calculate d by (Wasmund et al. 2010). .... 158

Table 6.1 Distribution of the substances with the highest concentrations in relation to target levels (i.e., the highest Contamination Ratio, CR) in the 137 assessment units classified as "areas disturbed by hazardous substances" in the different sub-basins of the Baltic Sea. Numbers in parentheses indicate the number of times the substance was found having the highest CR in the assessment units of the basin (HELCOM 2010c)..... 168